

PyCAMA report generated by trop12-proc

trop12-proc

2025-01-30 (01:35)

1 Short Introduction

1.1 The list of parameters

You may want to keep the list given in table 1 at hand when viewing the results.

2 Definitions

The averages shown here are *unweighted* averages:

$$\bar{x} = \frac{1}{N} \sum_{i=1}^N x_i \quad (1)$$

with N the number of observations in the dataset.

The spread of the measurements is indicated with the variance $V(x)$, or rather the standard deviation $\sigma(x) = \sqrt{V(x)}$.

$$V(x) = \frac{1}{N-1} \sum_{i=1}^N (x_i - \bar{x})^2 \quad (2)$$

We also report the more robust statistics median, minimum, maximum, various percentiles and inter quartile range.

The median m is the value of parameter x for which half of the observations of x is smaller than m :

$$P(x \leq m) = P(x \geq m) = \int_{-\infty}^m f(x) dx = \frac{1}{2} \quad (3)$$

with $f(x)$ the probability density function.

The median is a special case of a percentile. Instead of $1/2$ in equation 3, other threshold values can be used. We report results for 1 %, 5 %, 10 %, 15.9 %, 25 %, 75 %, 84.1 %, 90 %, 95 % and 99 %. The inter quartile range is the difference between the 75 % and 25 % percentiles. Similarly the minimum and maximum values correspond to the 0 % and 100 % percentiles respectively.

For normally distributed parameters the mean and median are the same, while the $\mu \pm \sigma$ values and the 15.9 % and 84.1 % percentiles coincide.

To get a measure for the relation of one variable $x_{(k)}$ with another $x_{(l)}$, we calculate the covariance matrix C_{kl} .

$$C_{kl} = C(x_{(k)}, x_{(l)}) = \frac{1}{N-1} \sum_{i=1}^N (x_{(k),i} - \bar{x}_{(k)})(x_{(l),i} - \bar{x}_{(l)}) \quad (4)$$

Rather than a dimensionally dependent covariance, it is often easier to interpret a correlation matrix R_{kl} , a matrix of Pearson's r coefficients:

$$R_{kl} = R(x_{(k)}, x_{(l)}) = \frac{C_{kl}}{\sqrt{C_{kk}C_{ll}}} = \frac{C_{kl}}{\sqrt{V(x_k)V(x_l)}} \quad (5)$$

The diagonal elements of the covariance matrix are the variances of the elements, $V(x_{(k)}) = C_{kk}$ and obviously $R_{kk} = 1$.

| Variable | Parameterlist and basic statistics for the analysis | | | | | | |
|--|---|----------|-------------------------|------------------------|------------------------|-------------------------|------------------------|
| | mean $\pm \sigma$ | Count | Mode | IQR | Median | Minimum | Maximum |
| qa value [1] | 0.908 \pm 0.183 | 24779226 | 0.995 | 0.1000 | 1.000 | 0.350 | 1.000 |
| cloud pressure crb [hPa] | 789 \pm 194 | 24779226 | 1.015×10^3 | 279 | 845 | 130 | 1.069×10^3 |
| cloud pressure crb precision [hPa] | 2.46 \pm 9.52 | 24779226 | 0.750 | 1.21 | 0.522 | 6.104×10^{-4} | 1.567×10^3 |
| cloud fraction crb [1] | 0.474 \pm 0.387 | 24779226 | 0.996 | 0.837 | 0.400 | 0.0 | 1.000 |
| cloud fraction crb precision [1] | $(1.594 \pm 7.005) \times 10^{-4}$ | 24779226 | 2.500×10^{-4} | 6.128×10^{-5} | 7.288×10^{-5} | 2.198×10^{-9} | 0.455 |
| scene albedo [1] | 0.451 \pm 0.333 | 24779226 | 1.500×10^{-2} | 0.609 | 0.423 | -2.569×10^{-2} | 4.93 |
| scene albedo precision [1] | $(7.723 \pm 8.632) \times 10^{-5}$ | 24779226 | 2.500×10^{-4} | 6.021×10^{-5} | 5.227×10^{-5} | 1.038×10^{-5} | 1.871×10^{-2} |
| apparent scene pressure [hPa] | 818 \pm 169 | 24779226 | 1.008×10^3 | 252 | 866 | 130 | 1.067×10^3 |
| apparent scene pressure precision [hPa] | 0.996 \pm 1.827 | 24779226 | 0.500 | 0.511 | 0.422 | 6.299×10^{-2} | 61.3 |
| chi square [1] | $(0.232 \pm 2.190) \times 10^5$ | 24779226 | 0.150 | 2.714×10^4 | 1.579×10^4 | 51.0 | 3.224×10^8 |
| number of iterations [1] | 3.31 \pm 1.04 | 24779226 | 3.23 | 1.000 | 3.00 | 1.000 | 14.0 |
| fluorescence [$\text{mol s}^{-1} \text{m}^{-2} \text{nm}^{-1} \text{sr}^{-1}$] | $(1.224 \pm 6.157) \times 10^{-9}$ | 24779226 | 2.500×10^{-10} | 5.037×10^{-9} | 1.122×10^{-9} | -1.688×10^{-6} | 1.528×10^{-6} |
| fluorescence precision [$\text{mol s}^{-1} \text{m}^{-2} \text{nm}^{-1} \text{sr}^{-1}$] | $(1.736 \pm 0.702) \times 10^{-9}$ | 24779226 | 8.500×10^{-10} | 1.048×10^{-9} | 1.664×10^{-9} | 4.175×10^{-10} | 5.538×10^{-9} |
| chi square fluorescence [1] | $(0.515 \pm 0.977) \times 10^5$ | 24779226 | 1.250×10^3 | 4.600×10^4 | 1.607×10^4 | 90.6 | 2.684×10^6 |
| degrees of freedom fluorescence [1] | 6.00 \pm 0.00 | 24779226 | 5.95 | 0.0 | 6.00 | 6.00 | 6.00 |
| number of spectral points in retrieval [1] | 50.0 \pm 0.1 | 24779226 | 49.7 | 0.0 | 50.0 | 46.0 | 50.0 |
| wavelength calibration offset [nm] | $(3.838 \pm 8.535) \times 10^{-3}$ | 24779226 | 3.600×10^{-3} | 5.447×10^{-3} | 3.864×10^{-3} | -9.665×10^{-2} | 0.153 |

Table 2: Percentile ranges

| Variable | 1 % | 5 % | 10 % | 15.9 % | 25 % | 75 % | 84.1 % | 90 % | 95 % | 99 % |
|--|-------------------------|-------------------------|-------------------------|-------------------------|-------------------------|------------------------|------------------------|------------------------|------------------------|------------------------|
| qa value [1] | 0.500 | 0.500 | 0.500 | 0.700 | 0.900 | 1.000 | 1.000 | 1.000 | 1.000 | 1.000 |
| cloud pressure crb [hPa] | 240 | 396 | 502 | 592 | 667 | 947 | 976 | 994 | 1.010×10^3 | 1.019×10^3 |
| cloud pressure crb precision [hPa] | 0.145 | 0.228 | 0.250 | 0.269 | 0.302 | 1.51 | 2.70 | 4.71 | 9.47 | 32.0 |
| cloud fraction crb [1] | 6.924×10^{-4} | 1.041×10^{-2} | 2.274×10^{-2} | 4.248×10^{-2} | 8.749×10^{-2} | 0.925 | 1.000 | 1.000 | 1.000 | 1.000 |
| cloud fraction crb precision [1] | 1.941×10^{-5} | 2.270×10^{-5} | 2.537×10^{-5} | 2.905×10^{-5} | 3.873×10^{-5} | 1.000×10^{-4} | 1.201×10^{-4} | 2.009×10^{-4} | 5.444×10^{-4} | 1.953×10^{-3} |
| scene albedo [1] | 7.755×10^{-3} | 1.853×10^{-2} | 3.434×10^{-2} | 6.062×10^{-2} | 0.128 | 0.738 | 0.860 | 0.918 | 0.964 | 1.09 |
| scene albedo precision [1] | 1.284×10^{-5} | 1.500×10^{-5} | 1.815×10^{-5} | 2.265×10^{-5} | 3.072×10^{-5} | 9.093×10^{-5} | 1.170×10^{-4} | 1.511×10^{-4} | 2.244×10^{-4} | 4.543×10^{-4} |
| apparent scene pressure [hPa] | 345 | 480 | 574 | 635 | 705 | 957 | 982 | 999 | 1.011×10^3 | 1.020×10^3 |
| apparent scene pressure precision [hPa] | 0.210 | 0.236 | 0.254 | 0.272 | 0.301 | 0.812 | 1.33 | 2.17 | 3.89 | 9.05 |
| chi square [1] | 270 | 626 | 1.292×10^3 | 2.582×10^3 | 5.335×10^3 | 3.247×10^4 | 4.122×10^4 | 4.849×10^4 | 5.775×10^4 | 7.802×10^4 |
| number of iterations [1] | 2.00 | 2.00 | 2.00 | 2.00 | 3.00 | 4.00 | 4.00 | 4.00 | 5.00 | 7.00 |
| fluorescence [$\text{mol s}^{-1} \text{m}^{-2} \text{nm}^{-1} \text{sr}^{-1}$] | -1.459×10^{-8} | -6.773×10^{-9} | -4.075×10^{-9} | -2.550×10^{-9} | -1.181×10^{-9} | 3.855×10^{-9} | 5.478×10^{-9} | 7.061×10^{-9} | 9.374×10^{-9} | 1.467×10^{-8} |
| fluorescence precision [$\text{mol s}^{-1} \text{m}^{-2} \text{nm}^{-1} \text{sr}^{-1}$] | 7.119×10^{-10} | 8.054×10^{-10} | 8.775×10^{-10} | 9.684×10^{-10} | 1.146×10^{-9} | 2.194×10^{-9} | 2.479×10^{-9} | 2.659×10^{-9} | 2.982×10^{-9} | 3.625×10^{-9} |
| chi square fluorescence [1] | 406 | 1.067×10^3 | 1.698×10^3 | 2.566×10^3 | 4.417×10^3 | 5.042×10^4 | 8.682×10^4 | 1.367×10^5 | 2.369×10^5 | 4.957×10^5 |
| degrees of freedom fluorescence [1] | 6.00 | 6.00 | 6.00 | 6.00 | 6.00 | 6.00 | 6.00 | 6.00 | 6.00 | 6.00 |
| number of spectral points in retrieval [1] | 50.0 | 50.0 | 50.0 | 50.0 | 50.0 | 50.0 | 50.0 | 50.0 | 50.0 | 50.0 |
| wavelength calibration offset [nm] | -2.383×10^{-2} | -8.749×10^{-3} | -3.622×10^{-3} | -9.818×10^{-4} | 1.102×10^{-3} | 6.549×10^{-3} | 8.597×10^{-3} | 1.128×10^{-2} | 1.647×10^{-2} | 3.152×10^{-2} |

+

| Variable | mean $\pm \sigma$ | Count | IQR | Median | Minimum | Maximum | 25 % percentile | 75 % percentile |
|--|--------------------------------------|---------|-------------------------|-------------------------|-------------------------|------------------------|--------------------------|------------------------|
| qa value [1] | 0.986 ± 0.066 | 9583166 | 0.0 | 1.000 | 0.350 | 1.000 | 1.000 | 1.000 |
| cloud pressure crb [hPa] | 772 ± 215 | 9583166 | 326 | 843 | 130 | 1.069×10^3 | 623 | 949 |
| cloud pressure crb precision [hPa] | 3.38 ± 11.38 | 9583166 | 2.03 | 0.922 | 6.104×10^{-4} | 1.567×10^3 | 0.430 | 2.47 |
| cloud fraction crb [1] | 0.355 ± 0.344 | 9583166 | 0.569 | 0.214 | 0.0 | 1.000 | 5.464×10^{-2} | 0.624 |
| cloud fraction crb precision [1] | $(1.651 \pm 9.097) \times 10^{-4}$ | 9583166 | 7.820×10^{-5} | 7.941×10^{-5} | 2.198×10^{-9} | 0.455 | 4.237×10^{-5} | 1.206×10^{-4} |
| scene albedo [1] | 0.377 ± 0.295 | 9583166 | 0.494 | 0.325 | -2.328×10^{-2} | 3.97 | 0.104 | 0.598 |
| scene albedo precision [1] | $(8.096 \pm 9.049) \times 10^{-5}$ | 9583166 | 6.022×10^{-5} | 5.272×10^{-5} | 1.155×10^{-5} | 6.579×10^{-3} | 3.237×10^{-5} | 9.259×10^{-5} |
| apparent scene pressure [hPa] | 817 ± 180 | 9583166 | 249 | 874 | 130 | 1.067×10^3 | 711 | 960 |
| apparent scene pressure precision [hPa] | 1.19 ± 2.09 | 9583166 | 0.644 | 0.524 | 6.299×10^{-2} | 60.4 | 0.364 | 1.01 |
| chi square [1] | $(0.159 \pm 1.866) \times 10^5$ | 9583166 | 1.698×10^4 | 1.083×10^4 | 51.0 | 1.001×10^8 | 3.798×10^3 | 2.078×10^4 |
| number of iterations [1] | 3.36 ± 1.07 | 9583166 | 1.000 | 3.00 | 1.000 | 14.0 | 3.00 | 4.00 |
| fluorescence [$\text{mol s}^{-1} \text{m}^{-2} \text{nm}^{-1} \text{sr}^{-1}$] | $(7.609 \pm 46.496) \times 10^{-10}$ | 9583166 | 3.730×10^{-9} | 8.851×10^{-10} | -1.527×10^{-6} | 1.191×10^{-6} | -8.822×10^{-10} | 2.848×10^{-9} |
| fluorescence precision [$\text{mol s}^{-1} \text{m}^{-2} \text{nm}^{-1} \text{sr}^{-1}$] | $(1.505 \pm 0.608) \times 10^{-9}$ | 9583166 | 8.307×10^{-10} | 1.404×10^{-9} | 4.246×10^{-10} | 5.283×10^{-9} | 1.013×10^{-9} | 1.843×10^{-9} |
| chi square fluorescence [1] | $(0.403 \pm 0.837) \times 10^5$ | 9583166 | 3.636×10^4 | 1.169×10^4 | 108 | 1.758×10^6 | 3.432×10^3 | 3.979×10^4 |
| degrees of freedom fluorescence [1] | 6.00 ± 0.00 | 9583166 | 0.0 | 6.00 | 6.00 | 6.00 | 6.00 | 6.00 |
| number of spectral points in retrieval [1] | 50.0 ± 0.1 | 9583166 | 0.0 | 50.0 | 48.0 | 50.0 | 50.0 | 50.0 |
| wavelength calibration offset [nm] | $(3.843 \pm 9.433) \times 10^{-3}$ | 9583166 | 6.636×10^{-3} | 3.764×10^{-3} | -8.504×10^{-2} | 8.765×10^{-2} | 4.625×10^{-4} | 7.098×10^{-3} |

Table 4: Parameterlist and basic statistics for the analysis for observations in the southern hemisphere

| Variable | mean $\pm \sigma$ | Count | IQR | Median | Minimum | Maximum | 25 % percentile | 75 % percentile |
|--|------------------------------------|----------|------------------------|------------------------|-------------------------|------------------------|-------------------------|------------------------|
| qa value [1] | 0.859 ± 0.214 | 15196060 | 0.300 | 1.000 | 0.350 | 1.000 | 0.700 | 1.000 |
| cloud pressure crb [hPa] | 799 ± 178 | 15196060 | 263 | 845 | 130 | 1.034×10^3 | 682 | 945 |
| cloud pressure crb precision [hPa] | 1.88 ± 8.07 | 15196060 | 0.679 | 0.382 | 2.075×10^{-3} | 557 | 0.276 | 0.954 |
| cloud fraction crb [1] | 0.550 ± 0.393 | 15196060 | 0.870 | 0.577 | 0.0 | 1.000 | 0.130 | 1.000 |
| cloud fraction crb precision [1] | $(1.558 \pm 5.275) \times 10^{-4}$ | 15196060 | 6.334×10^{-5} | 6.923×10^{-5} | 5.319×10^{-8} | 0.121 | 3.666×10^{-5} | 1.000×10^{-4} |
| scene albedo [1] | 0.498 ± 0.346 | 15196060 | 0.677 | 0.510 | -2.569×10^{-2} | 4.93 | 0.145 | 0.822 |
| scene albedo precision [1] | $(7.488 \pm 8.349) \times 10^{-5}$ | 15196060 | 6.039×10^{-5} | 5.202×10^{-5} | 1.038×10^{-5} | 1.871×10^{-2} | 2.956×10^{-5} | 8.995×10^{-5} |
| apparent scene pressure [hPa] | 818 ± 162 | 15196060 | 252 | 861 | 130 | 1.034×10^3 | 703 | 955 |
| apparent scene pressure precision [hPa] | 0.873 ± 1.628 | 15196060 | 0.408 | 0.364 | 0.143 | 61.3 | 0.280 | 0.688 |
| chi square [1] | $(0.278 \pm 2.371) \times 10^5$ | 15196060 | 3.263×10^4 | 2.187×10^4 | 57.8 | 3.224×10^8 | 6.928×10^3 | 3.956×10^4 |
| number of iterations [1] | 3.28 ± 1.02 | 15196060 | 1.000 | 3.00 | 1.000 | 14.0 | 3.00 | 4.00 |
| fluorescence [$\text{mol s}^{-1} \text{m}^{-2} \text{nm}^{-1} \text{sr}^{-1}$] | $(1.516 \pm 6.926) \times 10^{-9}$ | 15196060 | 6.067×10^{-9} | 1.377×10^{-9} | -1.688×10^{-6} | 1.528×10^{-6} | -1.409×10^{-9} | 4.659×10^{-9} |
| fluorescence precision [$\text{mol s}^{-1} \text{m}^{-2} \text{nm}^{-1} \text{sr}^{-1}$] | $(1.881 \pm 0.717) \times 10^{-9}$ | 15196060 | 1.109×10^{-9} | 1.879×10^{-9} | 4.175×10^{-10} | 5.538×10^{-9} | 1.282×10^{-9} | 2.391×10^{-9} |
| chi square fluorescence [1] | $(0.585 \pm 1.050) \times 10^5$ | 15196060 | 5.352×10^4 | 1.930×10^4 | 90.6 | 2.684×10^6 | 5.290×10^3 | 5.881×10^4 |
| degrees of freedom fluorescence [1] | 6.00 ± 0.00 | 15196060 | 0.0 | 6.00 | 6.00 | 6.00 | 6.00 | 6.00 |
| number of spectral points in retrieval [1] | 50.0 ± 0.1 | 15196060 | 0.0 | 50.0 | 46.0 | 50.0 | 50.0 | 50.0 |
| wavelength calibration offset [nm] | $(3.836 \pm 7.917) \times 10^{-3}$ | 15196060 | 4.817×10^{-3} | 3.909×10^{-3} | -9.665×10^{-2} | 0.153 | 1.453×10^{-3} | 6.270×10^{-3} |

Table 5: Parameterlist and basic statistics for the analysis for observations over water

| Variable | mean $\pm \sigma$ | Count | IQR | Median | Minimum | Maximum | 25 % percentile | 75 % percentile |
|--|--------------------------------------|----------|------------------------|-------------------------|-------------------------|------------------------|-------------------------|------------------------|
| qa value [1] | 0.982 ± 0.045 | 16051604 | 0.0 | 1.000 | 0.350 | 1.000 | 1.000 | 1.000 |
| cloud pressure crb [hPa] | 824 ± 184 | 16051604 | 233 | 889 | 130 | 1.037×10^3 | 731 | 964 |
| cloud pressure crb precision [hPa] | 2.63 ± 10.27 | 16051604 | 1.26 | 0.602 | 2.075×10^{-3} | 1.434×10^3 | 0.333 | 1.60 |
| cloud fraction crb [1] | 0.381 ± 0.339 | 16051604 | 0.610 | 0.273 | 0.0 | 1.000 | 6.574×10^{-2} | 0.676 |
| cloud fraction crb precision [1] | $(8.246 \pm 24.963) \times 10^{-5}$ | 16051604 | 5.125×10^{-5} | 5.063×10^{-5} | 2.198×10^{-9} | 0.157 | 2.929×10^{-5} | 8.055×10^{-5} |
| scene albedo [1] | 0.326 ± 0.286 | 16051604 | 0.505 | 0.240 | -2.569×10^{-2} | 4.93 | 6.276×10^{-2} | 0.567 |
| scene albedo precision [1] | $(5.757 \pm 7.221) \times 10^{-5}$ | 16051604 | 4.012×10^{-5} | 4.219×10^{-5} | 1.038×10^{-5} | 1.871×10^{-2} | 2.300×10^{-5} | 6.311×10^{-5} |
| apparent scene pressure [hPa] | 842 ± 172 | 16051604 | 211 | 900 | 130 | 1.057×10^3 | 763 | 975 |
| apparent scene pressure precision [hPa] | 1.32 ± 2.20 | 16051604 | 0.962 | 0.553 | 6.299×10^{-2} | 61.3 | 0.324 | 1.29 |
| chi square [1] | $(0.177 \pm 1.765) \times 10^5$ | 16051604 | 2.421×10^4 | 1.019×10^4 | 51.0 | 3.224×10^8 | 2.762×10^3 | 2.698×10^4 |
| number of iterations [1] | 2.91 ± 0.76 | 16051604 | 1.000 | 3.00 | 1.000 | 14.0 | 2.00 | 3.00 |
| fluorescence [$\text{mol s}^{-1} \text{m}^{-2} \text{nm}^{-1} \text{sr}^{-1}$] | $(2.496 \pm 58.421) \times 10^{-10}$ | 16051604 | 4.346×10^{-9} | 1.867×10^{-10} | -1.579×10^{-6} | 1.363×10^{-6} | -1.870×10^{-9} | 2.476×10^{-9} |
| fluorescence precision [$\text{mol s}^{-1} \text{m}^{-2} \text{nm}^{-1} \text{sr}^{-1}$] | $(1.660 \pm 0.732) \times 10^{-9}$ | 16051604 | 1.147×10^{-9} | 1.517×10^{-9} | 4.175×10^{-10} | 5.472×10^{-9} | 1.025×10^{-9} | 2.172×10^{-9} |
| chi square fluorescence [1] | $(0.527 \pm 0.952) \times 10^5$ | 16051604 | 5.017×10^4 | 1.837×10^4 | 90.6 | 2.684×10^6 | 5.380×10^3 | 5.555×10^4 |
| degrees of freedom fluorescence [1] | 6.00 ± 0.00 | 16051604 | 0.0 | 6.00 | 6.00 | 6.00 | 6.00 | 6.00 |
| number of spectral points in retrieval [1] | 50.0 ± 0.1 | 16051604 | 0.0 | 50.0 | 48.0 | 50.0 | 50.0 | 50.0 |
| wavelength calibration offset [nm] | $(3.800 \pm 10.006) \times 10^{-3}$ | 16051604 | 6.993×10^{-3} | 3.831×10^{-3} | -9.665×10^{-2} | 0.153 | 2.699×10^{-4} | 7.263×10^{-3} |

| Variable | mean $\pm \sigma$ | Count | IQR | Median | Minimum | Maximum | 25 % percentile | 75 % percentile |
|--|-------------------------------------|---------|-------------------------|------------------------|-------------------------|------------------------|------------------------|------------------------|
| qa value [1] | 0.727 ± 0.252 | 7172134 | 0.500 | 0.500 | 0.350 | 1.000 | 0.500 | 1.000 |
| cloud pressure crb [hPa] | 722 ± 185 | 7172134 | 233 | 727 | 130 | 1.062×10^3 | 632 | 865 |
| cloud pressure crb precision [hPa] | 1.97 ± 7.52 | 7172134 | 0.834 | 0.338 | 6.104×10^{-4} | 1.488×10^3 | 0.264 | 1.10 |
| cloud fraction crb [1] | 0.695 ± 0.402 | 7172134 | 0.770 | 1.000 | 0.0 | 1.000 | 0.230 | 1.000 |
| cloud fraction crb precision [1] | $(3.107 \pm 10.778) \times 10^{-4}$ | 7172134 | 2.977×10^{-5} | 1.000×10^{-4} | 1.062×10^{-7} | 0.294 | 1.000×10^{-4} | 1.298×10^{-4} |
| scene albedo [1] | 0.717 ± 0.280 | 7172134 | 0.447 | 0.814 | 1.438×10^{-3} | 3.99 | 0.482 | 0.929 |
| scene albedo precision [1] | $(1.168 \pm 0.972) \times 10^{-4}$ | 7172134 | 7.887×10^{-5} | 9.320×10^{-5} | 1.392×10^{-5} | 1.756×10^{-3} | 5.511×10^{-5} | 1.340×10^{-4} |
| apparent scene pressure [hPa] | 764 ± 147 | 7172134 | 229 | 761 | 130 | 1.053×10^3 | 659 | 888 |
| apparent scene pressure precision [hPa] | 0.376 ± 0.158 | 7172134 | 0.155 | 0.329 | 7.477×10^{-2} | 34.3 | 0.275 | 0.430 |
| chi square [1] | $(0.347 \pm 2.430) \times 10^5$ | 7172134 | 2.660×10^4 | 2.630×10^4 | 150 | 3.212×10^8 | 1.460×10^4 | 4.120×10^4 |
| number of iterations [1] | 4.11 ± 1.03 | 7172134 | 0.0 | 4.00 | 1.000 | 14.0 | 4.00 | 4.00 |
| fluorescence [$\text{mol s}^{-1} \text{m}^{-2} \text{nm}^{-1} \text{sr}^{-1}$] | $(3.271 \pm 6.041) \times 10^{-9}$ | 7172134 | 4.491×10^{-9} | 3.163×10^{-9} | -1.688×10^{-6} | 1.496×10^{-6} | 1.138×10^{-9} | 5.629×10^{-9} |
| fluorescence precision [$\text{mol s}^{-1} \text{m}^{-2} \text{nm}^{-1} \text{sr}^{-1}$] | $(1.900 \pm 0.609) \times 10^{-9}$ | 7172134 | 7.965×10^{-10} | 1.875×10^{-9} | 4.402×10^{-10} | 5.535×10^{-9} | 1.450×10^{-9} | 2.247×10^{-9} |
| chi square fluorescence [1] | $(0.424 \pm 0.915) \times 10^5$ | 7172134 | 3.195×10^4 | 1.035×10^4 | 127 | 1.931×10^6 | 3.031×10^3 | 3.498×10^4 |
| degrees of freedom fluorescence [1] | 6.00 ± 0.00 | 7172134 | 0.0 | 6.00 | 6.00 | 6.00 | 6.00 | 6.00 |
| number of spectral points in retrieval [1] | 50.0 ± 0.1 | 7172134 | 0.0 | 50.0 | 48.0 | 50.0 | 50.0 | 50.0 |
| wavelength calibration offset [nm] | $(3.878 \pm 4.085) \times 10^{-3}$ | 7172134 | 3.339×10^{-3} | 3.891×10^{-3} | -7.865×10^{-2} | 6.456×10^{-2} | 2.213×10^{-3} | 5.553×10^{-3} |

Table 6: Parameterlist and basic statistics for the analysis for observations over land

| Variable | mean $\pm \sigma$ | Count | IQR | Median | Minimum | Maximum | 25 % percentile | 75 % percentile |
|--|-------------------------------------|---------|-------------------------|------------------------|-------------------------|------------------------|------------------------|------------------------|
| qa value [1] | 0.727 ± 0.252 | 7172134 | 0.500 | 0.500 | 0.350 | 1.000 | 0.500 | 1.000 |
| cloud pressure crb [hPa] | 722 ± 185 | 7172134 | 233 | 727 | 130 | 1.062×10^3 | 632 | 865 |
| cloud pressure crb precision [hPa] | 1.97 ± 7.52 | 7172134 | 0.834 | 0.338 | 6.104×10^{-4} | 1.488×10^3 | 0.264 | 1.10 |
| cloud fraction crb [1] | 0.695 ± 0.402 | 7172134 | 0.770 | 1.000 | 0.0 | 1.000 | 0.230 | 1.000 |
| cloud fraction crb precision [1] | $(3.107 \pm 10.778) \times 10^{-4}$ | 7172134 | 2.977×10^{-5} | 1.000×10^{-4} | 1.062×10^{-7} | 0.294 | 1.000×10^{-4} | 1.298×10^{-4} |
| scene albedo [1] | 0.717 ± 0.280 | 7172134 | 0.447 | 0.814 | 1.438×10^{-3} | 3.99 | 0.482 | 0.929 |
| scene albedo precision [1] | $(1.168 \pm 0.972) \times 10^{-4}$ | 7172134 | 7.887×10^{-5} | 9.320×10^{-5} | 1.392×10^{-5} | 1.756×10^{-3} | 5.511×10^{-5} | 1.340×10^{-4} |
| apparent scene pressure [hPa] | 764 ± 147 | 7172134 | 229 | 761 | 130 | 1.053×10^3 | 659 | 888 |
| apparent scene pressure precision [hPa] | 0.376 ± 0.158 | 7172134 | 0.155 | 0.329 | 7.477×10^{-2} | 34.3 | 0.275 | 0.430 |
| chi square [1] | $(0.347 \pm 2.430) \times 10^5$ | 7172134 | 2.660×10^4 | 2.630×10^4 | 150 | 3.212×10^8 | 1.460×10^4 | 4.120×10^4 |
| number of iterations [1] | 4.11 ± 1.03 | 7172134 | 0.0 | 4.00 | 1.000 | 14.0 | 4.00 | 4.00 |
| fluorescence [$\text{mol s}^{-1} \text{m}^{-2} \text{nm}^{-1} \text{sr}^{-1}$] | $(3.271 \pm 6.041) \times 10^{-9}$ | 7172134 | 4.491×10^{-9} | 3.163×10^{-9} | -1.688×10^{-6} | 1.496×10^{-6} | 1.138×10^{-9} | 5.629×10^{-9} |
| fluorescence precision [$\text{mol s}^{-1} \text{m}^{-2} \text{nm}^{-1} \text{sr}^{-1}$] | $(1.900 \pm 0.609) \times 10^{-9}$ | 7172134 | 7.965×10^{-10} | 1.875×10^{-9} | 4.402×10^{-10} | 5.535×10^{-9} | 1.450×10^{-9} | 2.247×10^{-9} |
| chi square fluorescence [1] | $(0.424 \pm 0.915) \times 10^5$ | 7172134 | 3.195×10^4 | 1.035×10^4 | 127 | 1.931×10^6 | 3.031×10^3 | 3.498×10^4 |
| degrees of freedom fluorescence [1] | 6.00 ± 0.00 | 7172134 | 0.0 | 6.00 | 6.00 | 6.00 | 6.00 | 6.00 |
| number of spectral points in retrieval [1] | 50.0 ± 0.1 | 7172134 | 0.0 | 50.0 | 48.0 | 50.0 | 50.0 | 50.0 |
| wavelength calibration offset [nm] | $(3.878 \pm 4.085) \times 10^{-3}$ | 7172134 | 3.339×10^{-3} | 3.891×10^{-3} | -7.865×10^{-2} | 6.456×10^{-2} | 2.213×10^{-3} | 5.553×10^{-3} |

Spectral offset ($\lambda_{\text{true}} - \lambda_{\text{nominal}}$)

| | Number of points in the spectrum | χ^2 of fluorescence retrieval |
|-------------------------|----------------------------------|------------------------------------|
| Viewing zenith angle | 1.674×10^{-2} | -9.827×10^{-3} |
| Solar zenith angle | 3.723×10^{-3} | -3.683×10^{-2} |
| Latitude | 9.700×10^{-4} | 6.015×10^{-3} |
| Cloud pressure | -5.734×10^{-3} | 3.256×10^{-2} |
| Cloud fraction | 1.381×10^{-4} | -2.181×10^{-2} |
| Scene albedo | 5.675×10^{-2} | 0.193 |
| Apparent scene pressure | 2.018×10^{-2} | -0.222 |
| χ^2 | 2.784×10^{-2} | 0.193 |
| Number of iterations | 2.061×10^{-2} | -4.385×10^{-3} |
| Fluorescence | 2.784×10^{-2} | 3.575×10^{-2} |

Table 7: Correlation matrix

| Spectral offset ($\lambda_{\text{true}} - \lambda_{\text{nominal}}$) | χ^2 of fluorescence retrieval | Number of points in the spectrum |
|--|------------------------------------|----------------------------------|
| 3.83×10^{-3} | 5.58×10^{-2} | 3.135×10^{-2} |
| 5.58×10^{-3} | 4.20×10^{-3} | 7.298×10^{-3} |
| 0.469×10^{-3} | 59.2×10^{-3} | 2.363×10^{-3} |
| -307×10^{-3} | 2.119×10^3 | 4.271×10^{-3} |
| 0.545×10^{-3} | -764×10^4 | 5.382×10^{-2} |
| 0.486×10^{-3} | 3.751×10^4 | 3.000×10^6 |
| -315×10^{-3} | -21.8×10^4 | -0.106×10^6 |
| $-6.424 \times 10^3 \times 10^{-3}$ | 0.121×10^4 | 5.106×10^{-6} |
| -0.609×10^{-3} | 0.111×10^4 | -7.196×10^{-5} |
| $8.484 \times 10^{-9} \times 10^{-3}$ | -27.1×10^4 | 1.807×10^{-5} |
| $2.658 \times 10^4 \times 10^{-3}$ | 4.058×10^4 | -5.337×10^{-5} |
| $3.135 \times 10^{-2} \times 10^{-3}$ | -1.010×10^5 | 7.285×10^{-5} |
| $-1.642 \times 10^{-3} \times 10^{-3}$ | 4.797×10^{10} | 2.890×10^{-7} |

Table 8: Covariance matrix

| Solar zenith angle | Latitude | Cloud pressure | Cloud fraction | Scene albedo | Apparent scene pressure | χ^2 | Number of iterations | χ^2 of fluorescence retrieval | Number of points in the spectrum | Spectral offset ($\lambda_{\text{true}} - \lambda_{\text{nominal}}$) |
|-------------------------|-------------------------|-------------------------|-------------------------|-------------------------|-------------------------|-------------------------|------------------------|------------------------------------|----------------------------------|--|
| 383 | 5.58 | 0.469 | -307 | 0.545 | 0.486 | -315 | -6.424 $\times 10^3$ | -0.609 | 8.484×10^{-9} | 2.658×10^4 |
| 5.58 | 420 | 59.2 | -998 | 3.80 | 3.76 | -976 | 1.023×10^5 | 8.06 | 3.132×10^{-8} | -7.155×10^5 |
| 0.469 | 59.2 | 2.119×10^3 | -764 | -6.94 | -5.01 | 24.3 | -4.066×10^5 | -2.02 | -3.992×10^{-8} | 2.511×10^4 |
| -307 | -998 | -764 | 3.751×10^4 | -21.8 | -23.1 | 2.922×10^4 | -2.227×10^5 | -72.8 | -2.253×10^{-7} | 3.000×10^6 |
| 0.545 | 3.80 | -6.94 | -21.8 | 0.149 | 0.121 | -31.6 | 4.583×10^3 | 6.666×10^{-2} | 8.473×10^{-10} | 1.040×10^3 |
| 0.486 | 3.76 | -5.01 | -23.1 | 0.121 | 0.111 | -27.1 | 4.058×10^3 | 0.109 | 7.803×10^{-10} | 1.059×10^3 |
| -315 | -976 | 24.3 | 2.922×10^4 | -31.6 | -27.1 | 2.862×10^4 | -1.010×10^5 | -39.1 | -2.413×10^{-7} | 3.195×10^6 |
| -6.424×10^3 | 1.023×10^5 | -4.066×10^5 | -2.227×10^5 | 4.583×10^3 | 4.058×10^3 | -1.010×10^5 | 4.797×10^{10} | 1.533×10^4 | 2.722×10^{-5} | 4.409×10^8 |
| -0.609 | 8.06 | -2.02 | -72.8 | 6.666×10^{-2} | 0.109 | -39.1 | 1.533×10^4 | 1.09 | 1.283×10^{-9} | -1.665×10^4 |
| 8.484×10^{-9} | 3.132×10^{-8} | -3.992×10^{-8} | -2.253×10^{-7} | 8.473×10^{-10} | 7.803×10^{-10} | -2.413×10^{-7} | 2.722×10^{-5} | 1.283×10^{-9} | 3.791×10^{-17} | -1.476×10^{-4} |
| 2.658×10^4 | -7.155×10^5 | 2.511×10^4 | 3.000×10^6 | 1.040×10^3 | 1.059×10^3 | 1.059×10^3 | 4.409×10^8 | -1.665×10^4 | -1.476×10^{-4} | 9.543×10^9 |
| 3.135×10^{-2} | 7.298×10^{-3} | 4.271×10^{-3} | -0.106 | 5.106×10^{-6} | 1.807×10^{-5} | -7.096×10^{-2} | 5.83 | 2.158×10^{-9} | -26.8 | 9.151×10^{-3} |
| -1.642×10^{-3} | -6.442×10^{-3} | 2.363×10^{-3} | 5.382×10^{-2} | -7.196×10^{-5} | -5.337×10^{-5} | 5.162×10^{-2} | -3.69 | -3.200×10^{-5} | 35.6 | 2.890×10^{-7} |

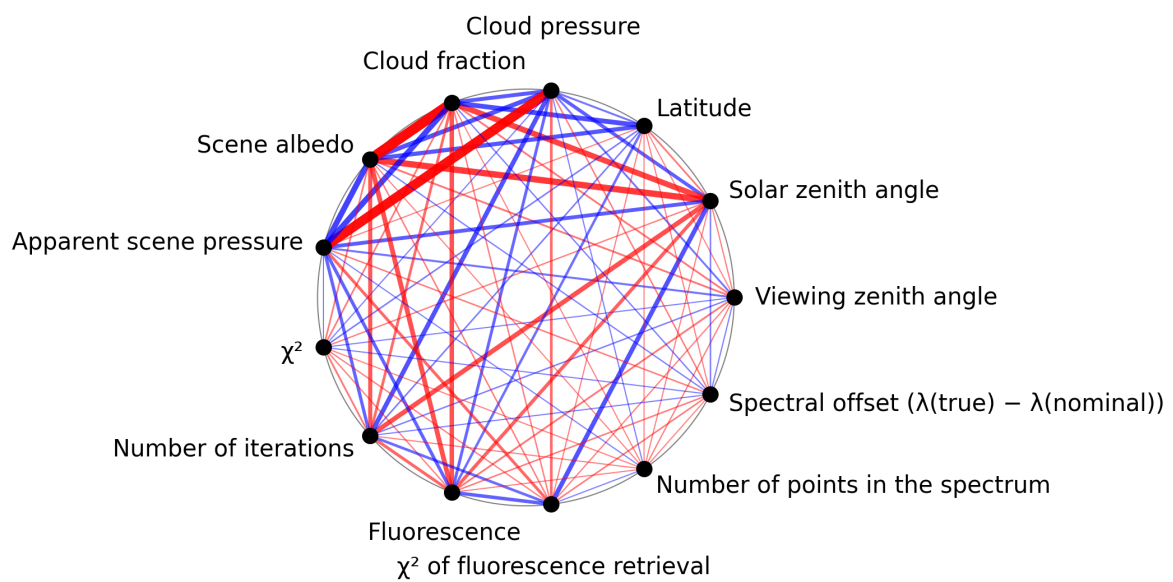


Figure 1: Map of correlation graph for 2025-01-14 to 2025-01-16.

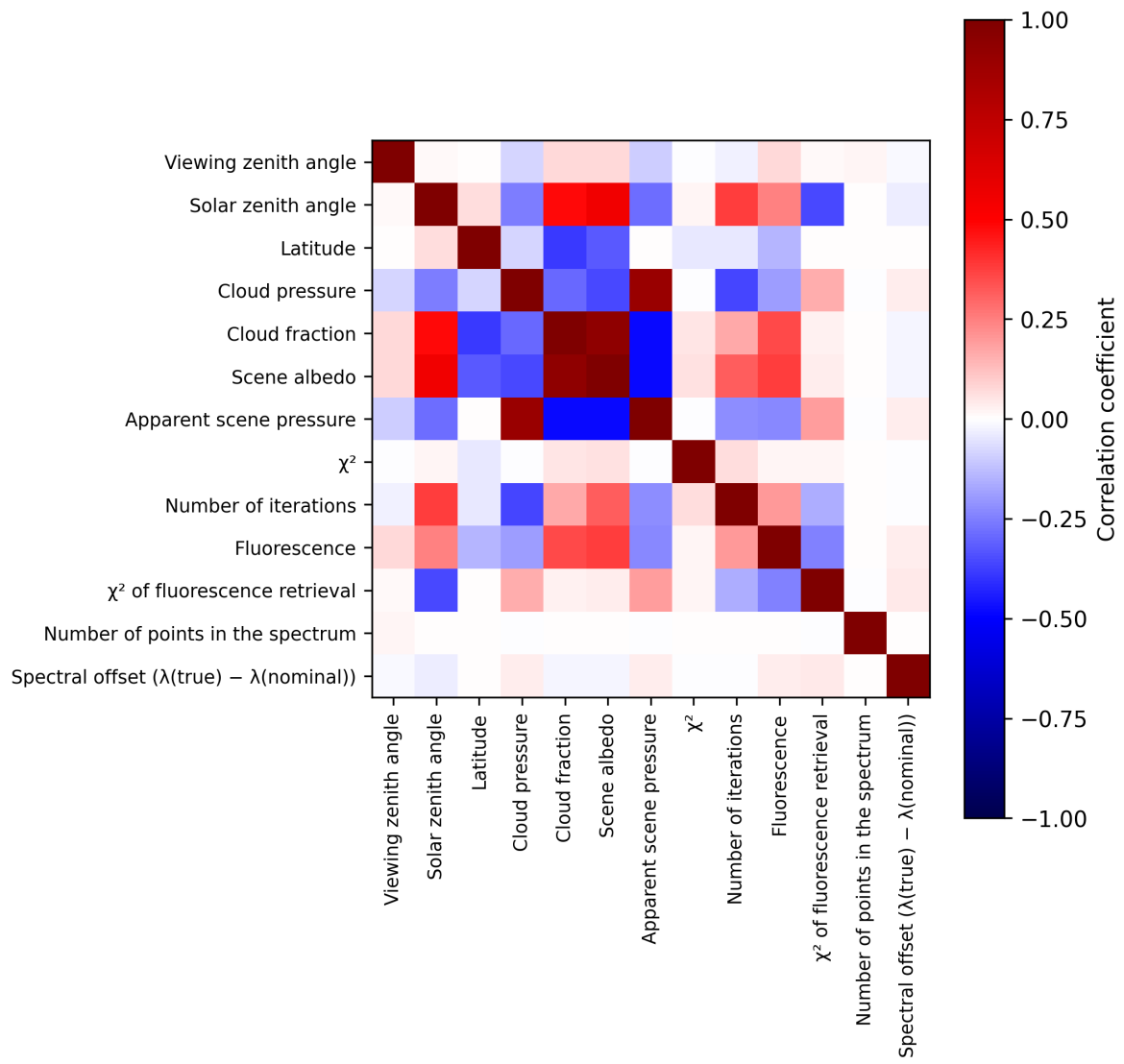


Figure 2: Map of correlation matrix for 2025-01-14 to 2025-01-16.

3 Granule outlines

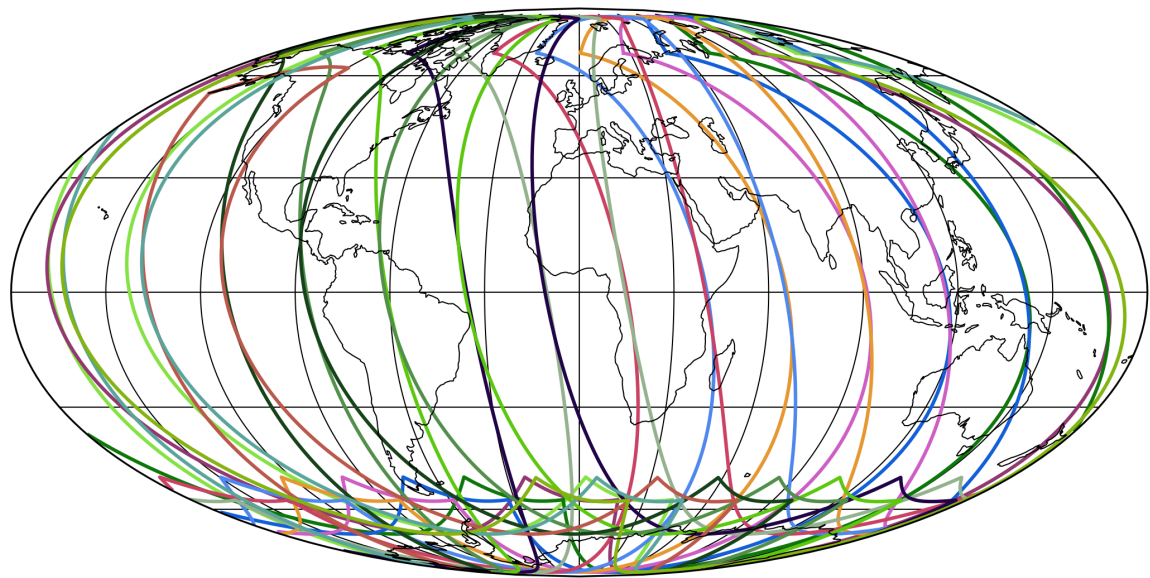


Figure 3: Outline of the granules.

4 Input data monitoring

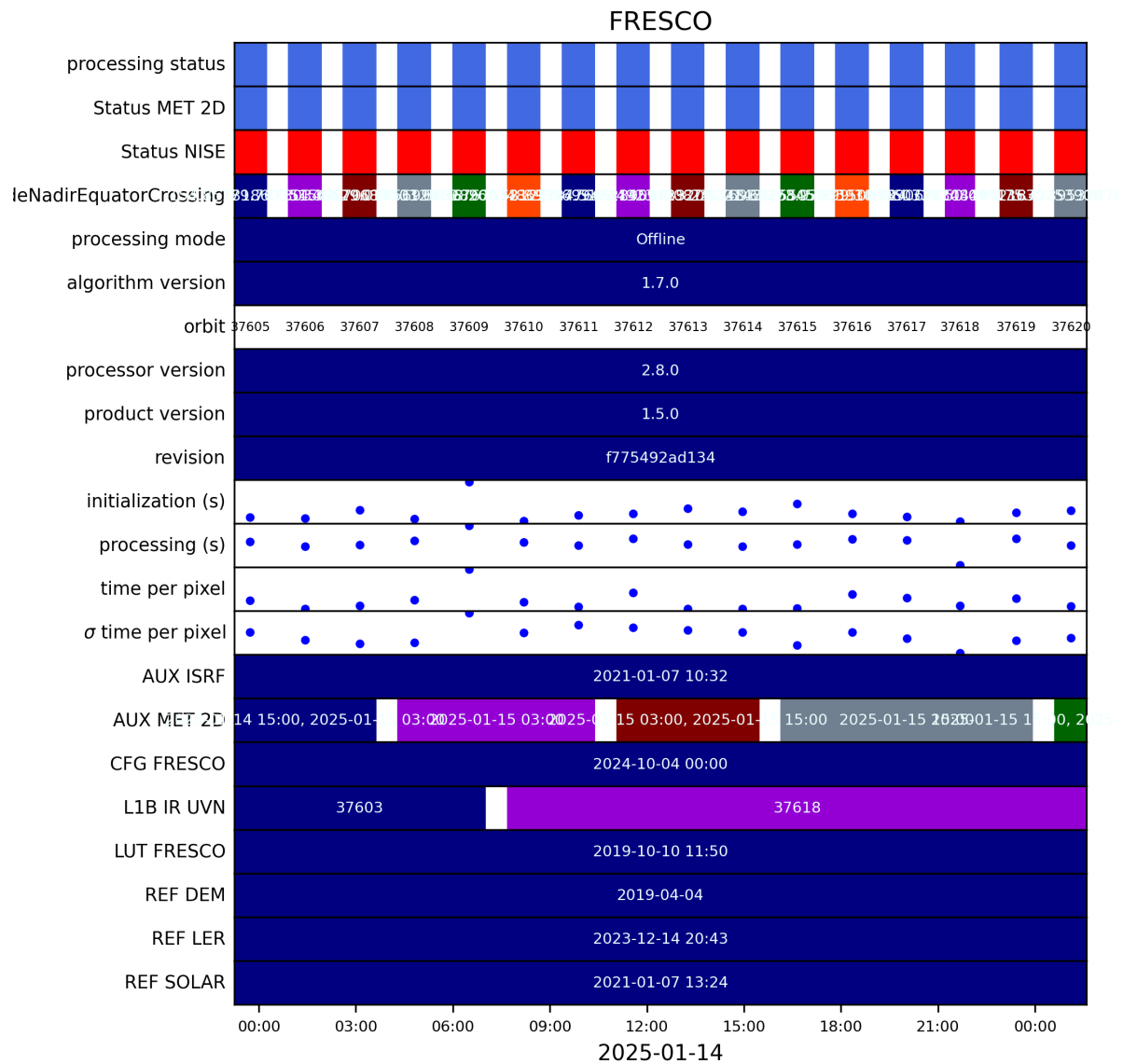


Figure 4: Input data per granule

5 Warnings and errors

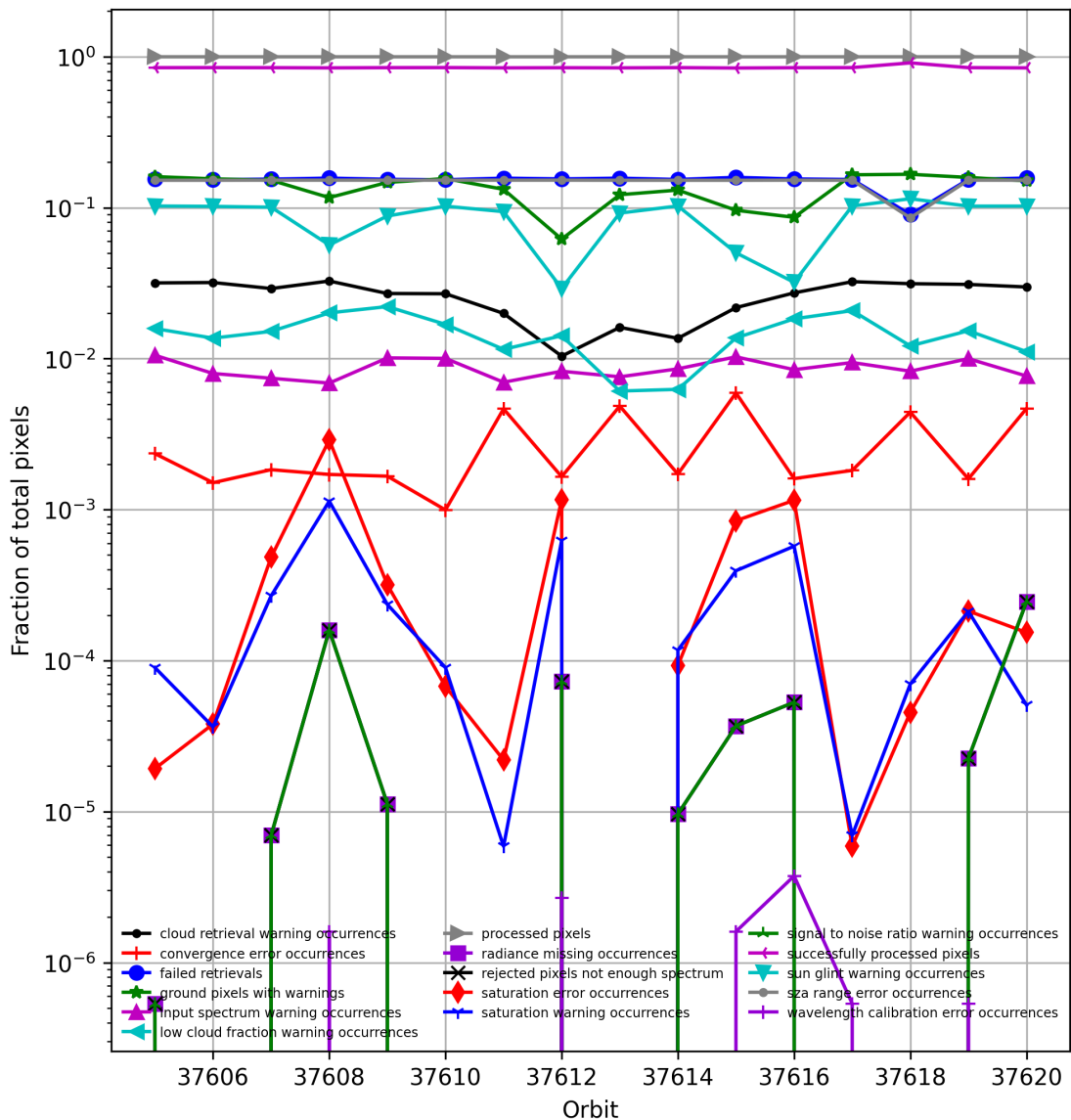


Figure 5: Fraction of pixels with specific warnings and errors during processing

6 World maps

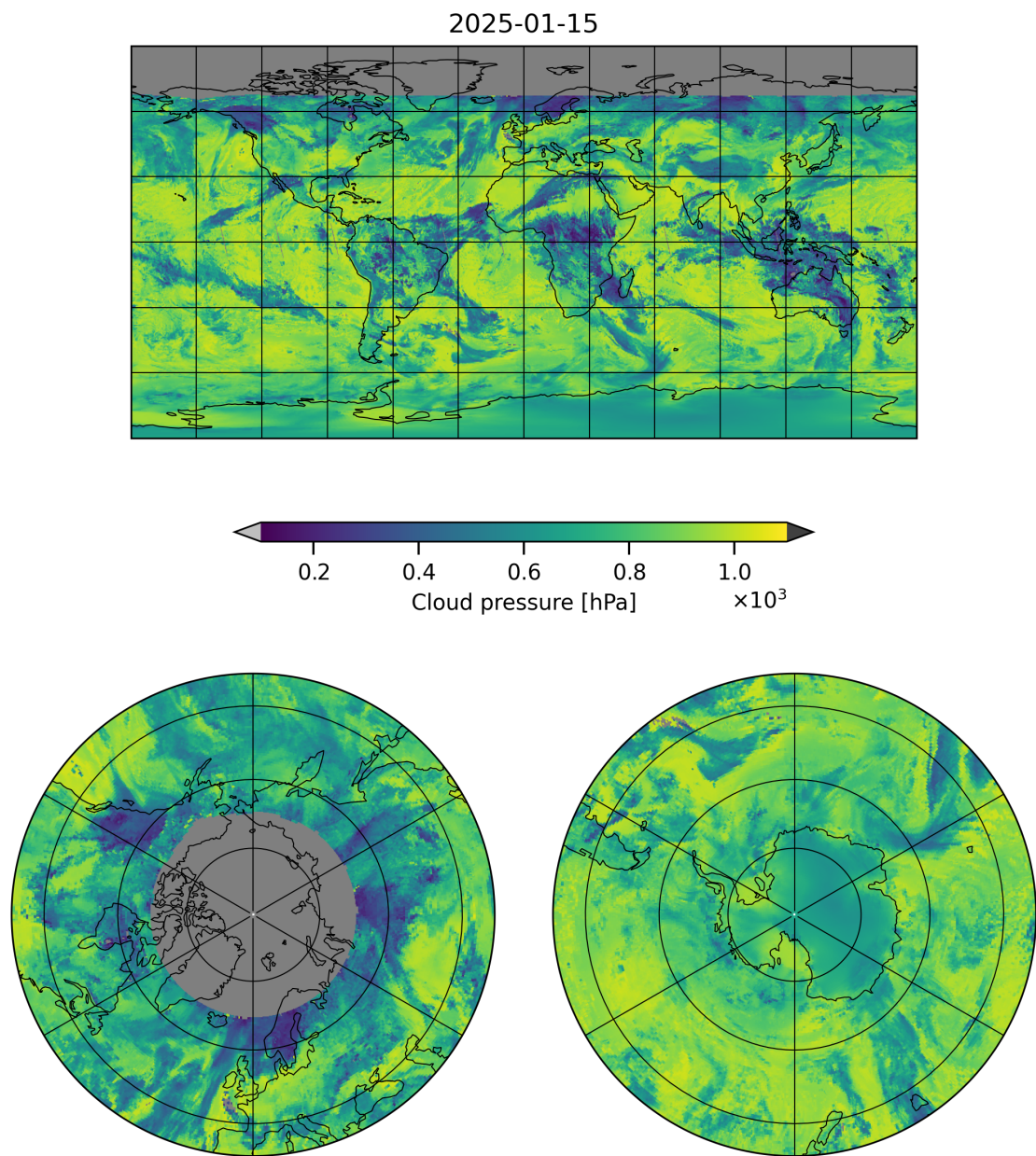


Figure 6: Map of “Cloud pressure” for 2025-01-14 to 2025-01-16

2025-01-15

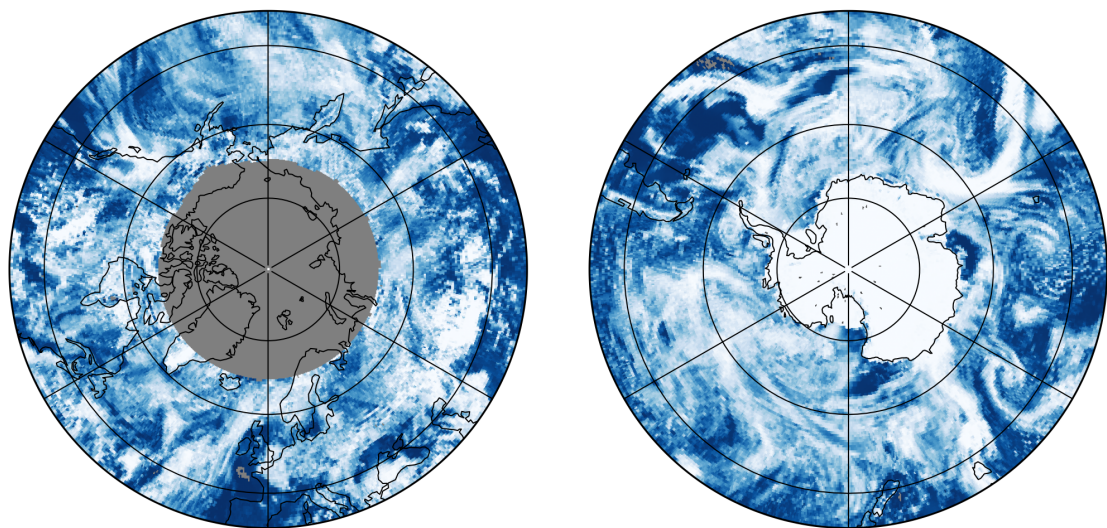
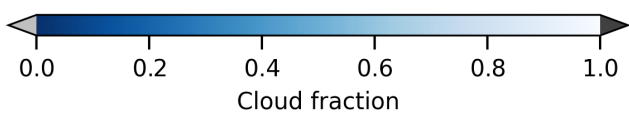
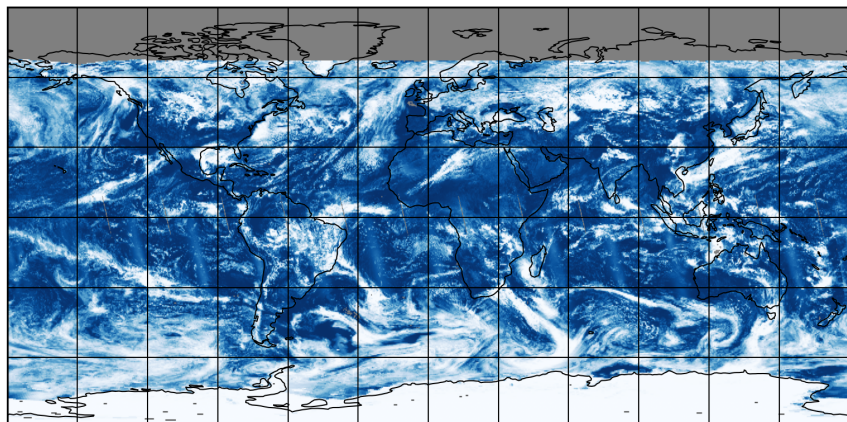


Figure 7: Map of “Cloud fraction” for 2025-01-14 to 2025-01-16

2025-01-15

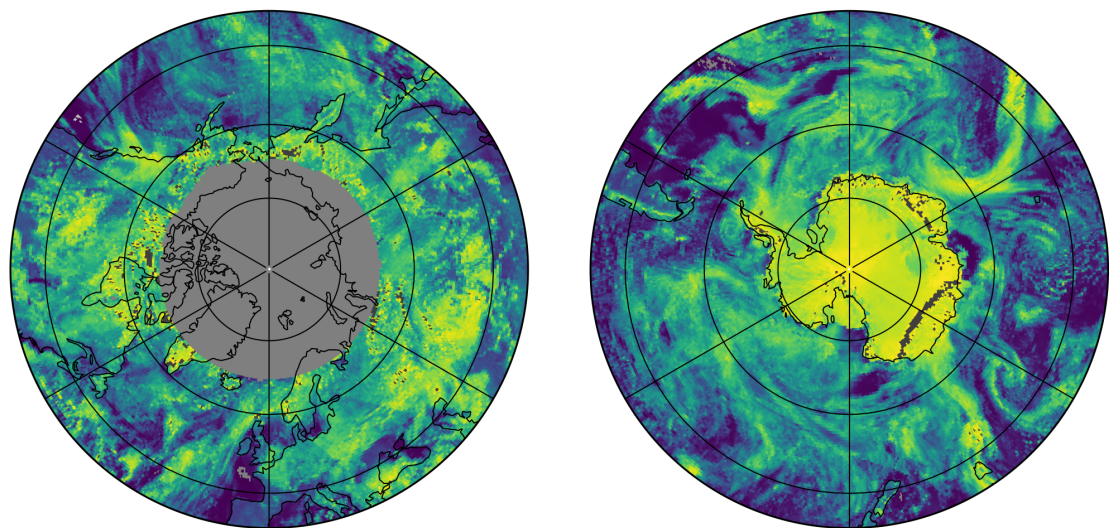
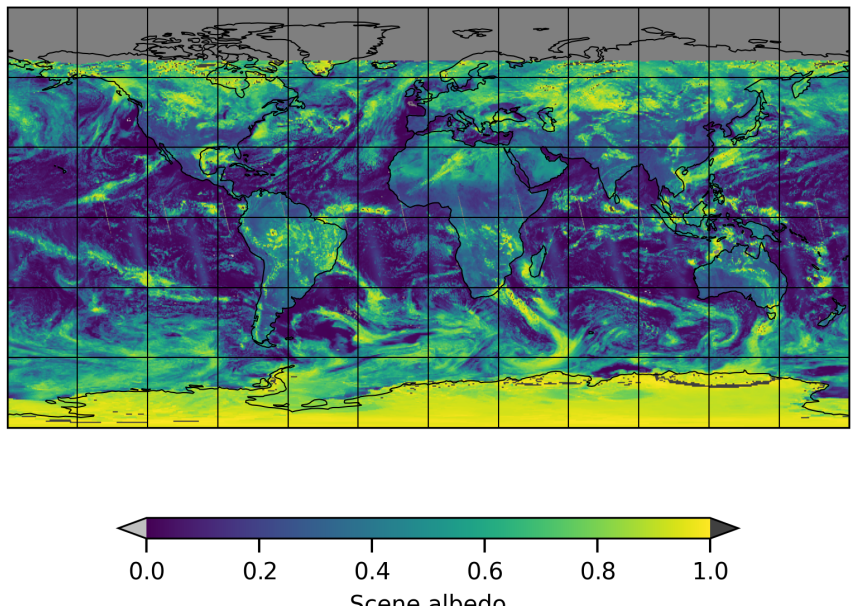


Figure 8: Map of “Scene albedo” for 2025-01-14 to 2025-01-16

2025-01-15

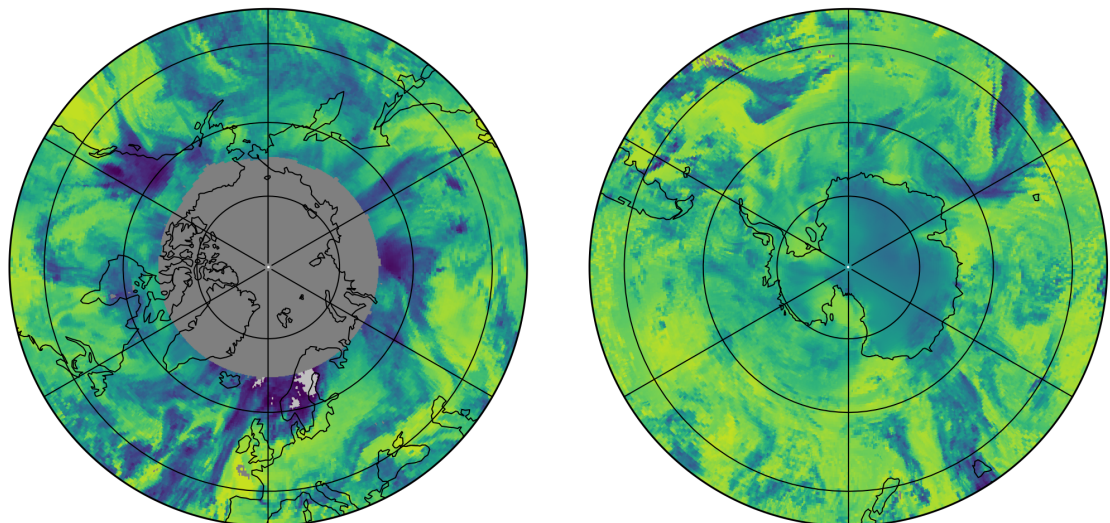
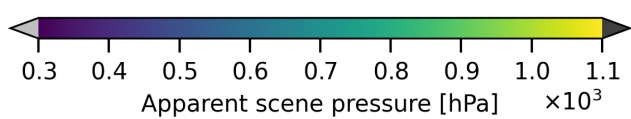
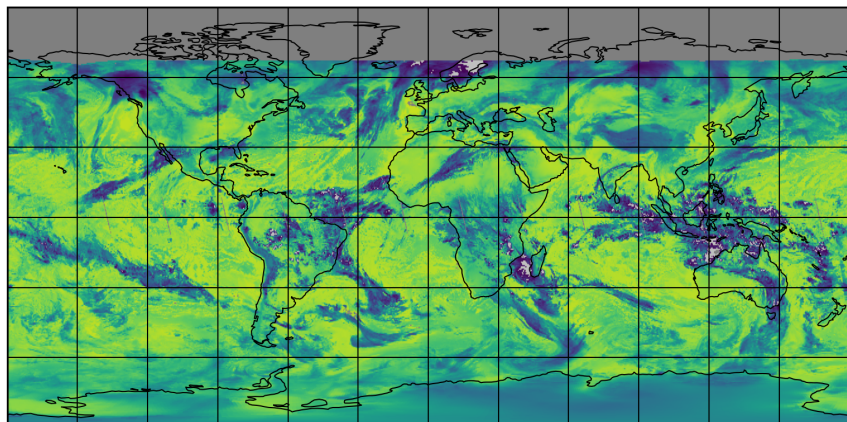


Figure 9: Map of “Apparent scene pressure” for 2025-01-14 to 2025-01-16

2025-01-15

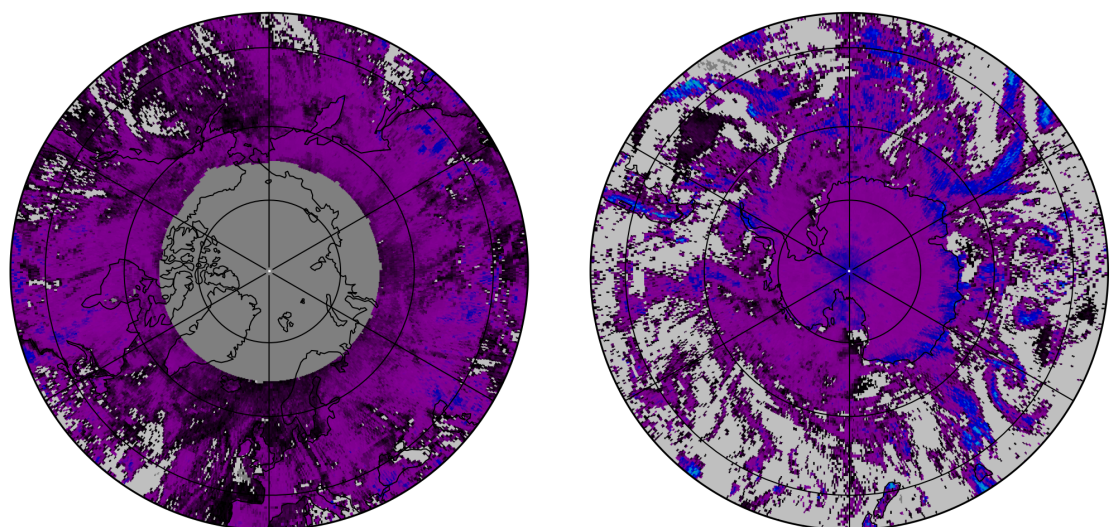
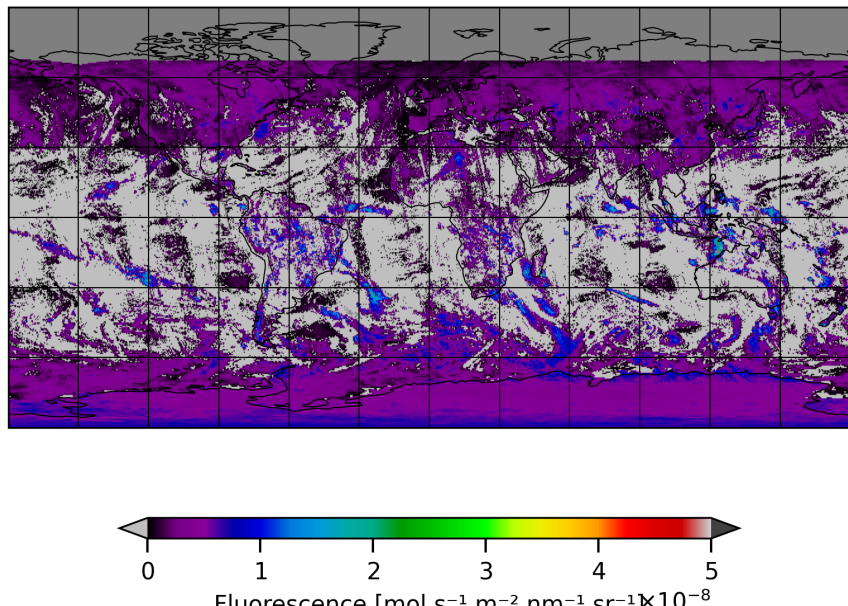


Figure 10: Map of “Fluorescence” for 2025-01-14 to 2025-01-16

2025-01-15

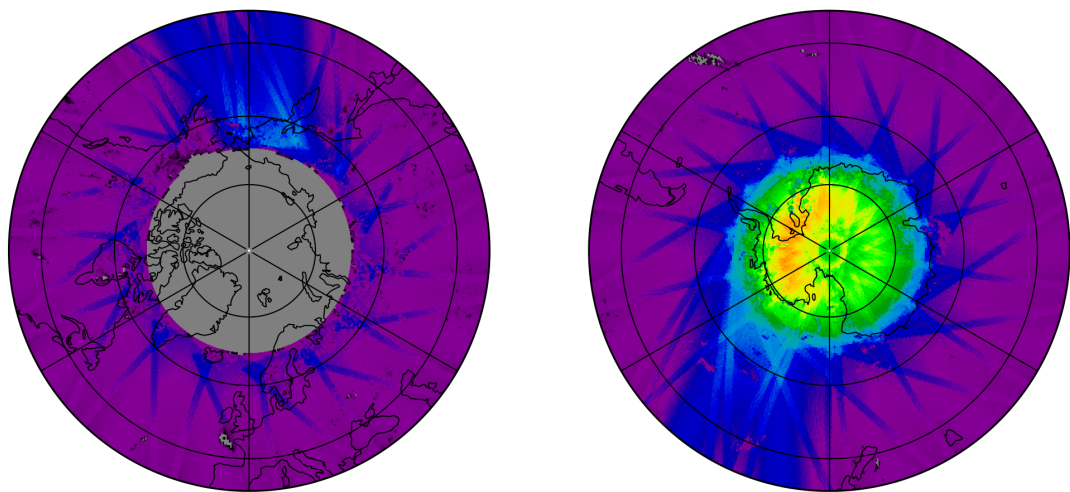
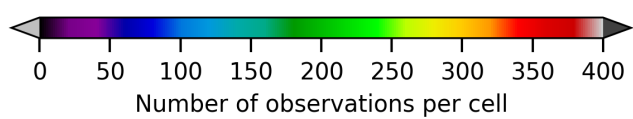
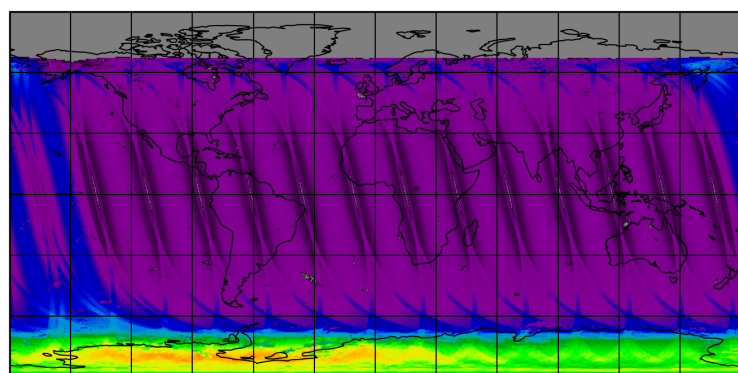


Figure 11: Map of the number of observations for 2025-01-14 to 2025-01-16

7 Zonal average

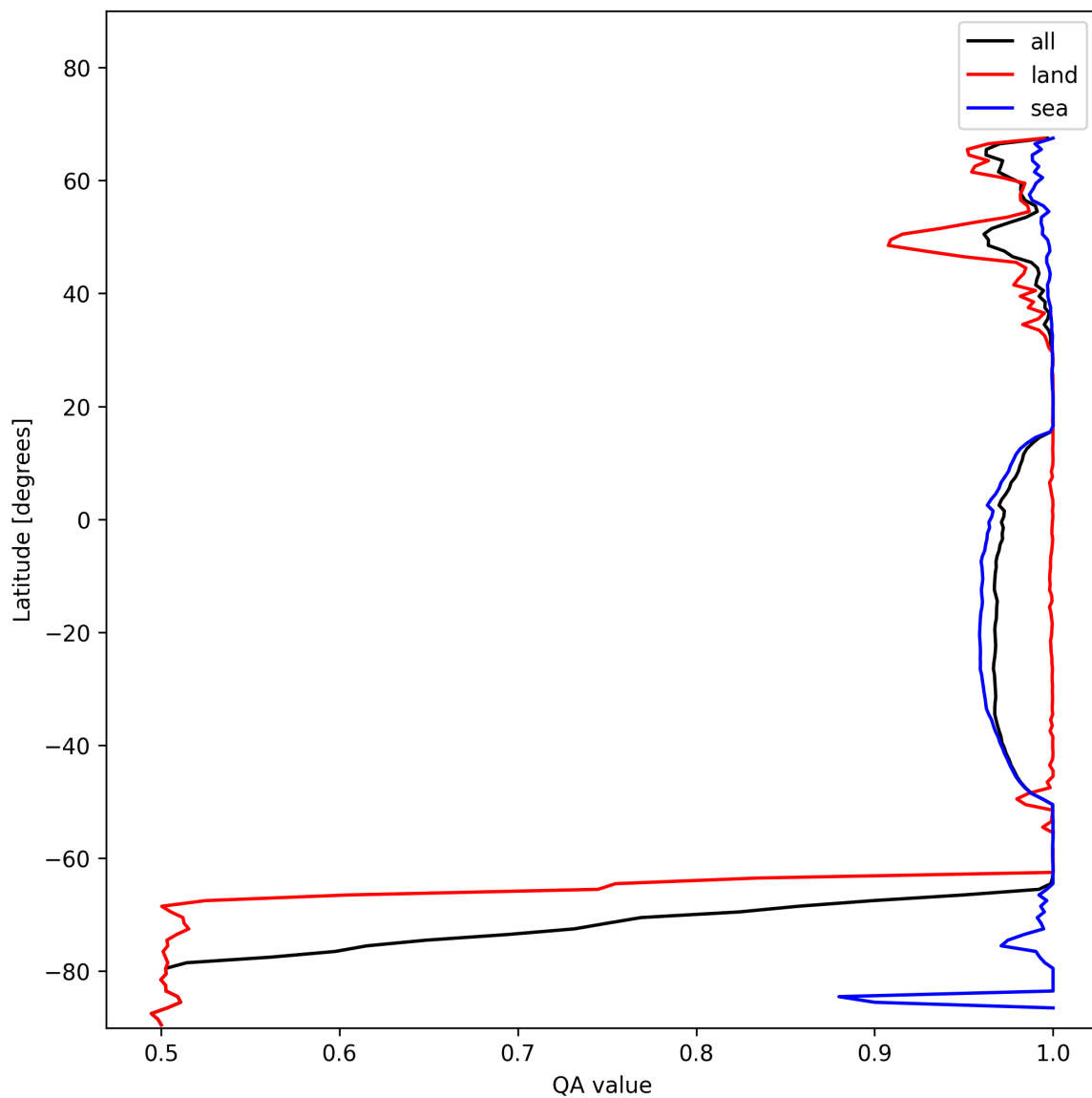


Figure 12: Zonal average of “QA value” for 2025-01-14 to 2025-01-16.

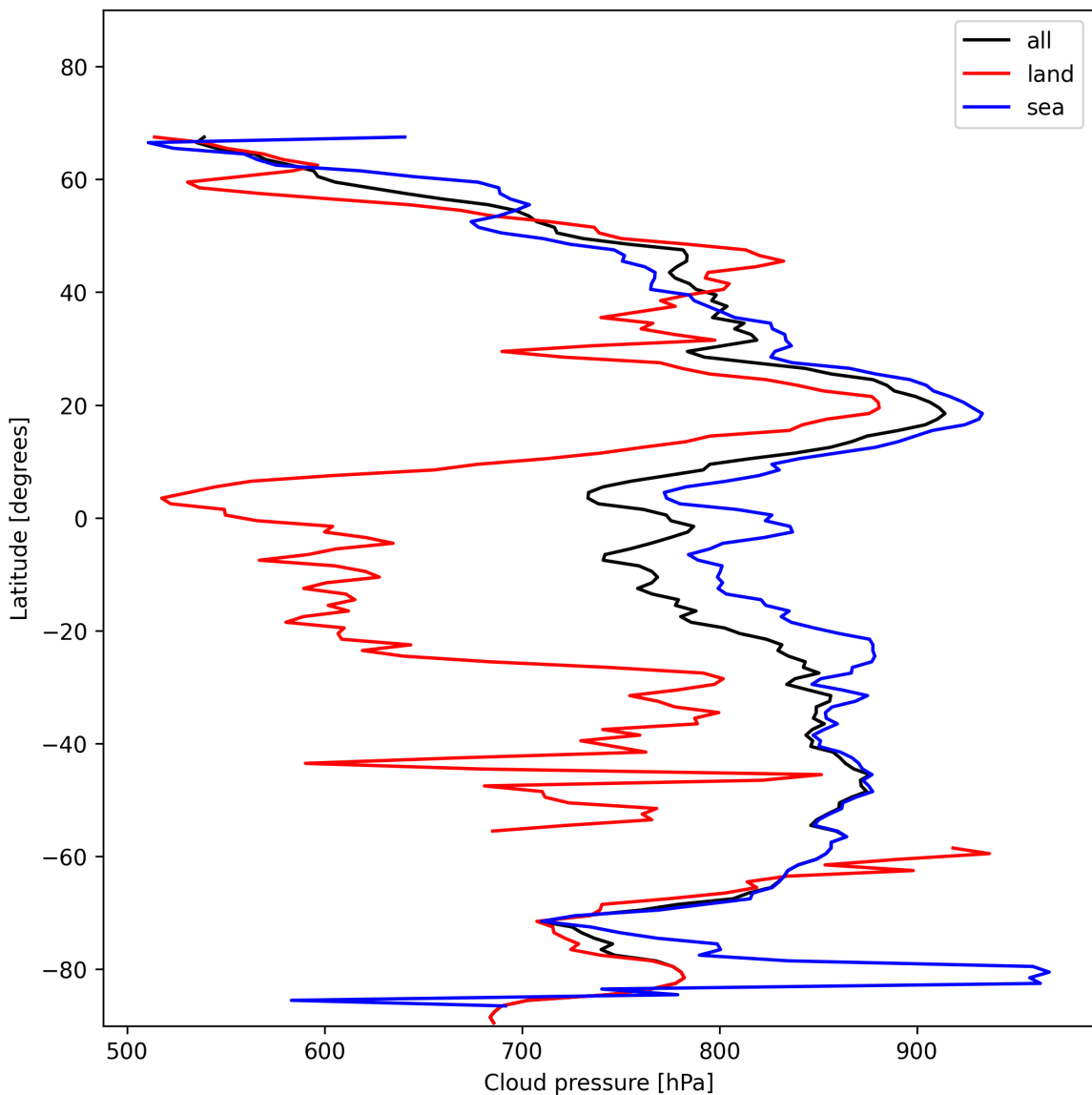


Figure 13: Zonal average of “Cloud pressure” for 2025-01-14 to 2025-01-16.

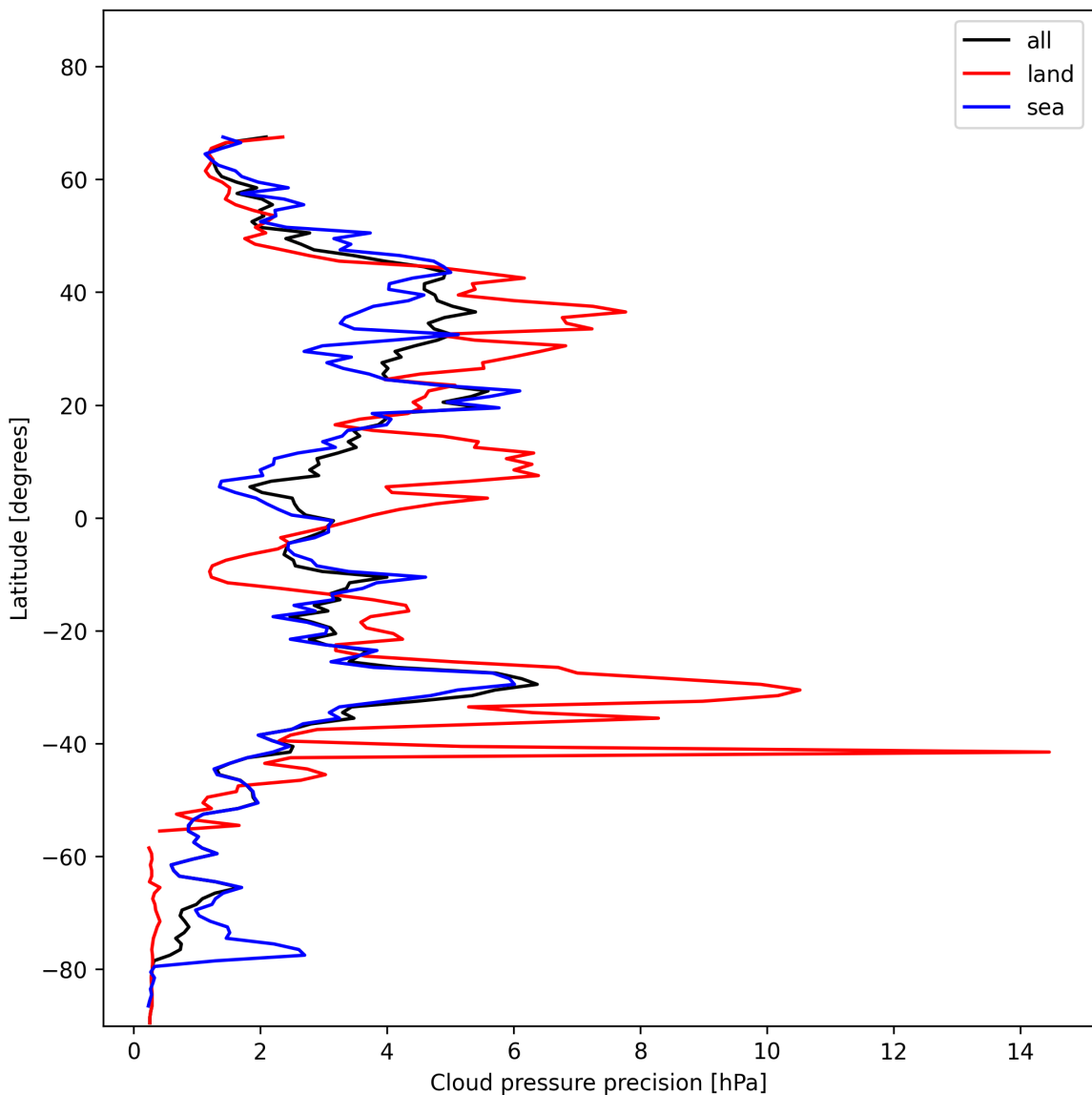


Figure 14: Zonal average of “Cloud pressure precision” for 2025-01-14 to 2025-01-16.

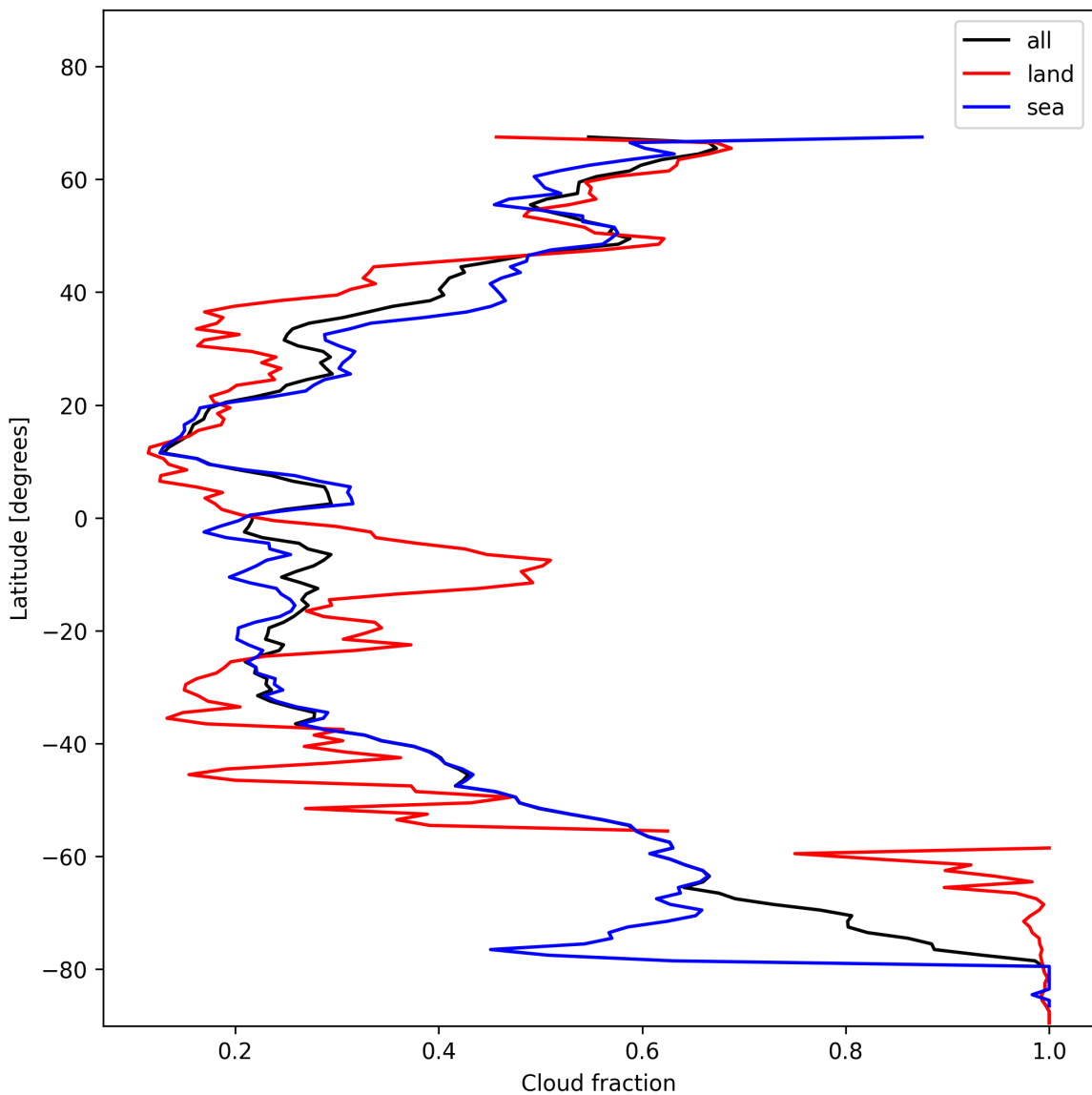


Figure 15: Zonal average of “Cloud fraction” for 2025-01-14 to 2025-01-16.

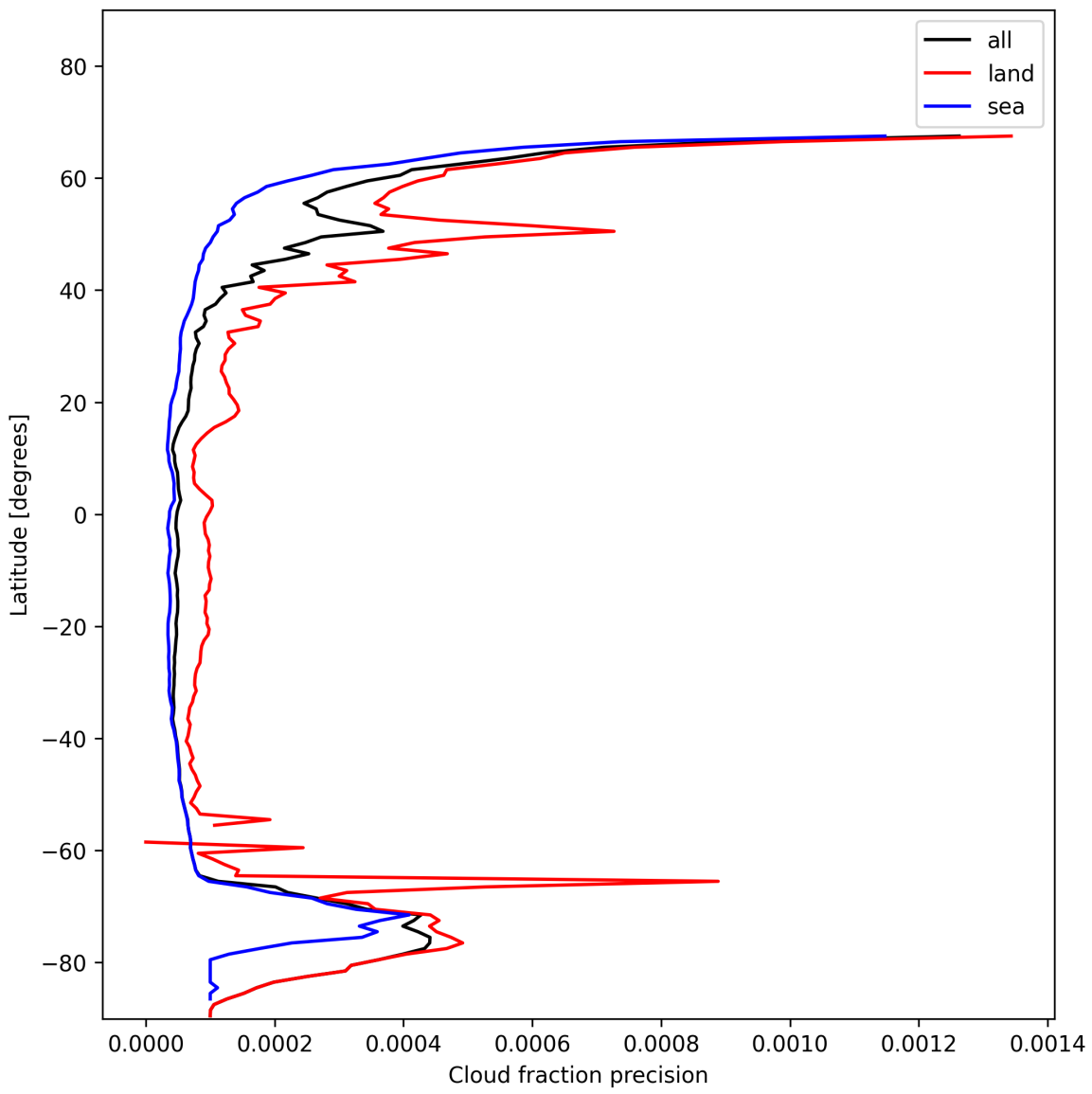


Figure 16: Zonal average of “Cloud fraction precision” for 2025-01-14 to 2025-01-16.

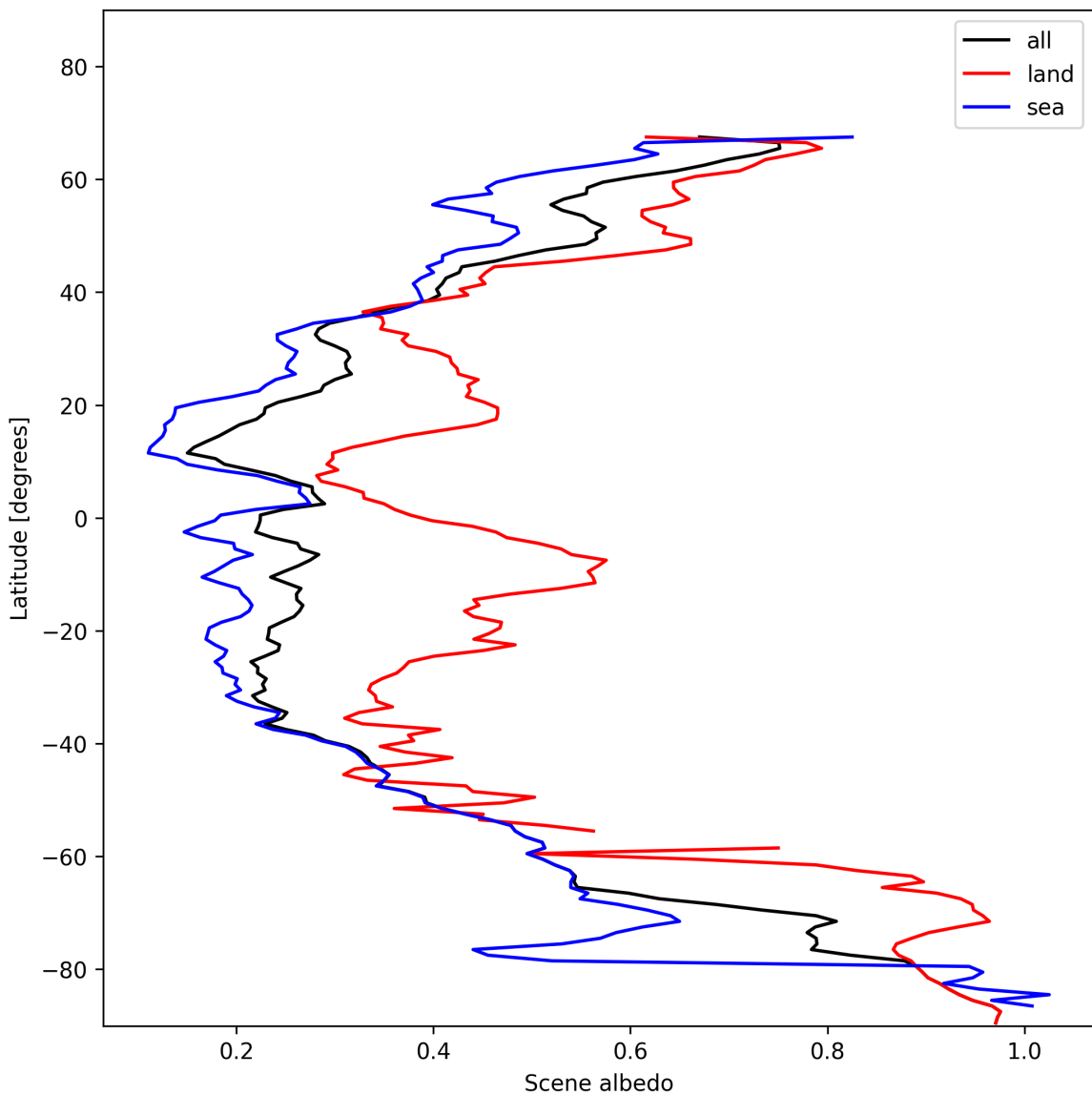


Figure 17: Zonal average of “Scene albedo” for 2025-01-14 to 2025-01-16.

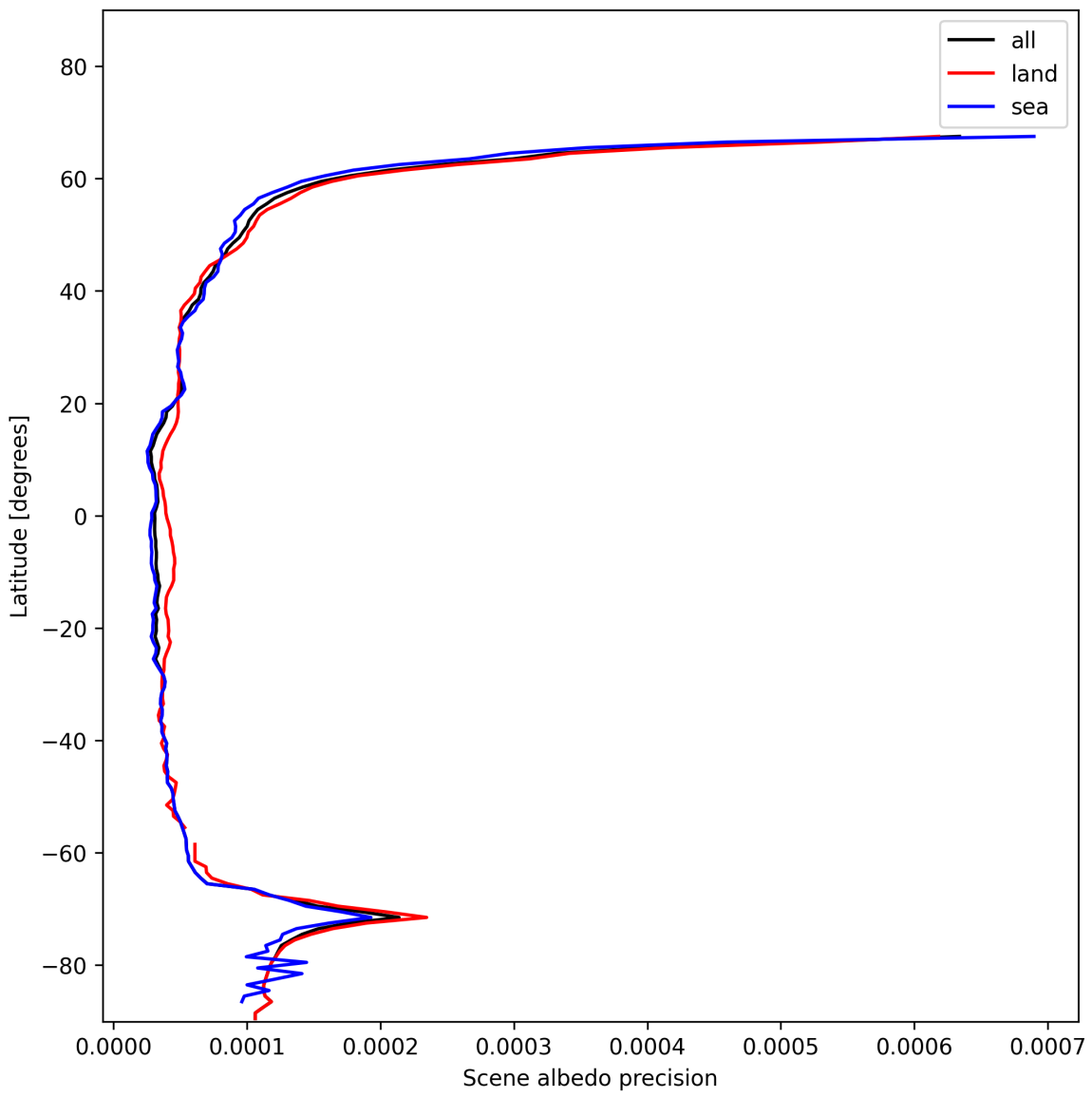


Figure 18: Zonal average of “Scene albedo precision” for 2025-01-14 to 2025-01-16.

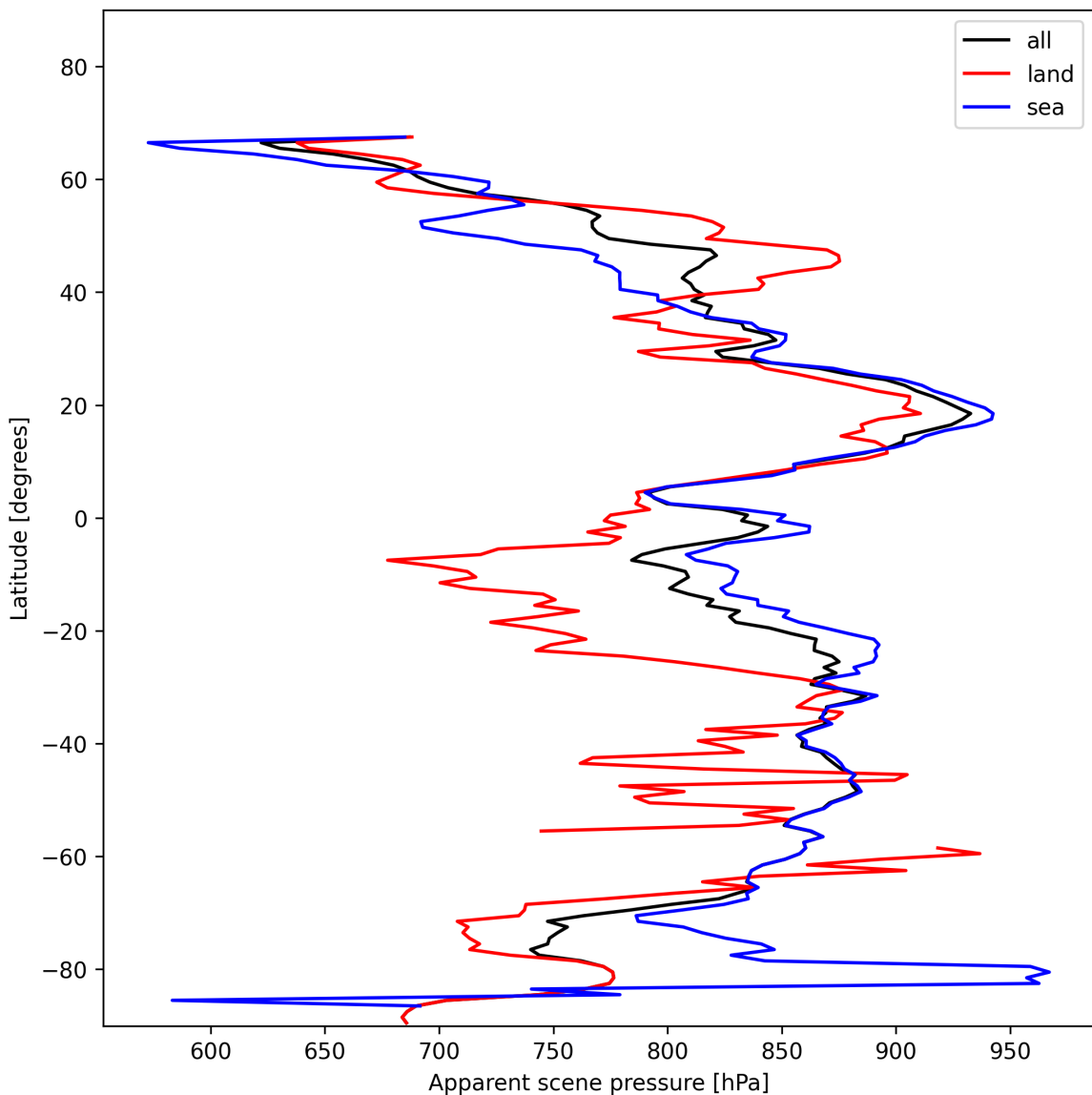


Figure 19: Zonal average of “Apparent scene pressure” for 2025-01-14 to 2025-01-16.

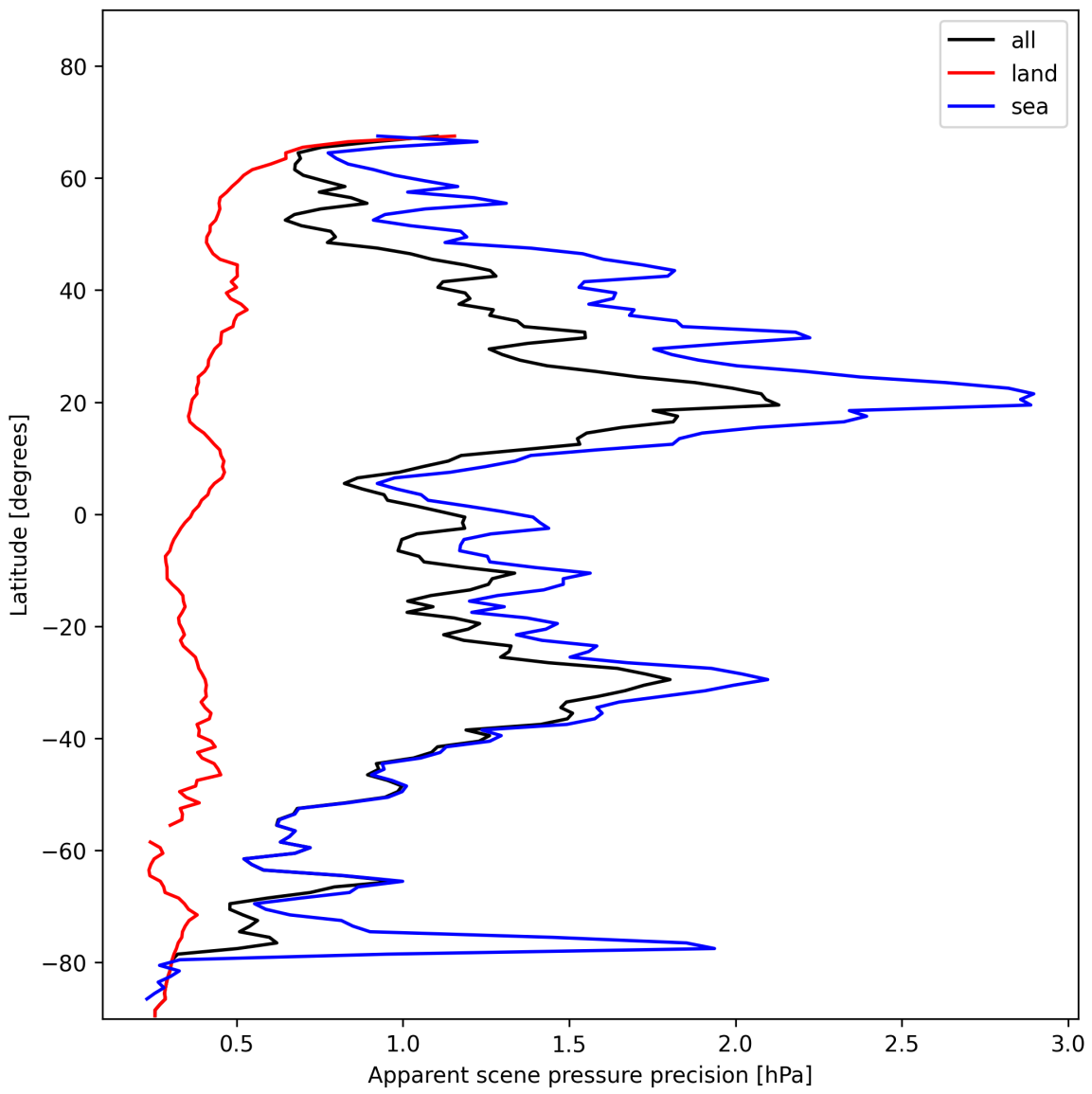


Figure 20: Zonal average of “Apparent scene pressure precision” for 2025-01-14 to 2025-01-16.

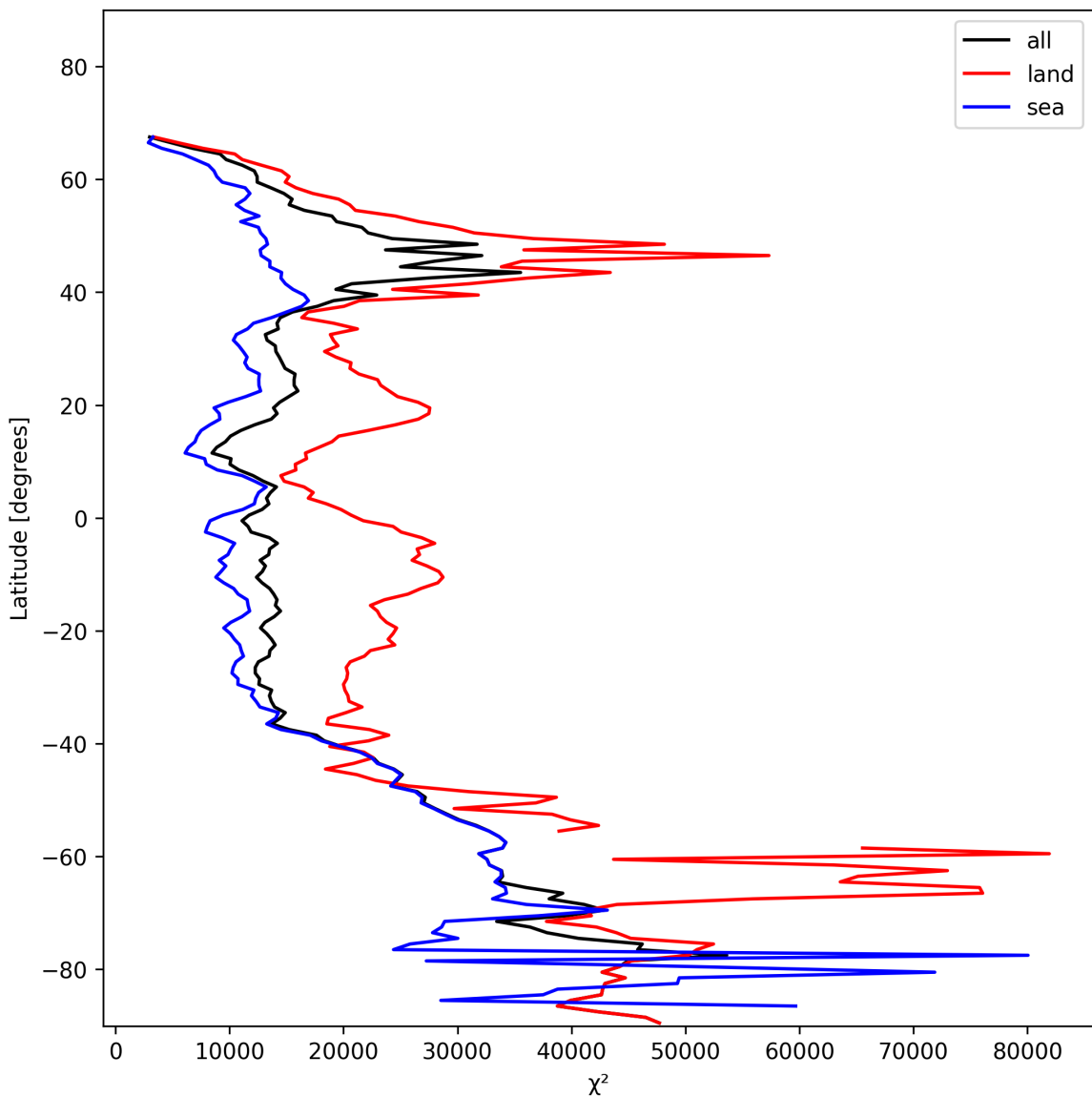


Figure 21: Zonal average of “ χ^2 ” for 2025-01-14 to 2025-01-16.

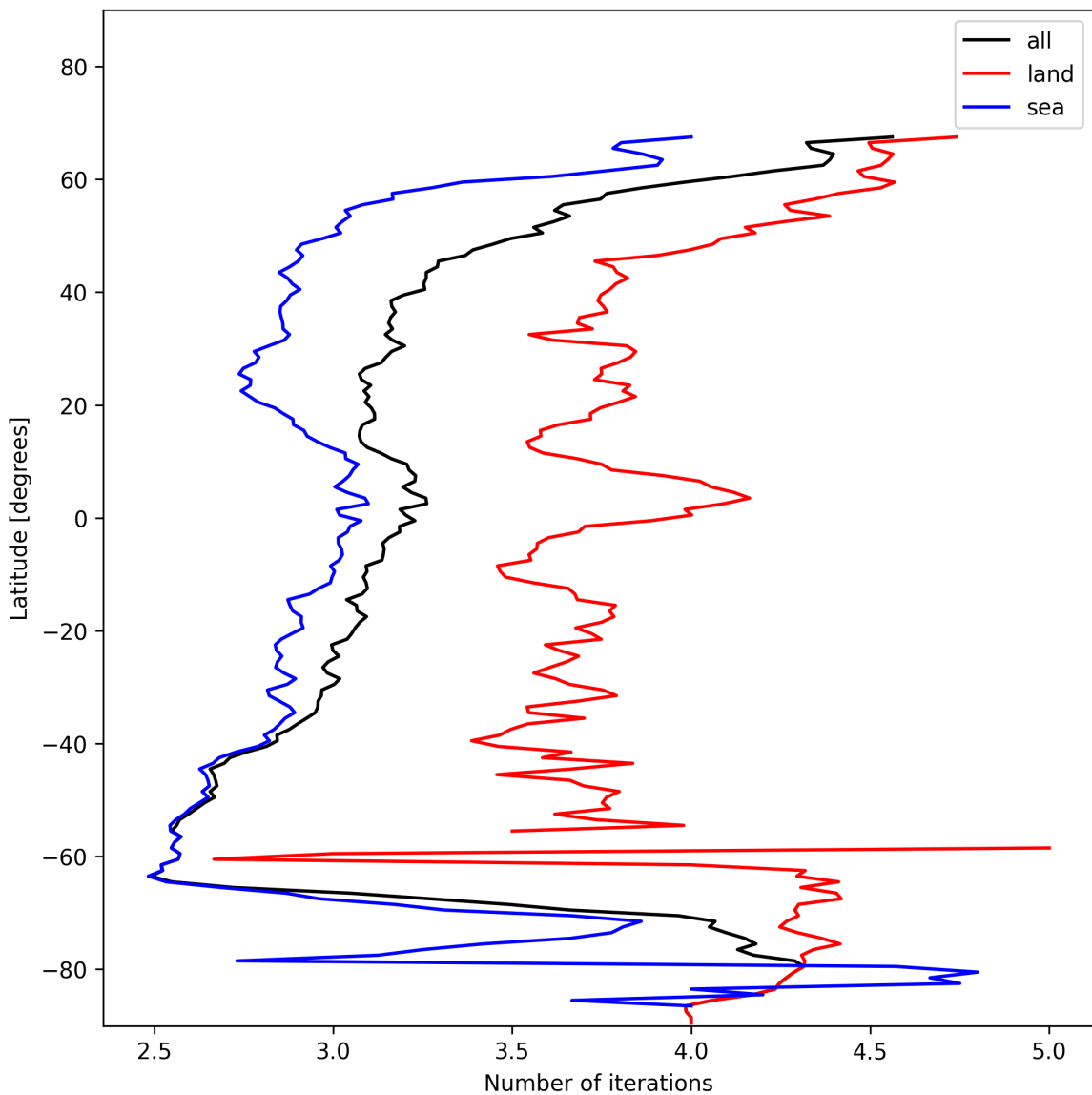


Figure 22: Zonal average of “Number of iterations” for 2025-01-14 to 2025-01-16.

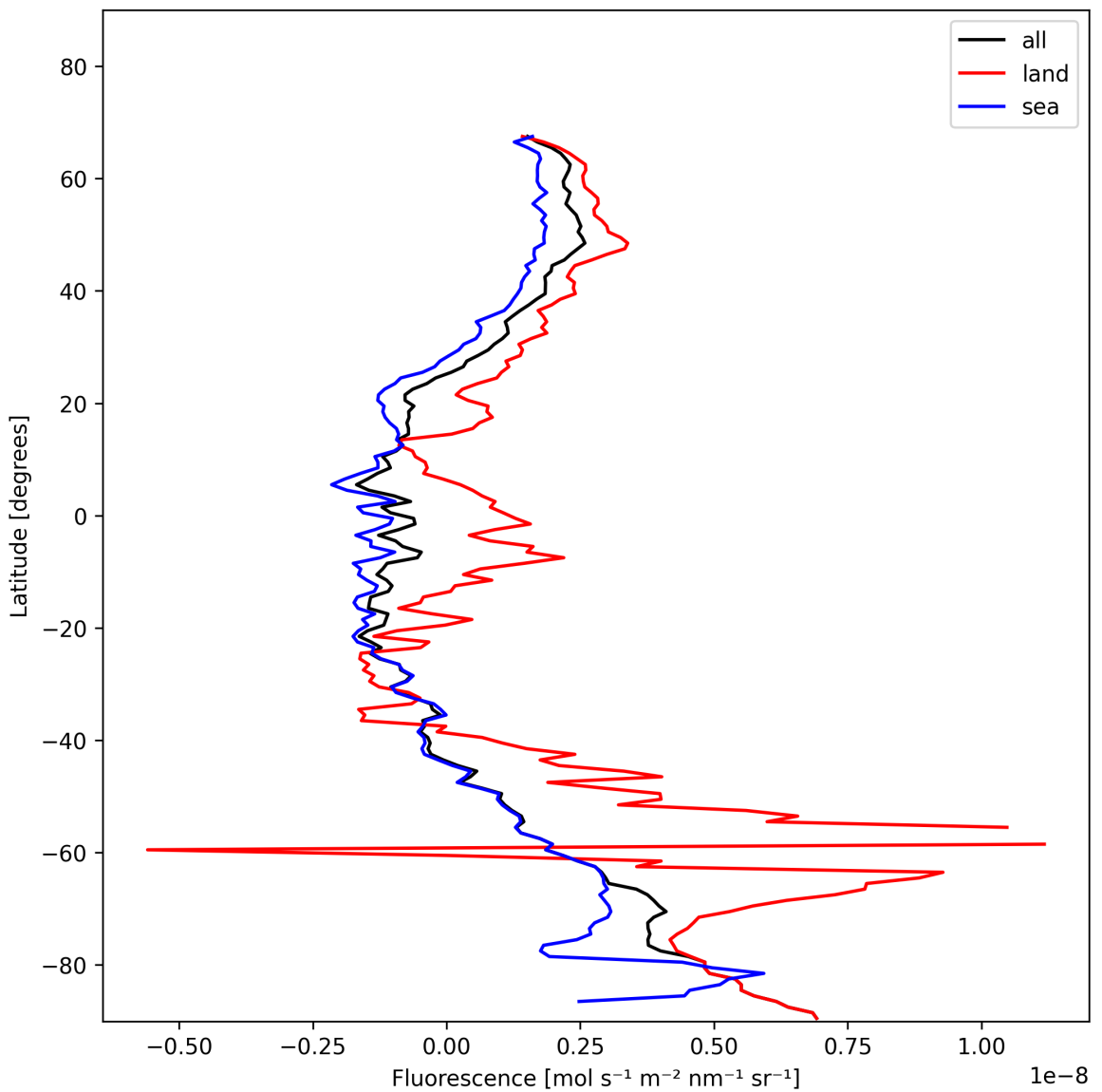


Figure 23: Zonal average of “Fluorescence” for 2025-01-14 to 2025-01-16.

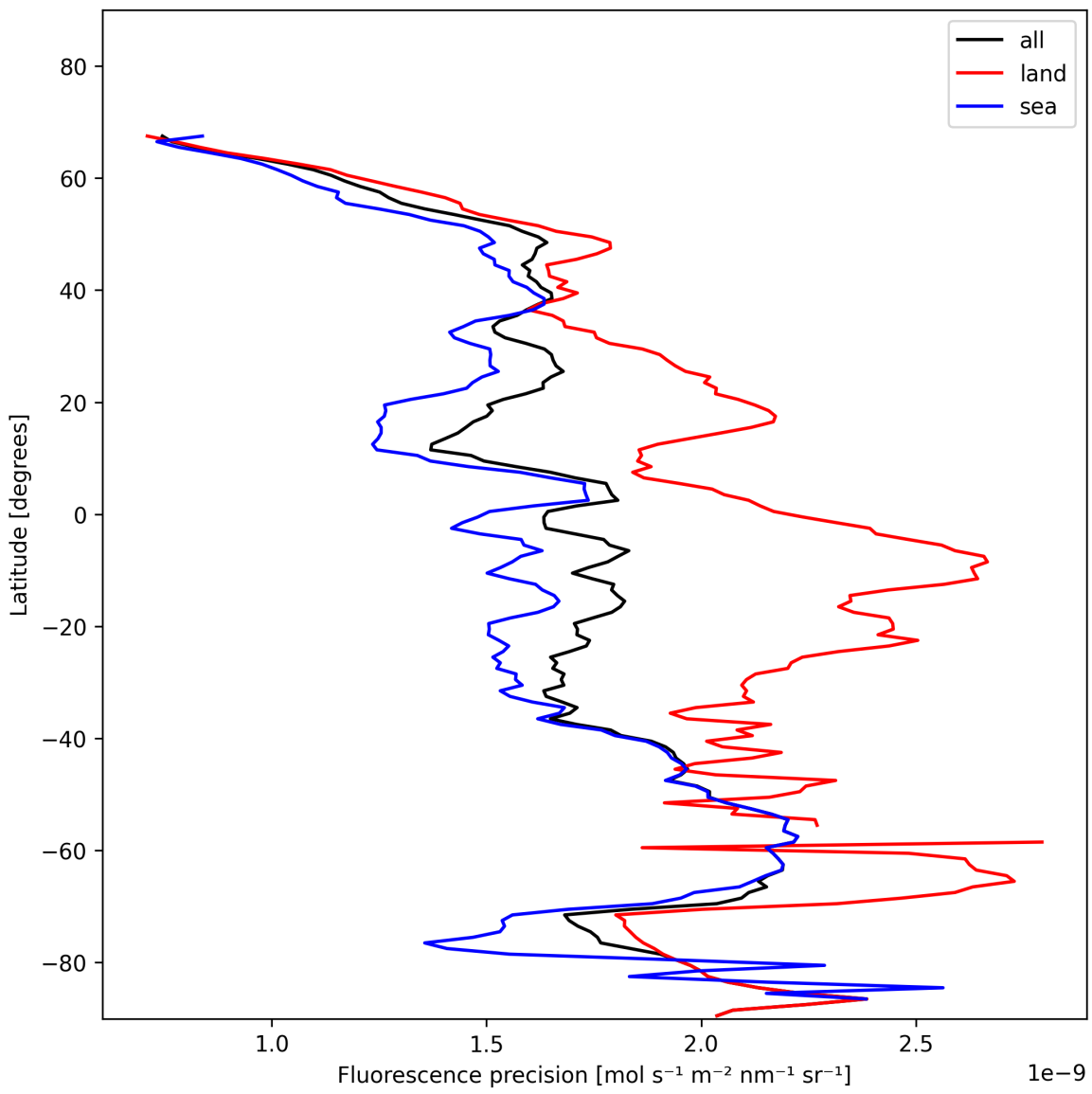


Figure 24: Zonal average of “Fluorescence precision” for 2025-01-14 to 2025-01-16.

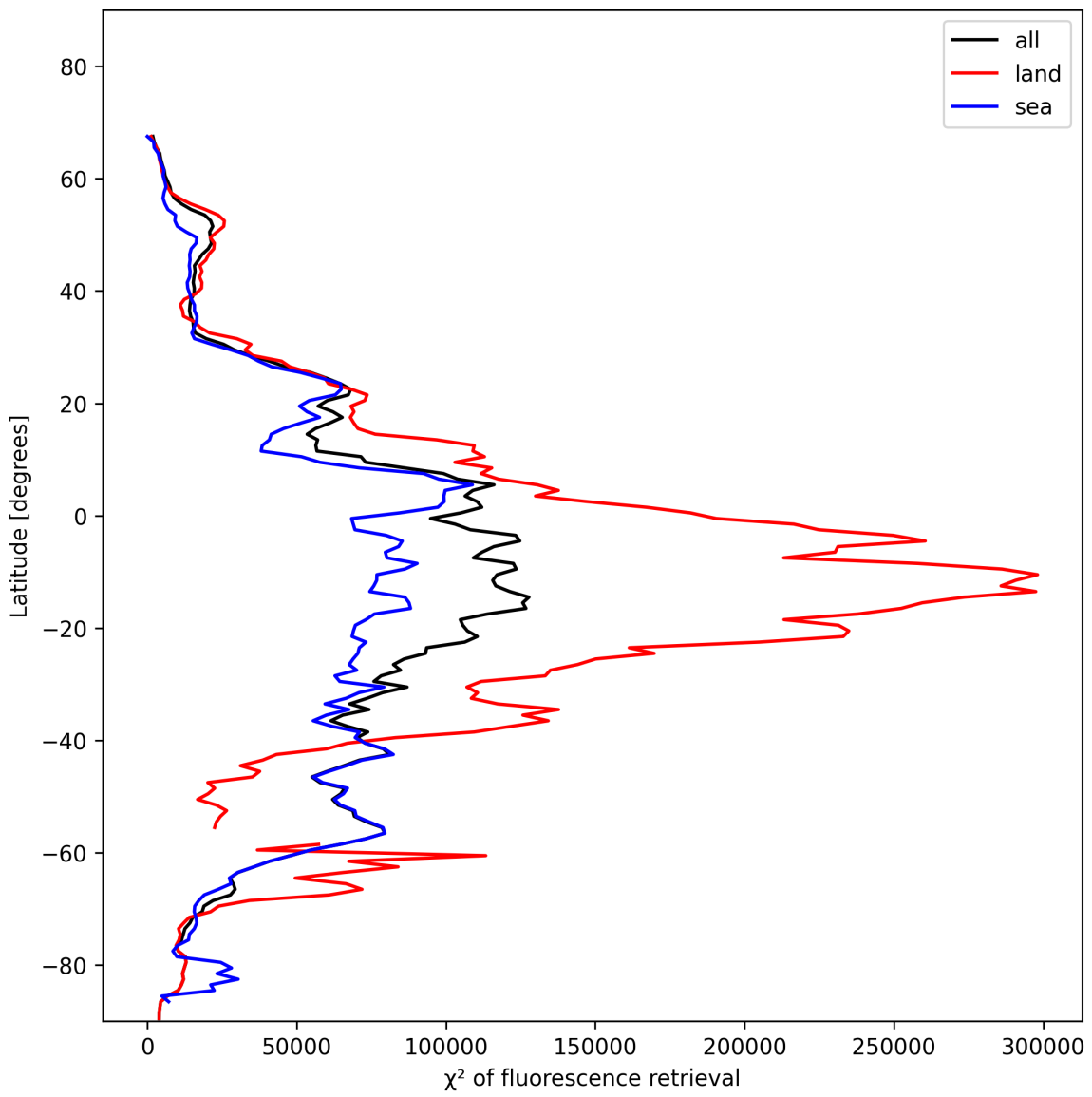


Figure 25: Zonal average of “ χ^2 of fluorescence retrieval” for 2025-01-14 to 2025-01-16.

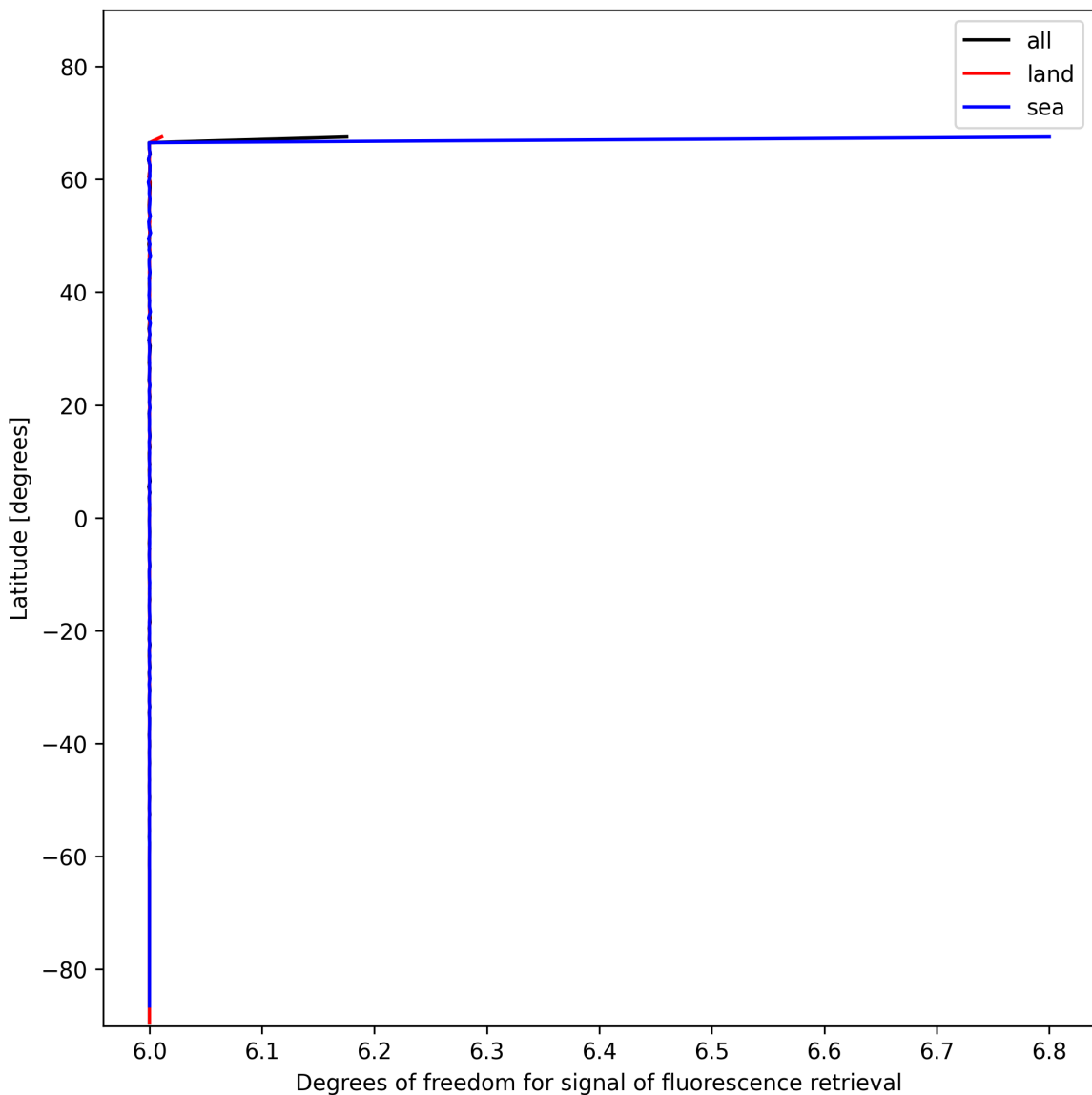


Figure 26: Zonal average of “Degrees of freedom for signal of fluorescence retrieval” for 2025-01-14 to 2025-01-16.

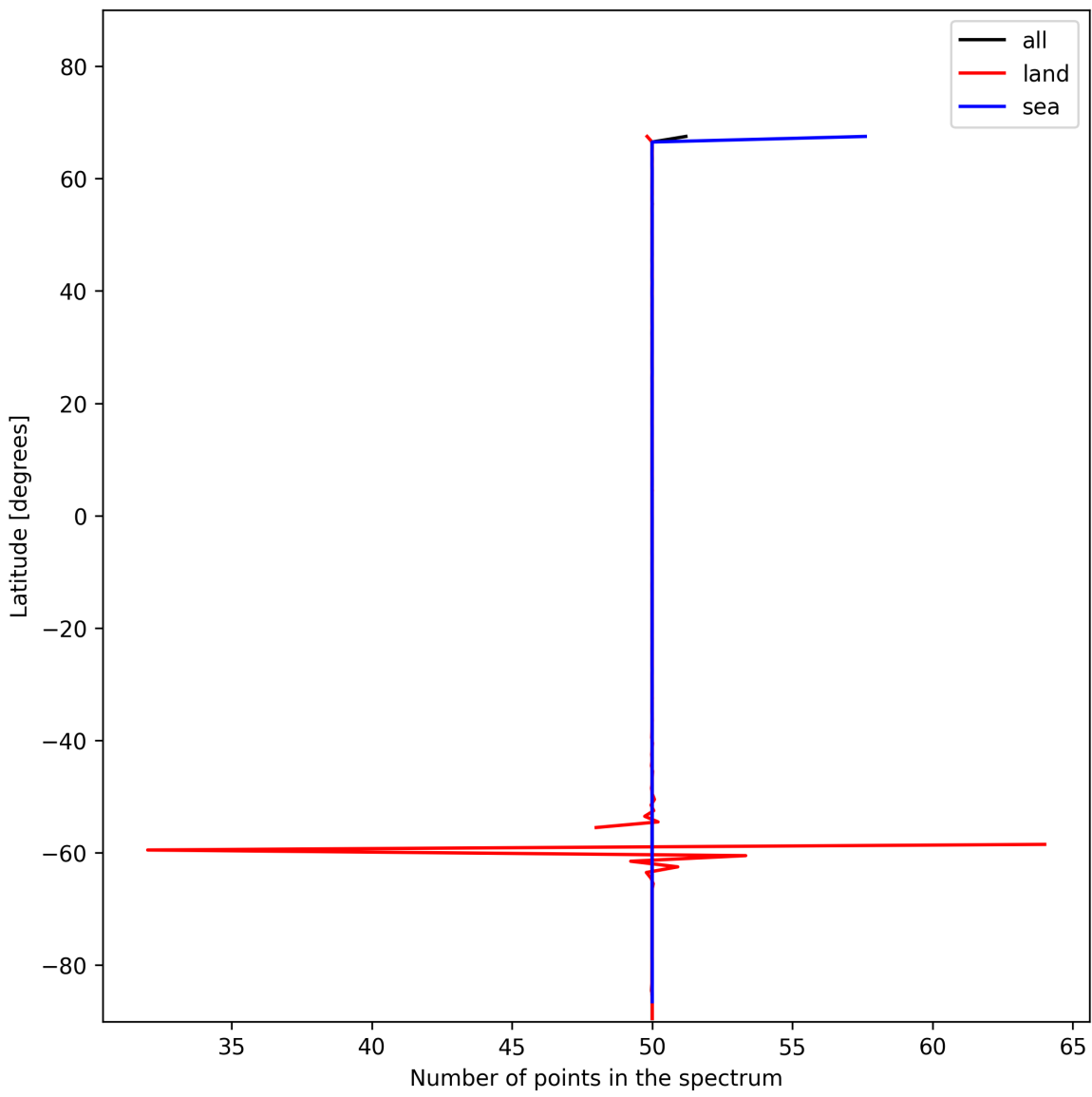


Figure 27: Zonal average of “Number of points in the spectrum” for 2025-01-14 to 2025-01-16.

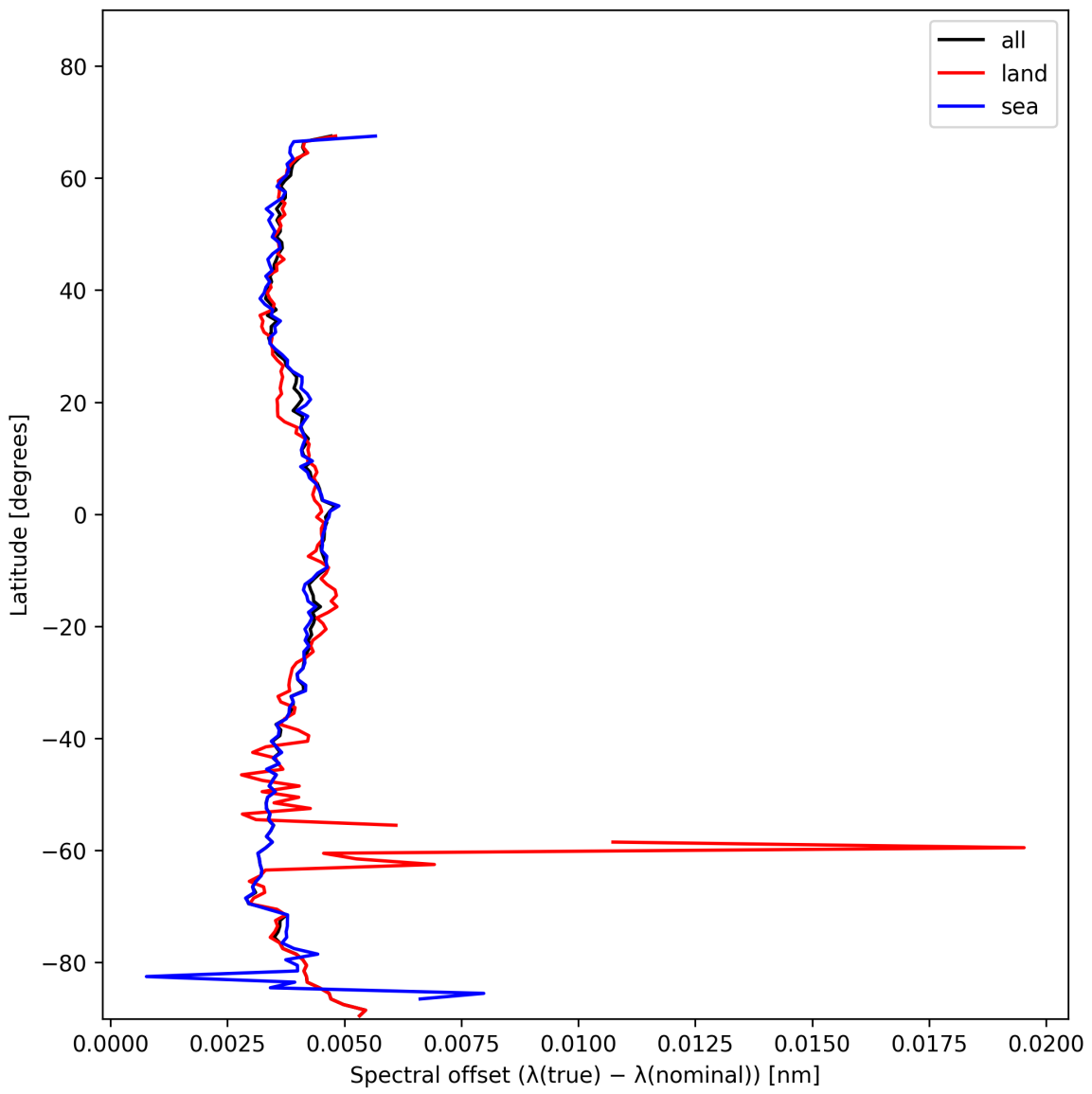


Figure 28: Zonal average of “Spectral offset ($\lambda_{\text{true}} - \lambda_{\text{nominal}}$)” for 2025-01-14 to 2025-01-16.

8 Histograms

The definitions of the parameters given in this section can be found in section 2.

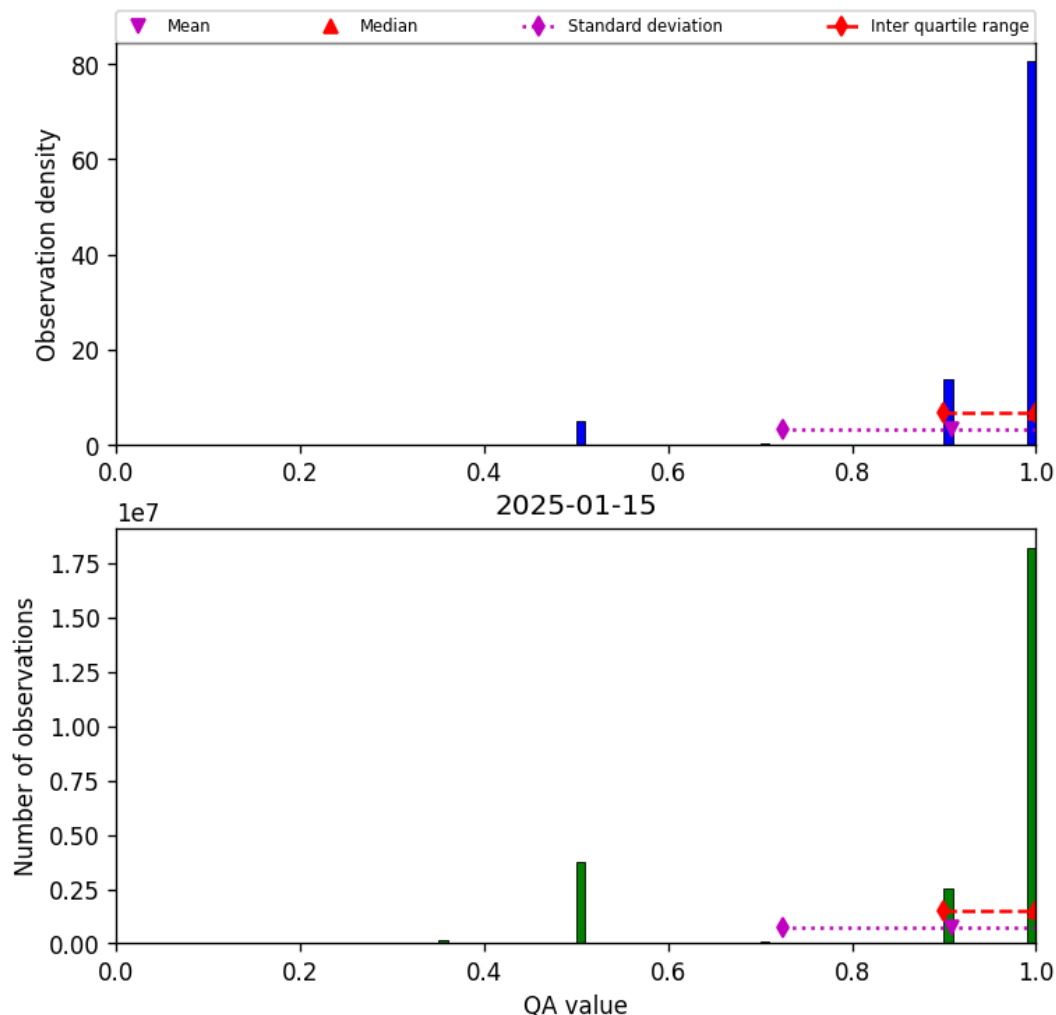


Figure 29: Histogram of “QA value” for 2025-01-14 to 2025-01-16

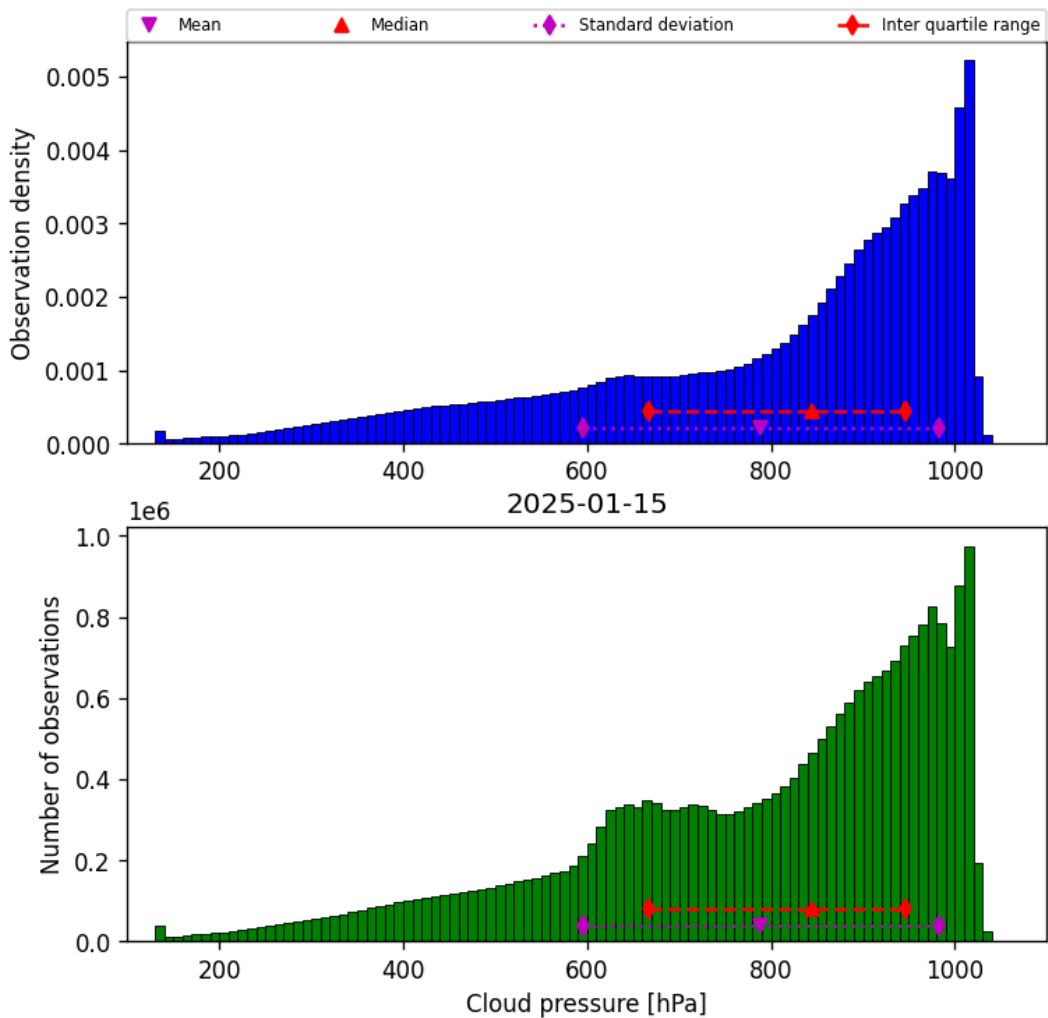


Figure 30: Histogram of “Cloud pressure” for 2025-01-14 to 2025-01-16

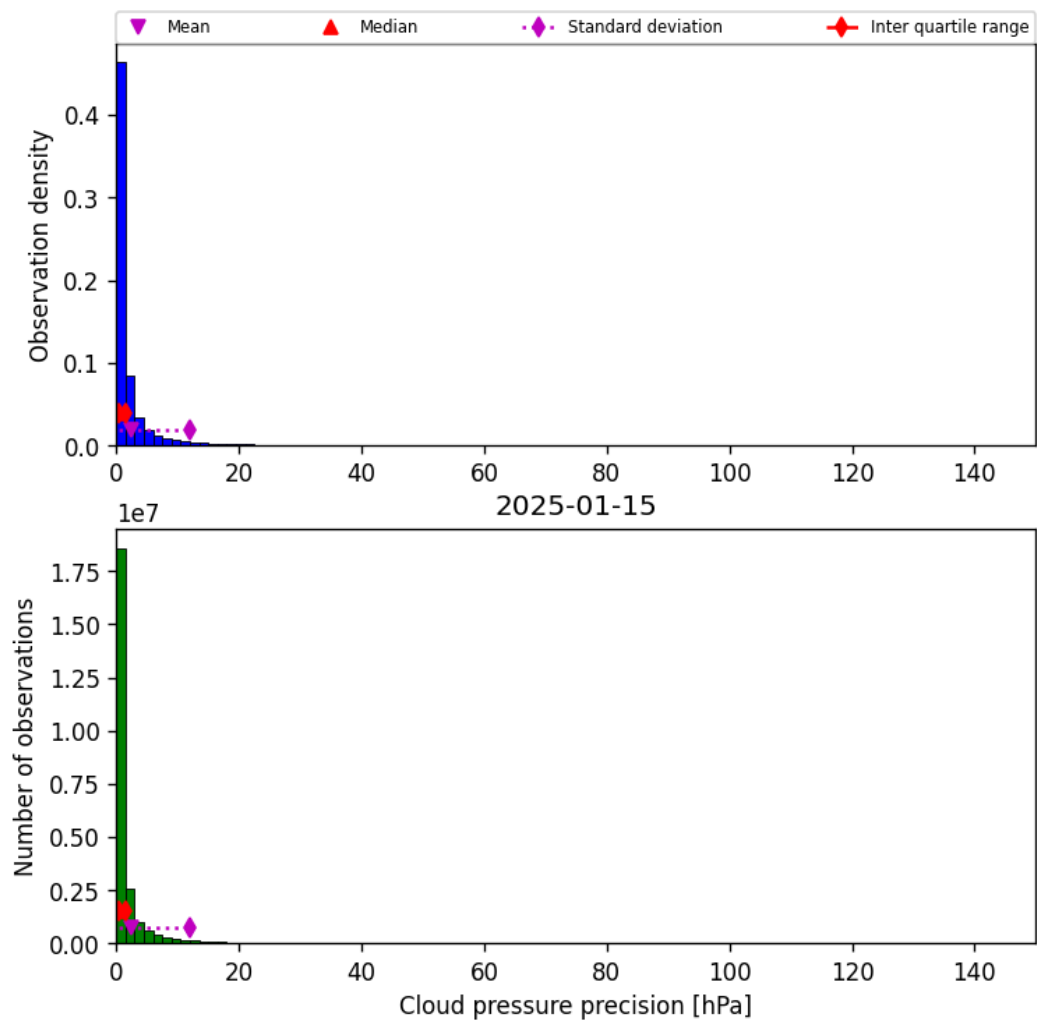


Figure 31: Histogram of “Cloud pressure precision” for 2025-01-14 to 2025-01-16

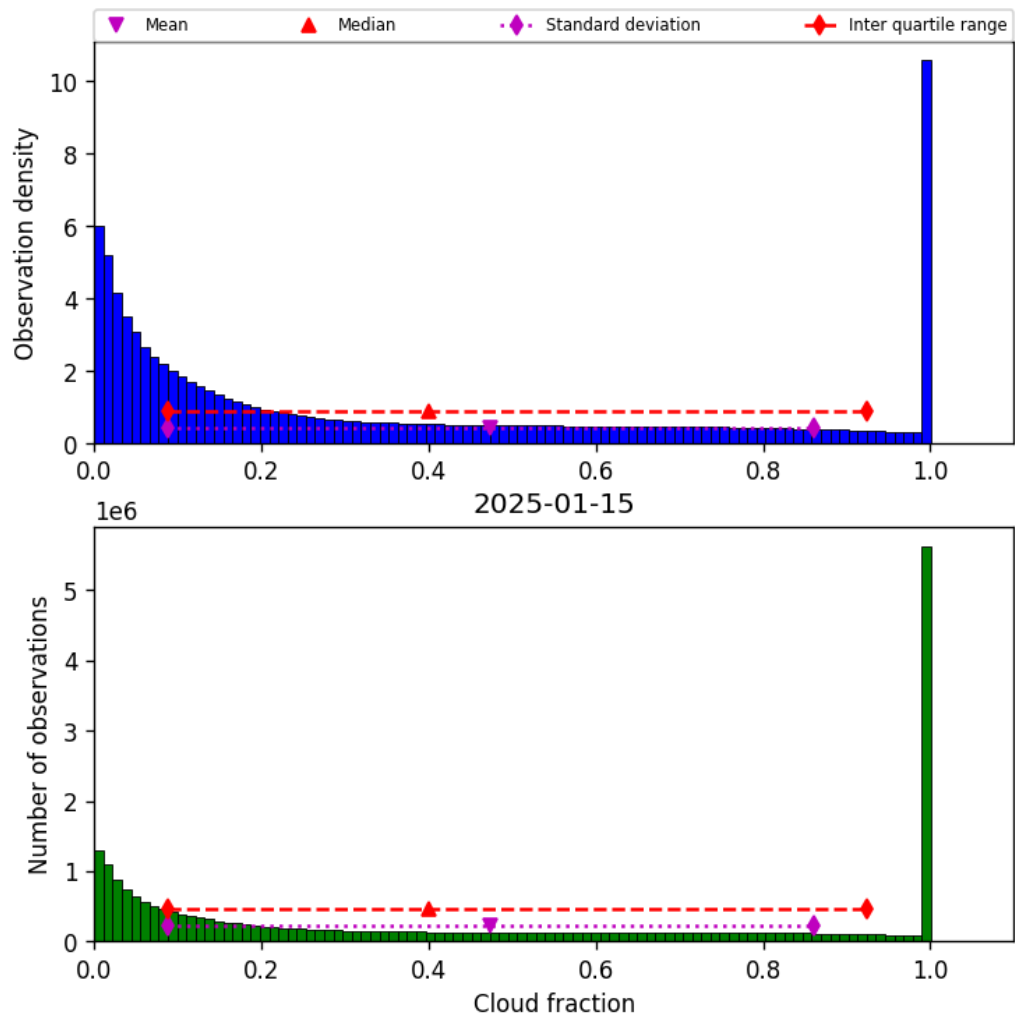


Figure 32: Histogram of “Cloud fraction” for 2025-01-14 to 2025-01-16

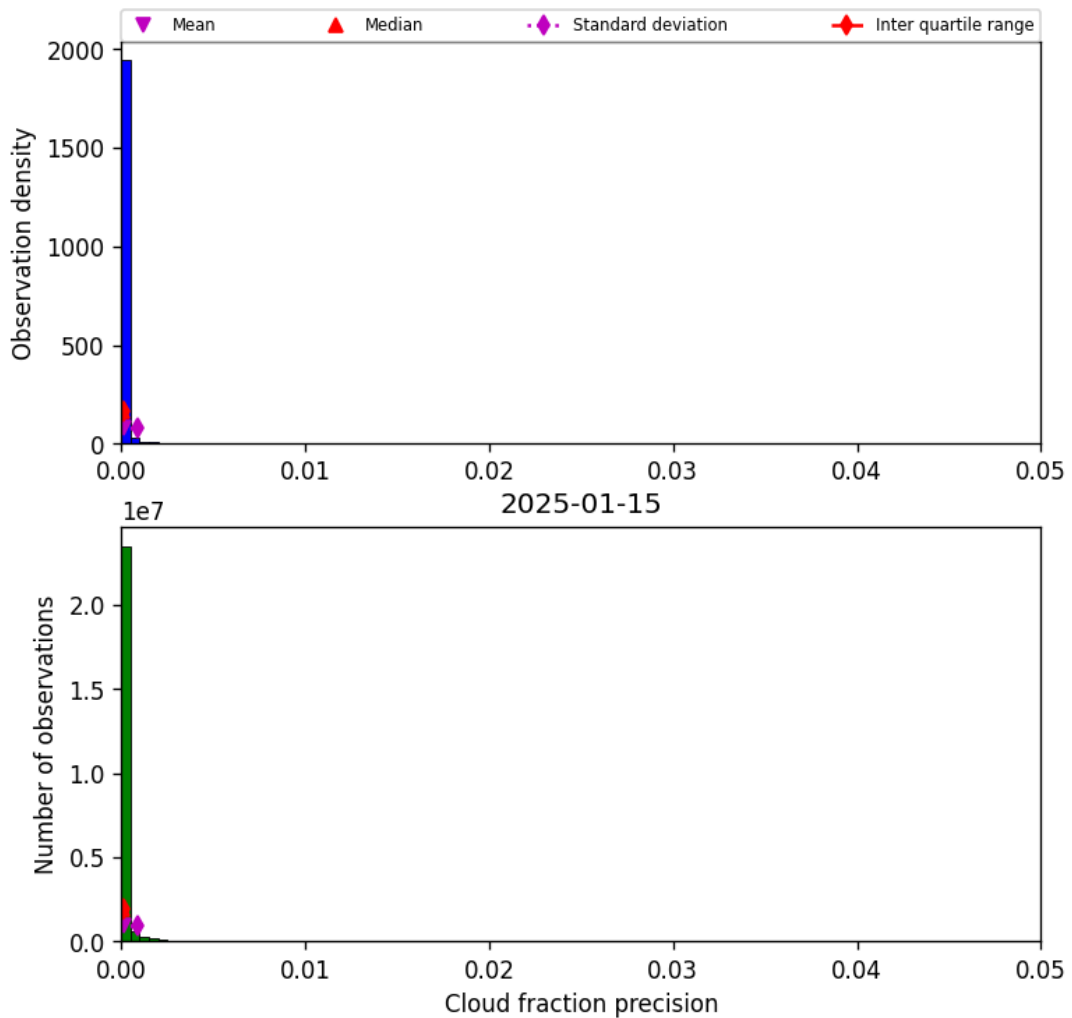


Figure 33: Histogram of “Cloud fraction precision” for 2025-01-14 to 2025-01-16

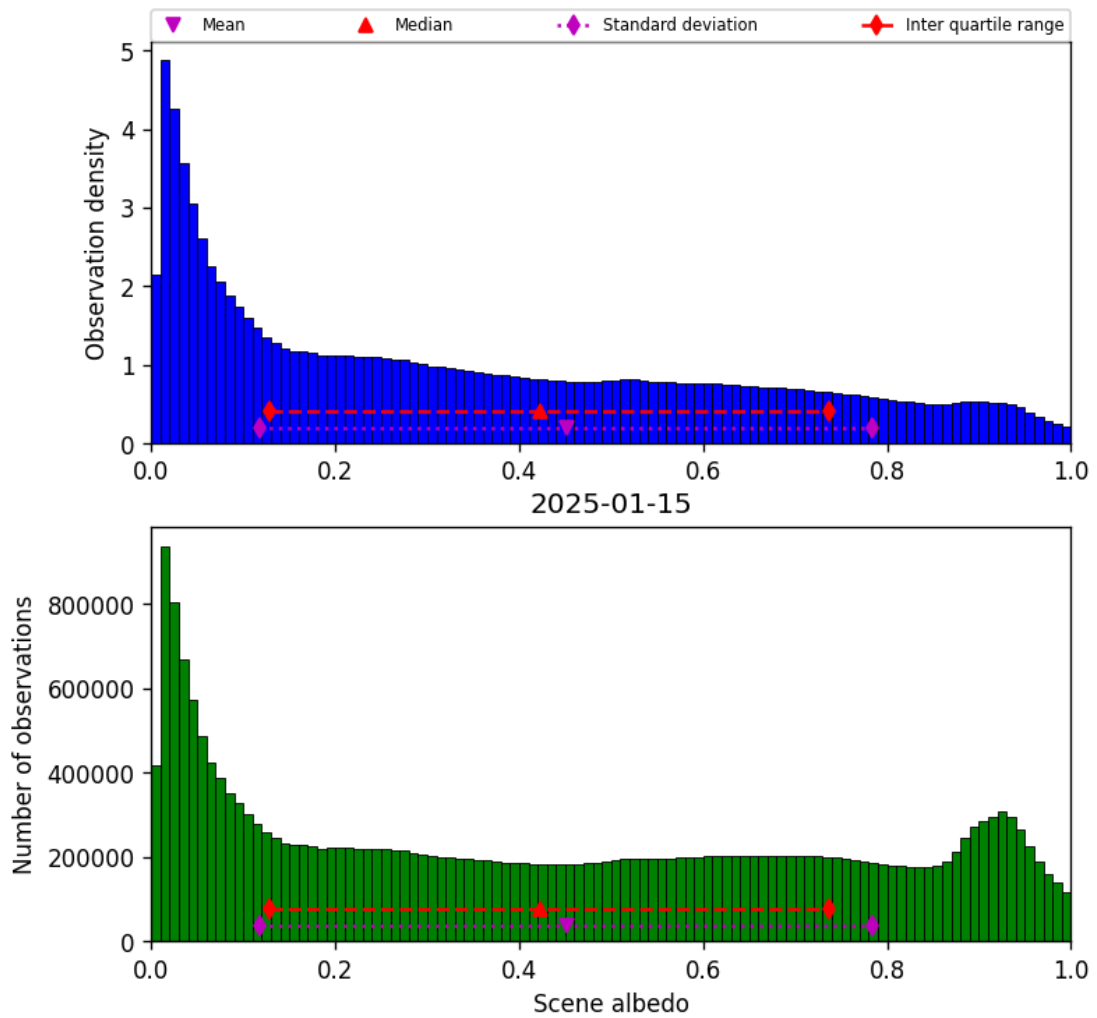


Figure 34: Histogram of “Scene albedo” for 2025-01-14 to 2025-01-16

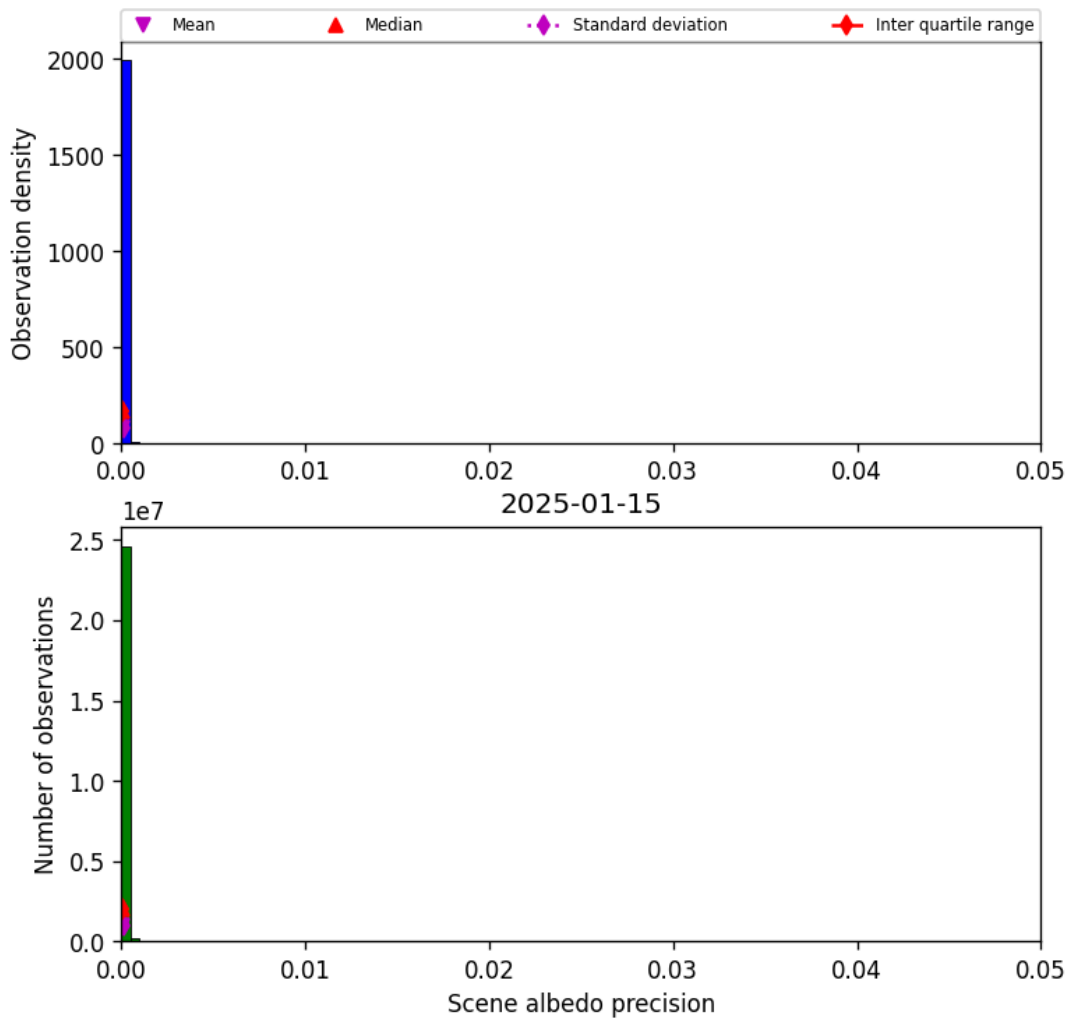


Figure 35: Histogram of “Scene albedo precision” for 2025-01-14 to 2025-01-16

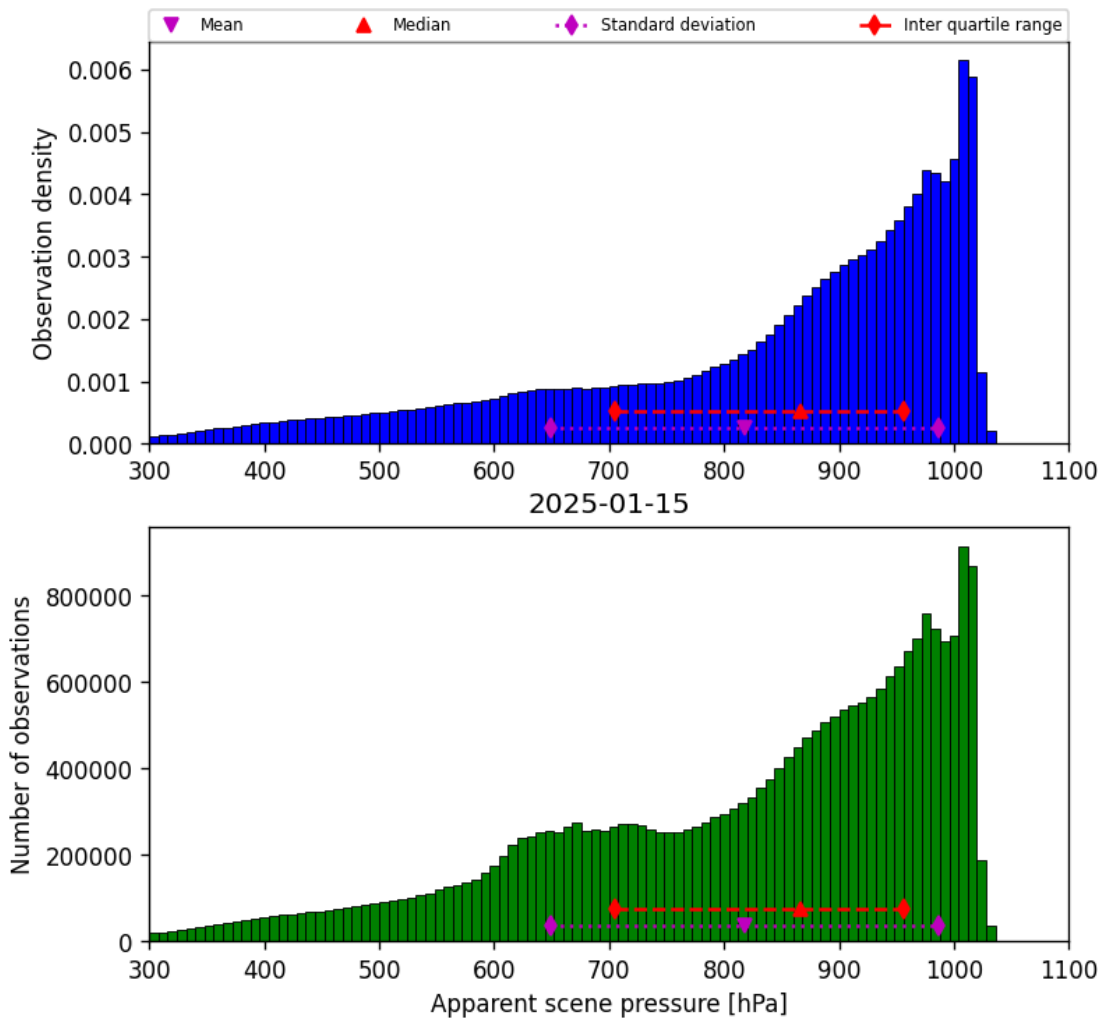


Figure 36: Histogram of “Apparent scene pressure” for 2025-01-14 to 2025-01-16

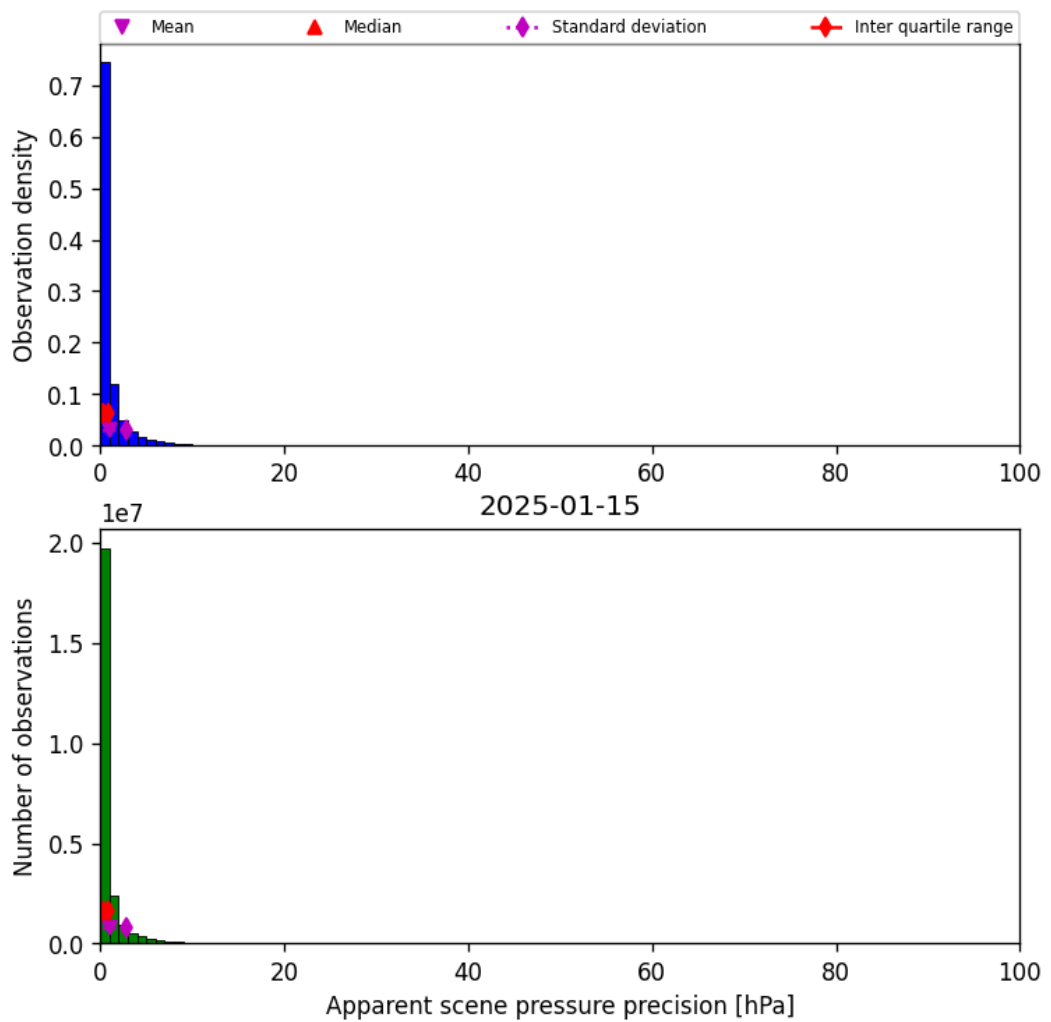


Figure 37: Histogram of “Apparent scene pressure precision” for 2025-01-14 to 2025-01-16

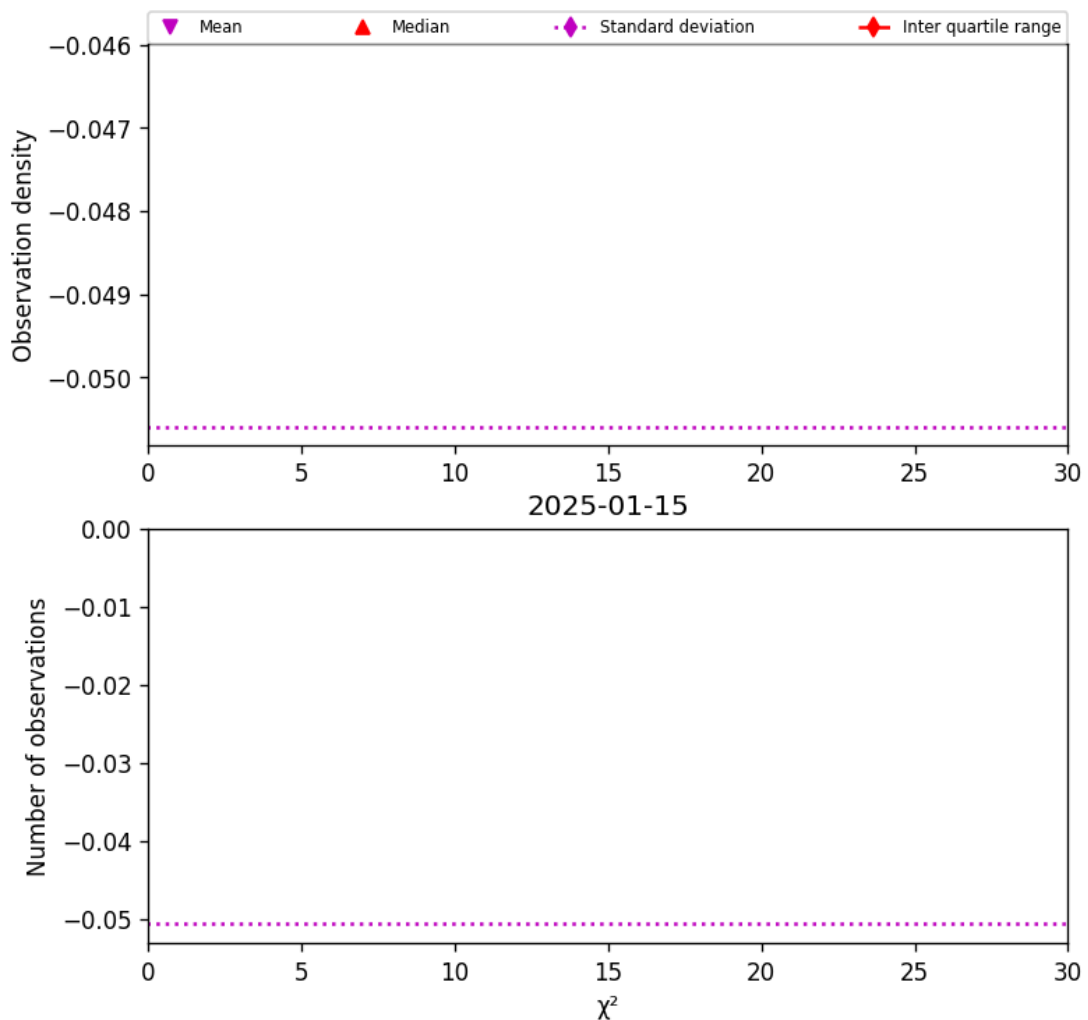


Figure 38: Histogram of " χ^2 " for 2025-01-14 to 2025-01-16

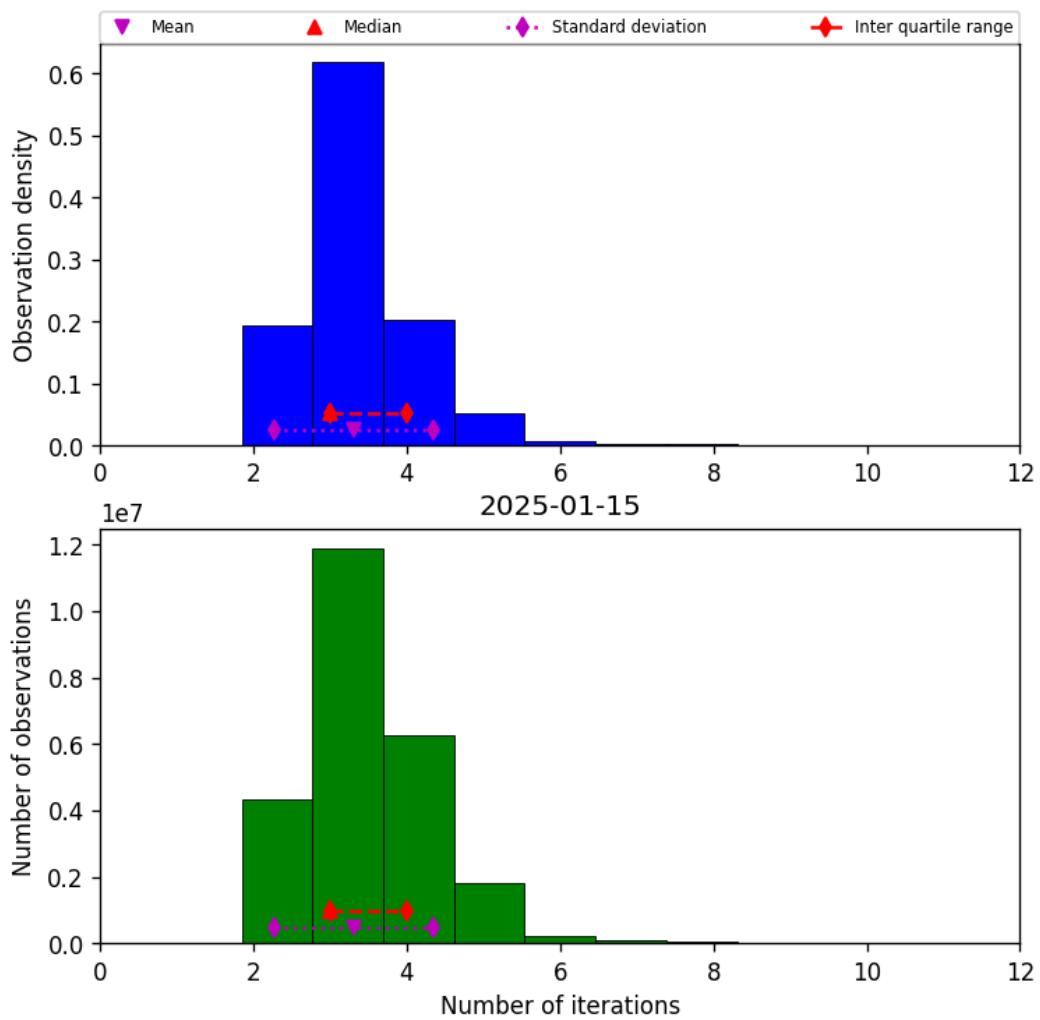


Figure 39: Histogram of “Number of iterations” for 2025-01-14 to 2025-01-16

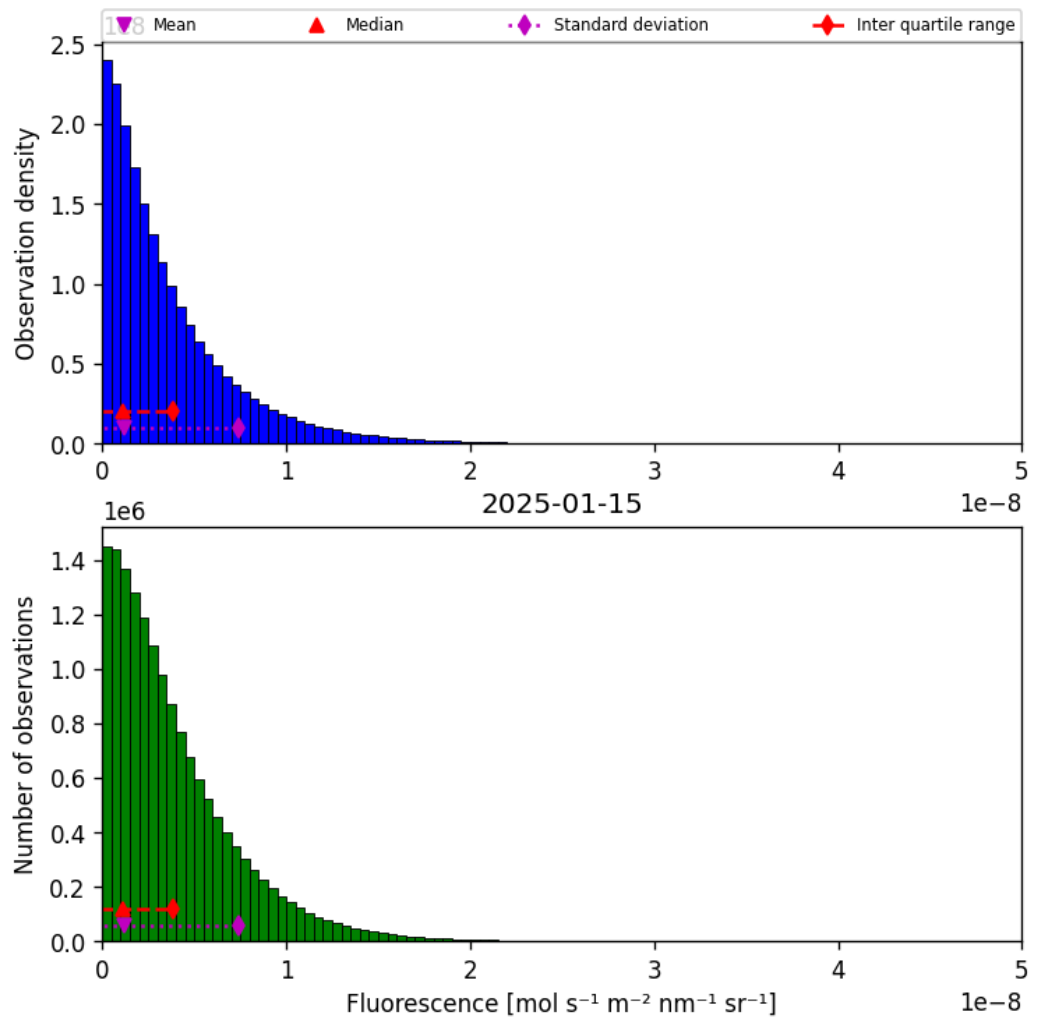


Figure 40: Histogram of “Fluorescence” for 2025-01-14 to 2025-01-16

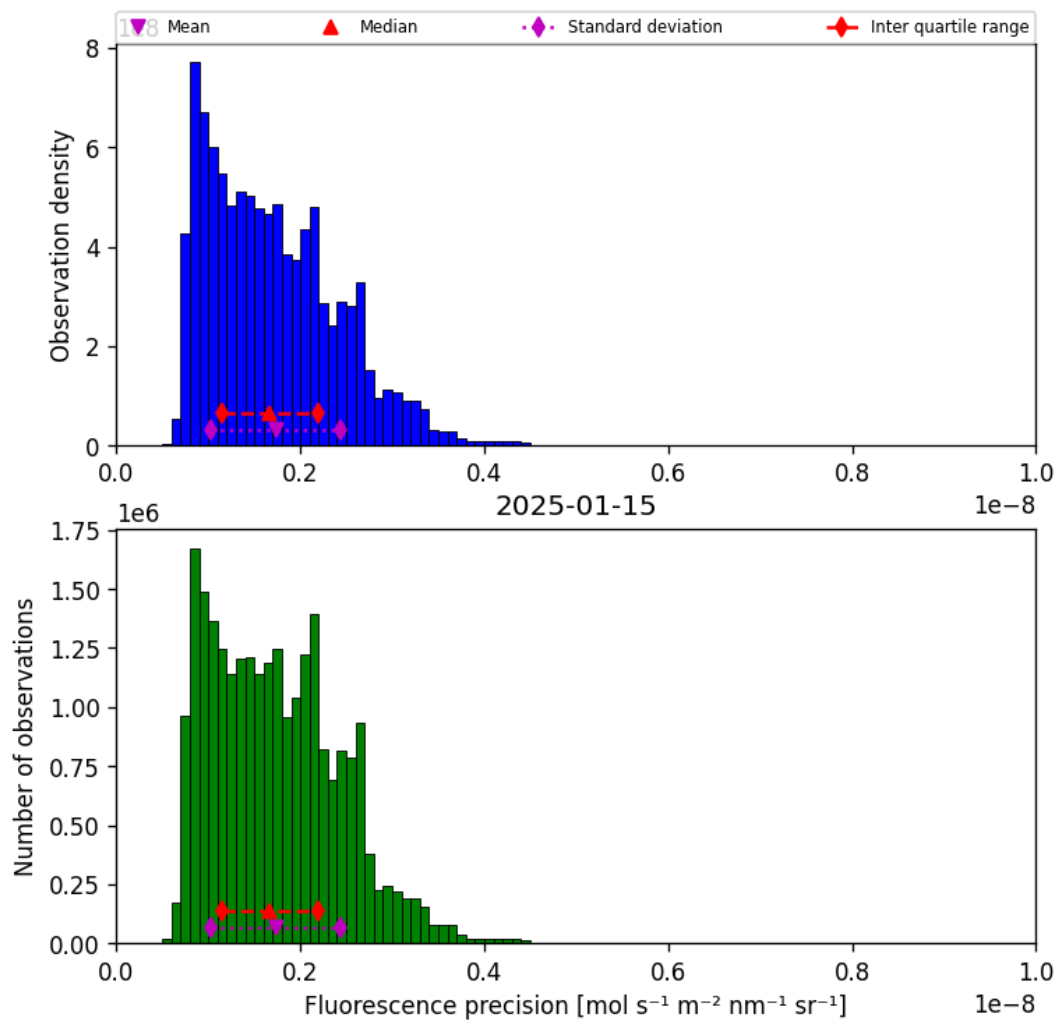


Figure 41: Histogram of “Fluorescence precision” for 2025-01-14 to 2025-01-16

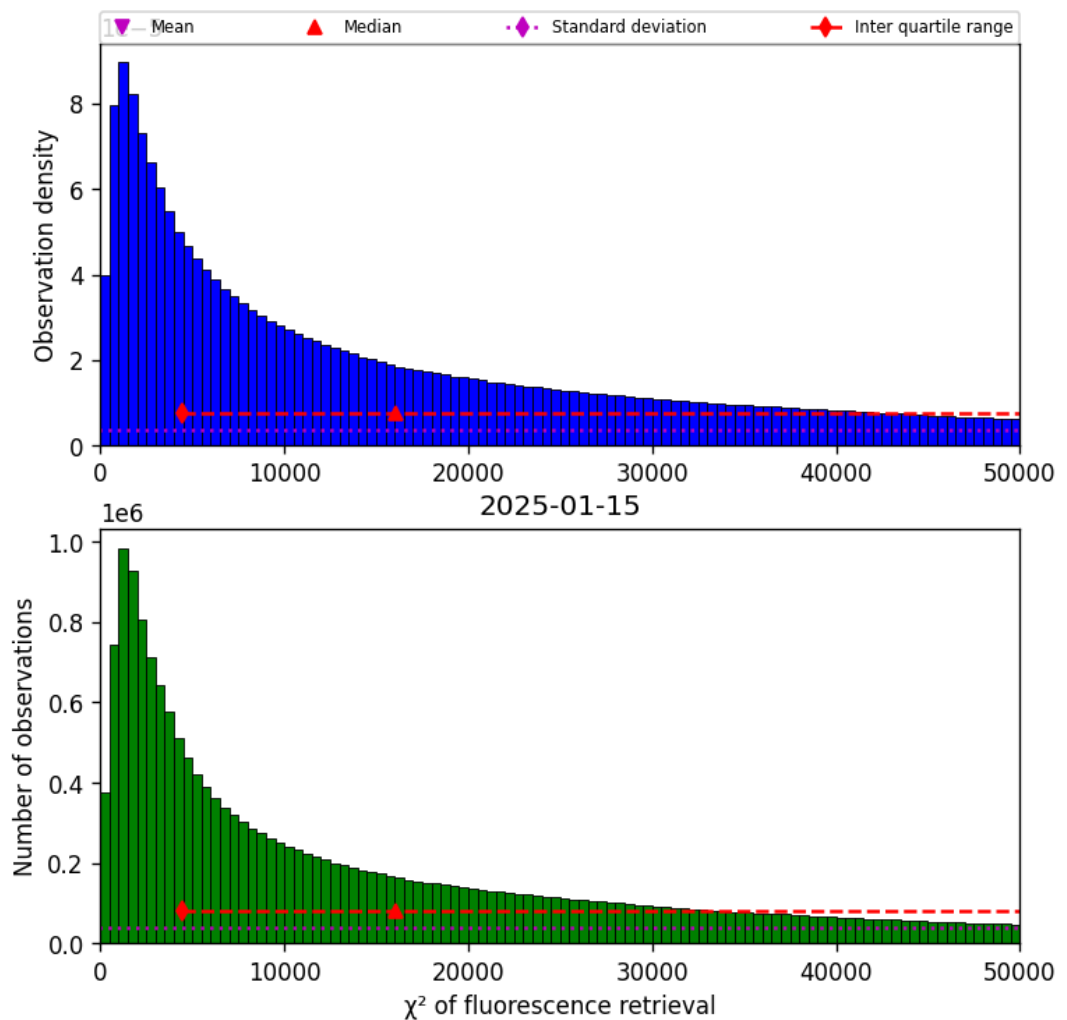


Figure 42: Histogram of “ χ^2 of fluorescence retrieval” for 2025-01-14 to 2025-01-16

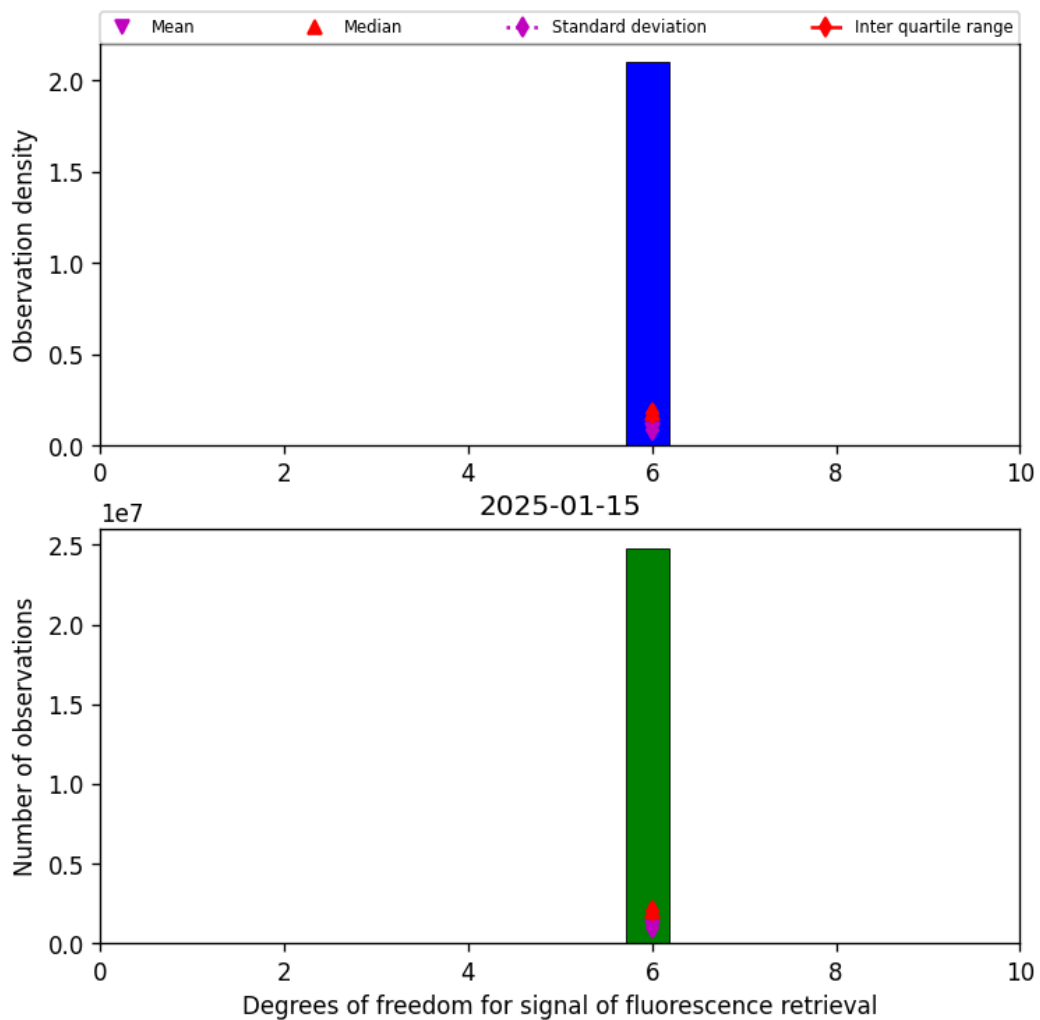


Figure 43: Histogram of “Degrees of freedom for signal of fluorescence retrieval” for 2025-01-14 to 2025-01-16

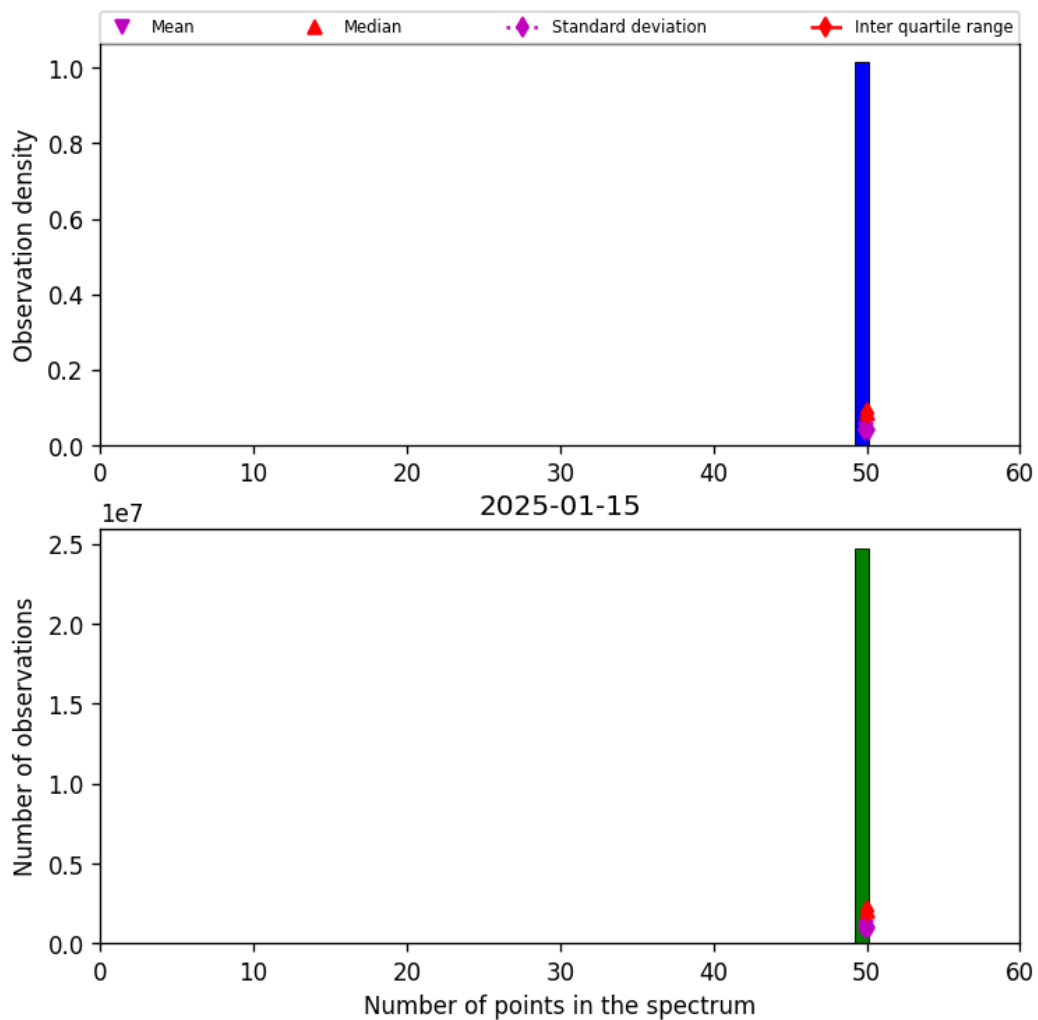


Figure 44: Histogram of “Number of points in the spectrum” for 2025-01-14 to 2025-01-16

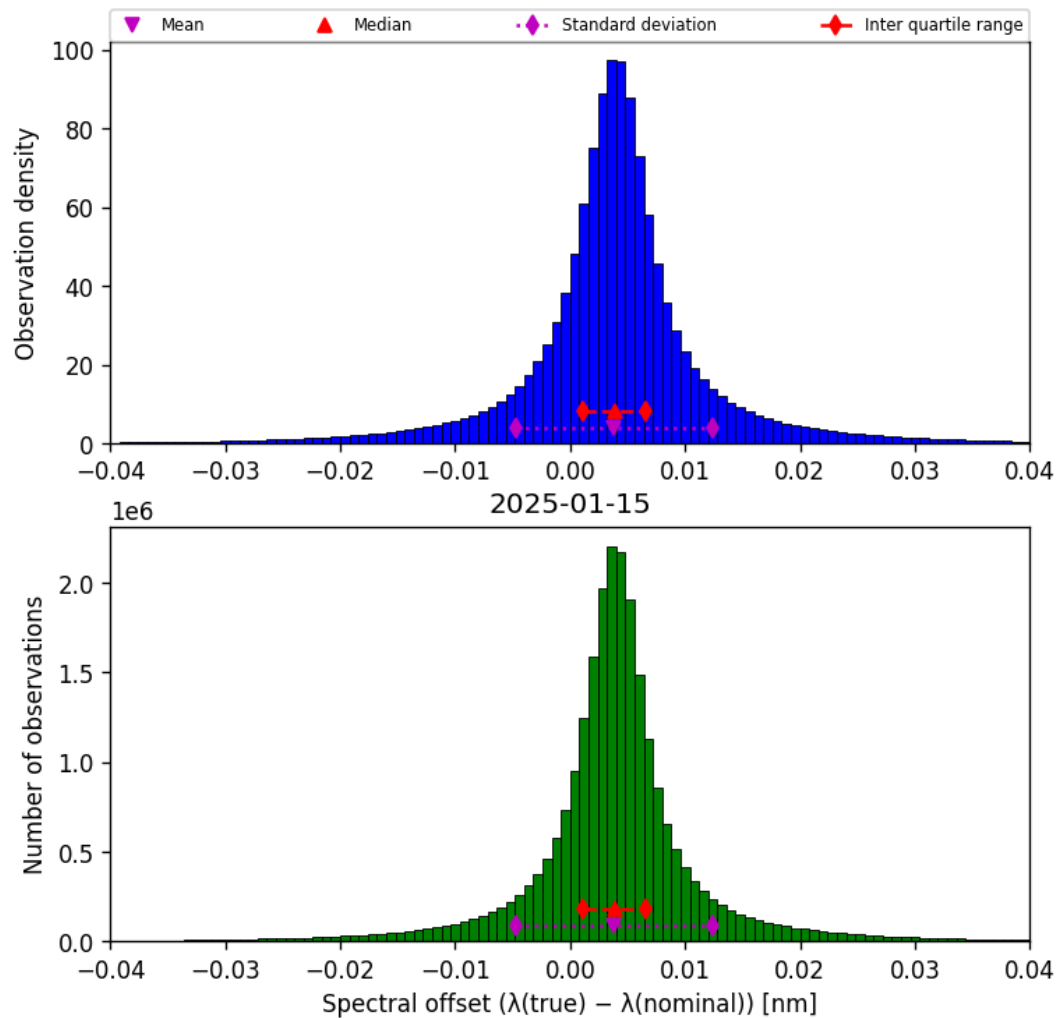


Figure 45: Histogram of “Spectral offset ($\lambda_{\text{true}} - \lambda_{\text{nominal}}$)” for 2025-01-14 to 2025-01-16

9 Along track statistics

The TROPOMI instrument uses different binned detector rows for different viewing directions. In this section statistics are presented for each of the binned rows in the instrument.

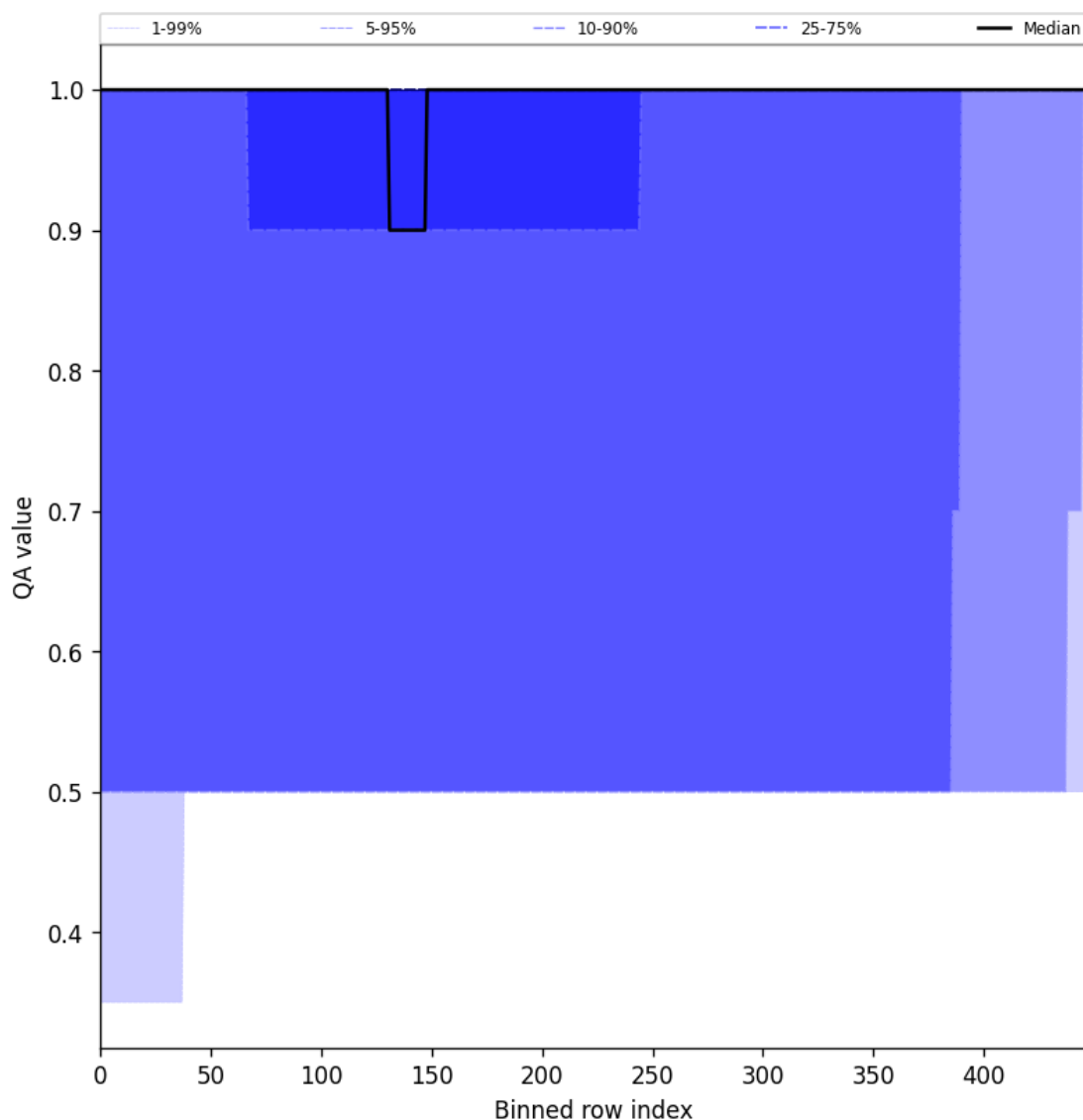


Figure 46: Along track statistics of “QA value” for 2025-01-14 to 2025-01-16

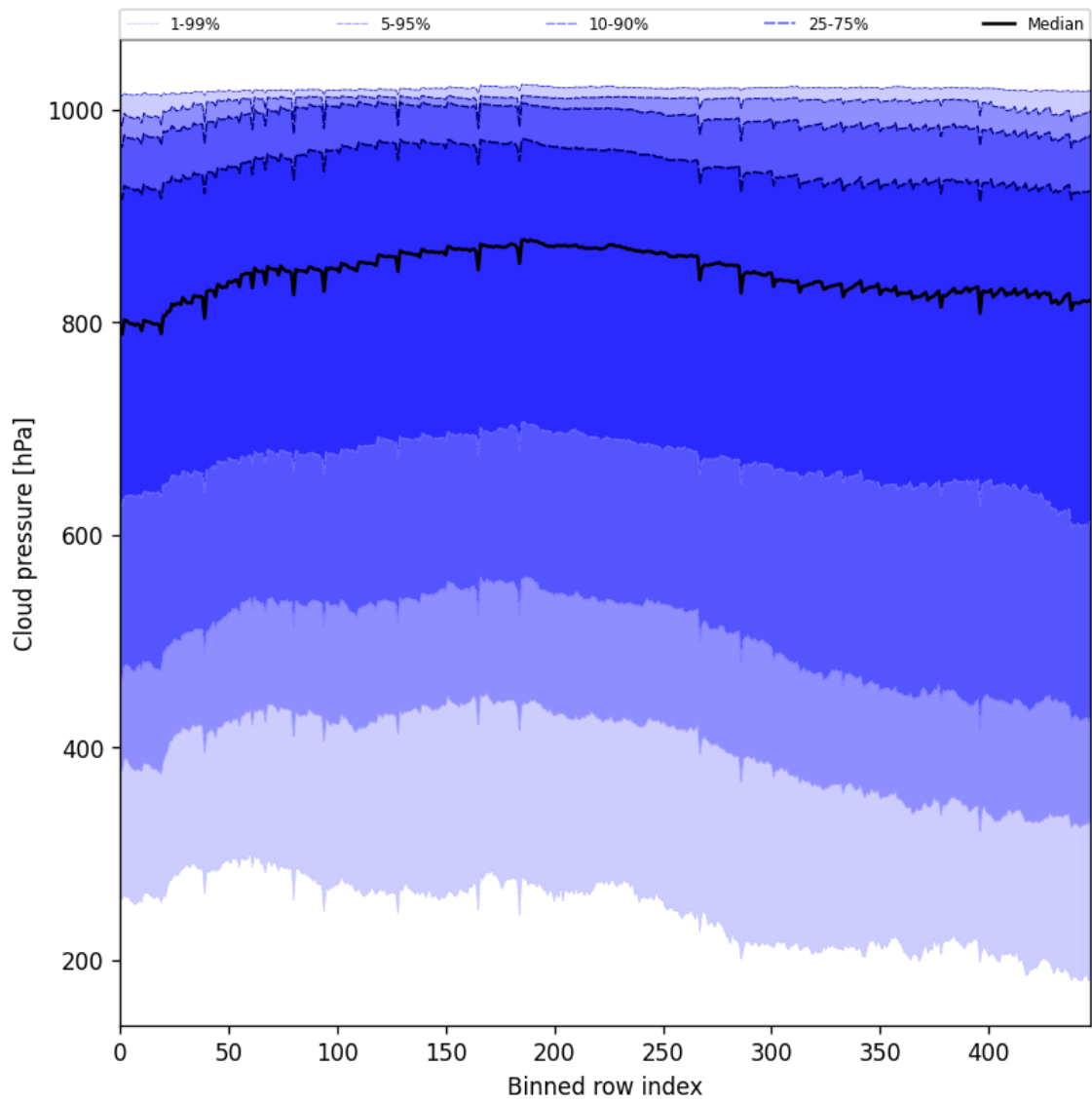


Figure 47: Along track statistics of “Cloud pressure” for 2025-01-14 to 2025-01-16

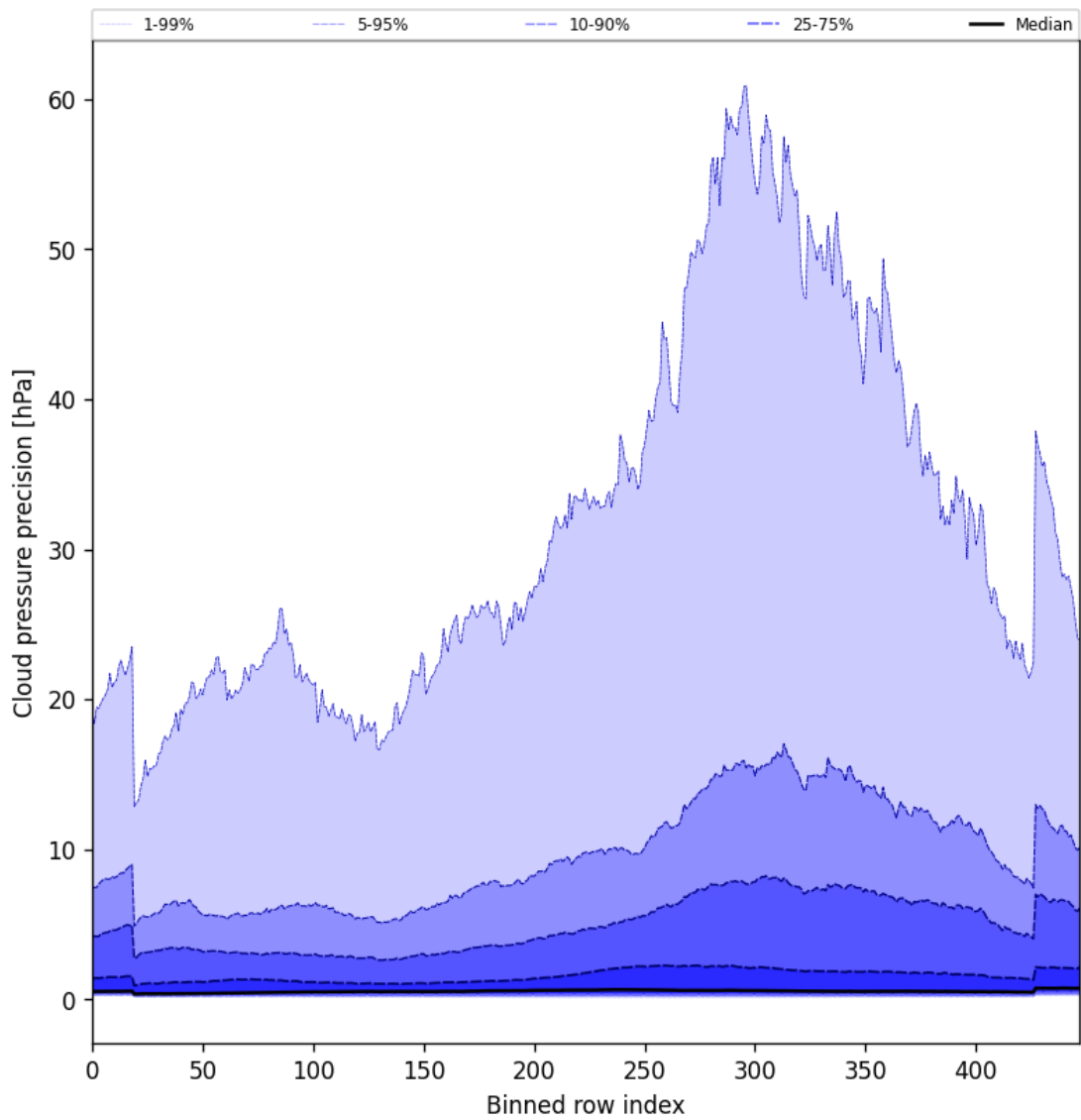


Figure 48: Along track statistics of “Cloud pressure precision” for 2025-01-14 to 2025-01-16

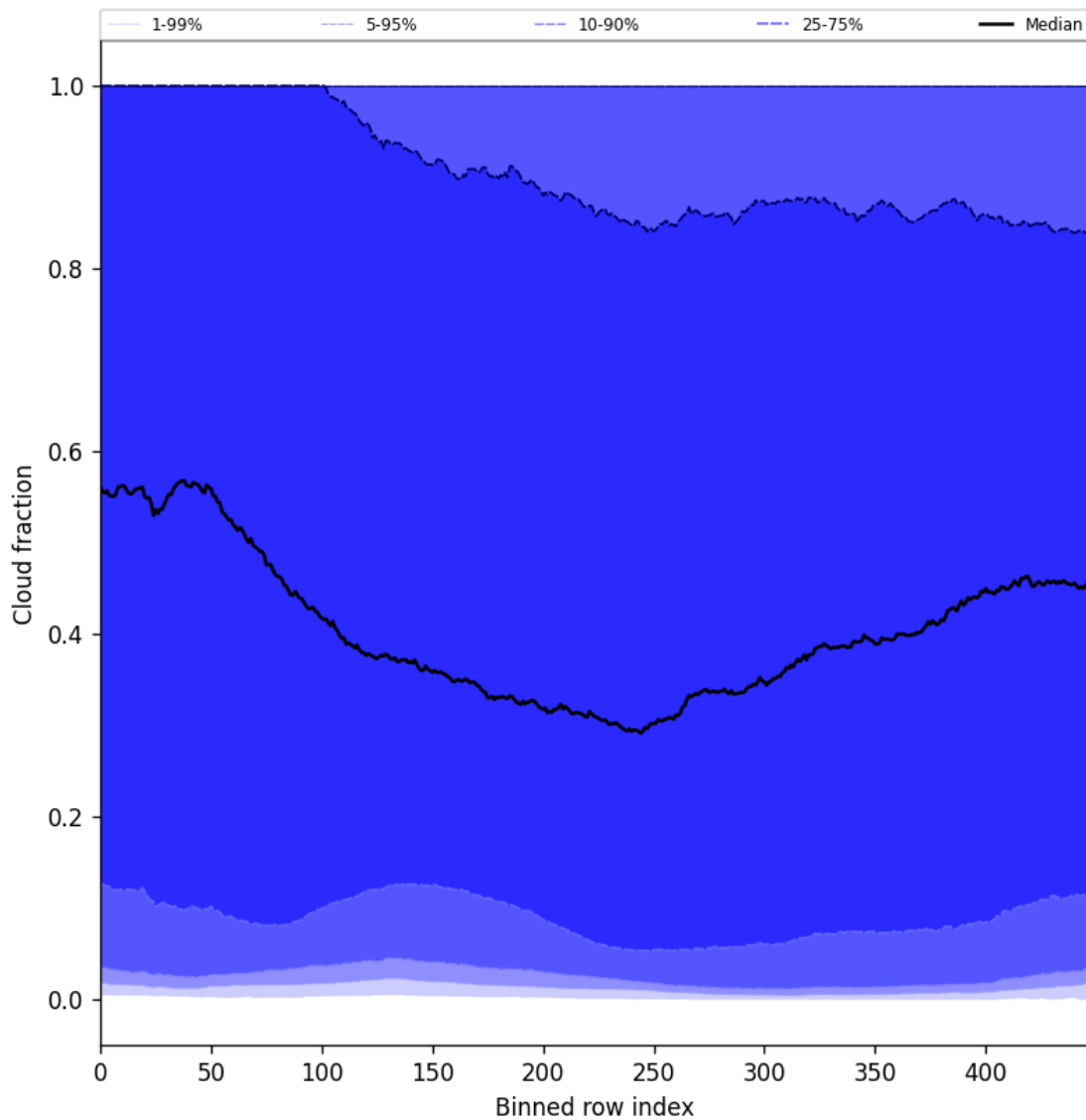


Figure 49: Along track statistics of “Cloud fraction” for 2025-01-14 to 2025-01-16

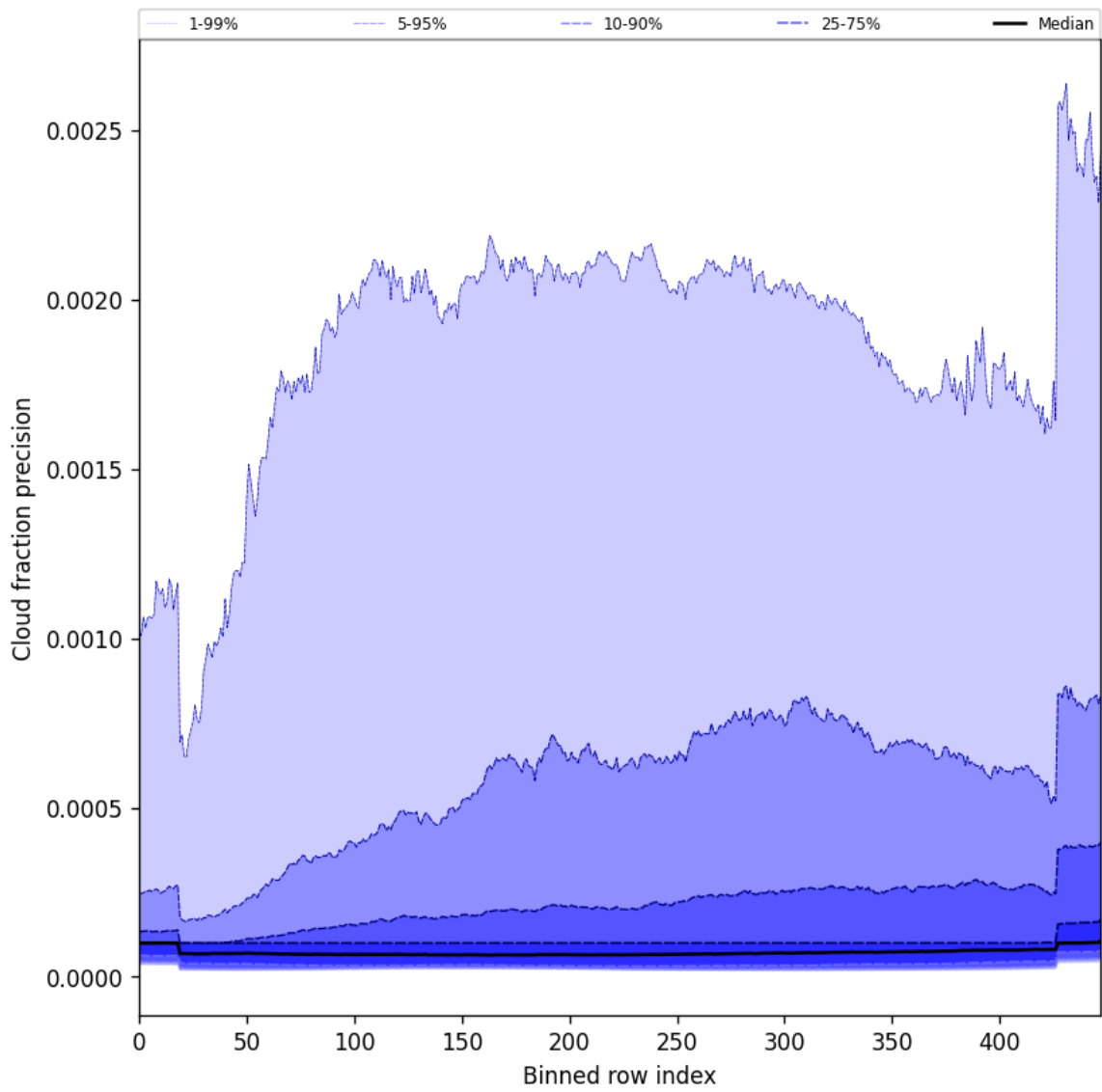


Figure 50: Along track statistics of “Cloud fraction precision” for 2025-01-14 to 2025-01-16

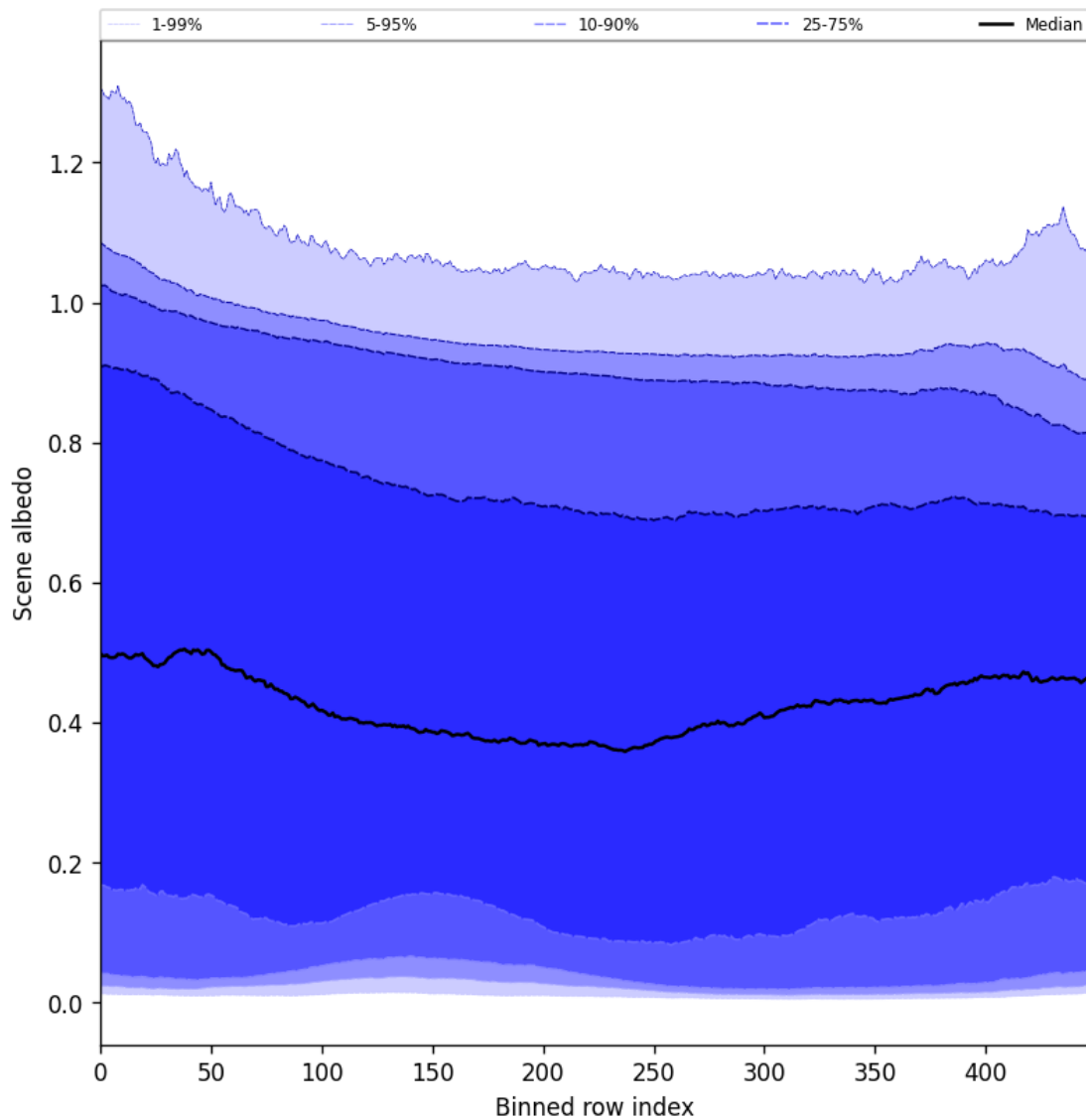


Figure 51: Along track statistics of “Scene albedo” for 2025-01-14 to 2025-01-16

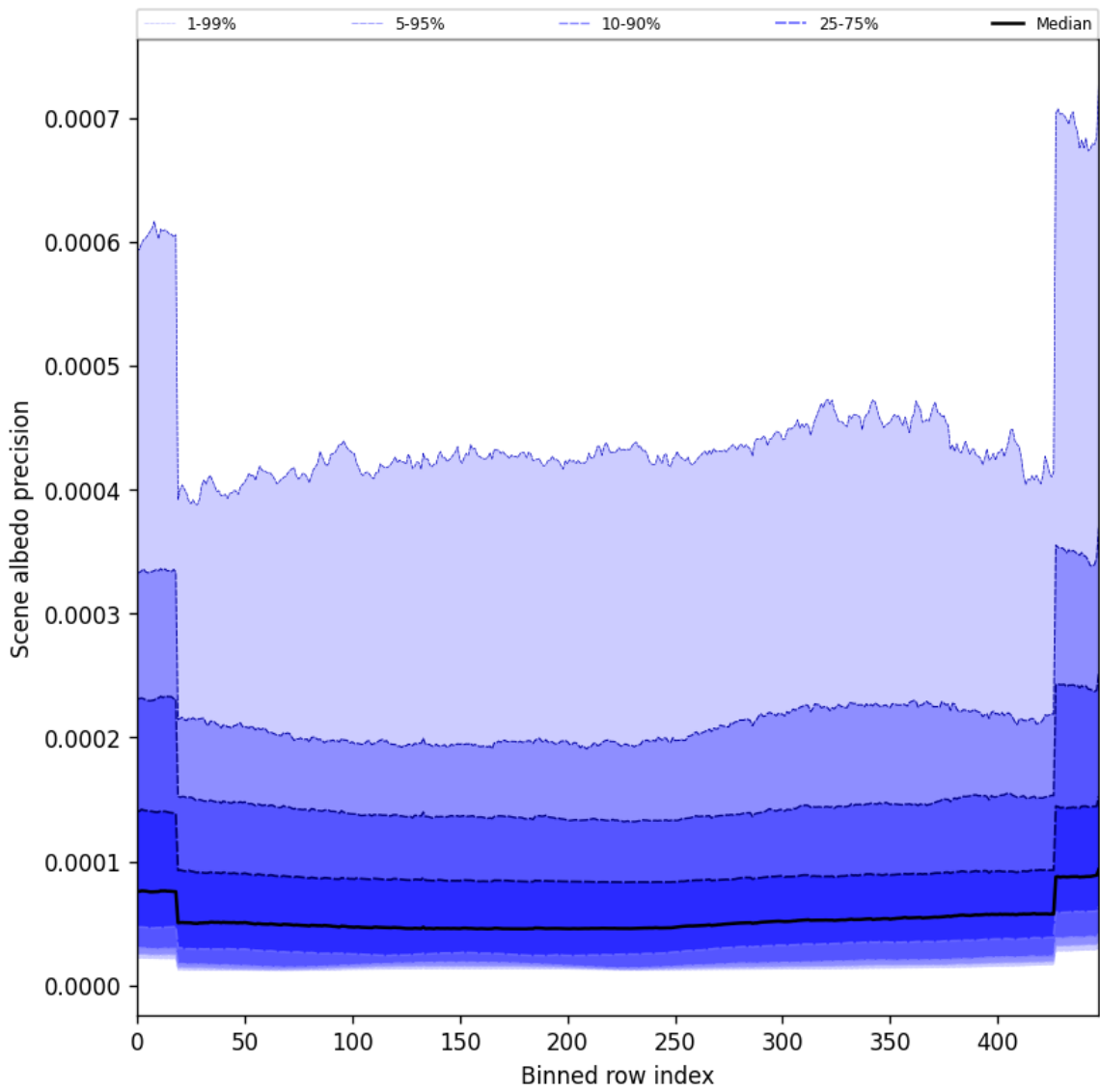


Figure 52: Along track statistics of “Scene albedo precision” for 2025-01-14 to 2025-01-16

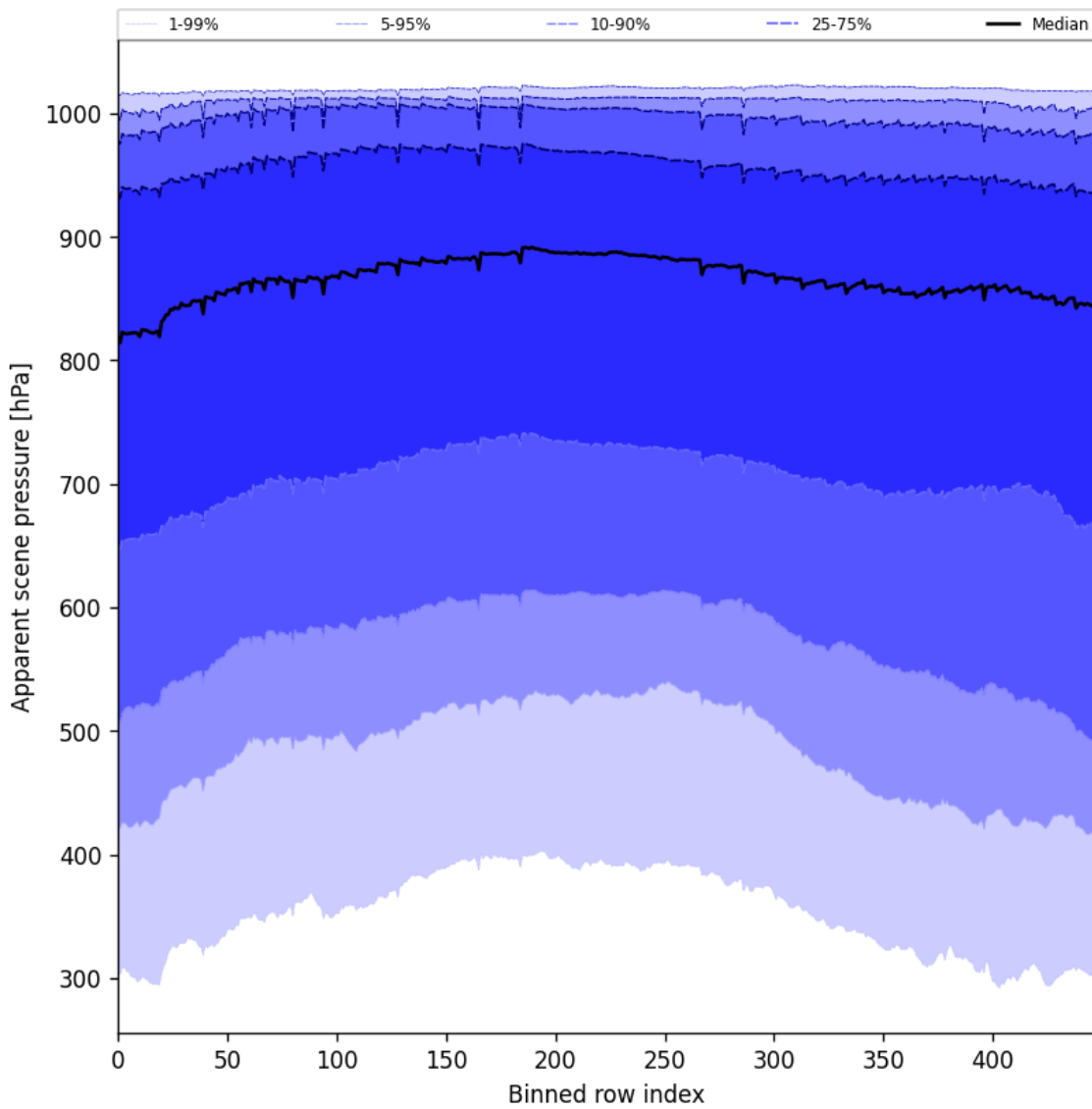


Figure 53: Along track statistics of “Apparent scene pressure” for 2025-01-14 to 2025-01-16

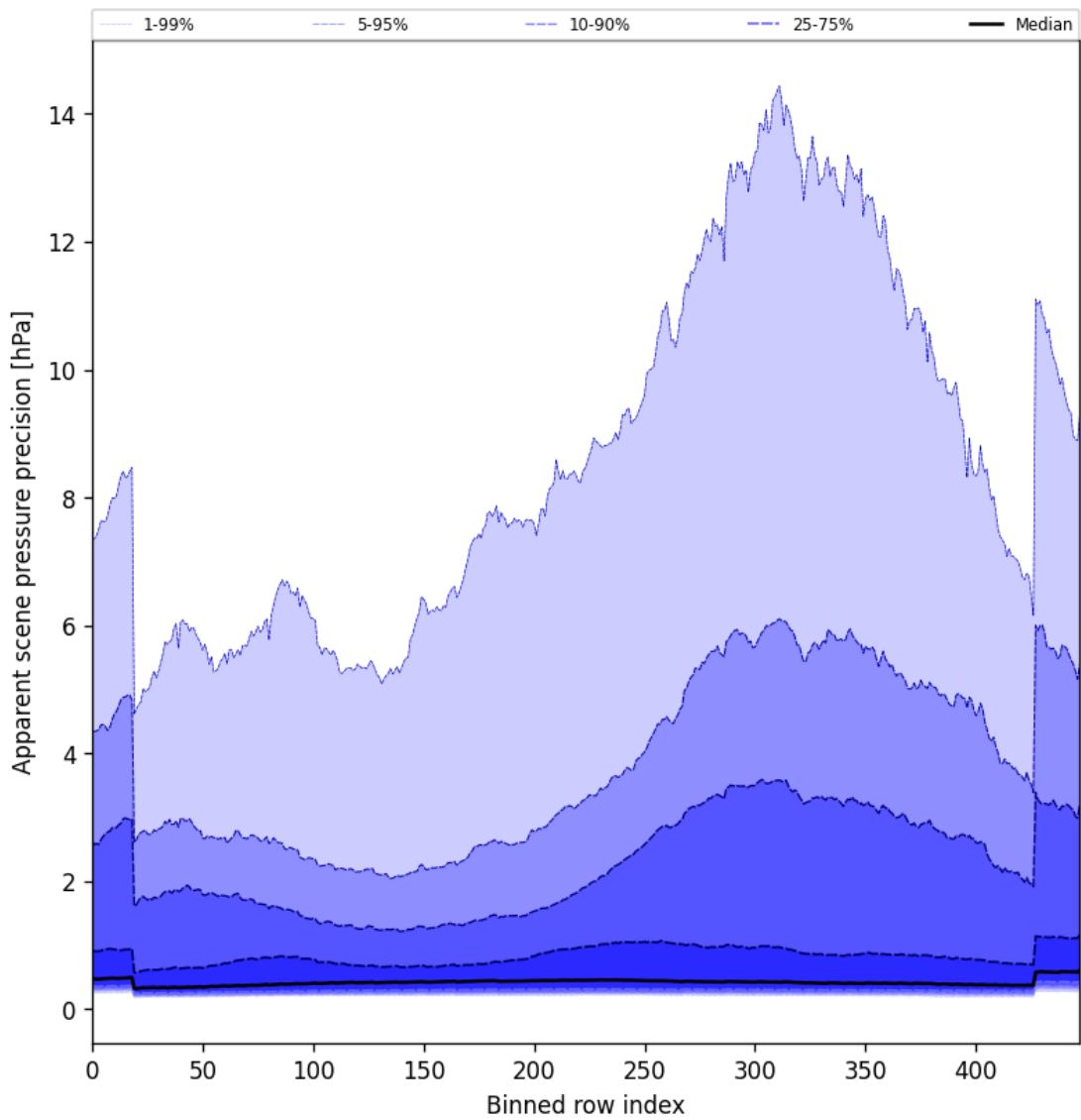


Figure 54: Along track statistics of “Apparent scene pressure precision” for 2025-01-14 to 2025-01-16

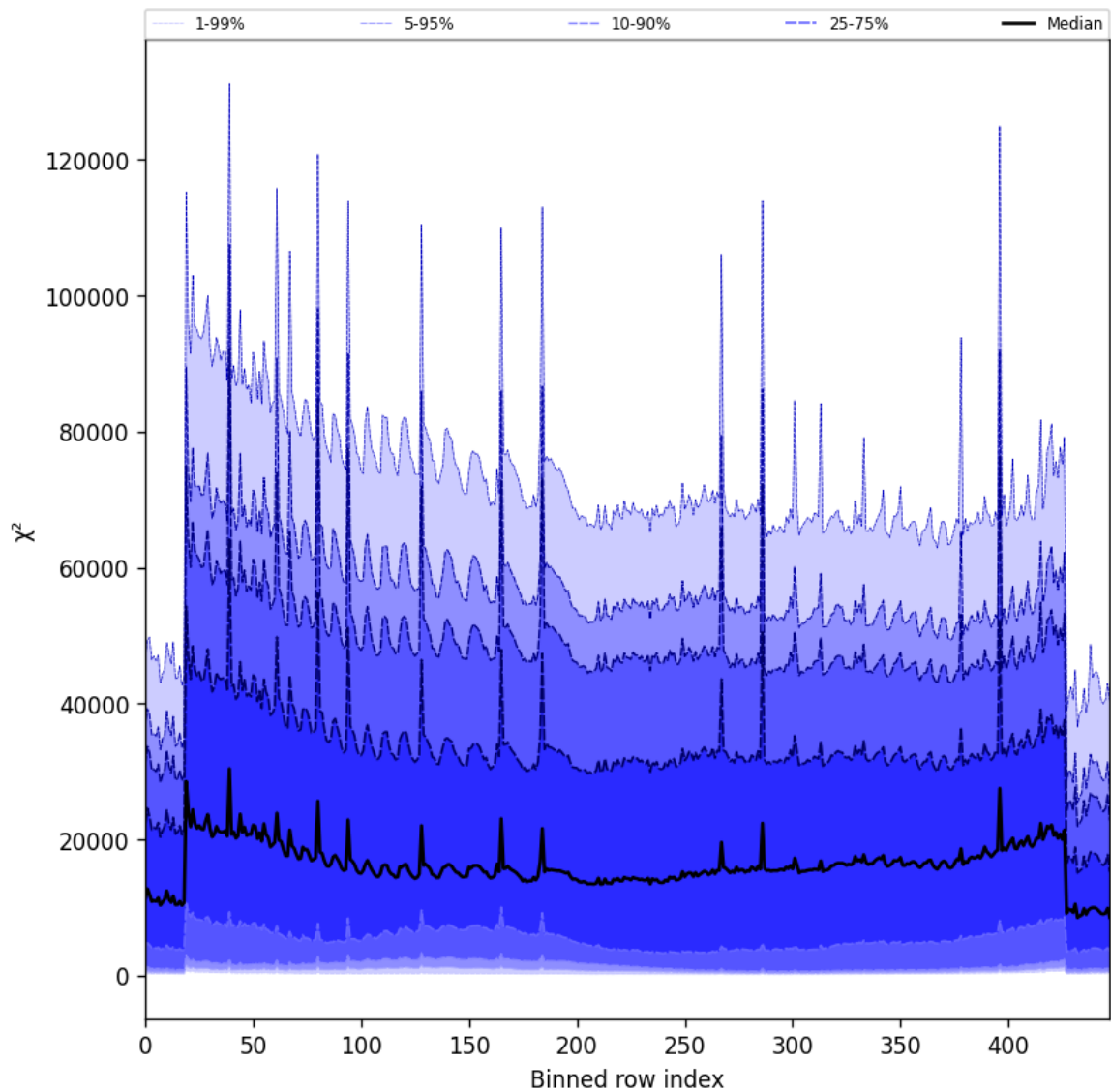


Figure 55: Along track statistics of “ χ^2 ” for 2025-01-14 to 2025-01-16

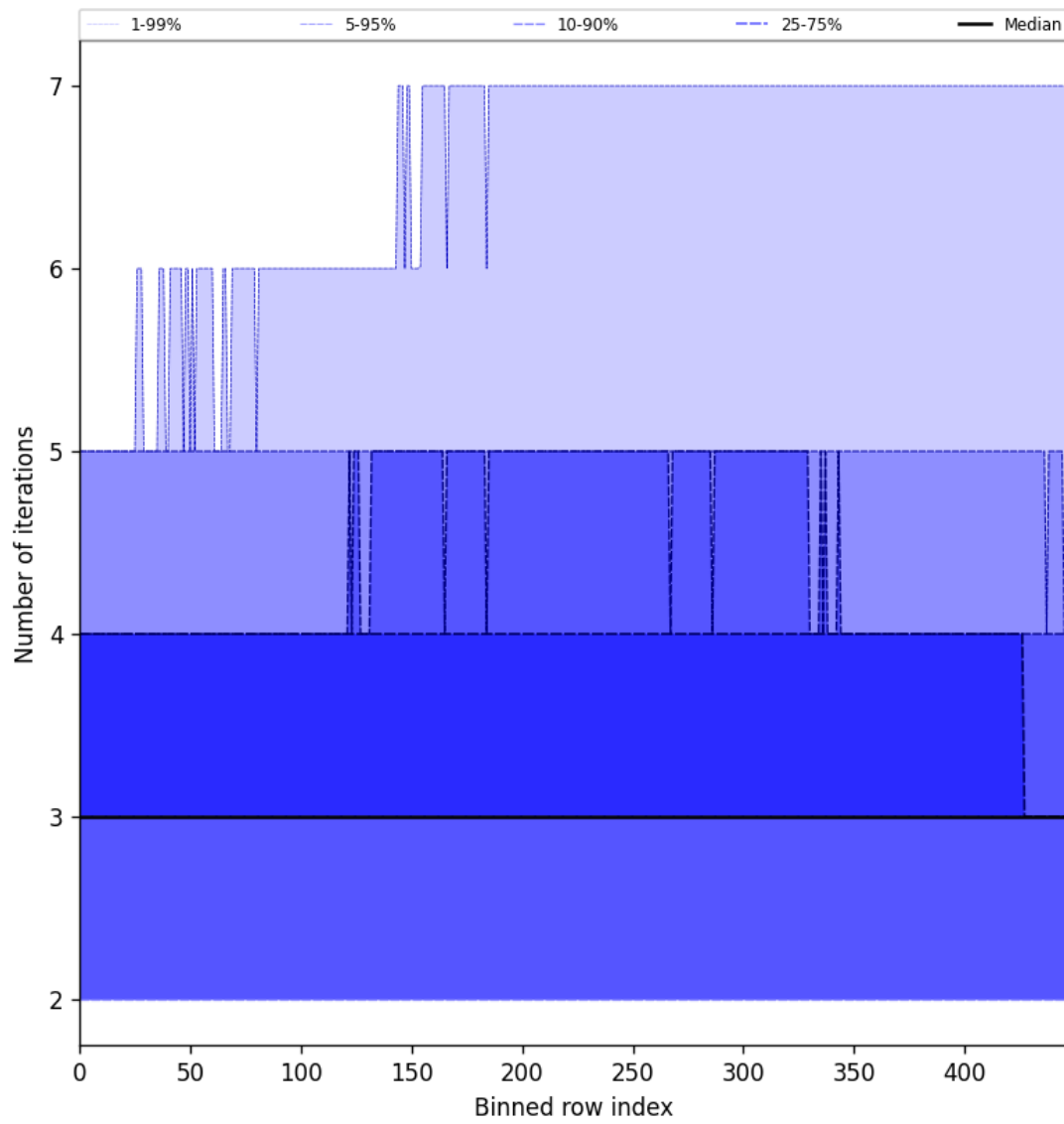


Figure 56: Along track statistics of “Number of iterations” for 2025-01-14 to 2025-01-16

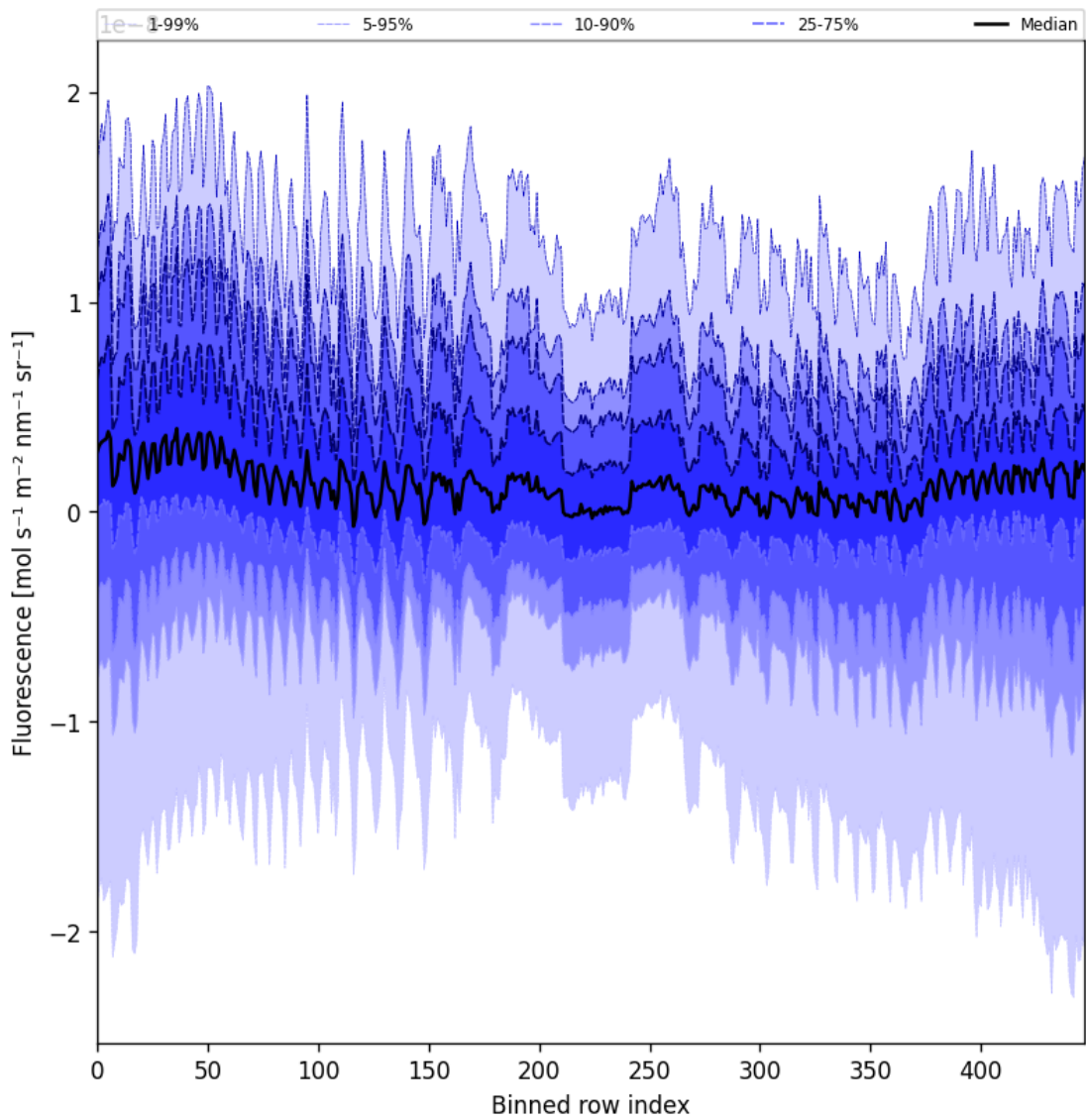


Figure 57: Along track statistics of “Fluorescence” for 2025-01-14 to 2025-01-16

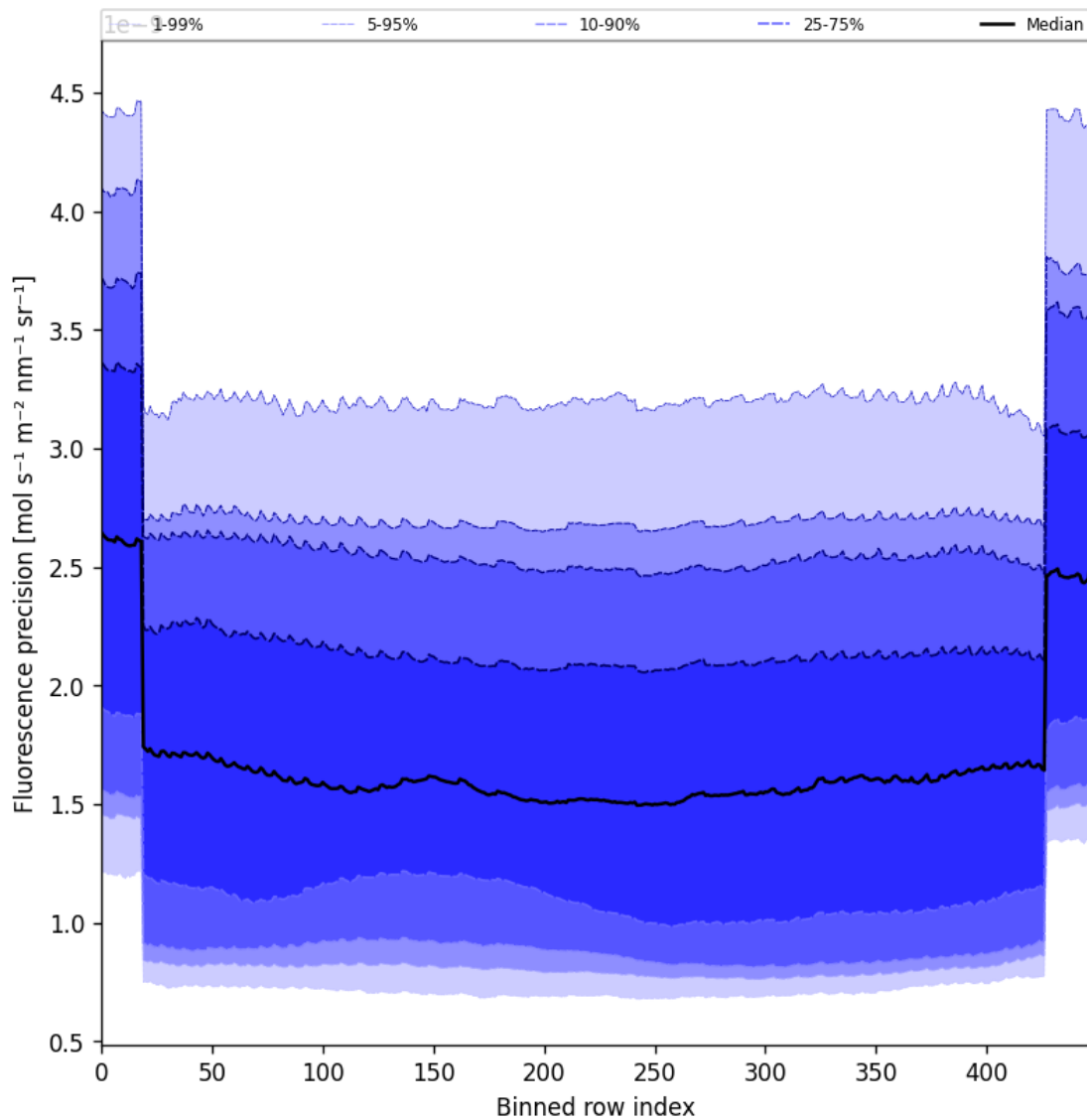


Figure 58: Along track statistics of “Fluorescence precision” for 2025-01-14 to 2025-01-16

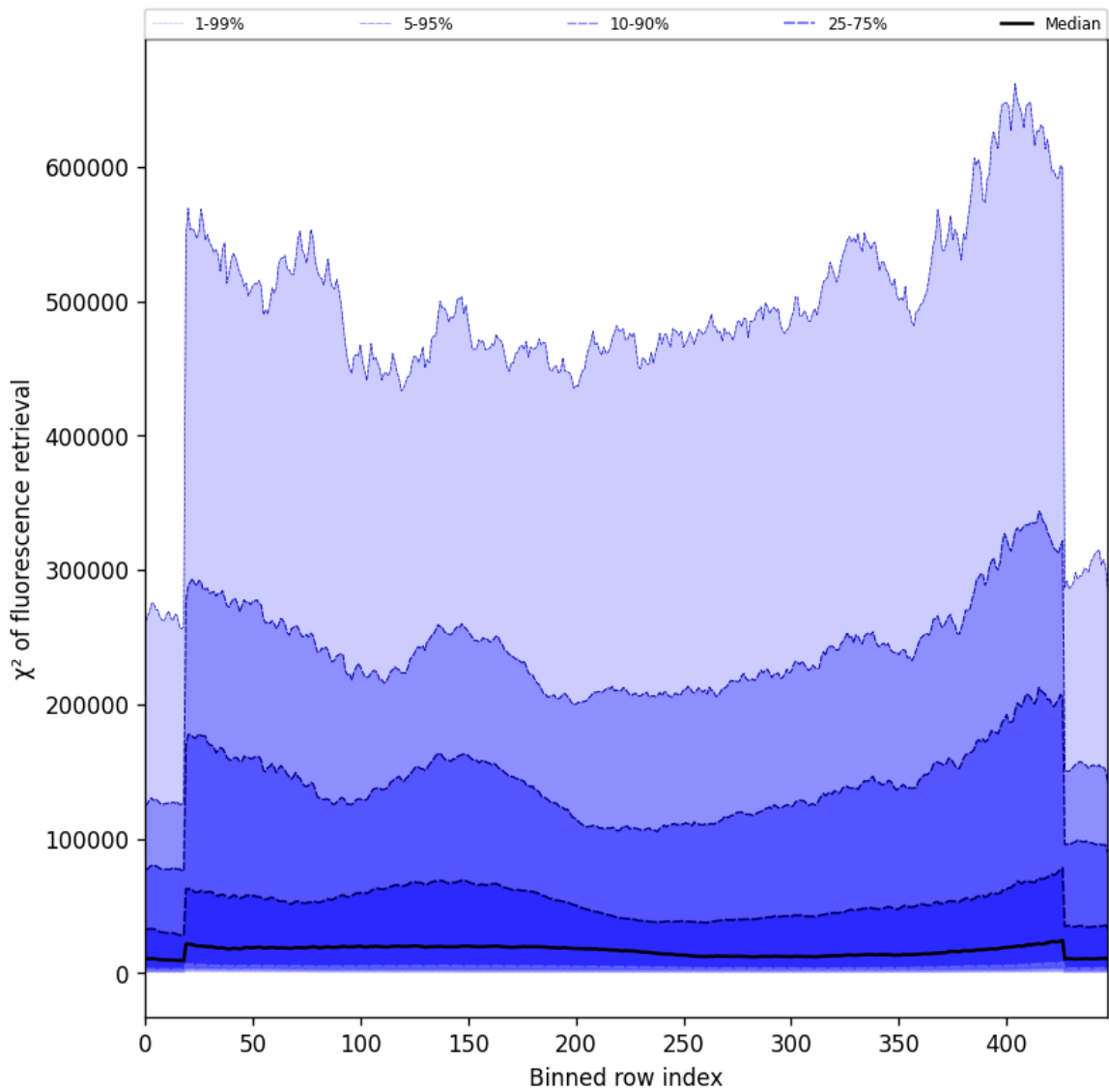


Figure 59: Along track statistics of “ χ^2 of fluorescence retrieval” for 2025-01-14 to 2025-01-16



Figure 60: Along track statistics of “Degrees of freedom for signal of fluorescence retrieval” for 2025-01-14 to 2025-01-16



Figure 61: Along track statistics of “Number of points in the spectrum” for 2025-01-14 to 2025-01-16

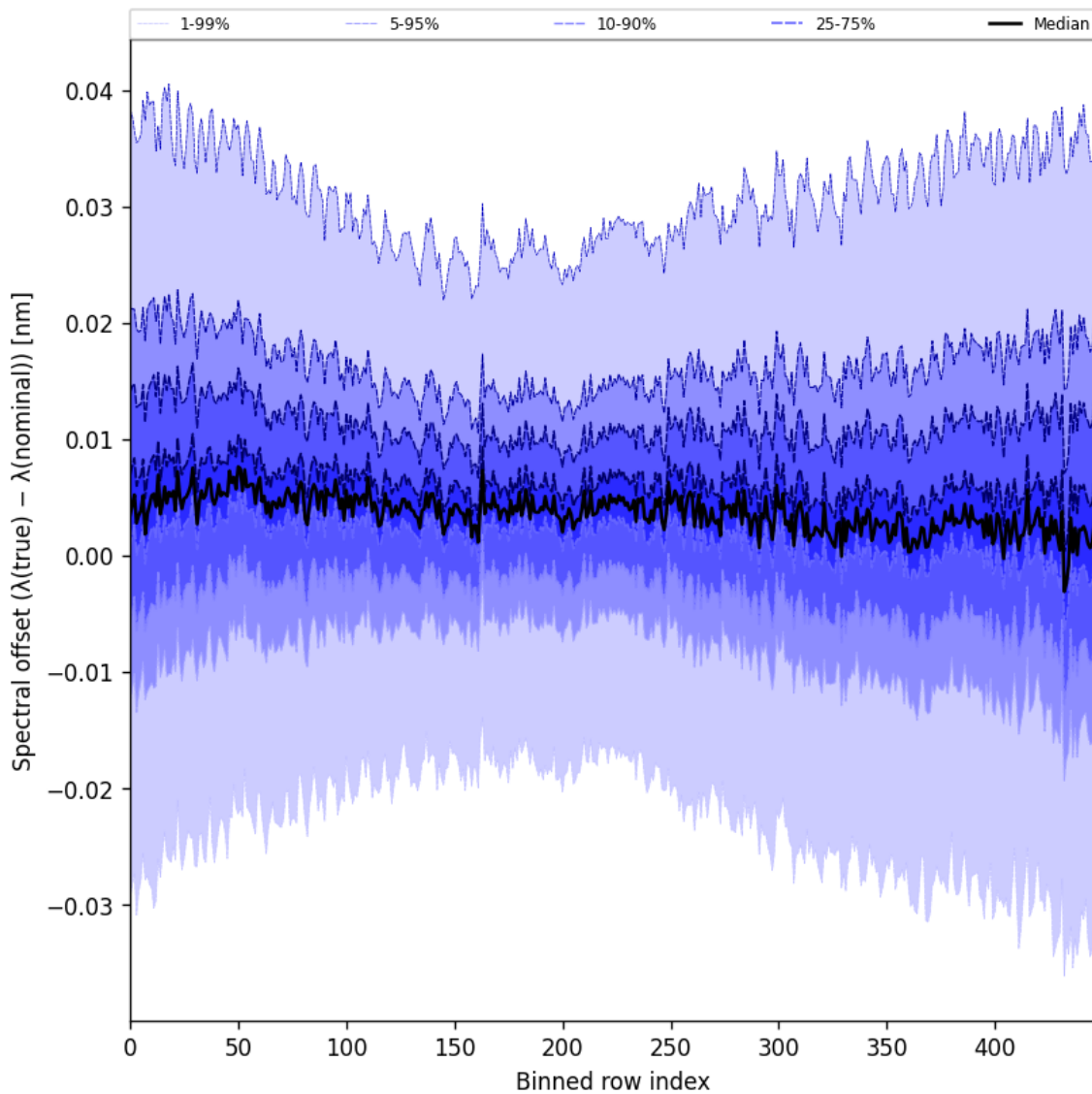


Figure 62: Along track statistics of “Spectral offset ($\lambda_{\text{true}} - \lambda_{\text{nominal}}$)” for 2025-01-14 to 2025-01-16

10 Coincidence density

To investigate the relation between parameters scatter density plots are produced. These include some ‘hidden’ parameters, latitude and the solar- and viewing geometries, in addition to all configured parameters. All combinations of pairs of parameters are included *once*, in one direction alone.

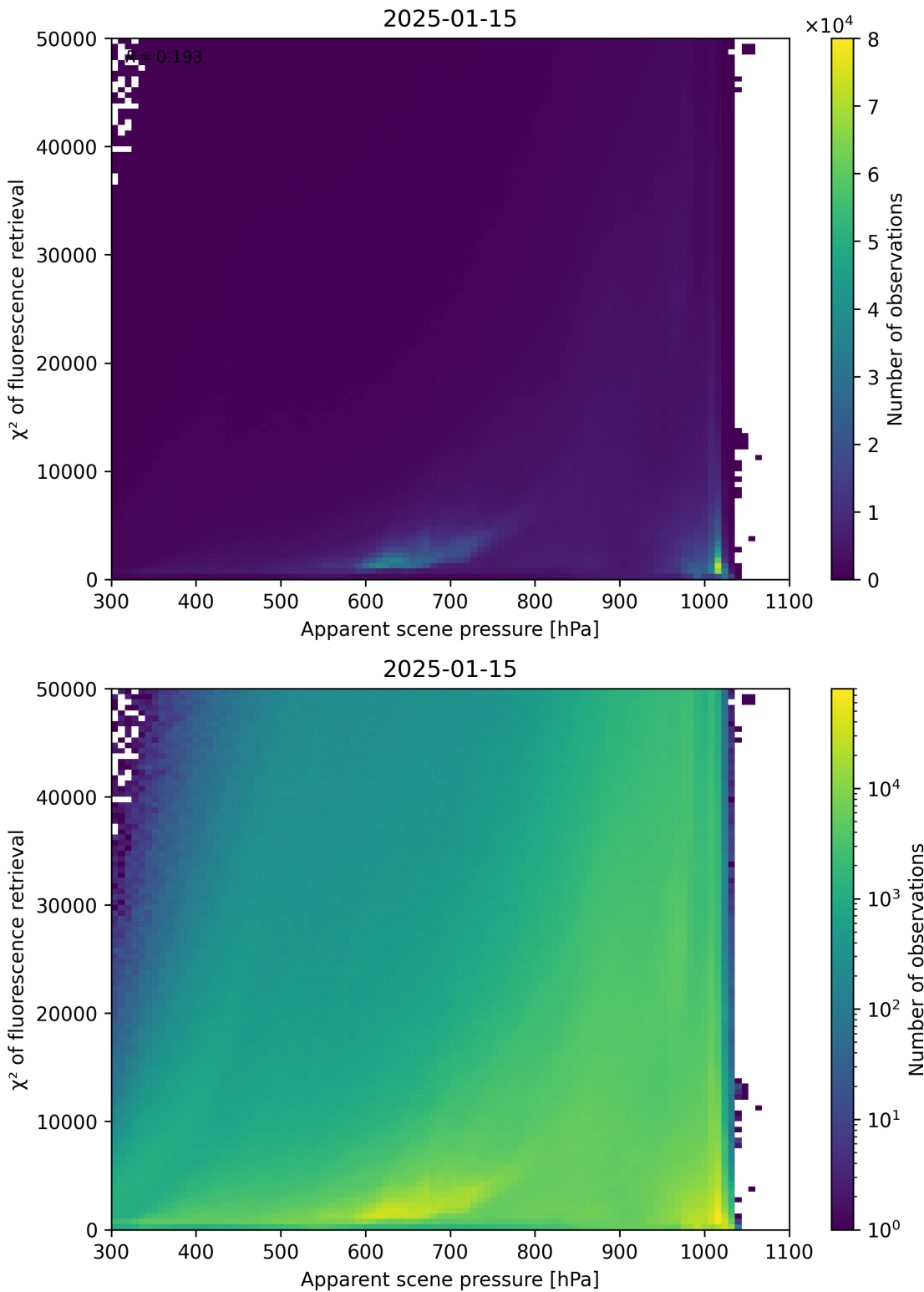


Figure 63: Scatter density plot of “Apparent scene pressure” against “ χ^2 of fluorescence retrieval” for 2025-01-14 to 2025-01-16.

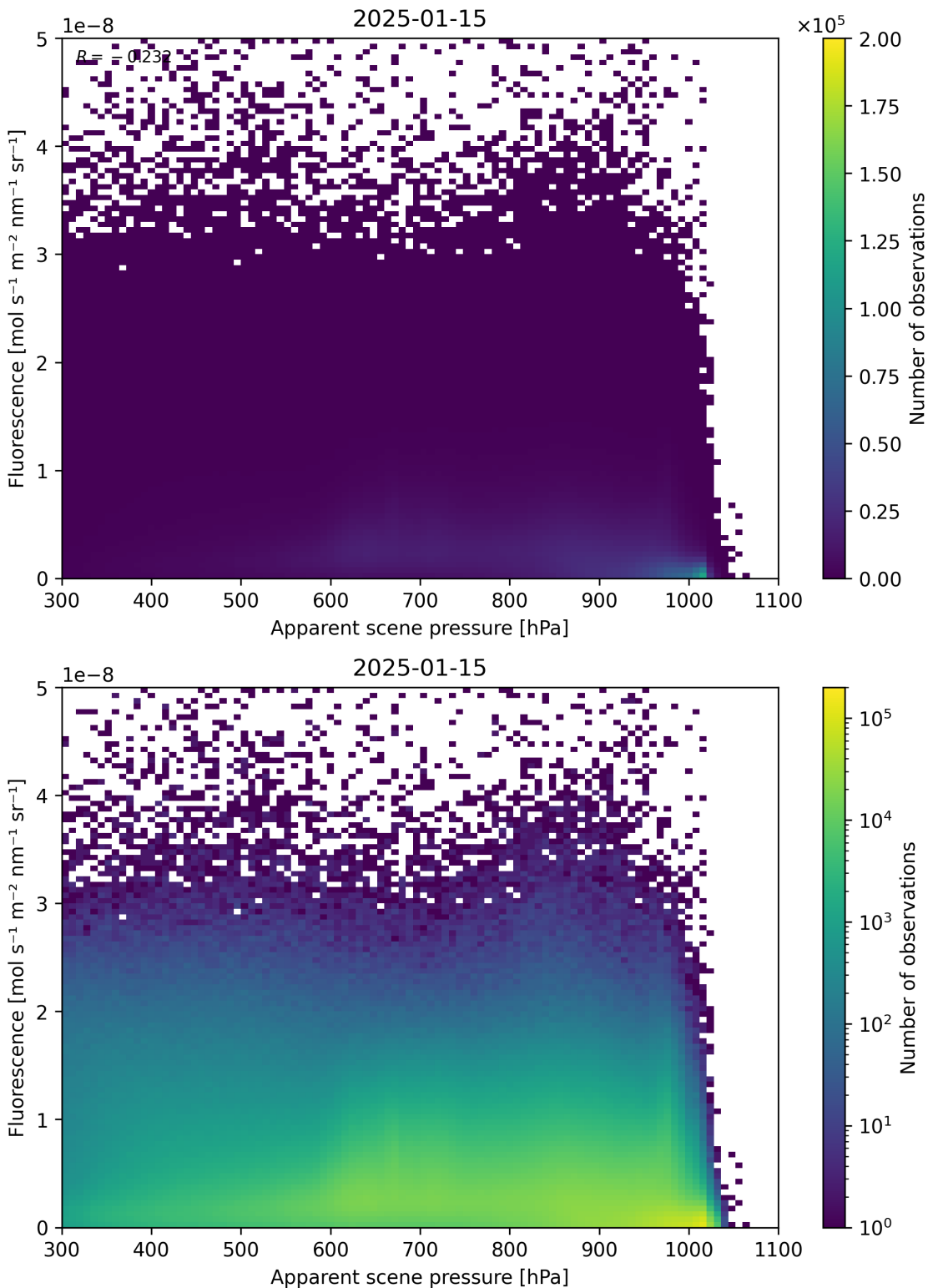


Figure 64: Scatter density plot of “Apparent scene pressure” against “Fluorescence” for 2025-01-14 to 2025-01-16.

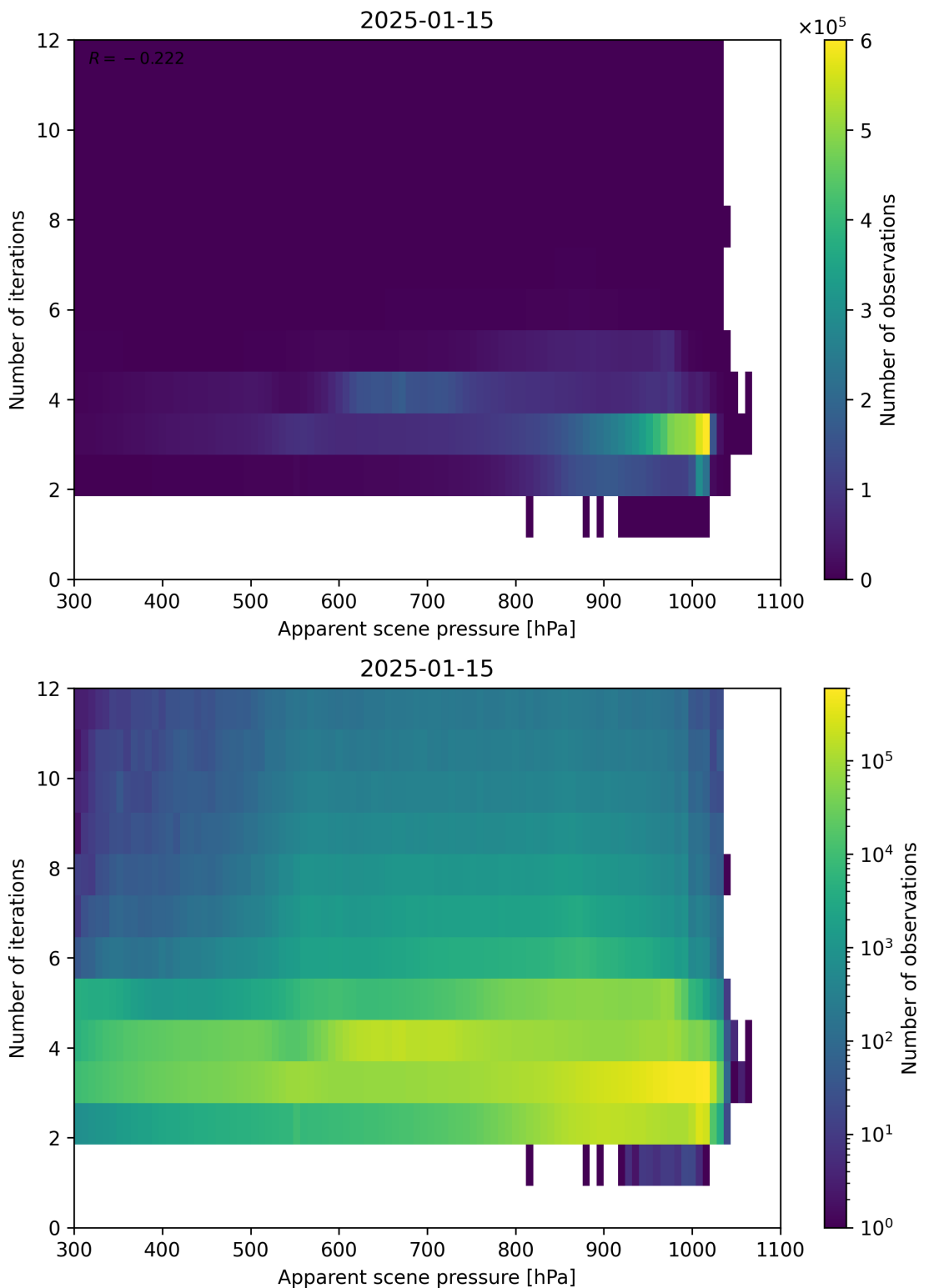


Figure 65: Scatter density plot of “Apparent scene pressure” against “Number of iterations” for 2025-01-14 to 2025-01-16.

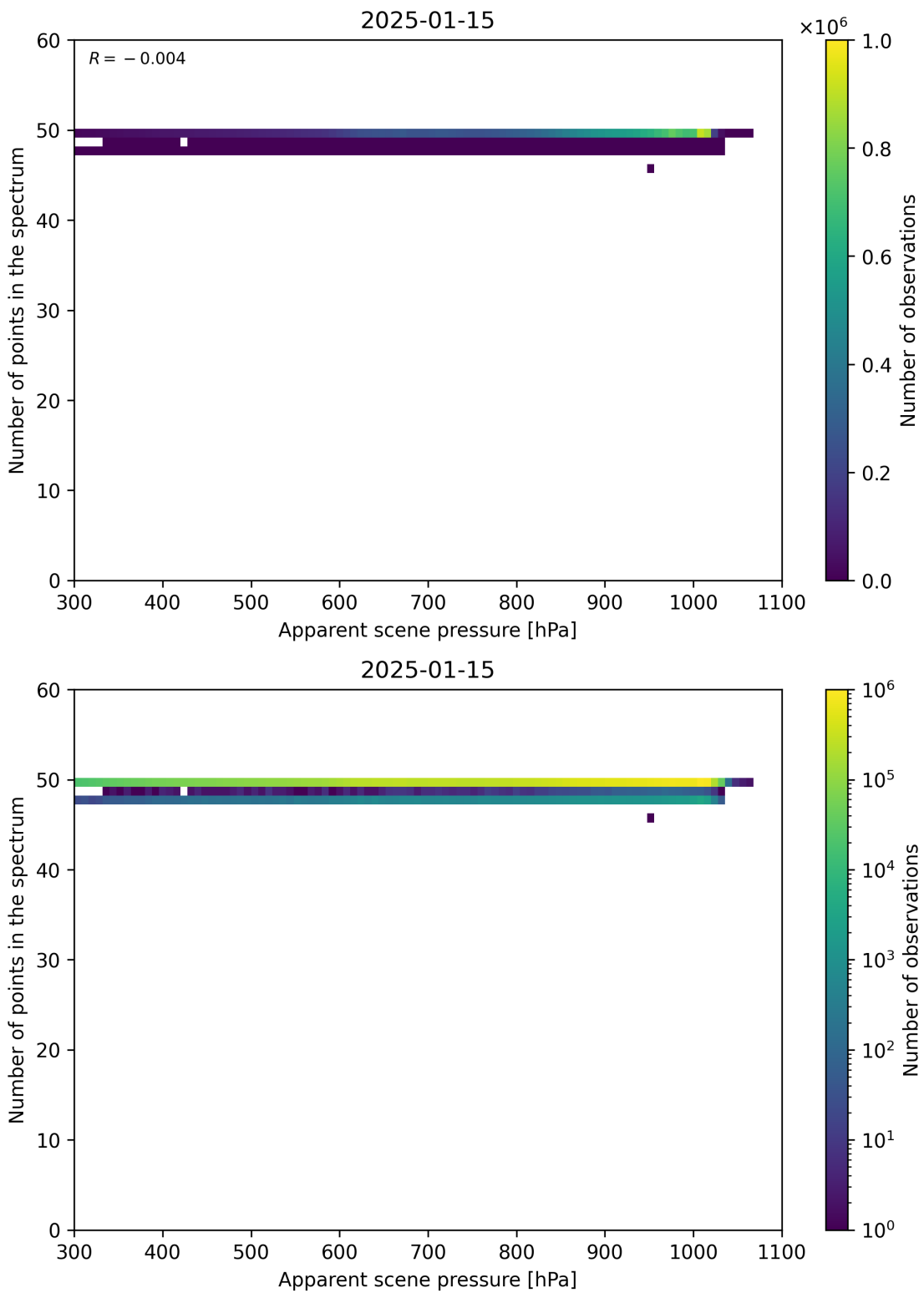


Figure 66: Scatter density plot of “Apparent scene pressure” against “Number of points in the spectrum” for 2025-01-14 to 2025-01-16.

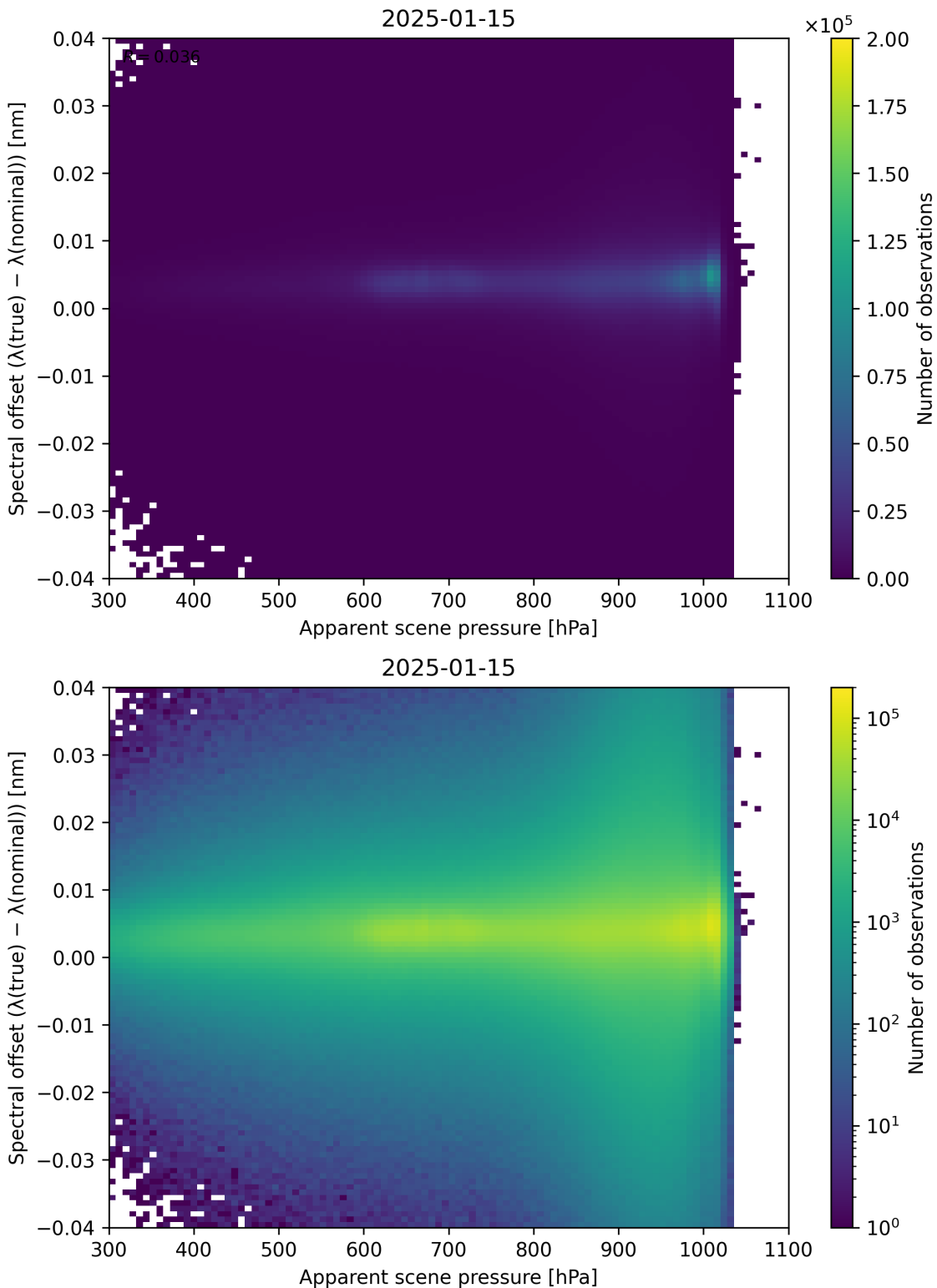


Figure 67: Scatter density plot of “Apparent scene pressure” against “Spectral offset ($\lambda_{\text{true}} - \lambda_{\text{nominal}}$)” for 2025-01-14 to 2025-01-16.

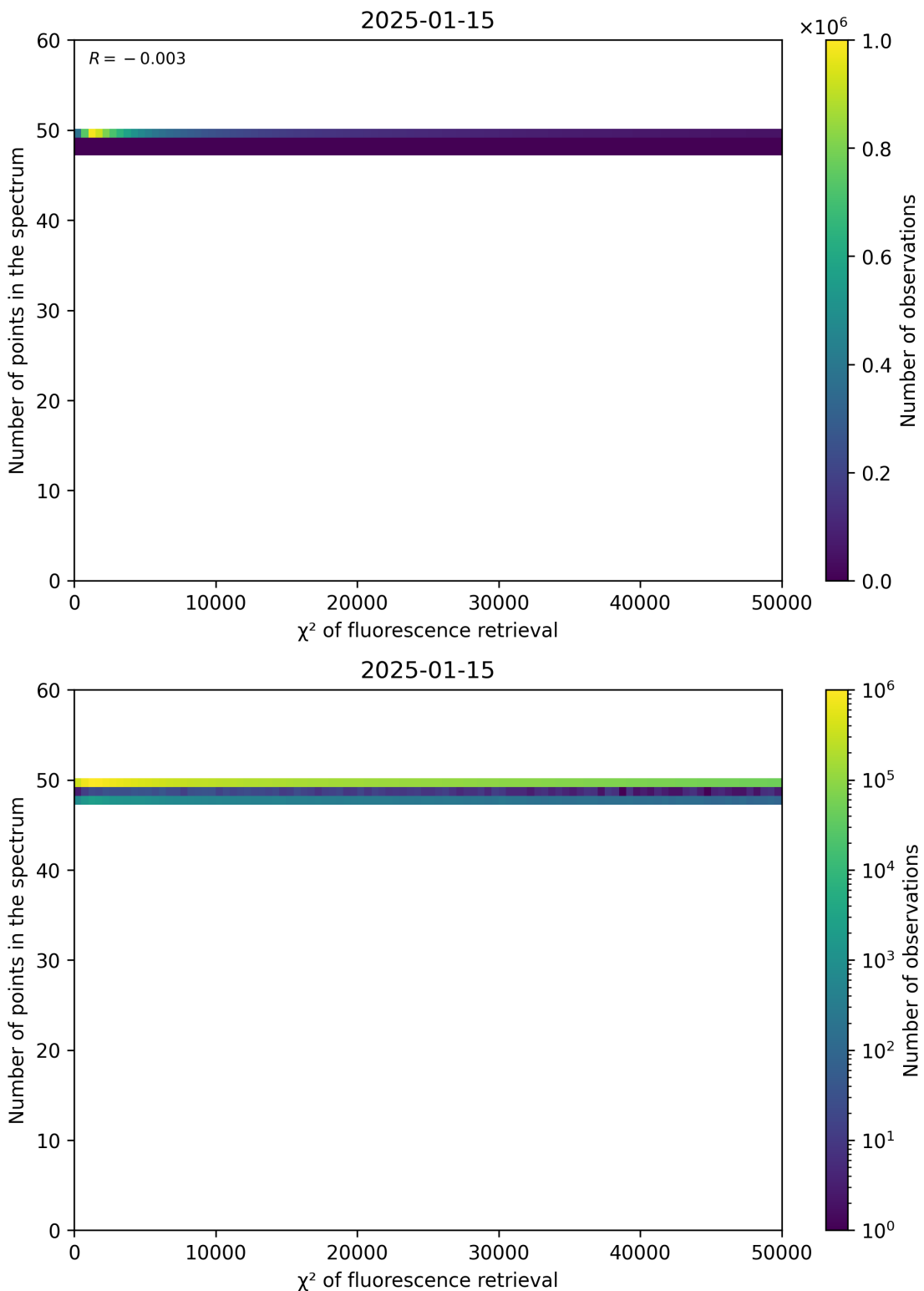


Figure 68: Scatter density plot of “ χ^2 of fluorescence retrieval” against “Number of points in the spectrum” for 2025-01-14 to 2025-01-16.

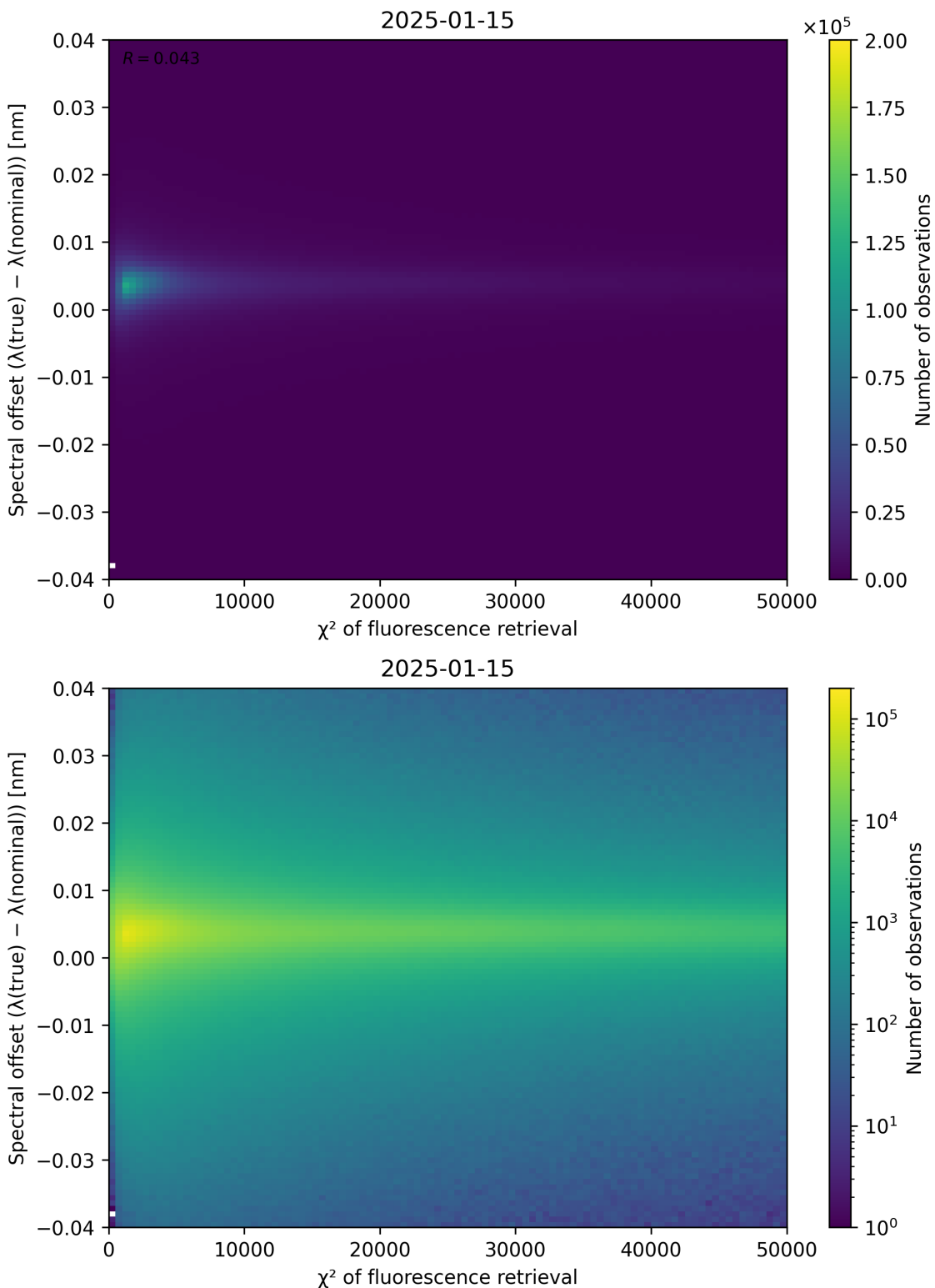


Figure 69: Scatter density plot of “ χ^2 of fluorescence retrieval” against “Spectral offset ($\lambda_{\text{true}} - \lambda_{\text{nominal}}$)” for 2025-01-14 to 2025-01-16.

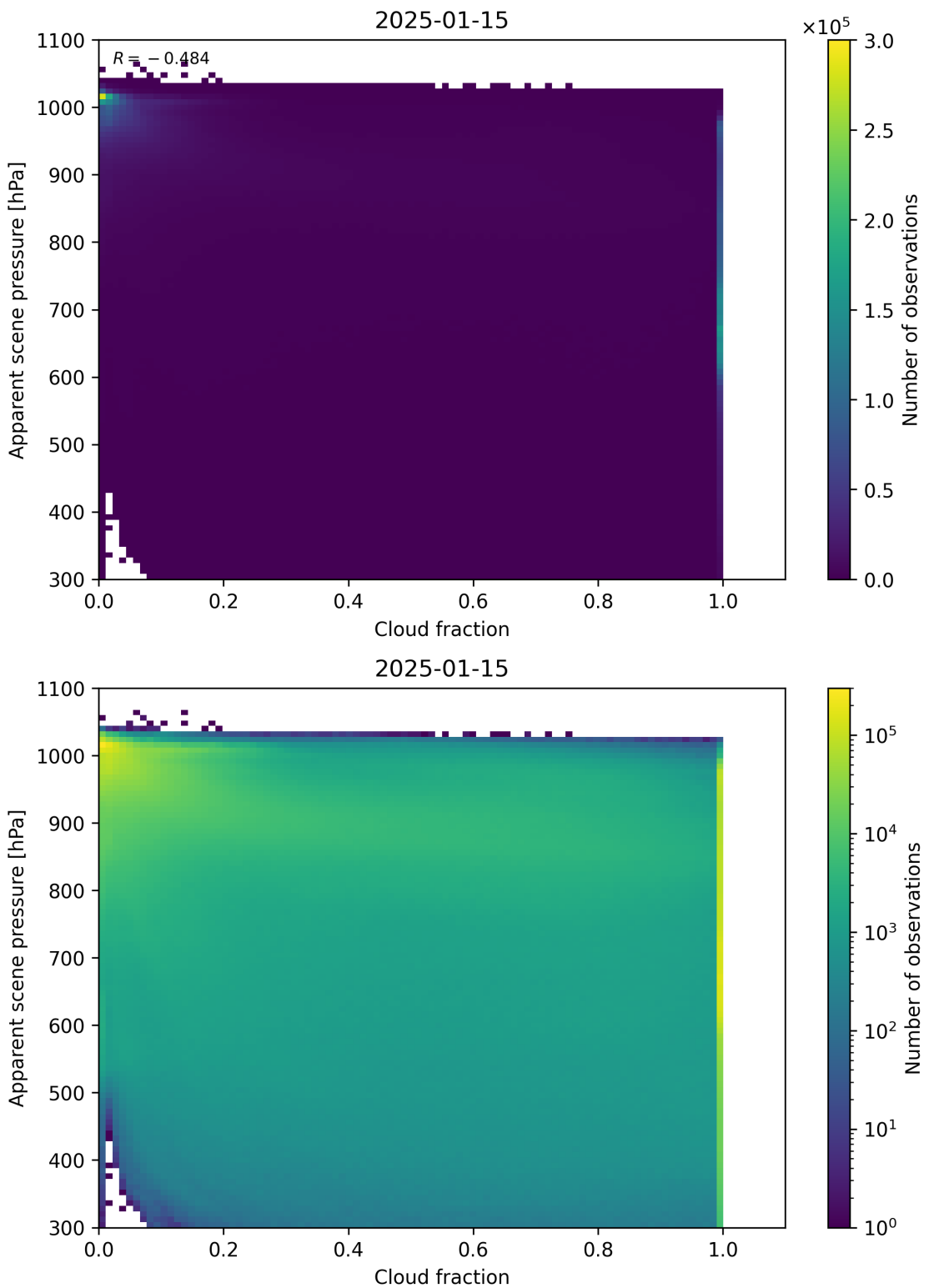


Figure 70: Scatter density plot of “Cloud fraction” against “Apparent scene pressure” for 2025-01-14 to 2025-01-16.

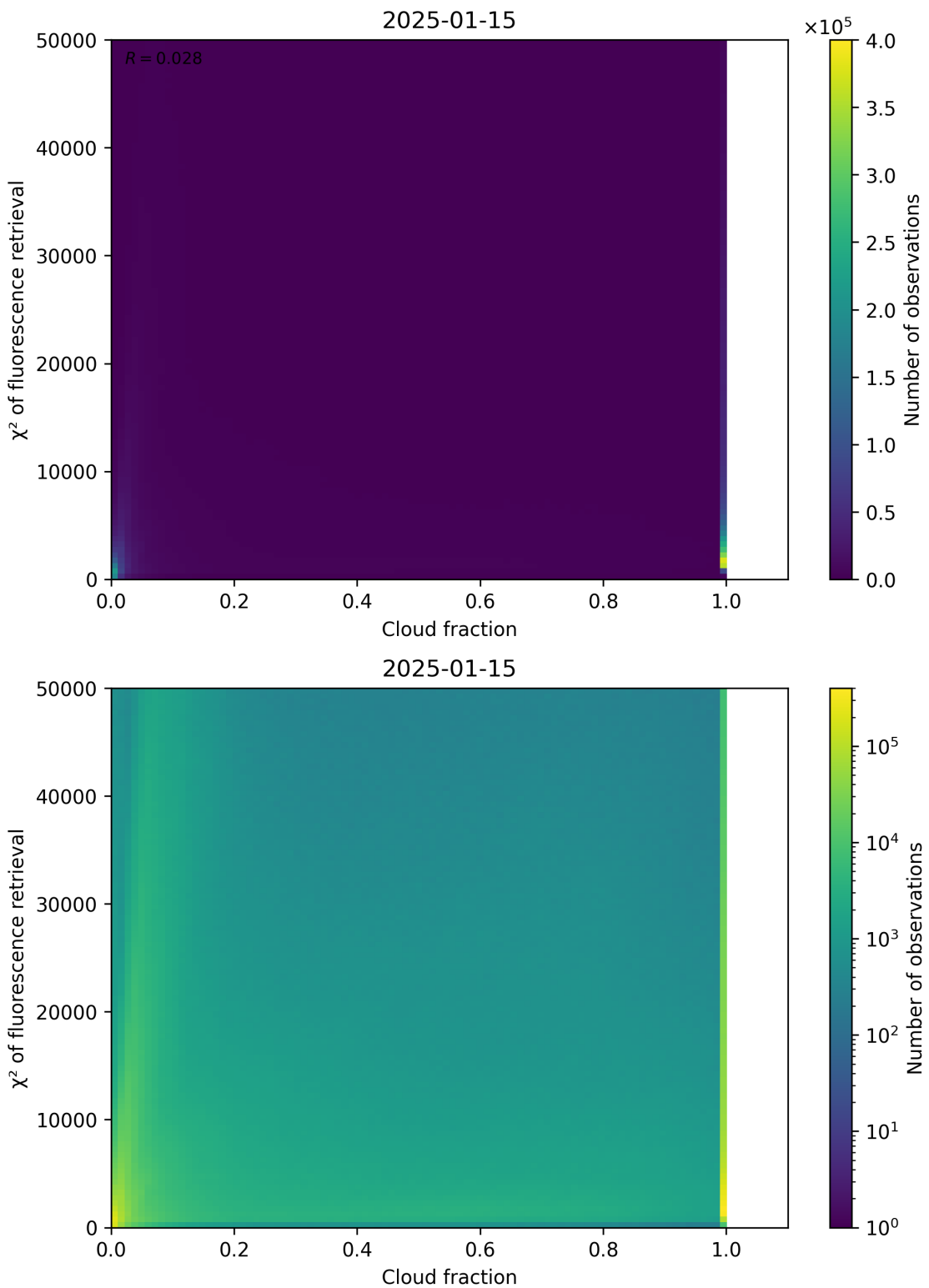


Figure 71: Scatter density plot of “Cloud fraction” against “ χ^2 of fluorescence retrieval” for 2025-01-14 to 2025-01-16.

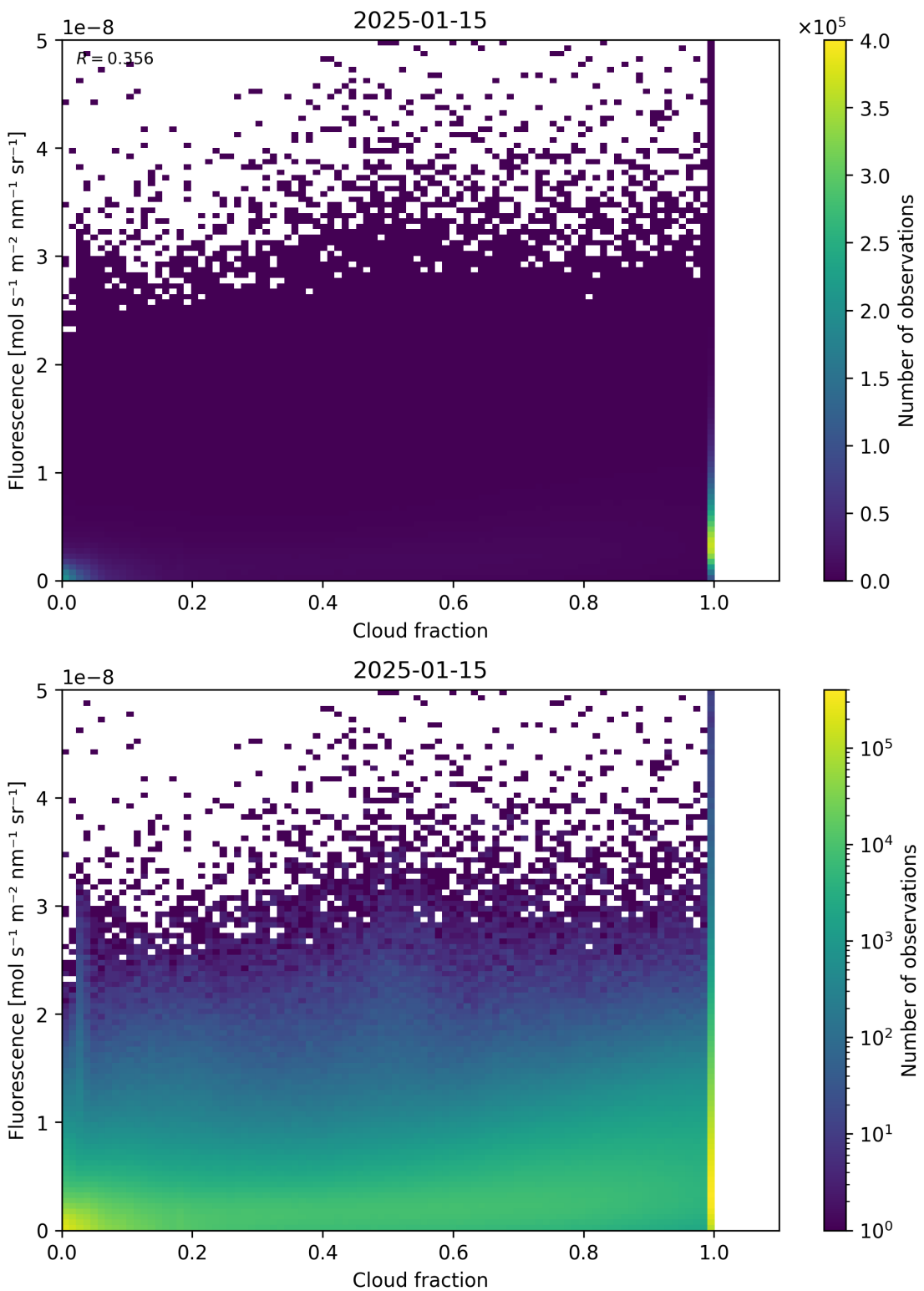


Figure 72: Scatter density plot of “Cloud fraction” against “Fluorescence” for 2025-01-14 to 2025-01-16.

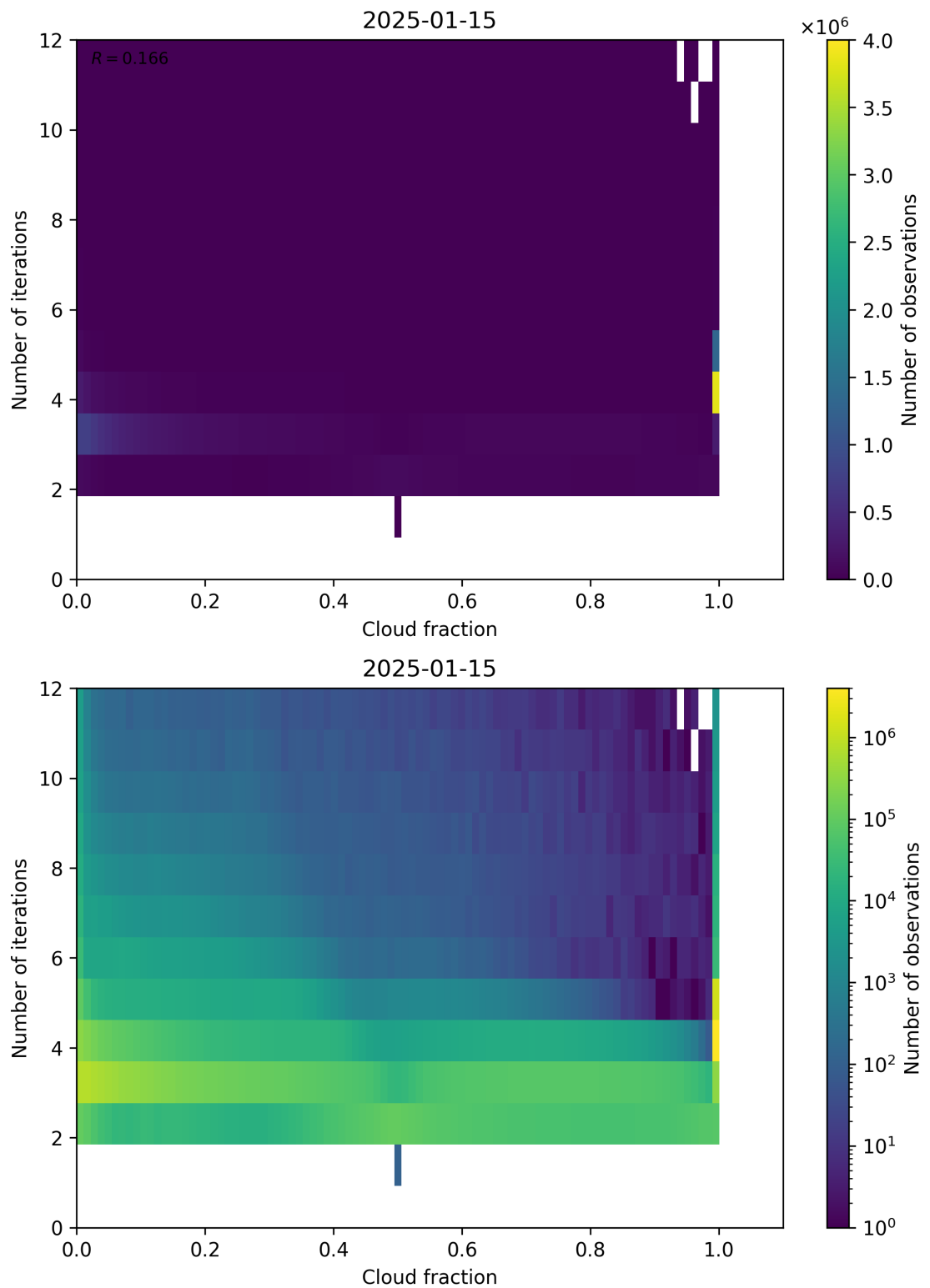


Figure 73: Scatter density plot of “Cloud fraction” against “Number of iterations” for 2025-01-14 to 2025-01-16.

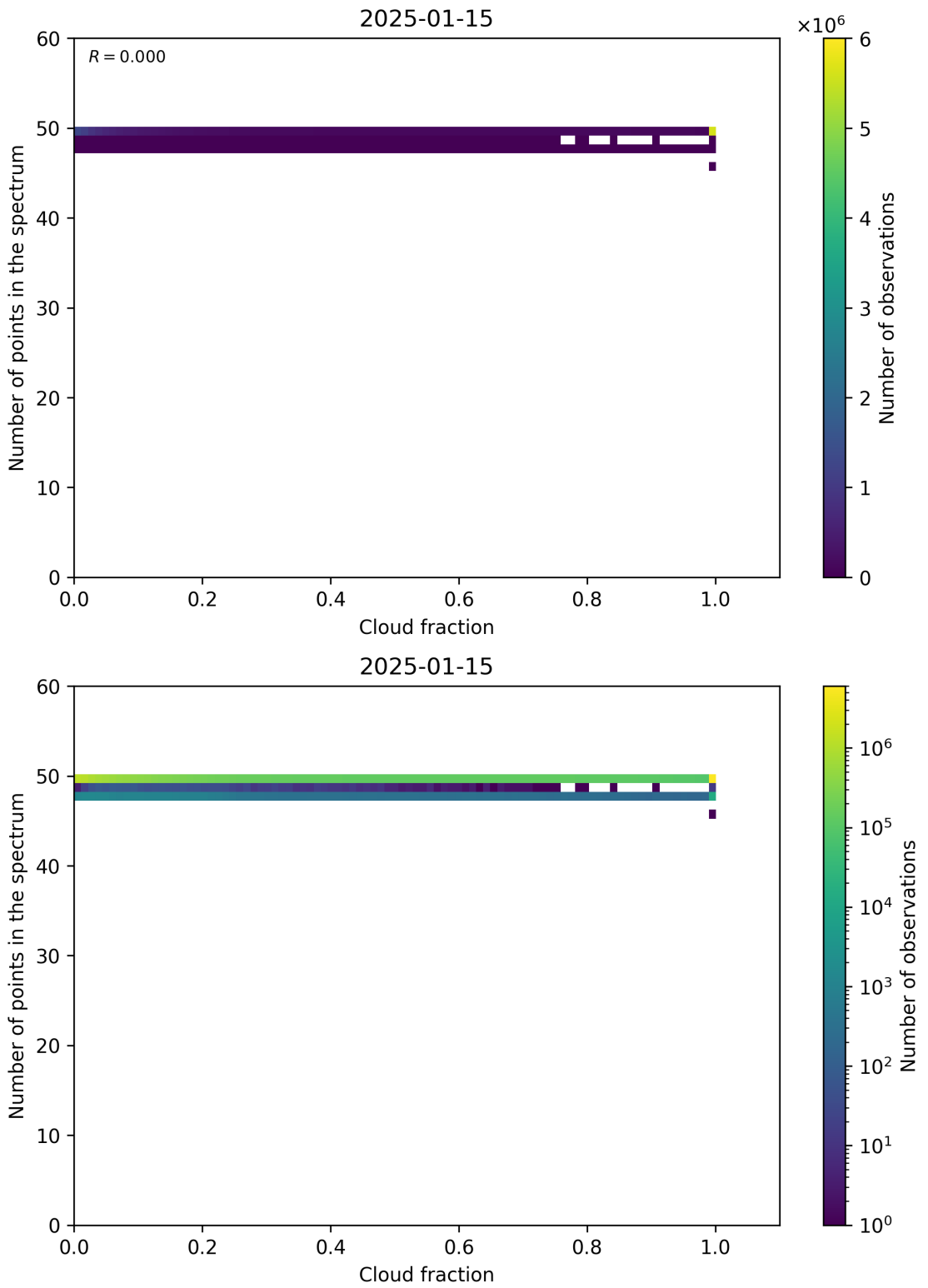


Figure 74: Scatter density plot of “Cloud fraction” against “Number of points in the spectrum” for 2025-01-14 to 2025-01-16.

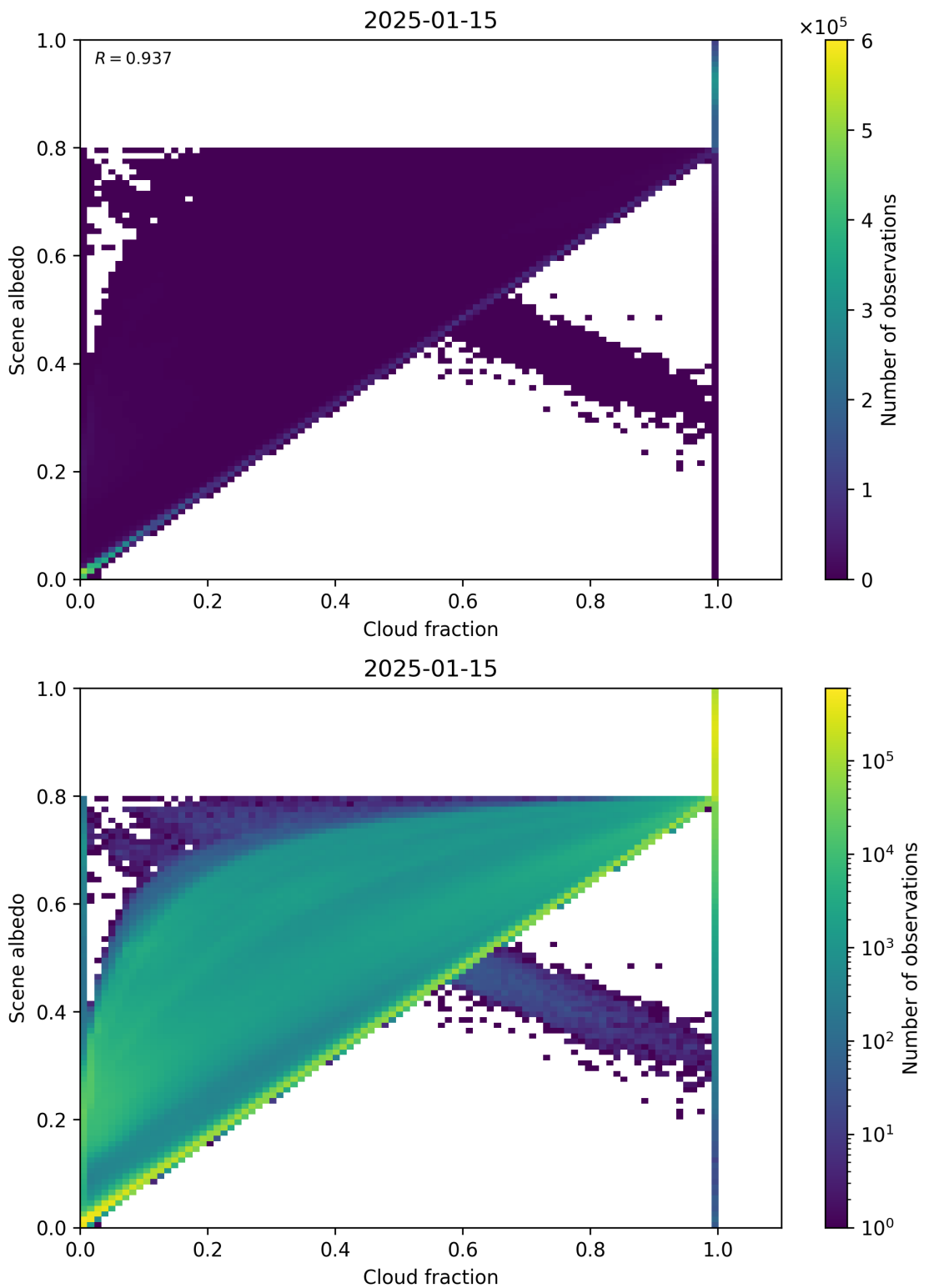


Figure 75: Scatter density plot of “Cloud fraction” against “Scene albedo” for 2025-01-14 to 2025-01-16.

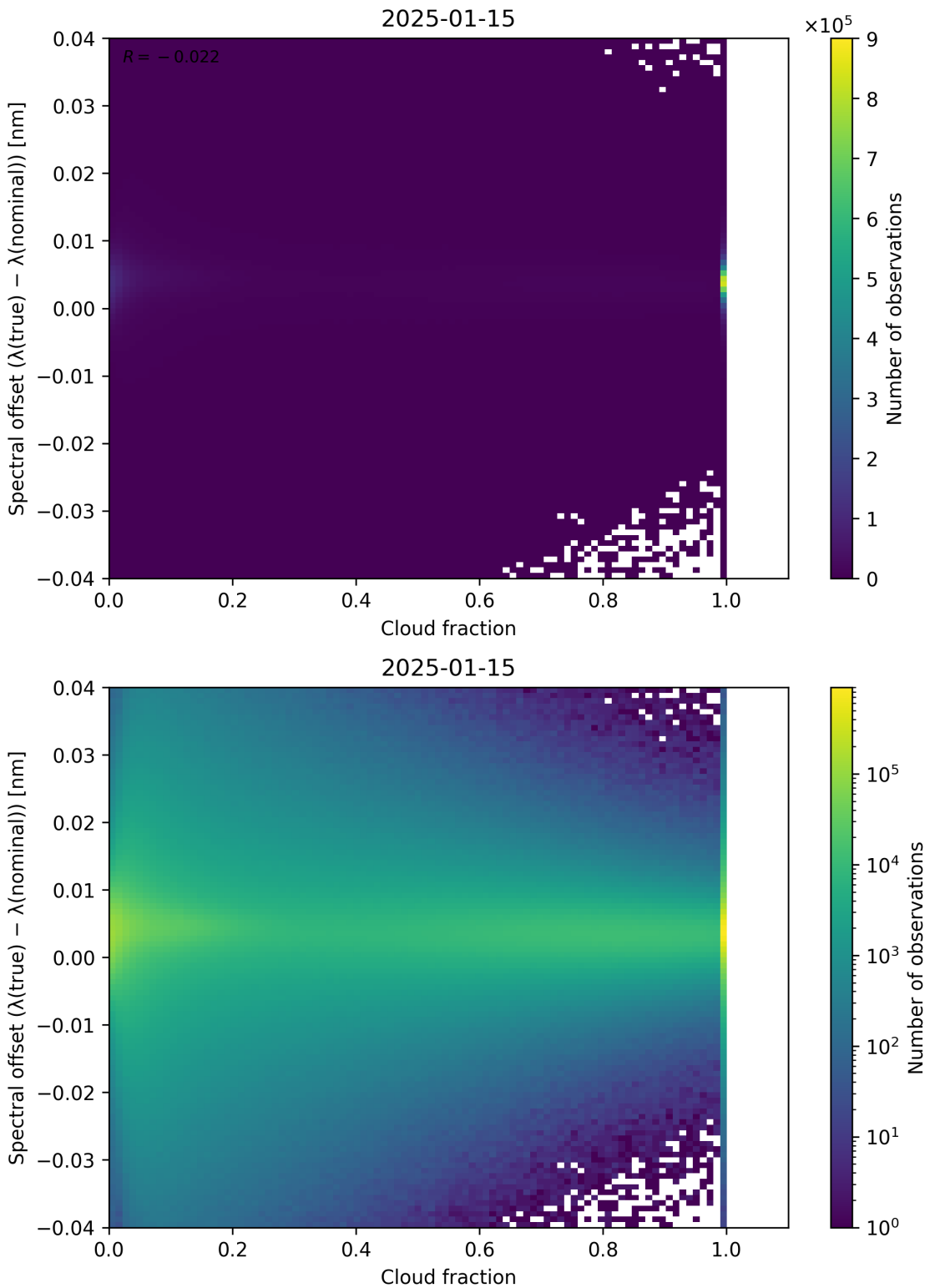


Figure 76: Scatter density plot of “Cloud fraction” against “Spectral offset ($\lambda_{\text{true}} - \lambda_{\text{nominal}}$)” for 2025-01-14 to 2025-01-16.

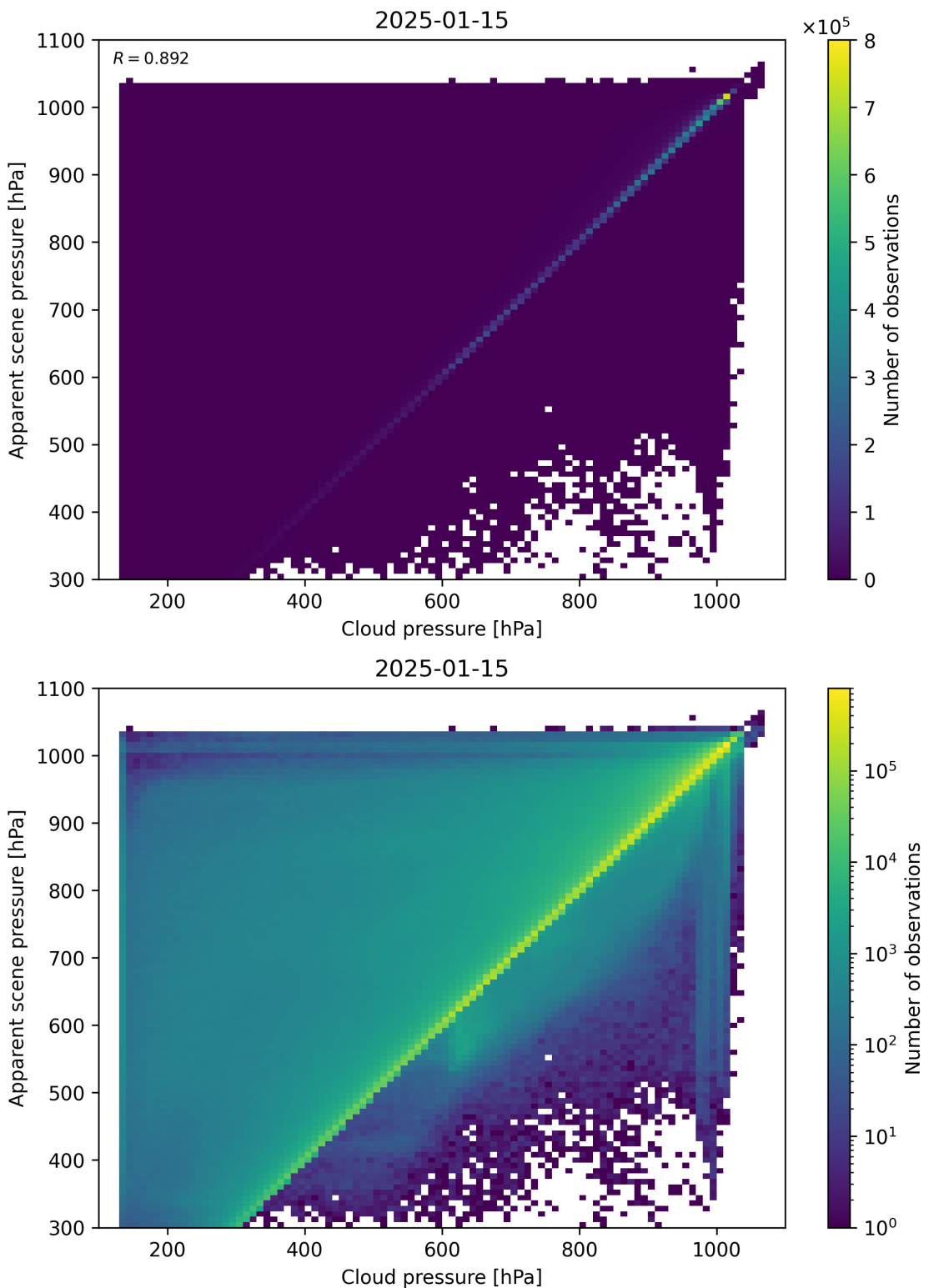


Figure 77: Scatter density plot of “Cloud pressure” against “Apparent scene pressure” for 2025-01-14 to 2025-01-16.

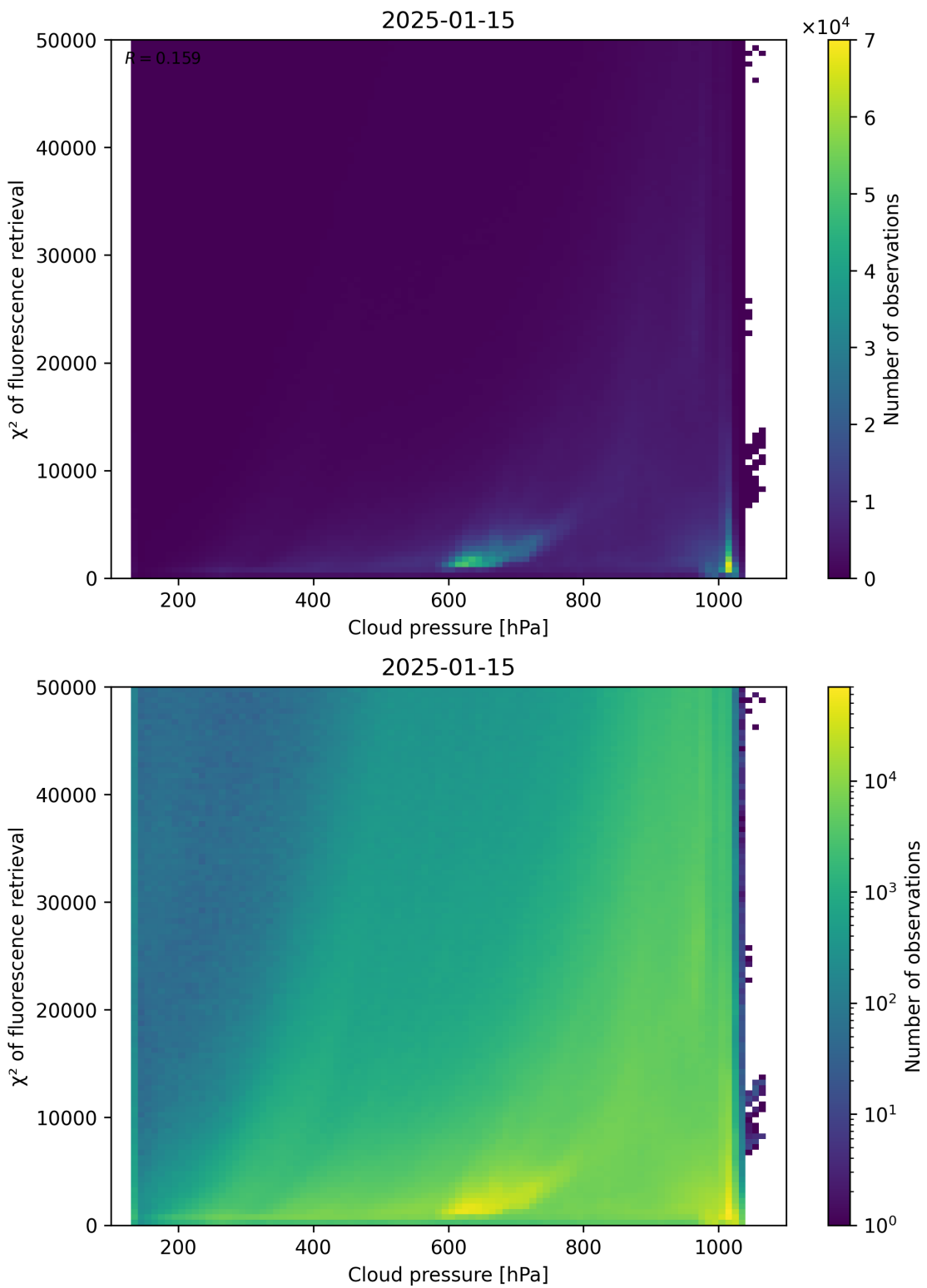


Figure 78: Scatter density plot of “Cloud pressure” against “ χ^2 of fluorescence retrieval” for 2025-01-14 to 2025-01-16.

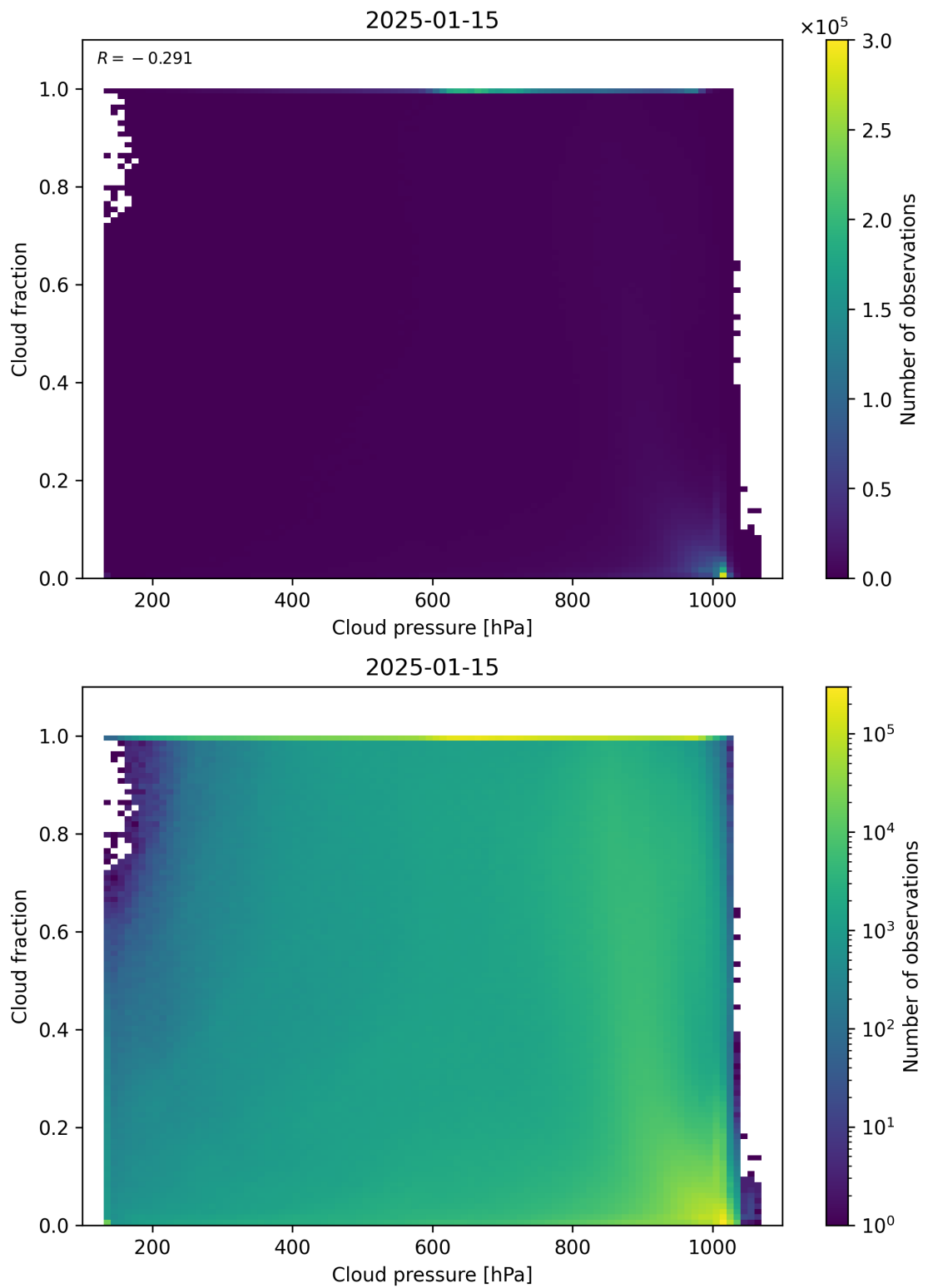


Figure 79: Scatter density plot of “Cloud pressure” against “Cloud fraction” for 2025-01-14 to 2025-01-16.

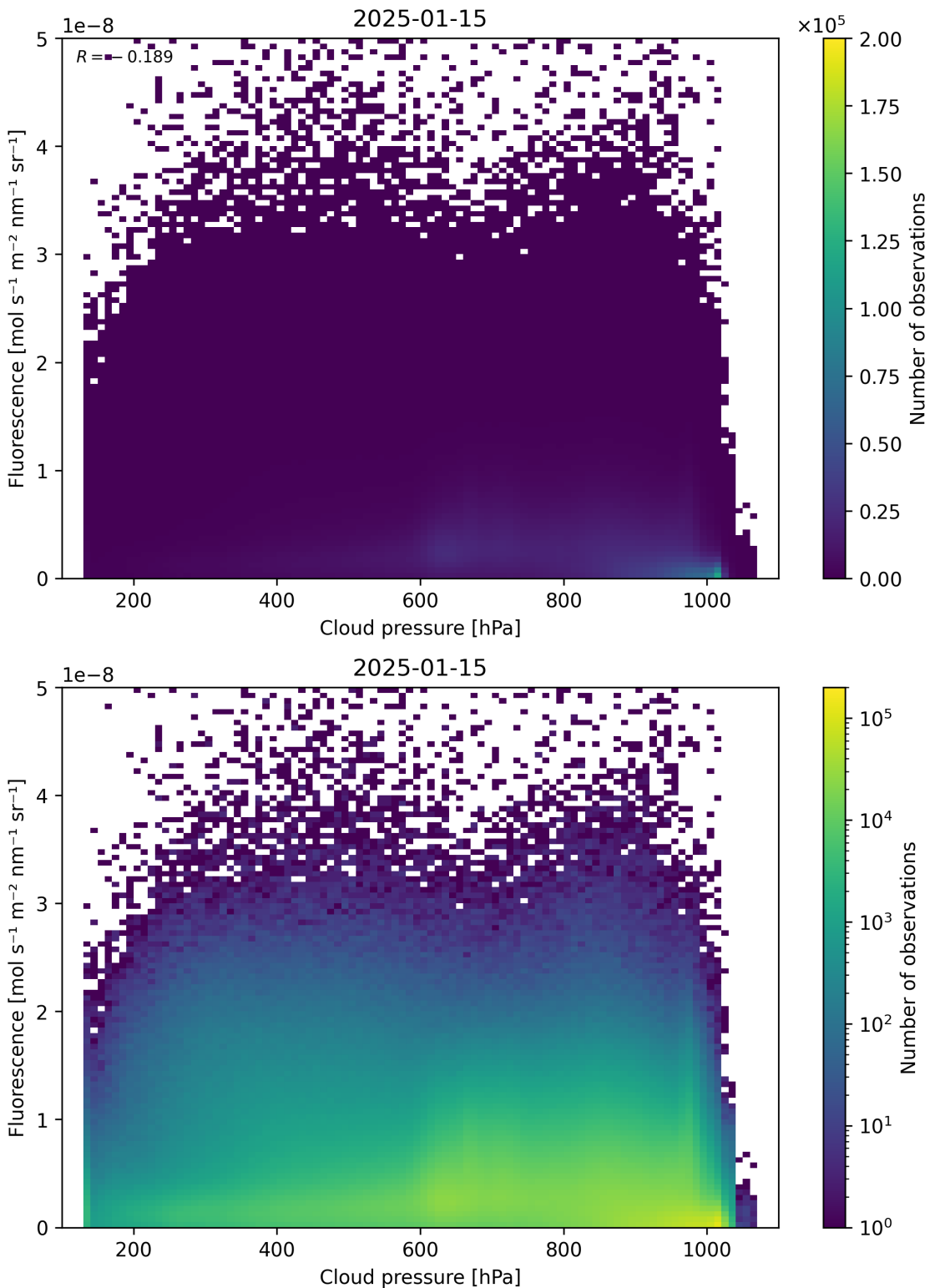


Figure 80: Scatter density plot of “Cloud pressure” against “Fluorescence” for 2025-01-14 to 2025-01-16.

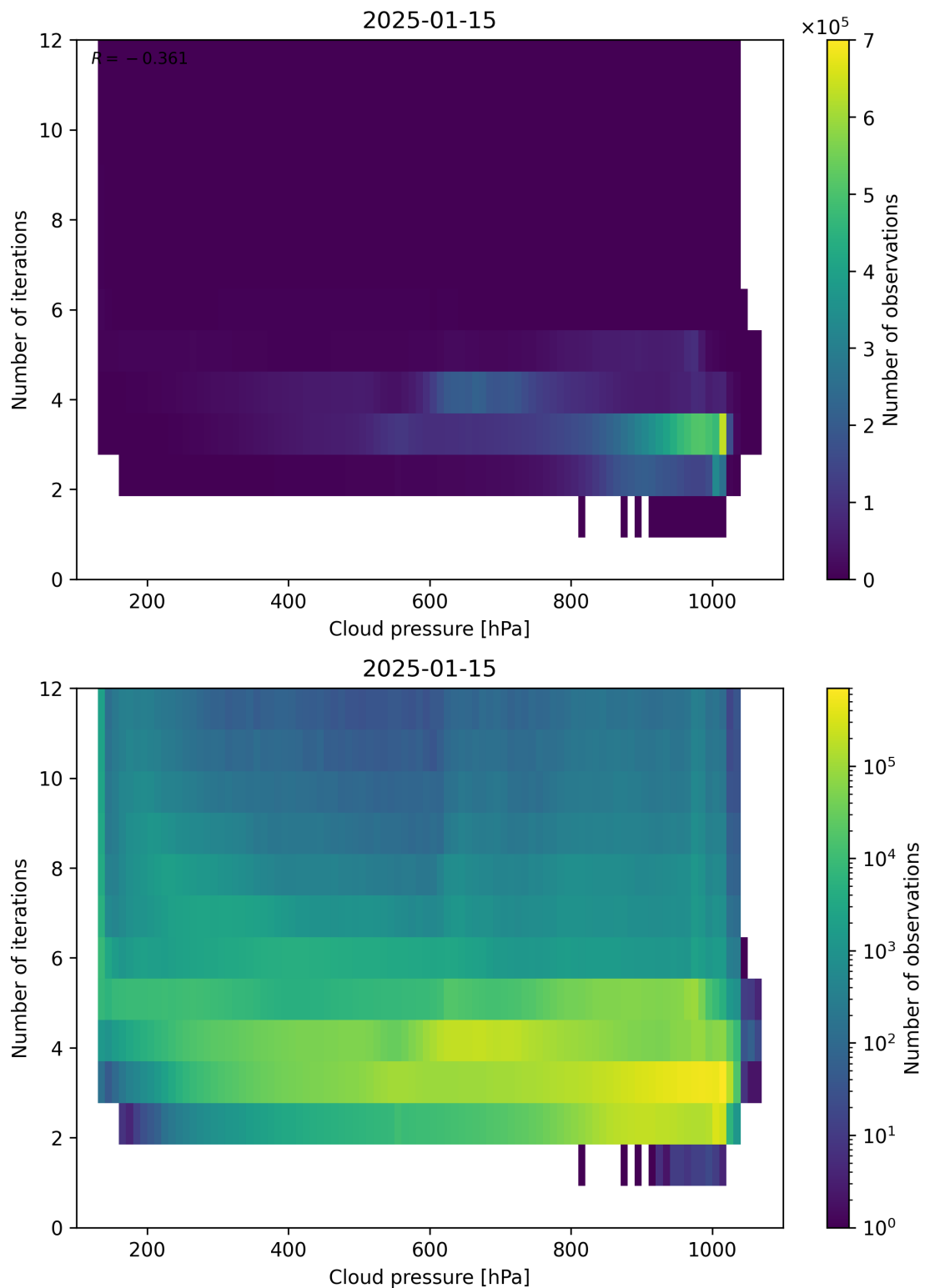


Figure 81: Scatter density plot of “Cloud pressure” against “Number of iterations” for 2025-01-14 to 2025-01-16.

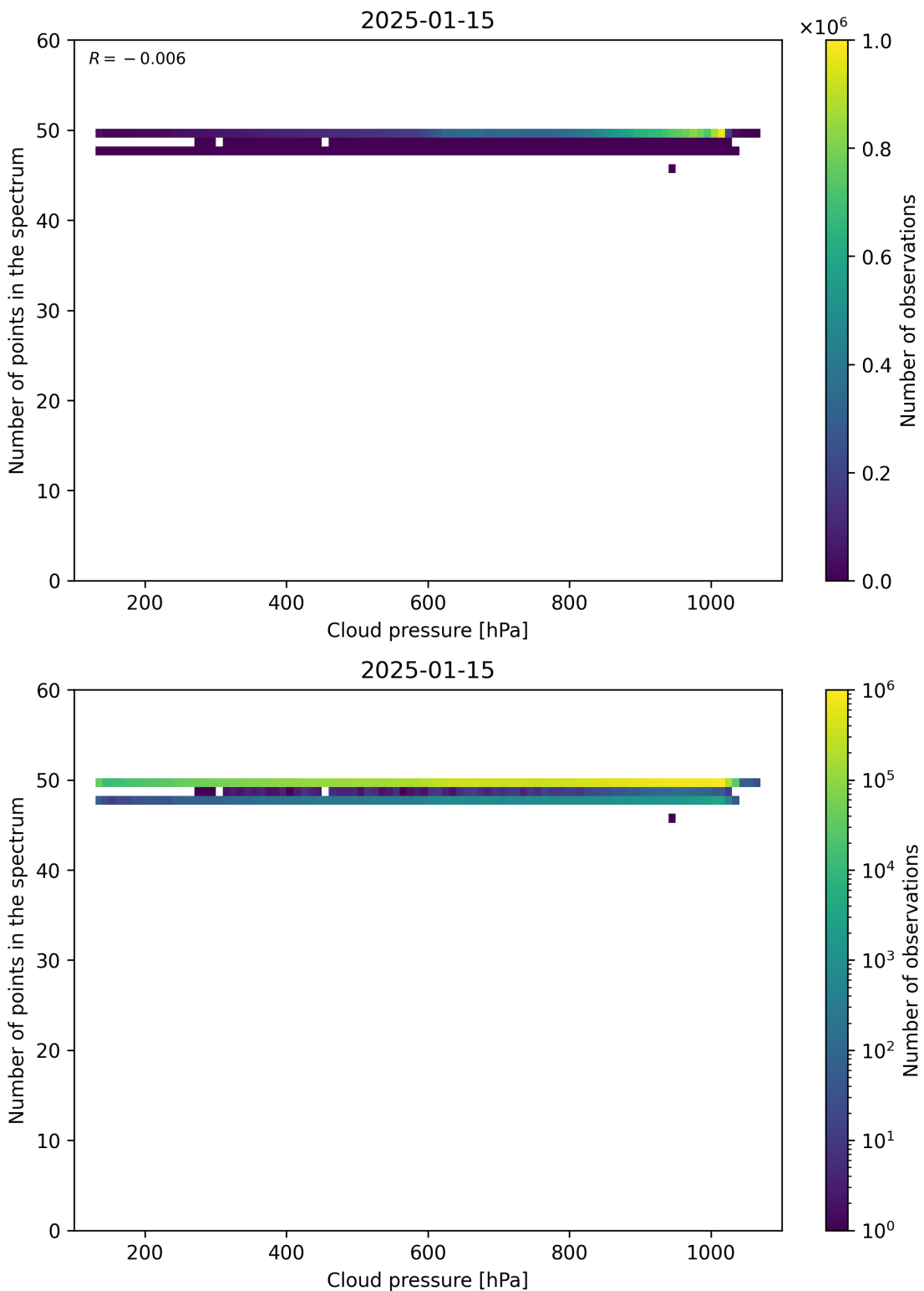


Figure 82: Scatter density plot of “Cloud pressure” against “Number of points in the spectrum” for 2025-01-14 to 2025-01-16.

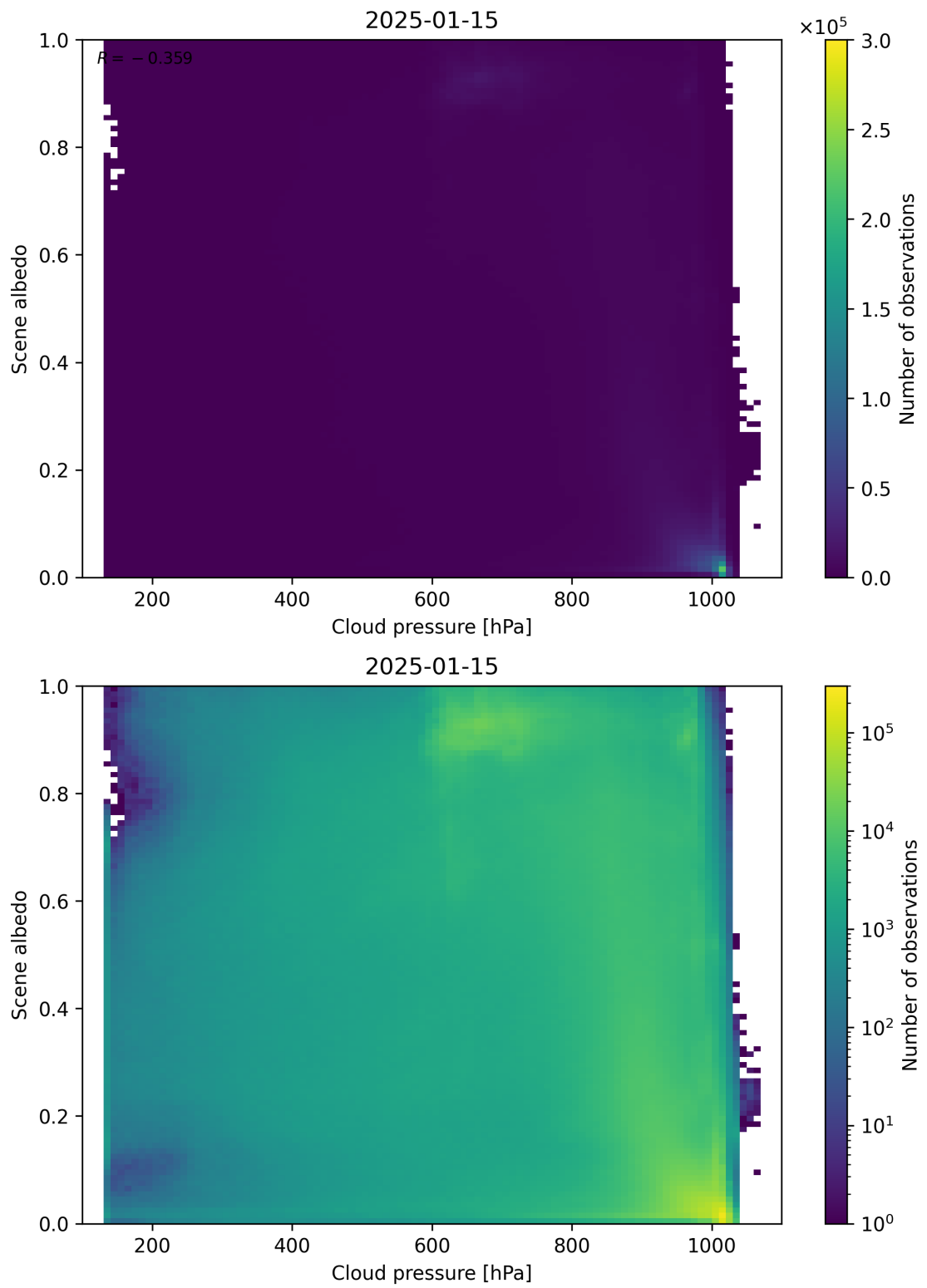


Figure 83: Scatter density plot of “Cloud pressure” against “Scene albedo” for 2025-01-14 to 2025-01-16.

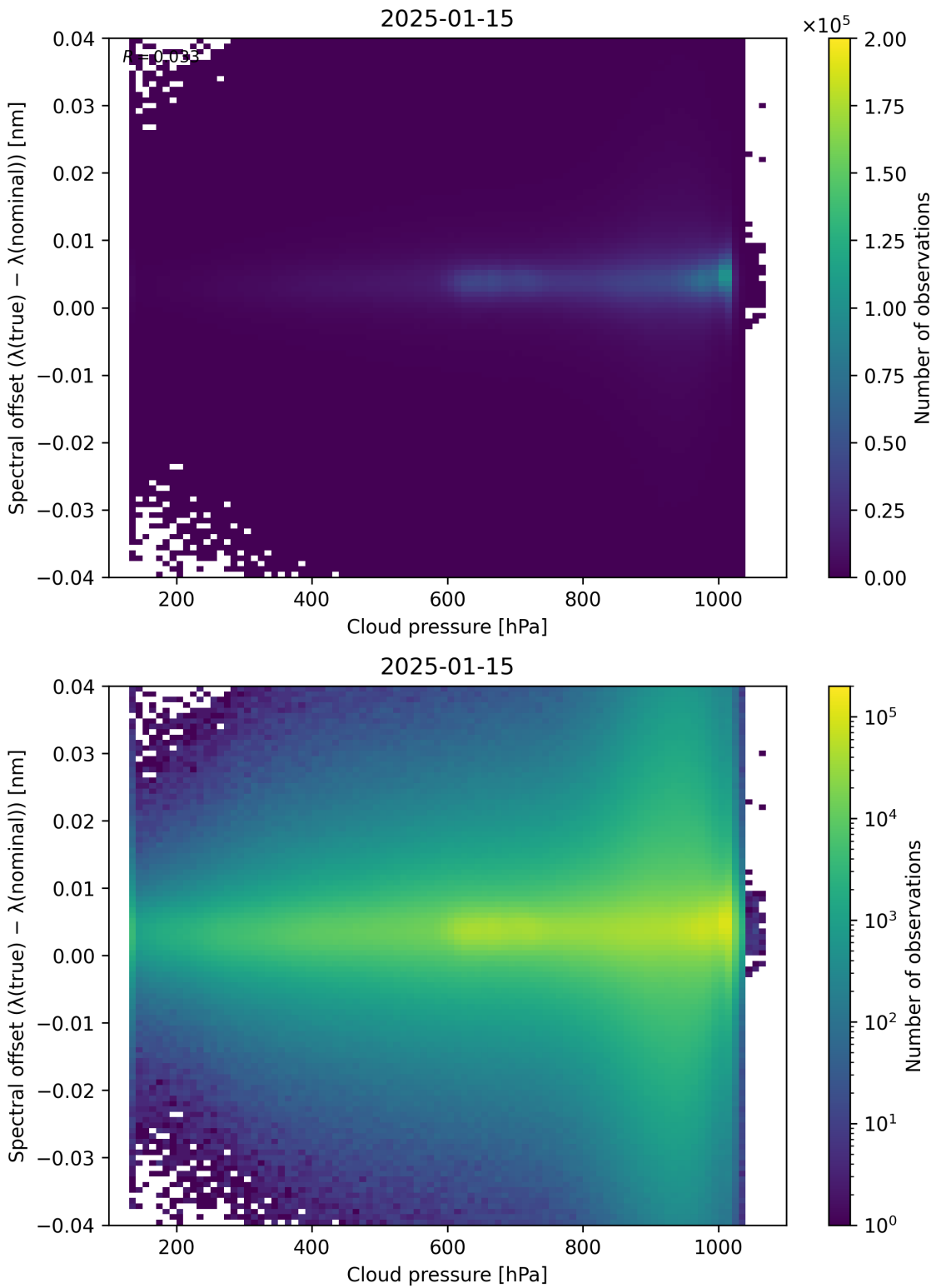


Figure 84: Scatter density plot of “Cloud pressure” against “Spectral offset ($\lambda_{\text{true}} - \lambda_{\text{nominal}}$)” for 2025-01-14 to 2025-01-16.

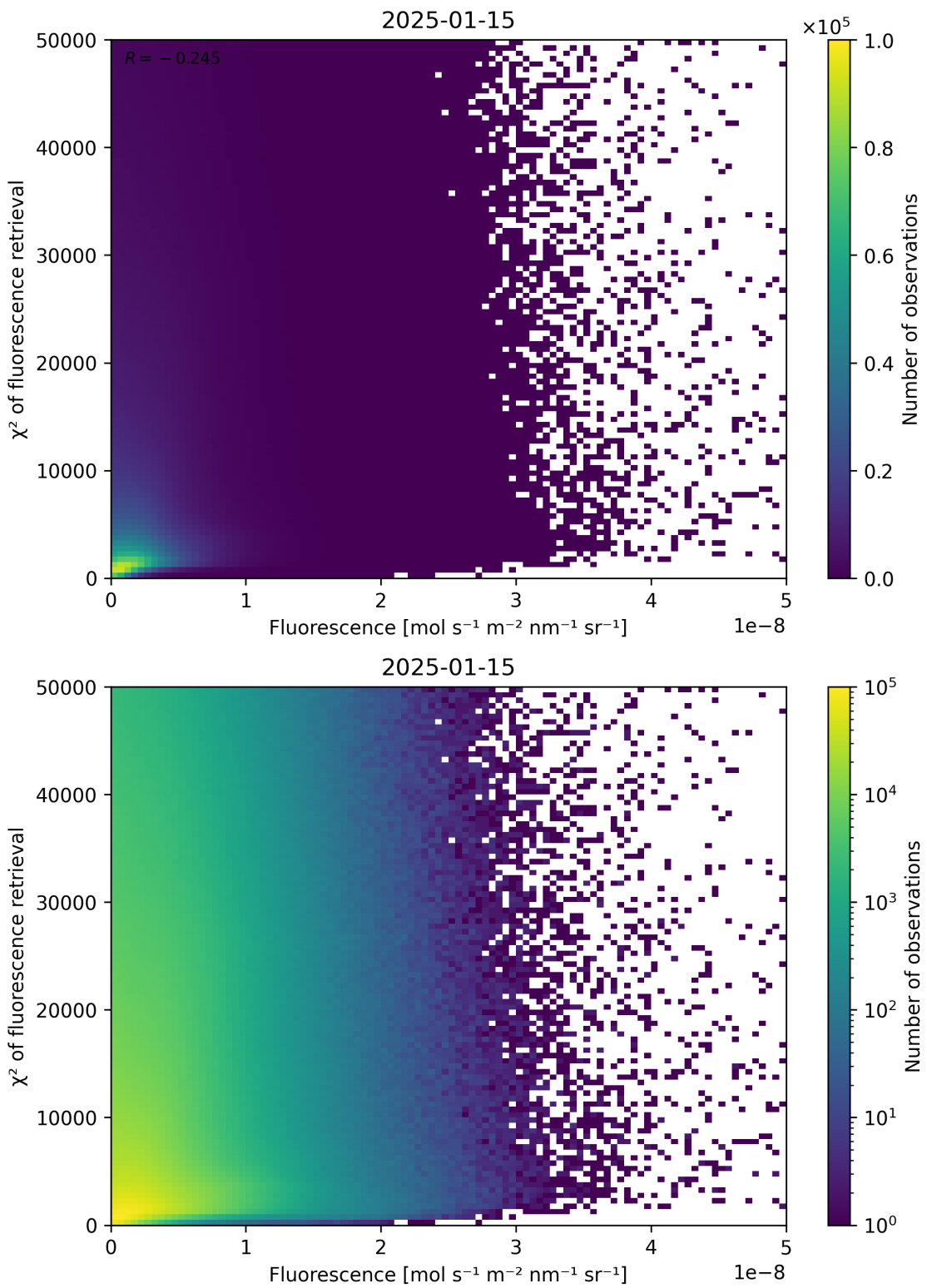


Figure 85: Scatter density plot of “Fluorescence” against “ χ^2 of fluorescence retrieval” for 2025-01-14 to 2025-01-16.

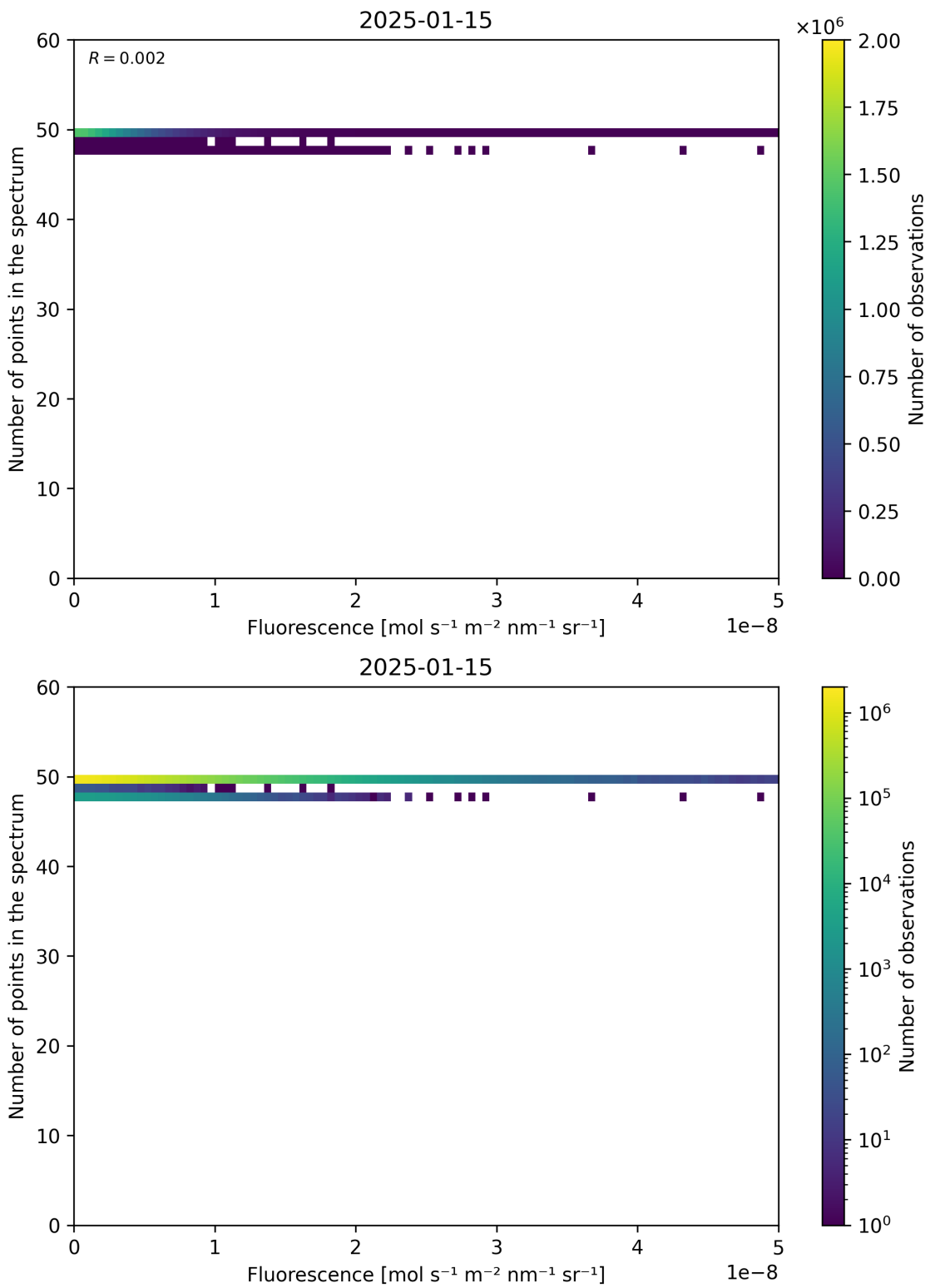


Figure 86: Scatter density plot of “Fluorescence” against “Number of points in the spectrum” for 2025-01-14 to 2025-01-16.

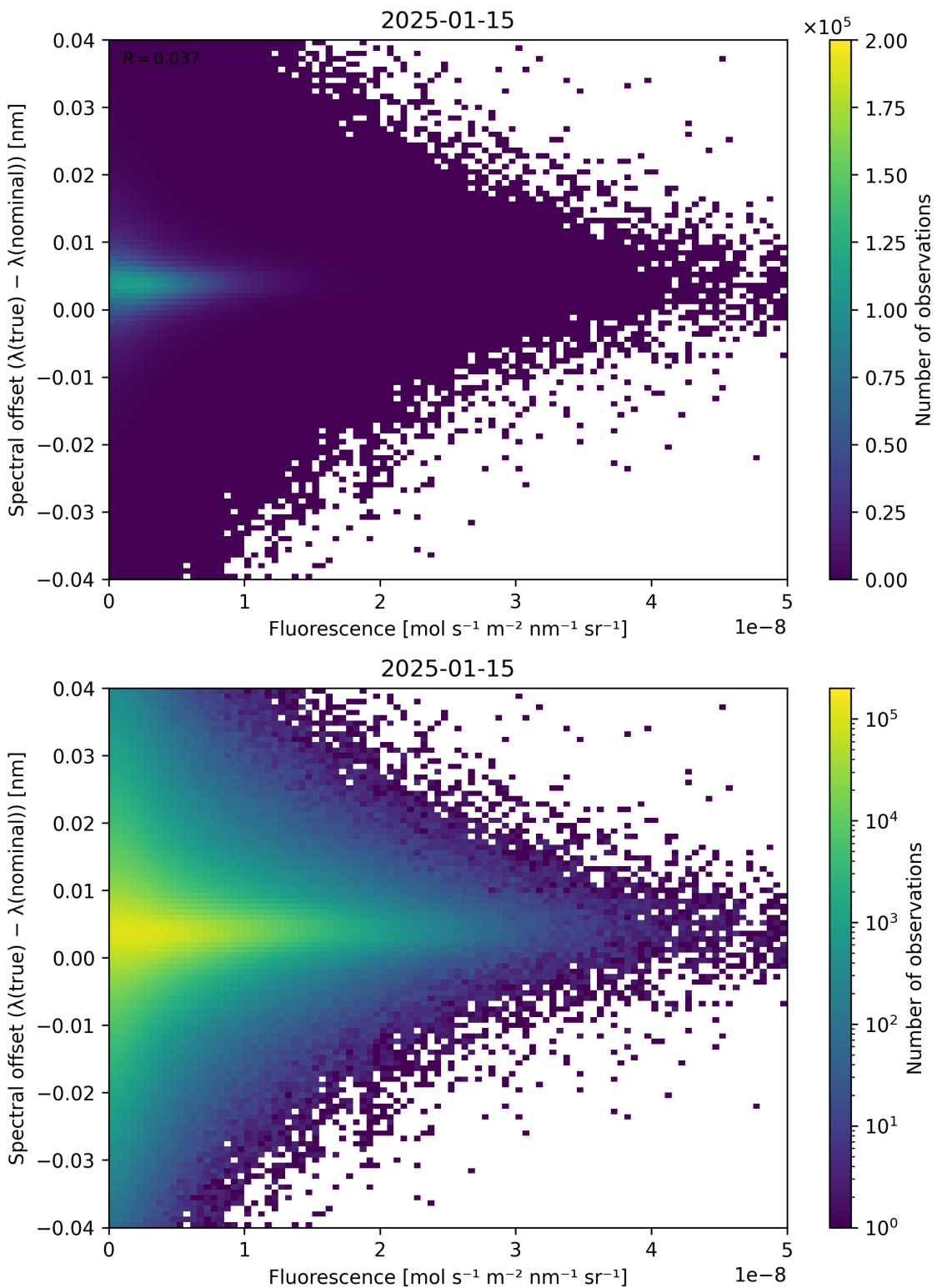


Figure 87: Scatter density plot of “Fluorescence” against “Spectral offset ($\lambda_{\text{true}} - \lambda_{\text{nominal}}$)” for 2025-01-14 to 2025-01-16.

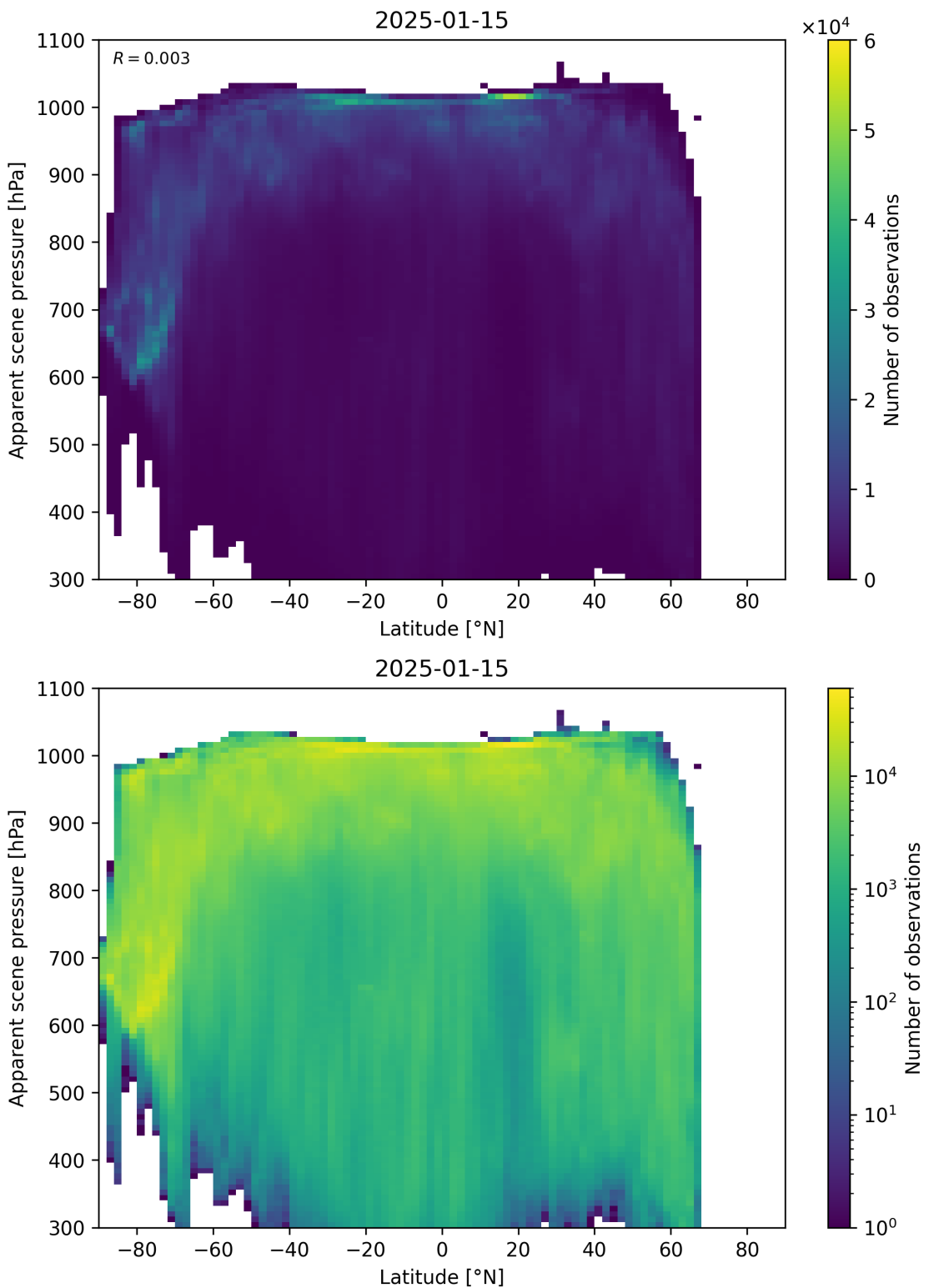


Figure 88: Scatter density plot of “Latitude” against “Apparent scene pressure” for 2025-01-14 to 2025-01-16.

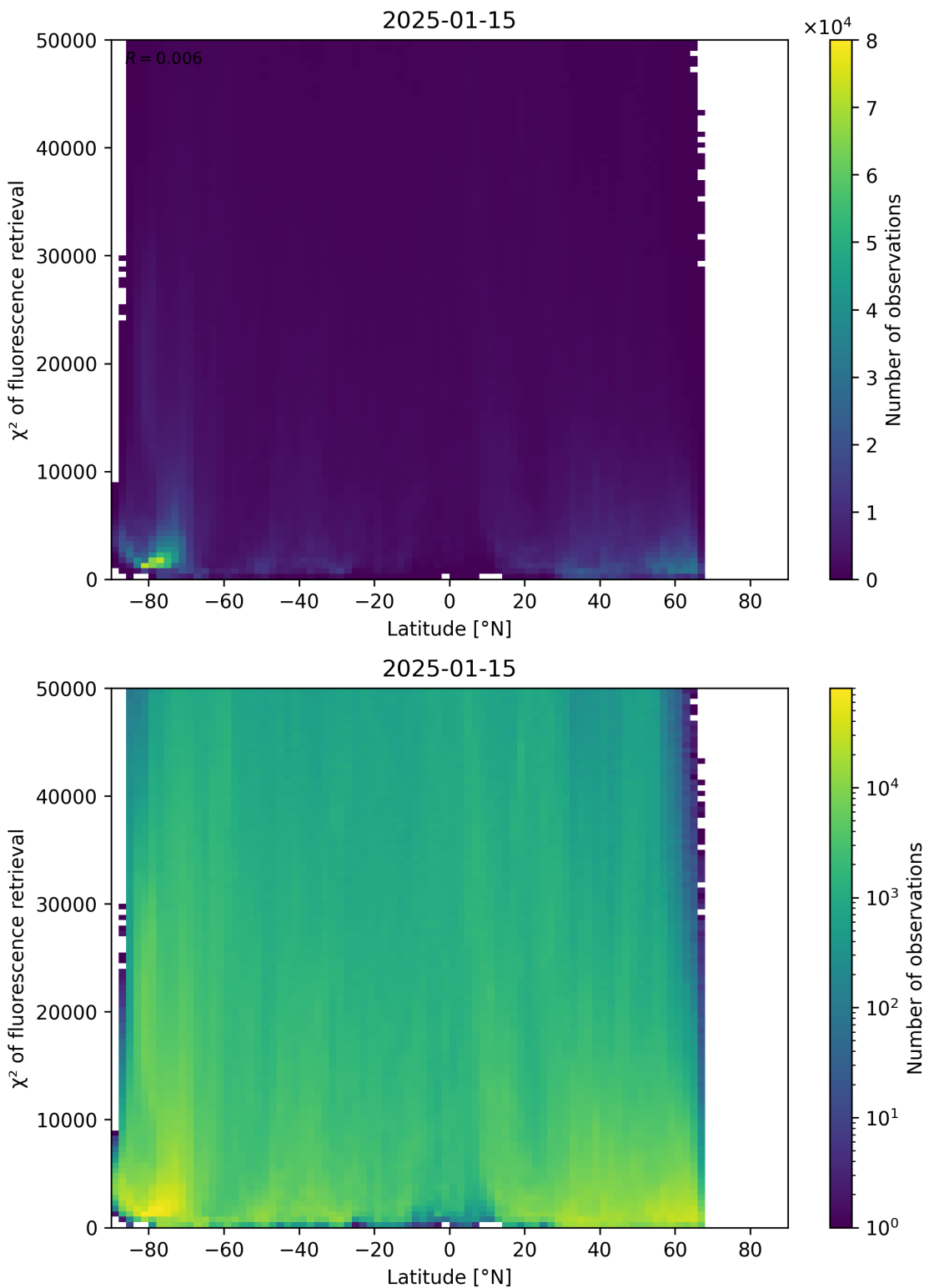


Figure 89: Scatter density plot of “Latitude” against “ χ^2 of fluorescence retrieval” for 2025-01-14 to 2025-01-16.

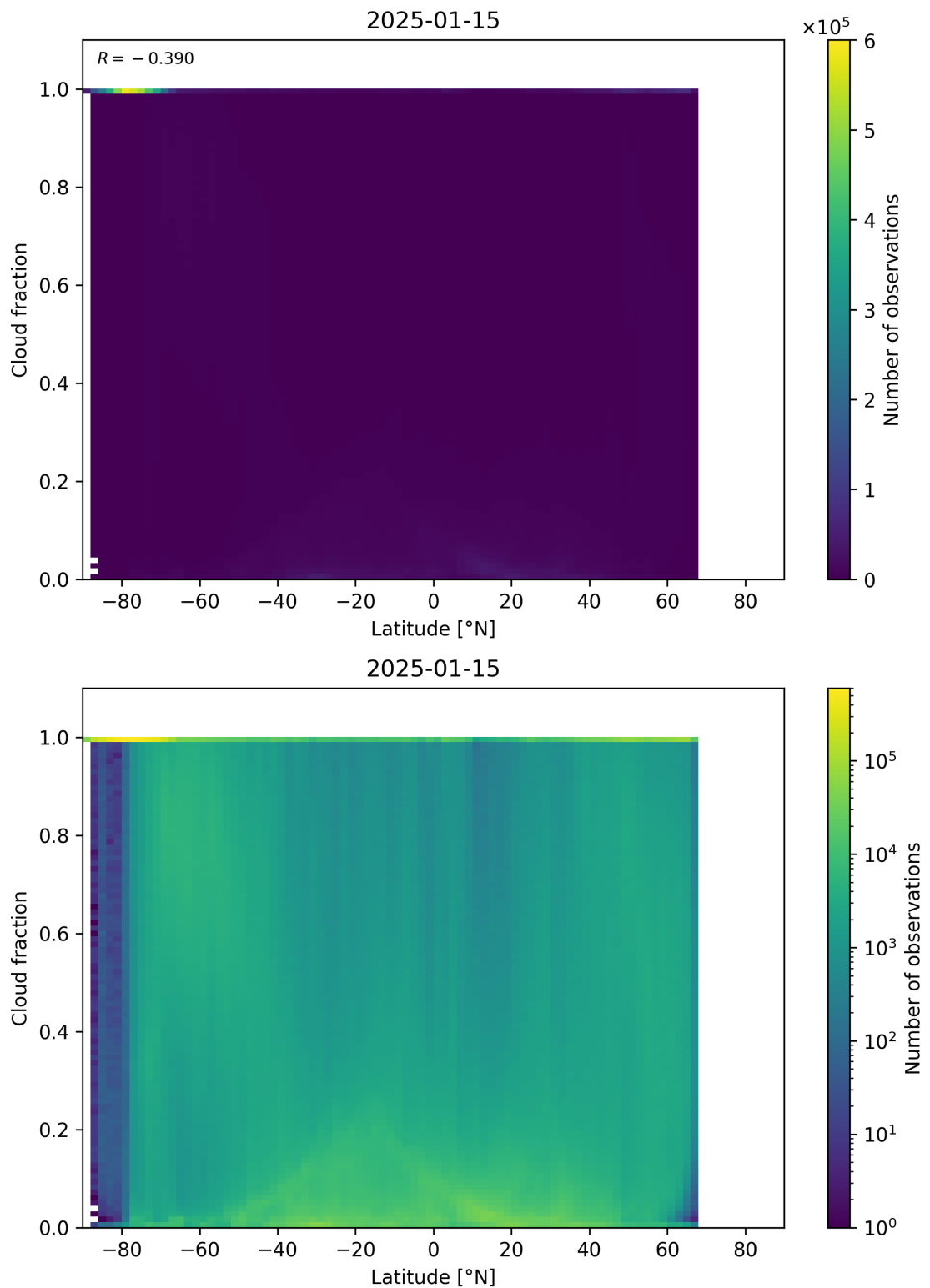


Figure 90: Scatter density plot of “Latitude” against “Cloud fraction” for 2025-01-14 to 2025-01-16.

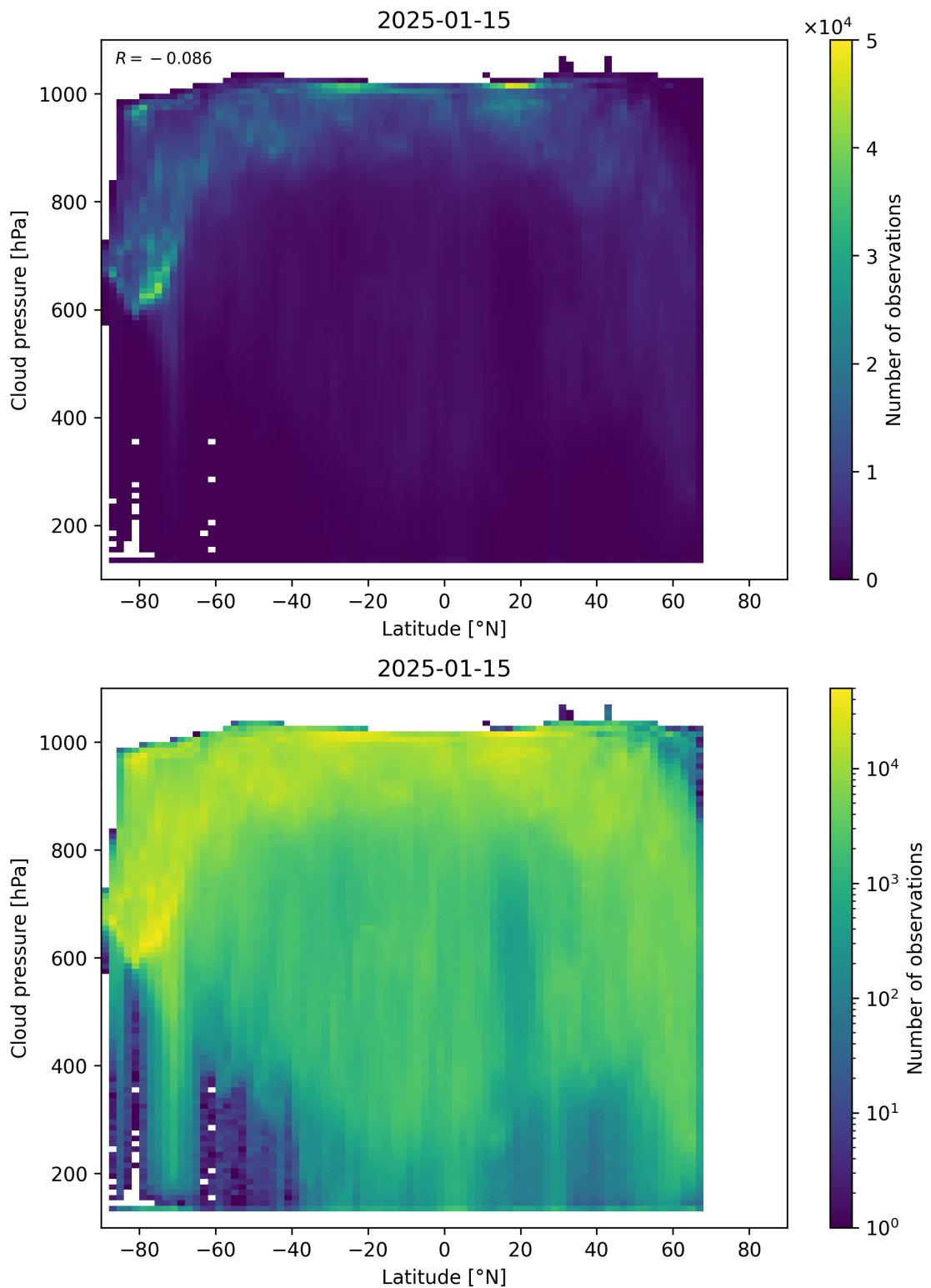


Figure 91: Scatter density plot of “Latitude” against “Cloud pressure” for 2025-01-14 to 2025-01-16.

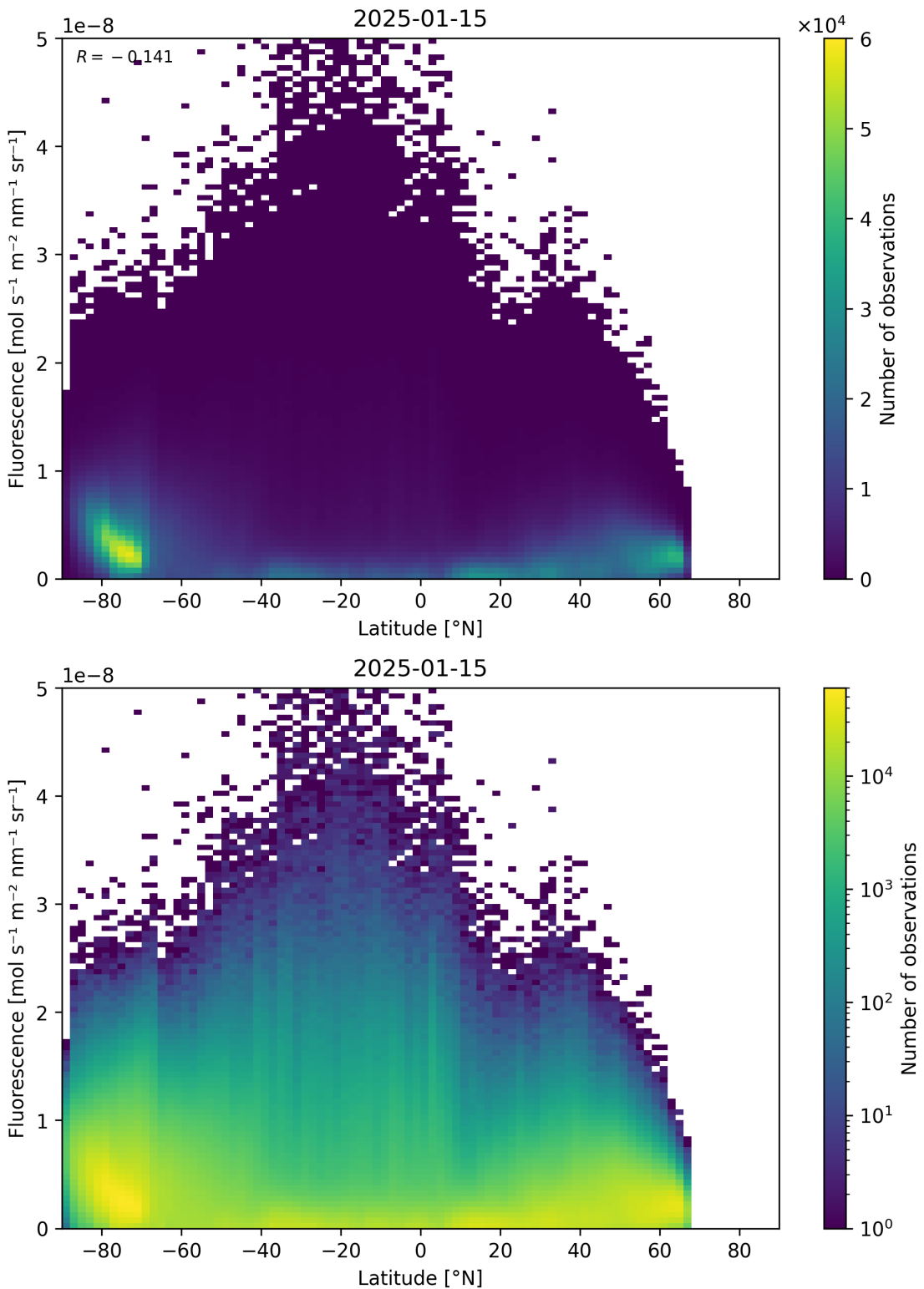


Figure 92: Scatter density plot of “Latitude” against “Fluorescence” for 2025-01-14 to 2025-01-16.

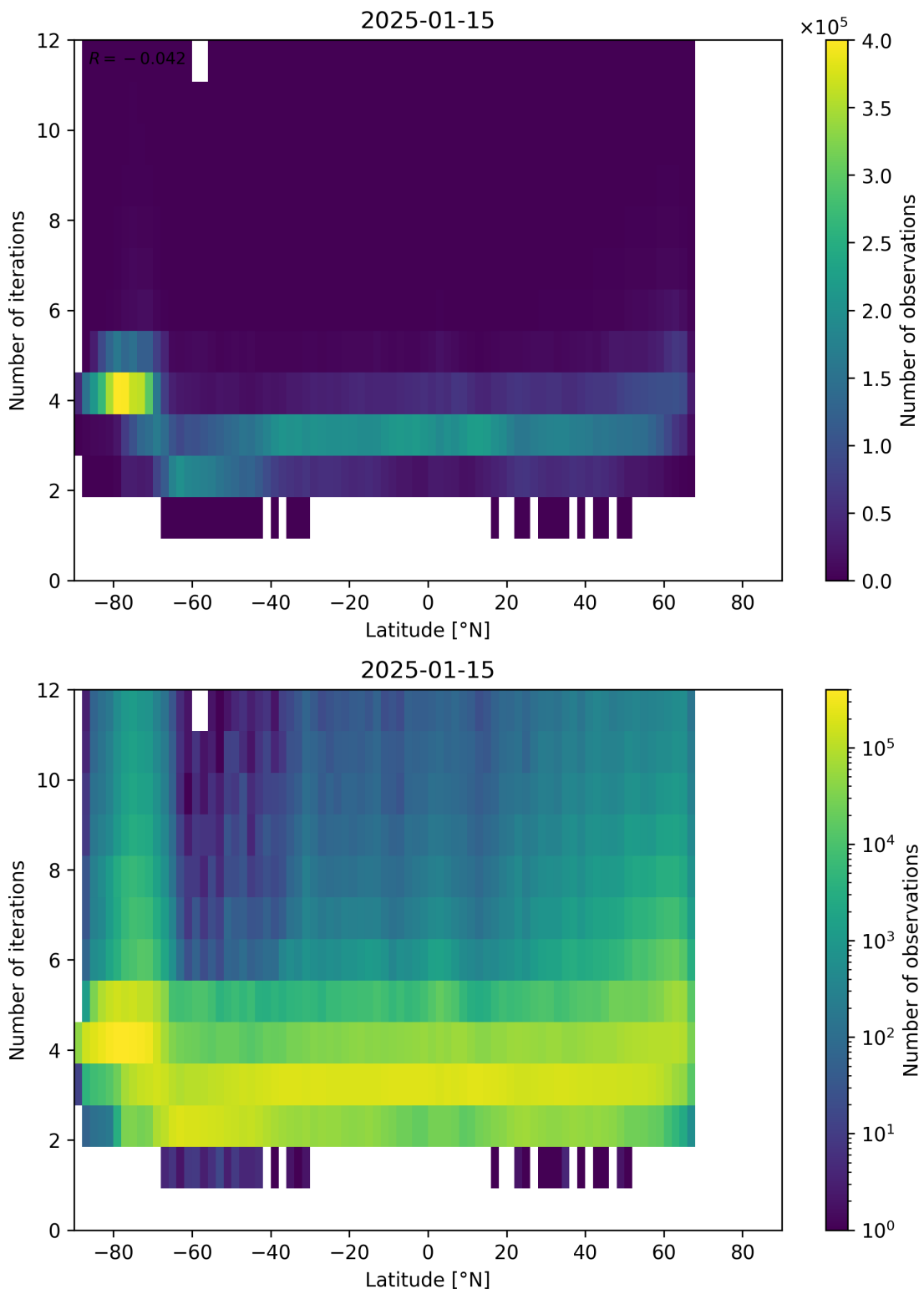


Figure 93: Scatter density plot of “Latitude” against “Number of iterations” for 2025-01-14 to 2025-01-16.

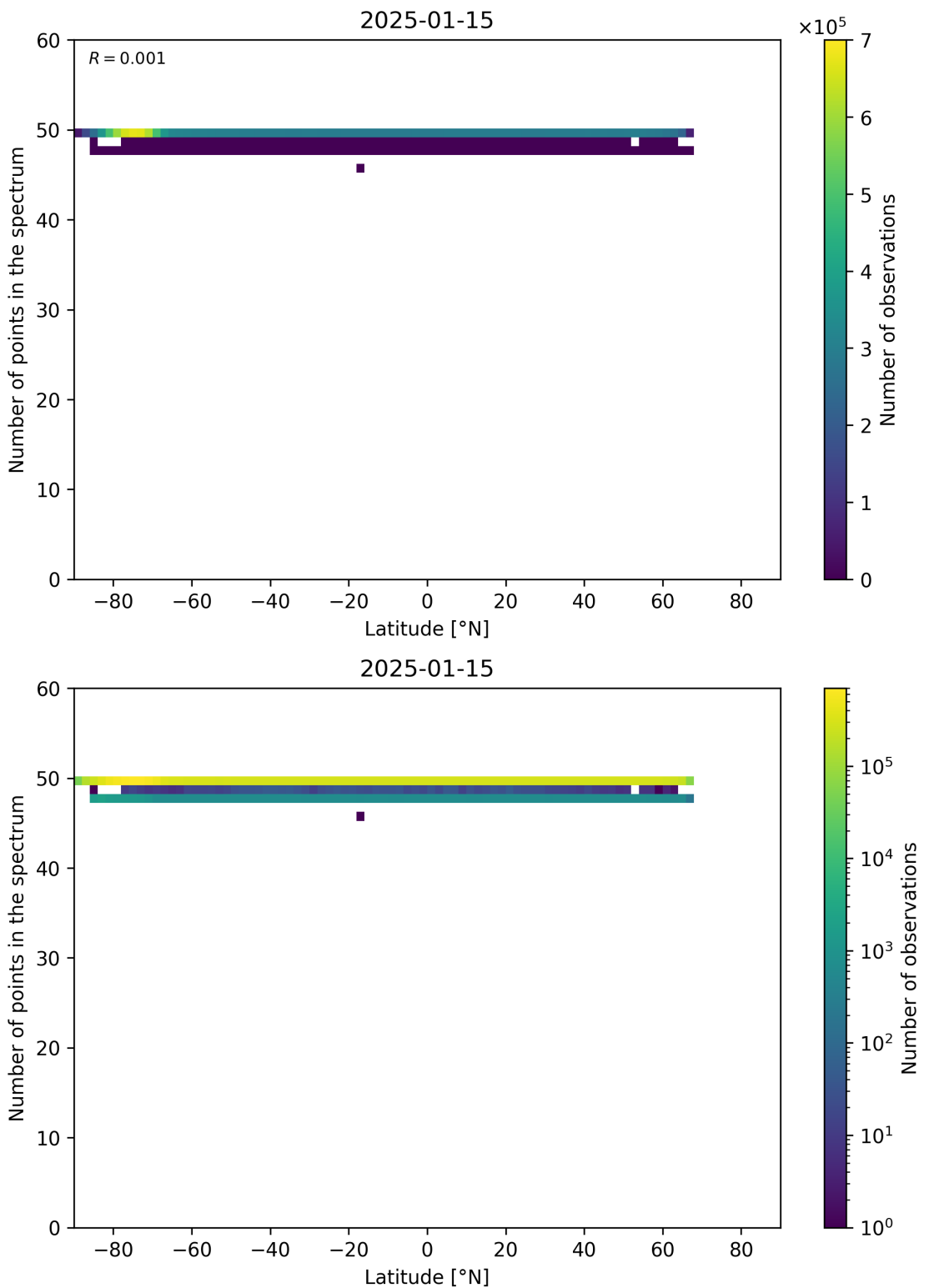


Figure 94: Scatter density plot of “Latitude” against “Number of points in the spectrum” for 2025-01-14 to 2025-01-16.

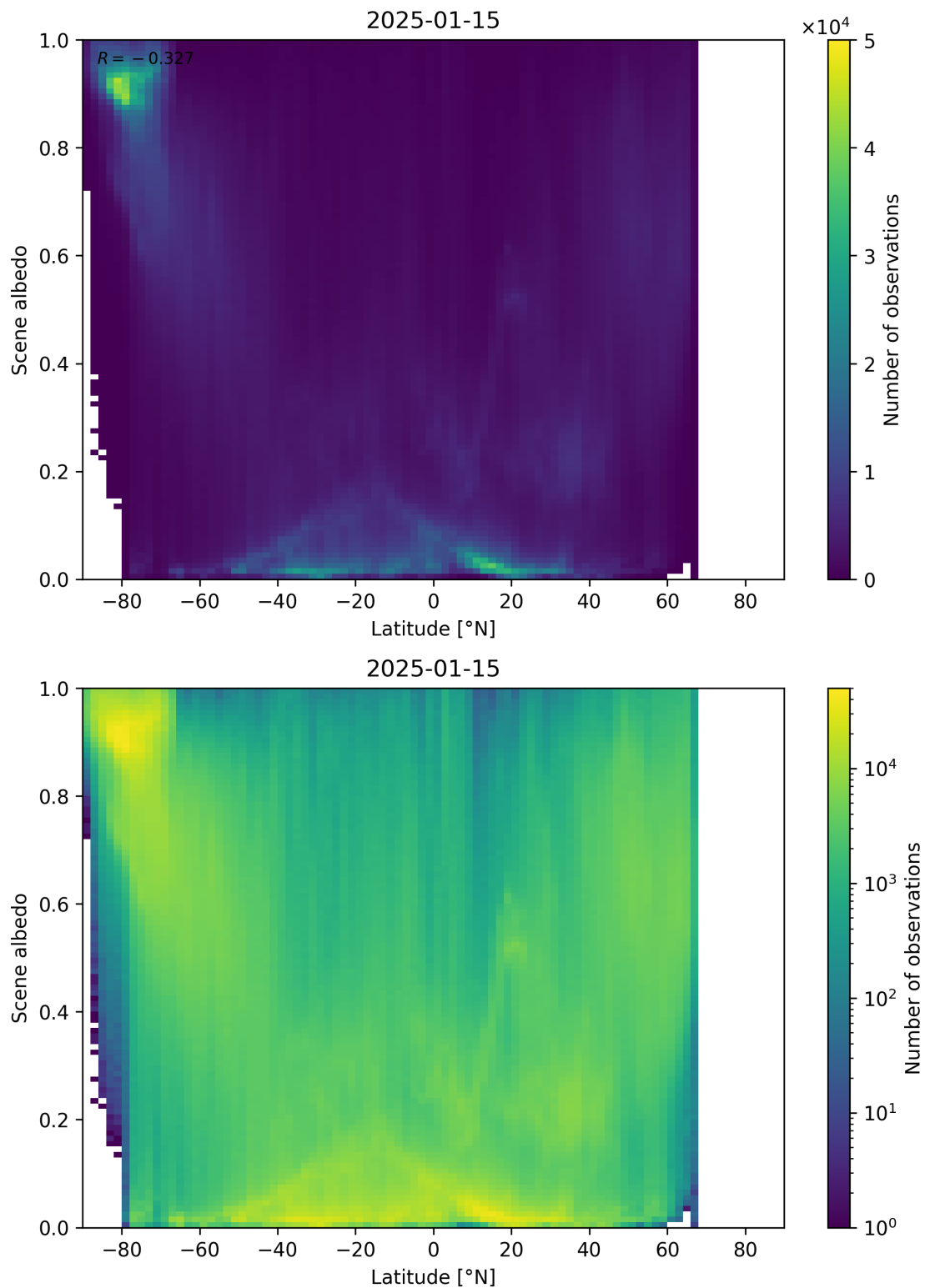


Figure 95: Scatter density plot of “Latitude” against “Scene albedo” for 2025-01-14 to 2025-01-16.

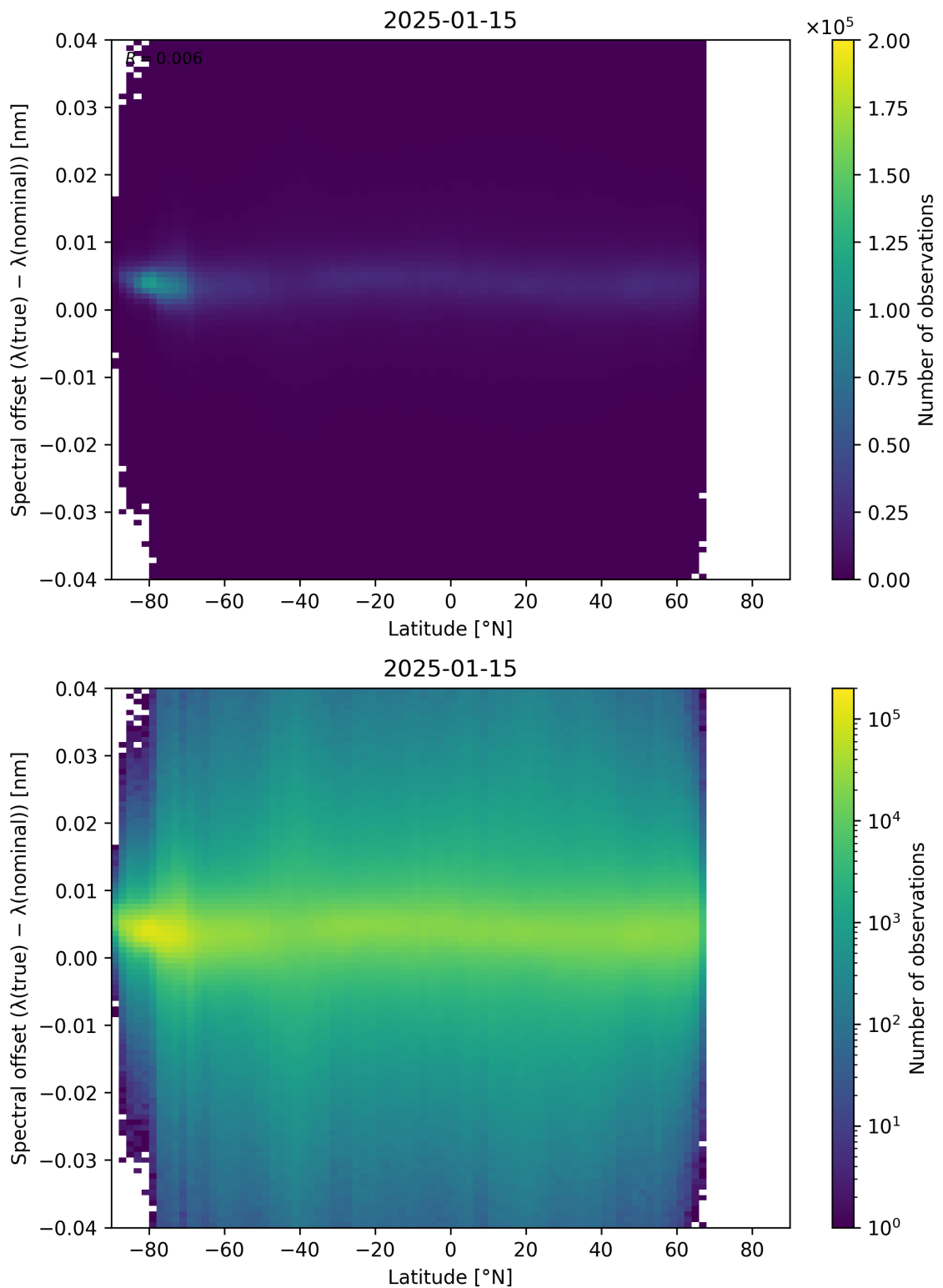


Figure 96: Scatter density plot of “Latitude” against “Spectral offset ($\lambda_{\text{true}} - \lambda_{\text{nominal}}$)” for 2025-01-14 to 2025-01-16.

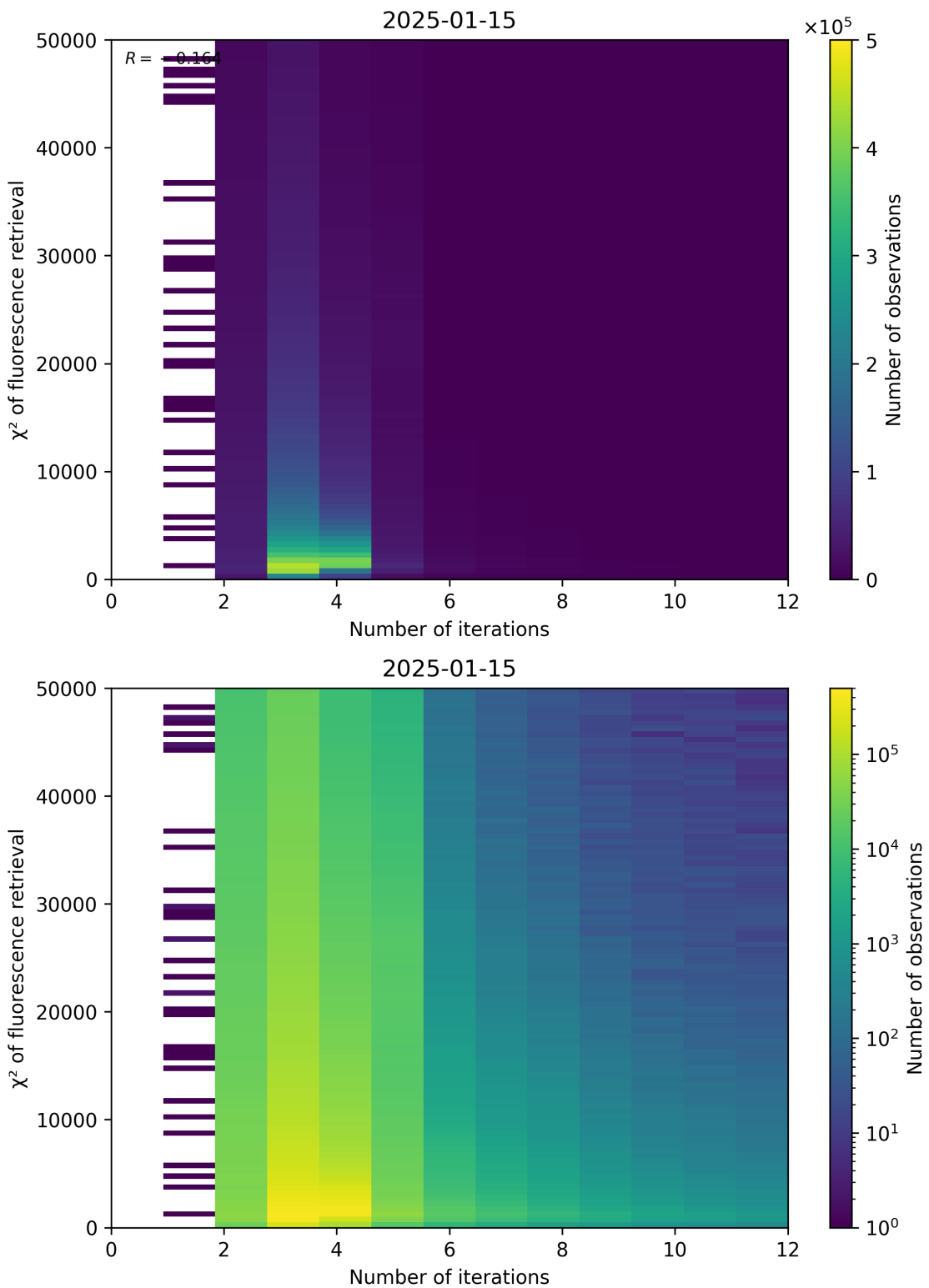


Figure 97: Scatter density plot of “Number of iterations” against “ χ^2 of fluorescence retrieval” for 2025-01-14 to 2025-01-16.

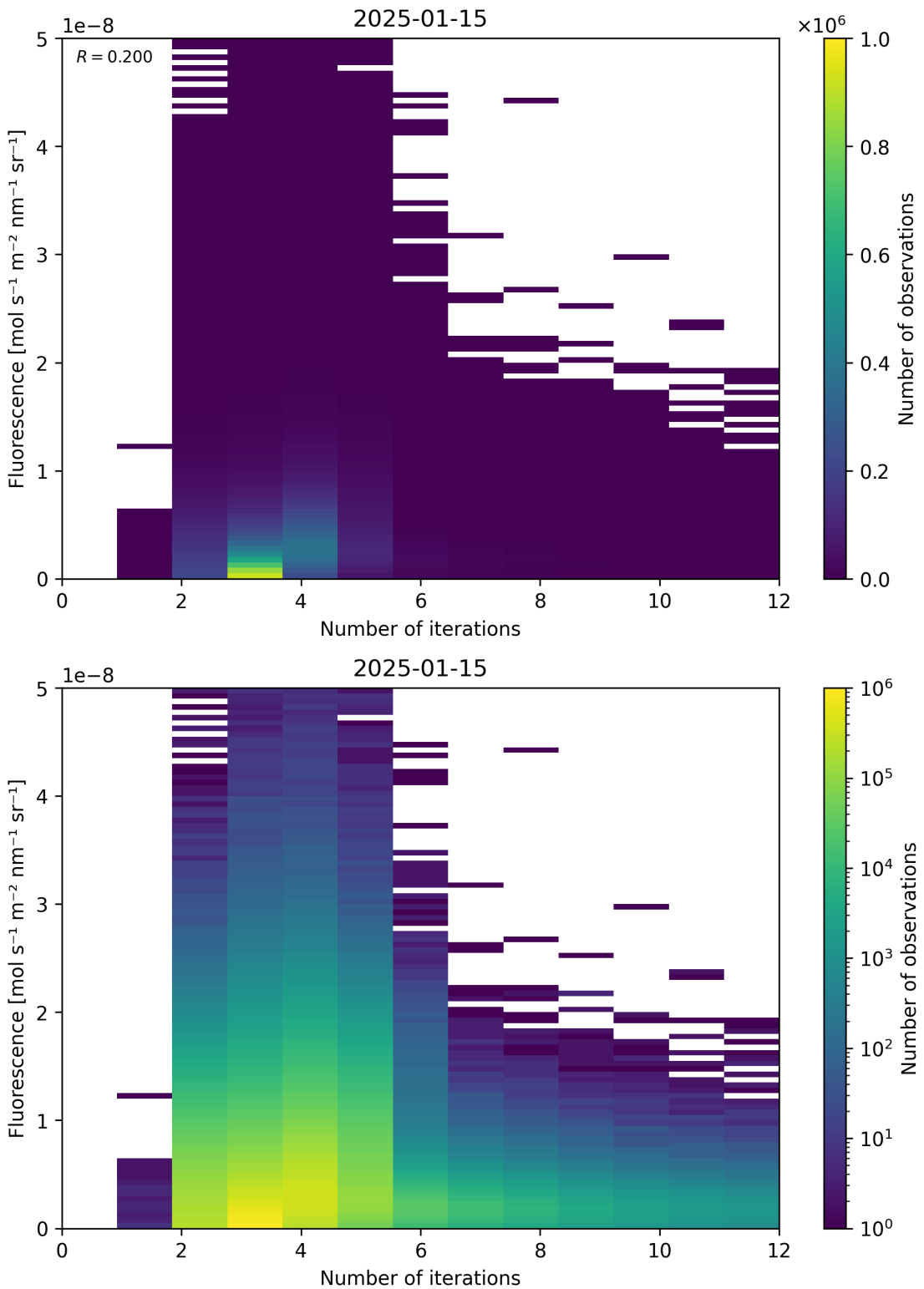


Figure 98: Scatter density plot of “Number of iterations” against “Fluorescence” for 2025-01-14 to 2025-01-16.

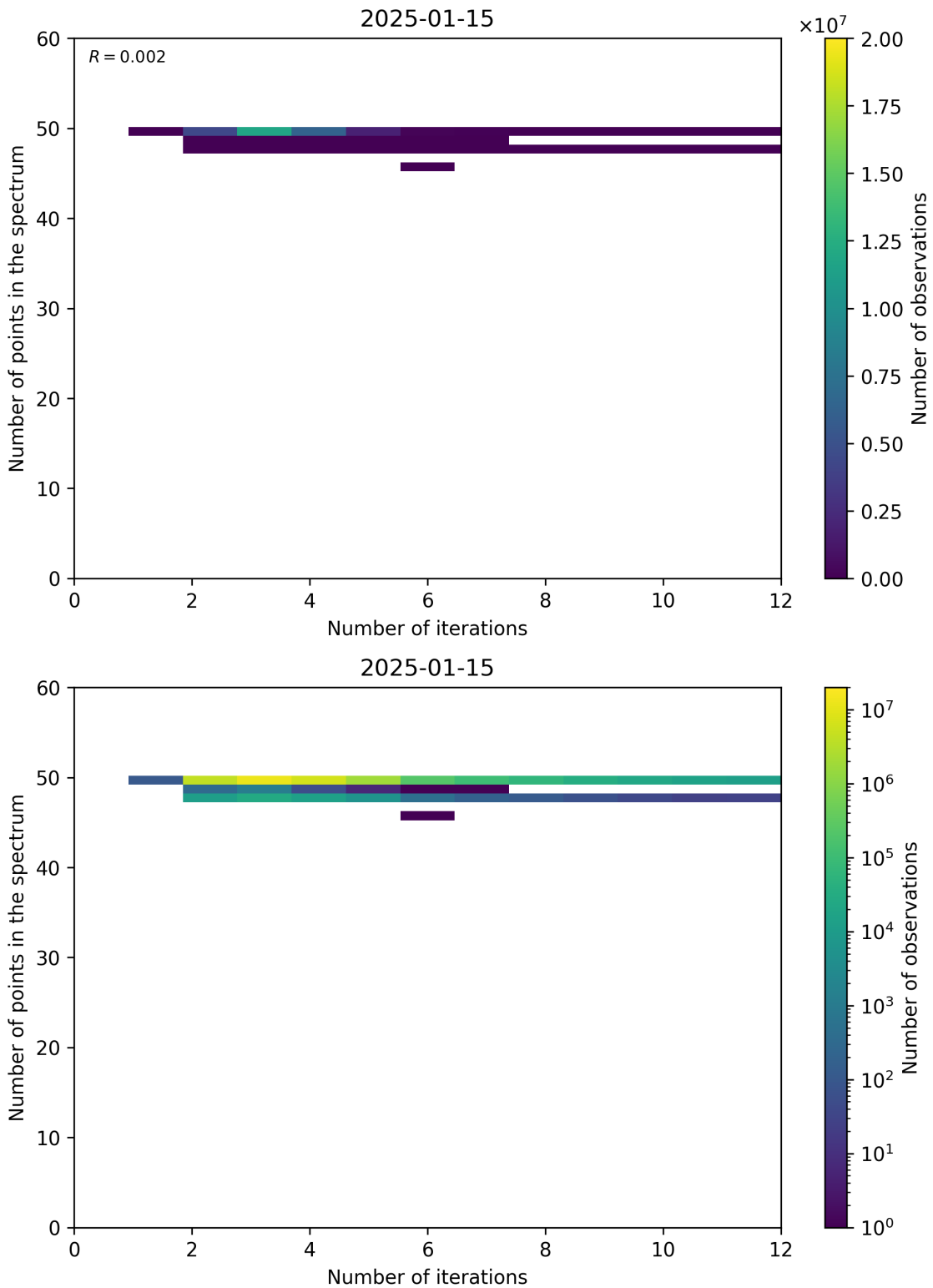


Figure 99: Scatter density plot of “Number of iterations” against “Number of points in the spectrum” for 2025-01-14 to 2025-01-16.

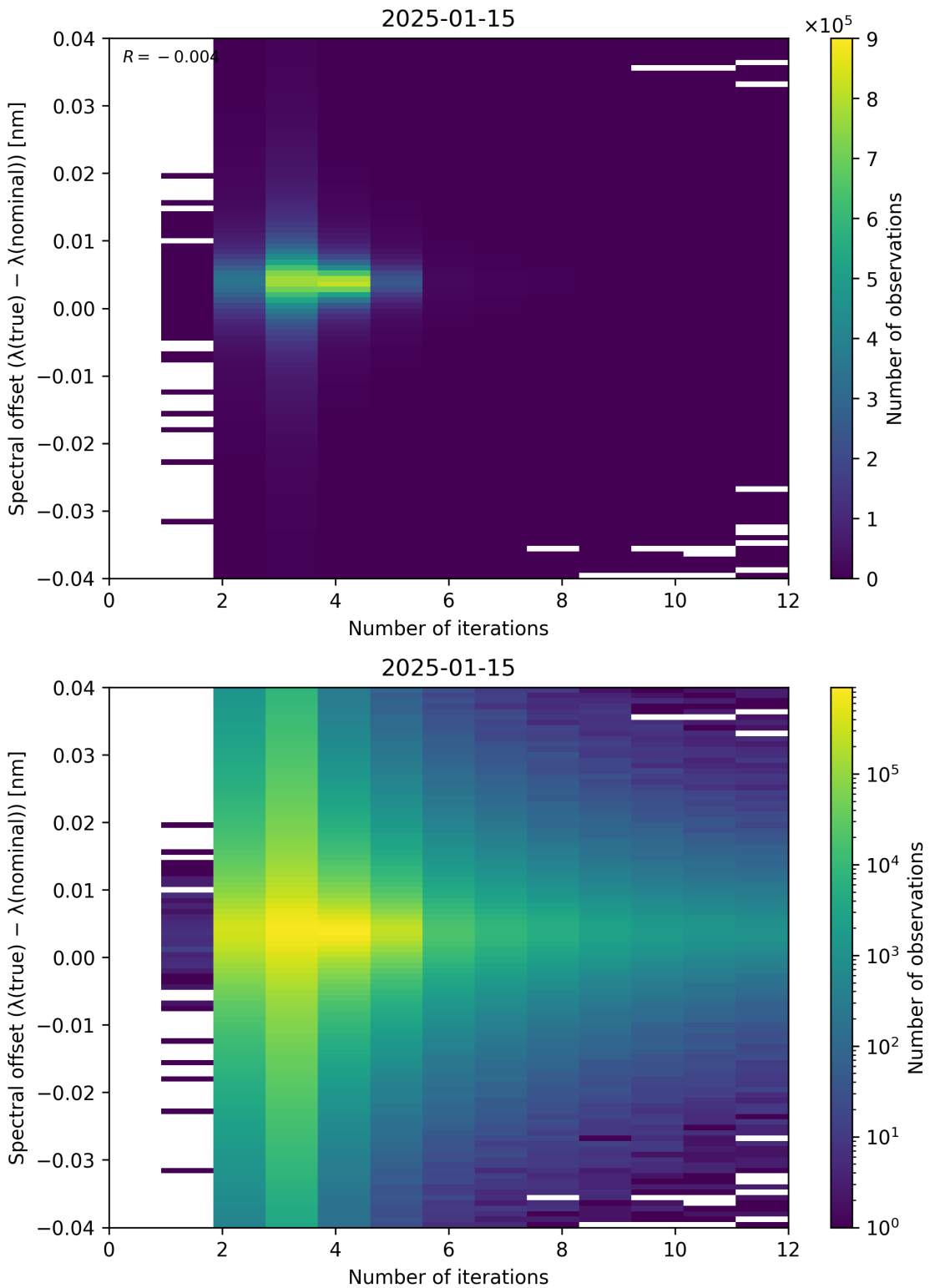


Figure 100: Scatter density plot of “Number of iterations” against “Spectral offset ($\lambda_{\text{true}} - \lambda_{\text{nominal}}$)” for 2025-01-14 to 2025-01-16.

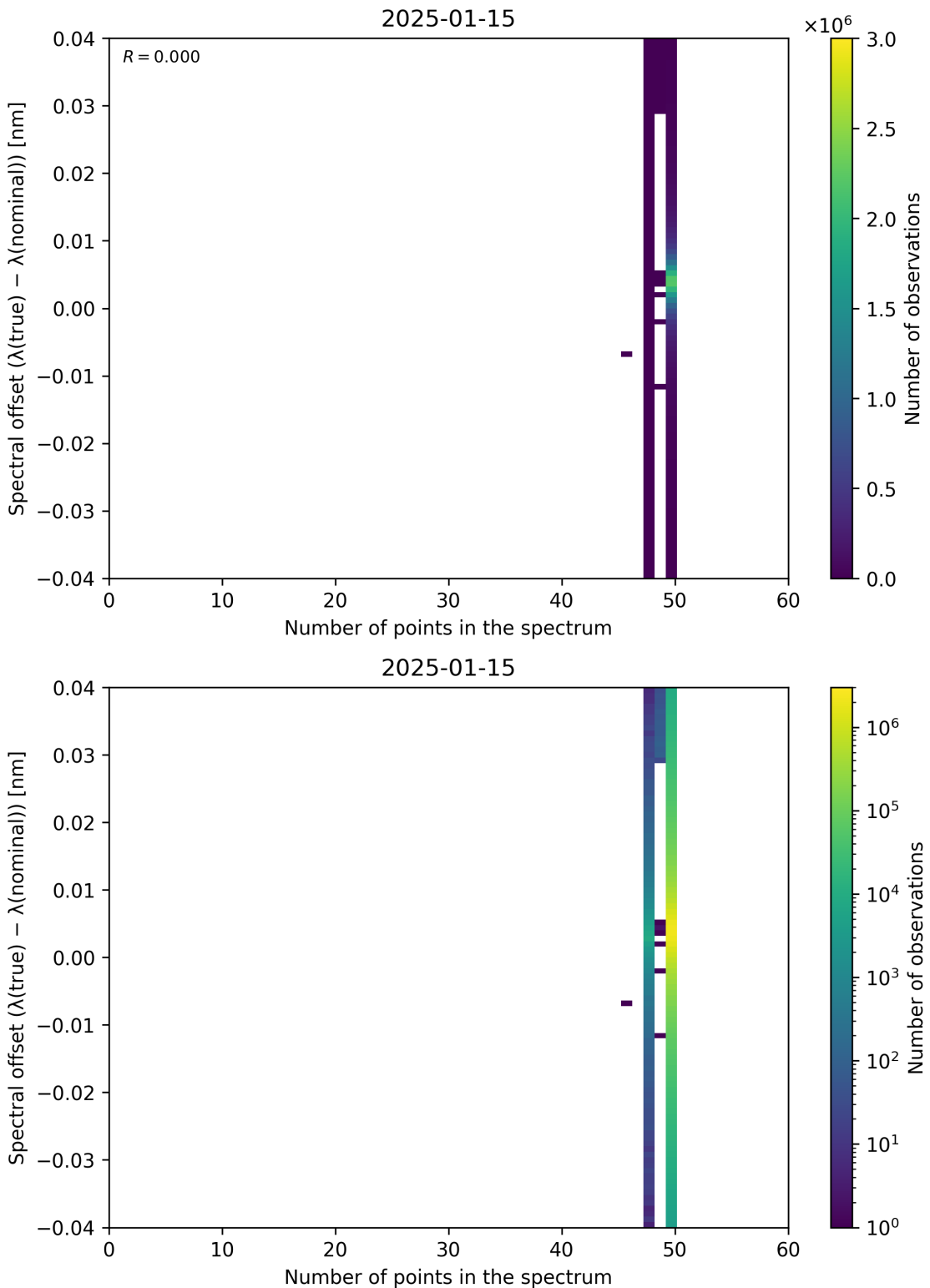


Figure 101: Scatter density plot of “Number of points in the spectrum” against “Spectral offset ($\lambda_{\text{true}} - \lambda_{\text{nominal}}$)” for 2025-01-14 to 2025-01-16.

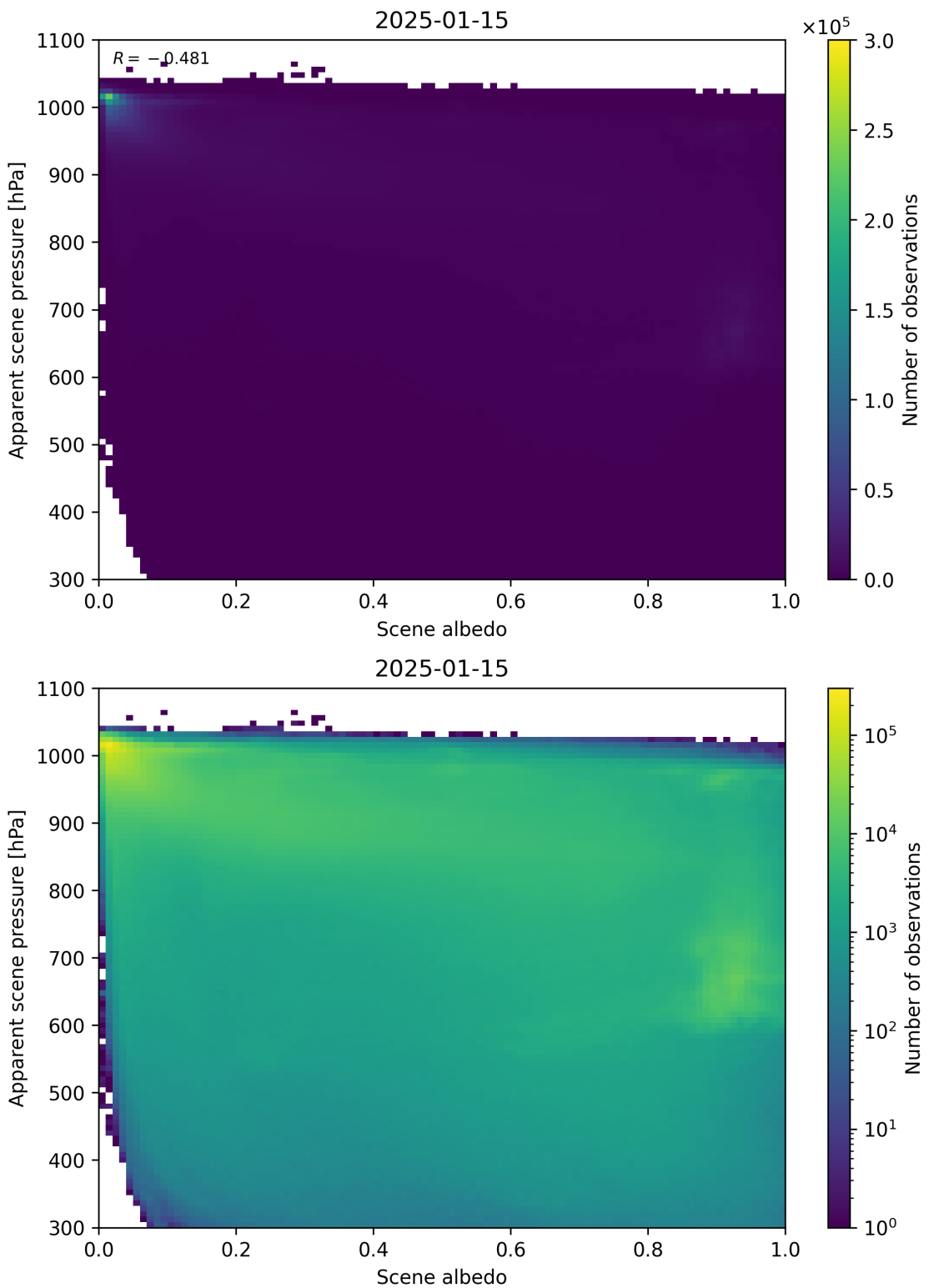


Figure 102: Scatter density plot of “Scene albedo” against “Apparent scene pressure” for 2025-01-14 to 2025-01-16.

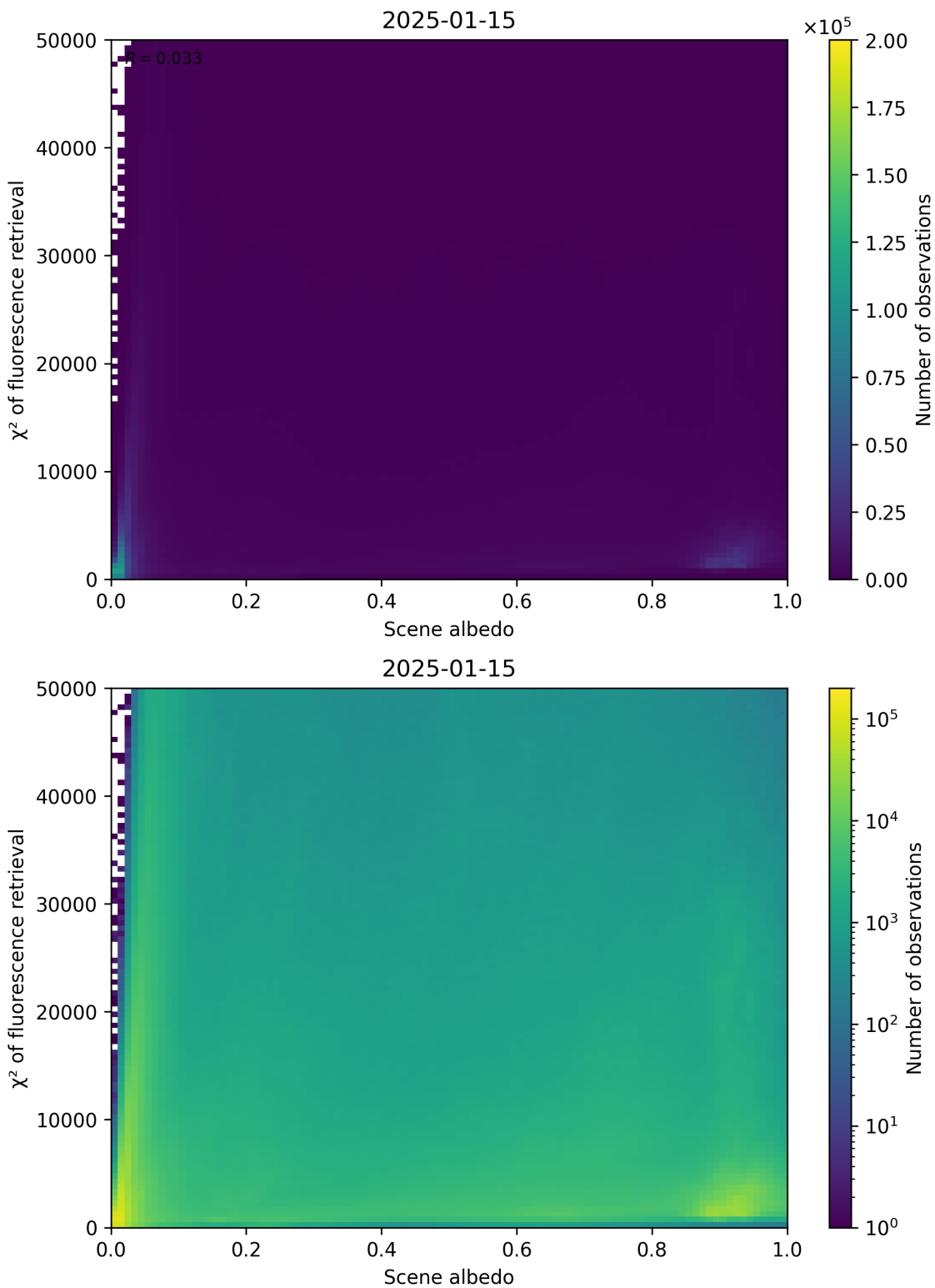


Figure 103: Scatter density plot of “Scene albedo” against “ χ^2 of fluorescence retrieval” for 2025-01-14 to 2025-01-16.

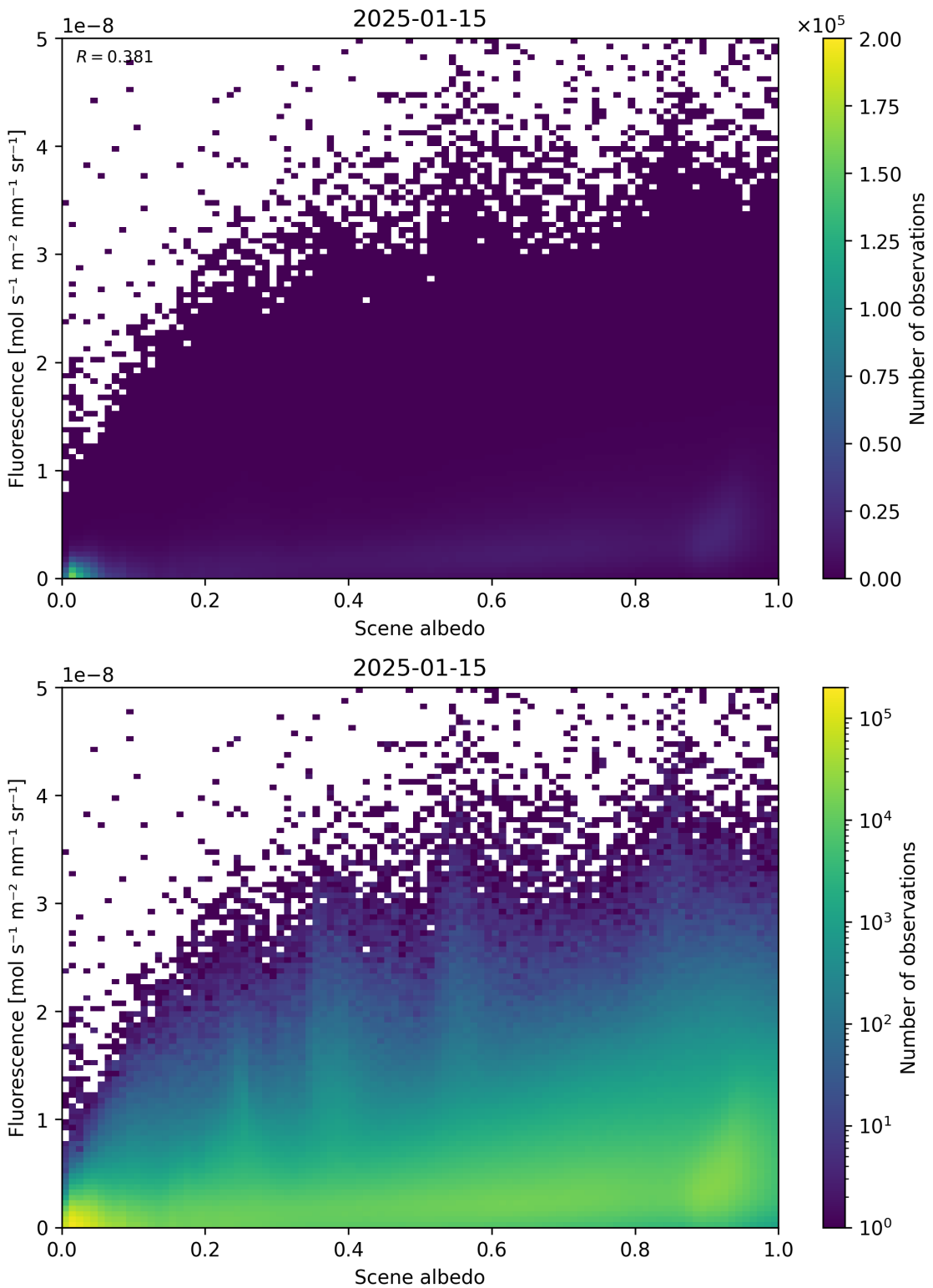


Figure 104: Scatter density plot of “Scene albedo” against “Fluorescence” for 2025-01-14 to 2025-01-16.

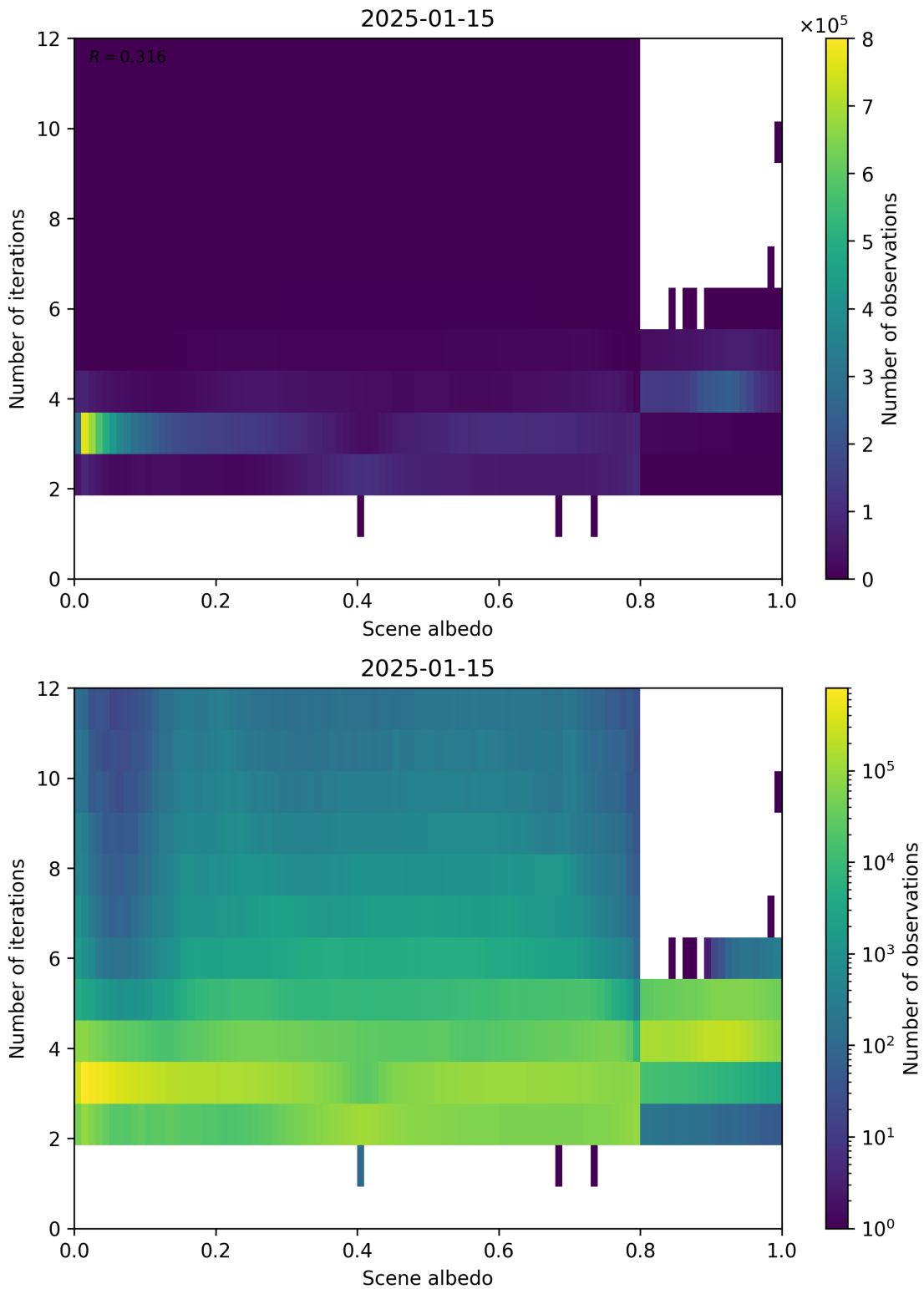


Figure 105: Scatter density plot of “Scene albedo” against “Number of iterations” for 2025-01-14 to 2025-01-16.

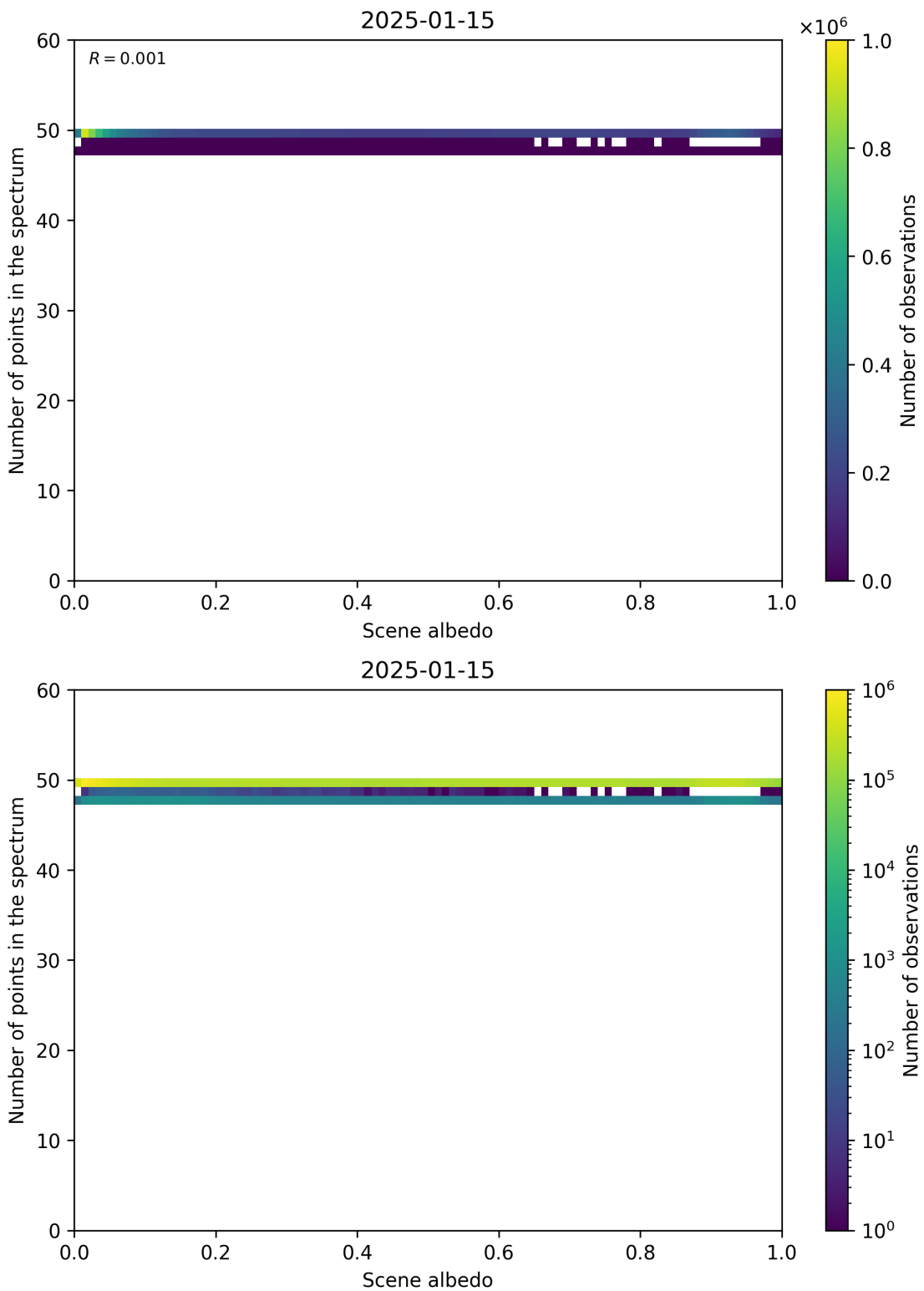


Figure 106: Scatter density plot of “Scene albedo” against “Number of points in the spectrum” for 2025-01-14 to 2025-01-16.

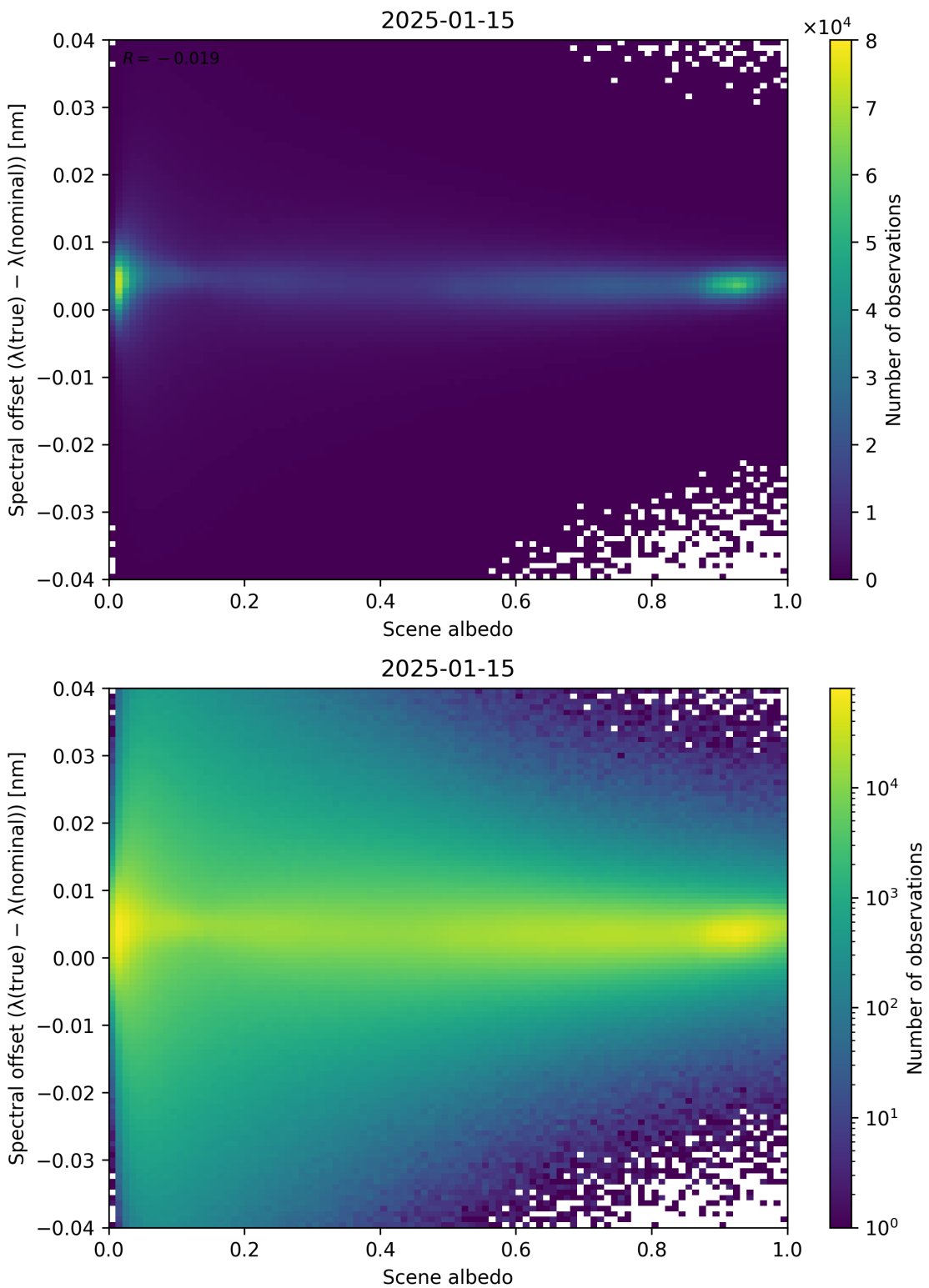


Figure 107: Scatter density plot of “Scene albedo” against “Spectral offset ($\lambda_{\text{true}} - \lambda_{\text{nominal}}$)” for 2025-01-14 to 2025-01-16.

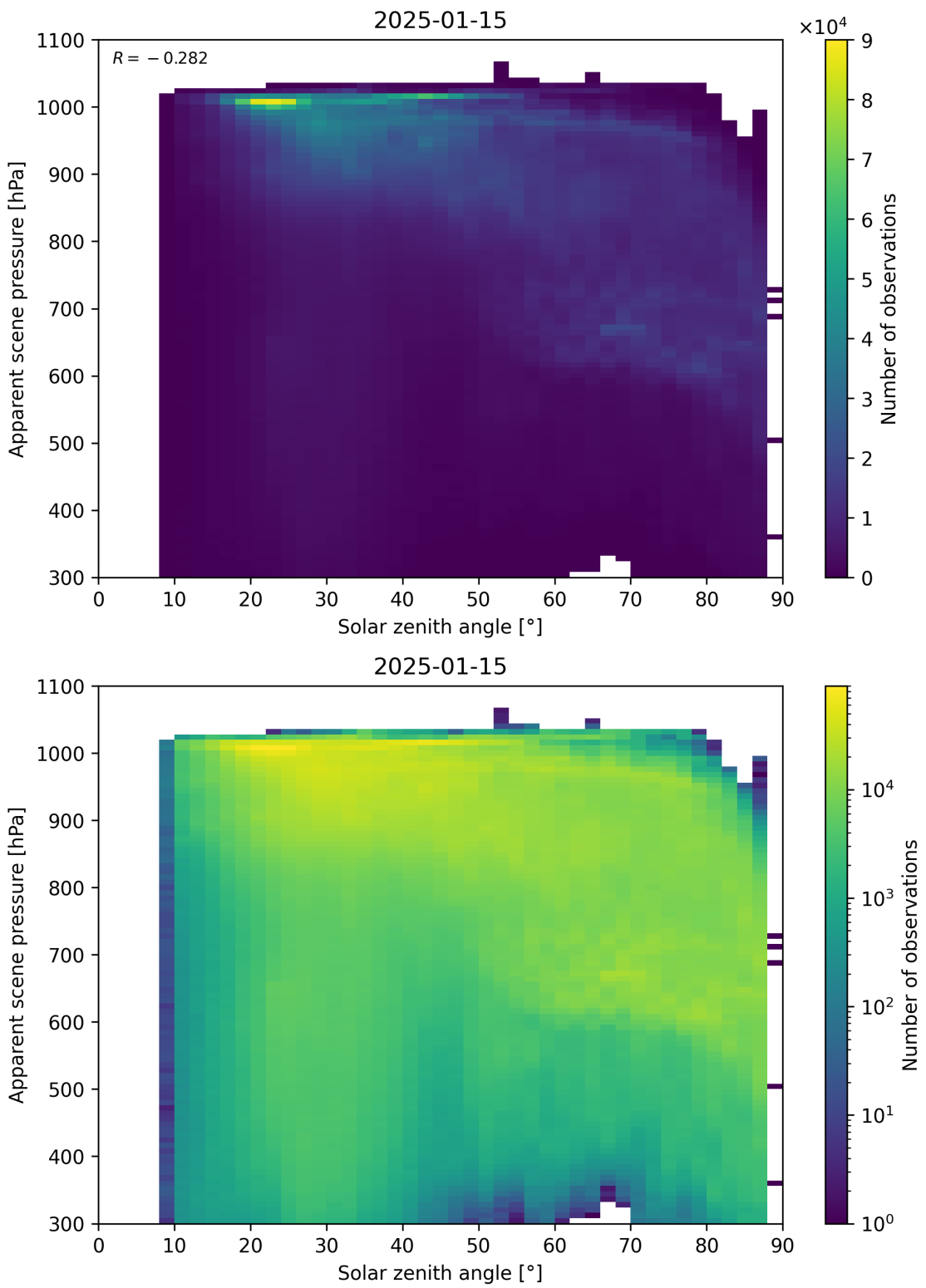


Figure 108: Scatter density plot of “Solar zenith angle” against “Apparent scene pressure” for 2025-01-14 to 2025-01-16.

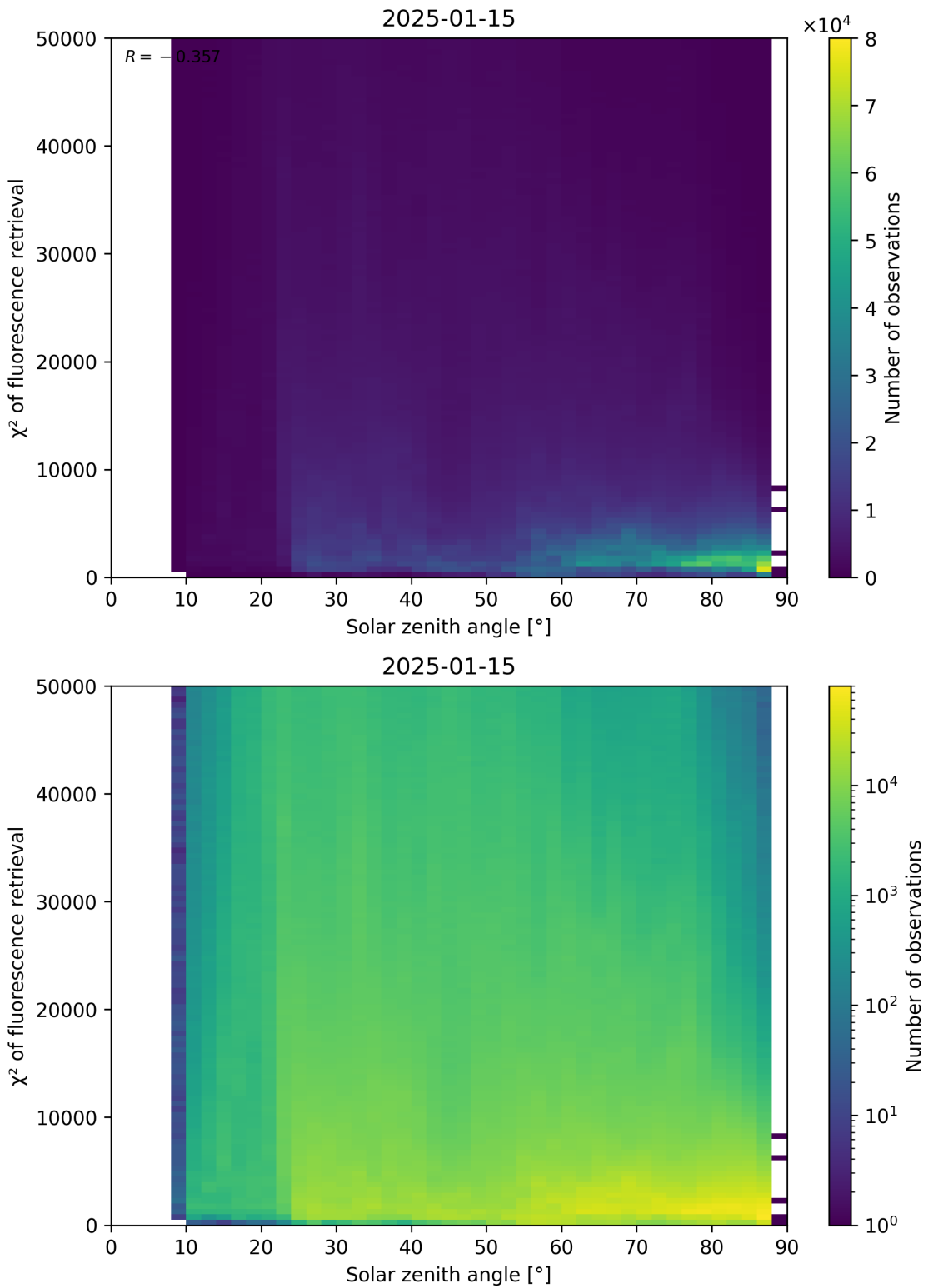


Figure 109: Scatter density plot of “Solar zenith angle” against “ χ^2 of fluorescence retrieval” for 2025-01-14 to 2025-01-16.

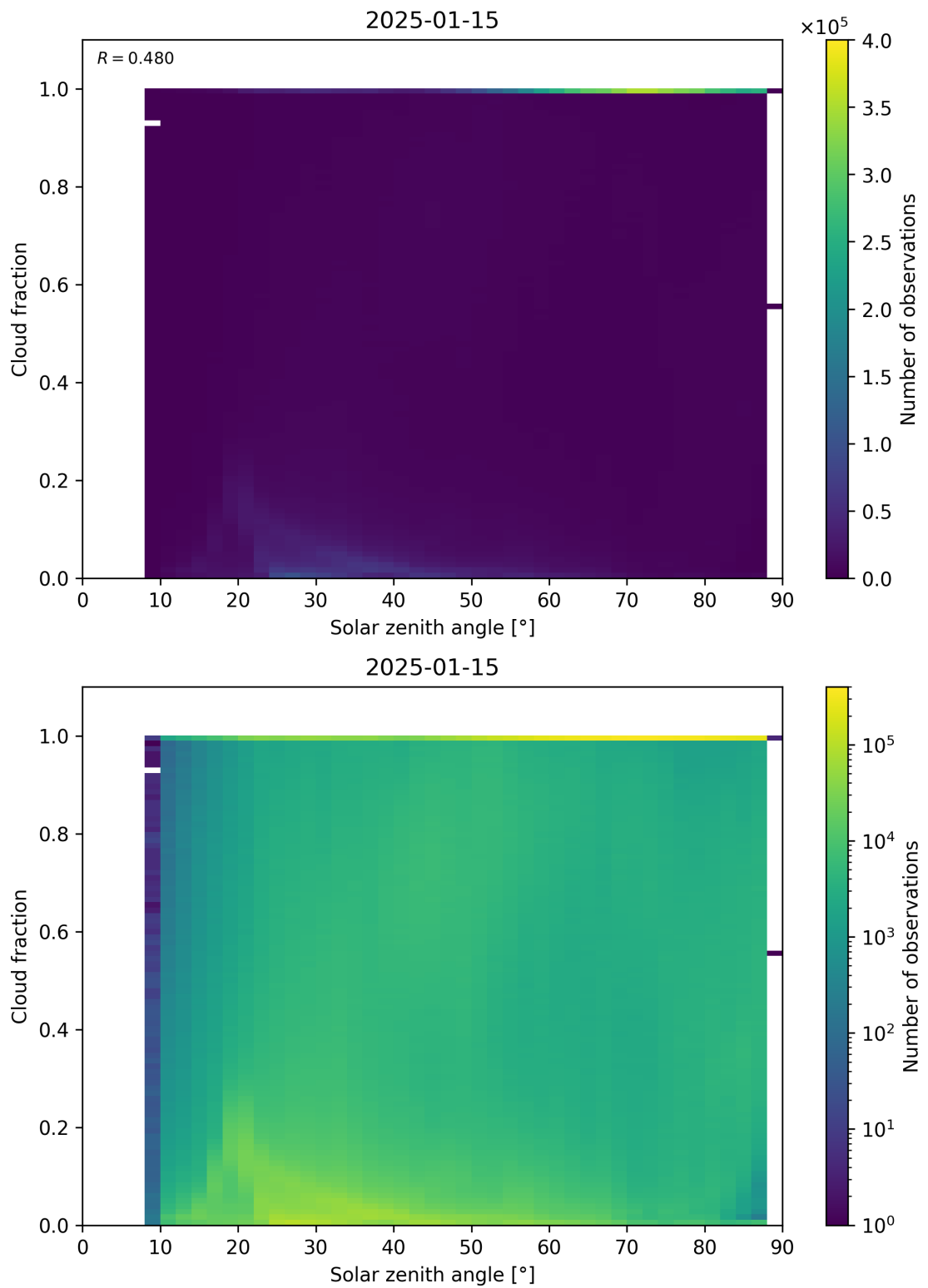


Figure 110: Scatter density plot of “Solar zenith angle” against “Cloud fraction” for 2025-01-14 to 2025-01-16.

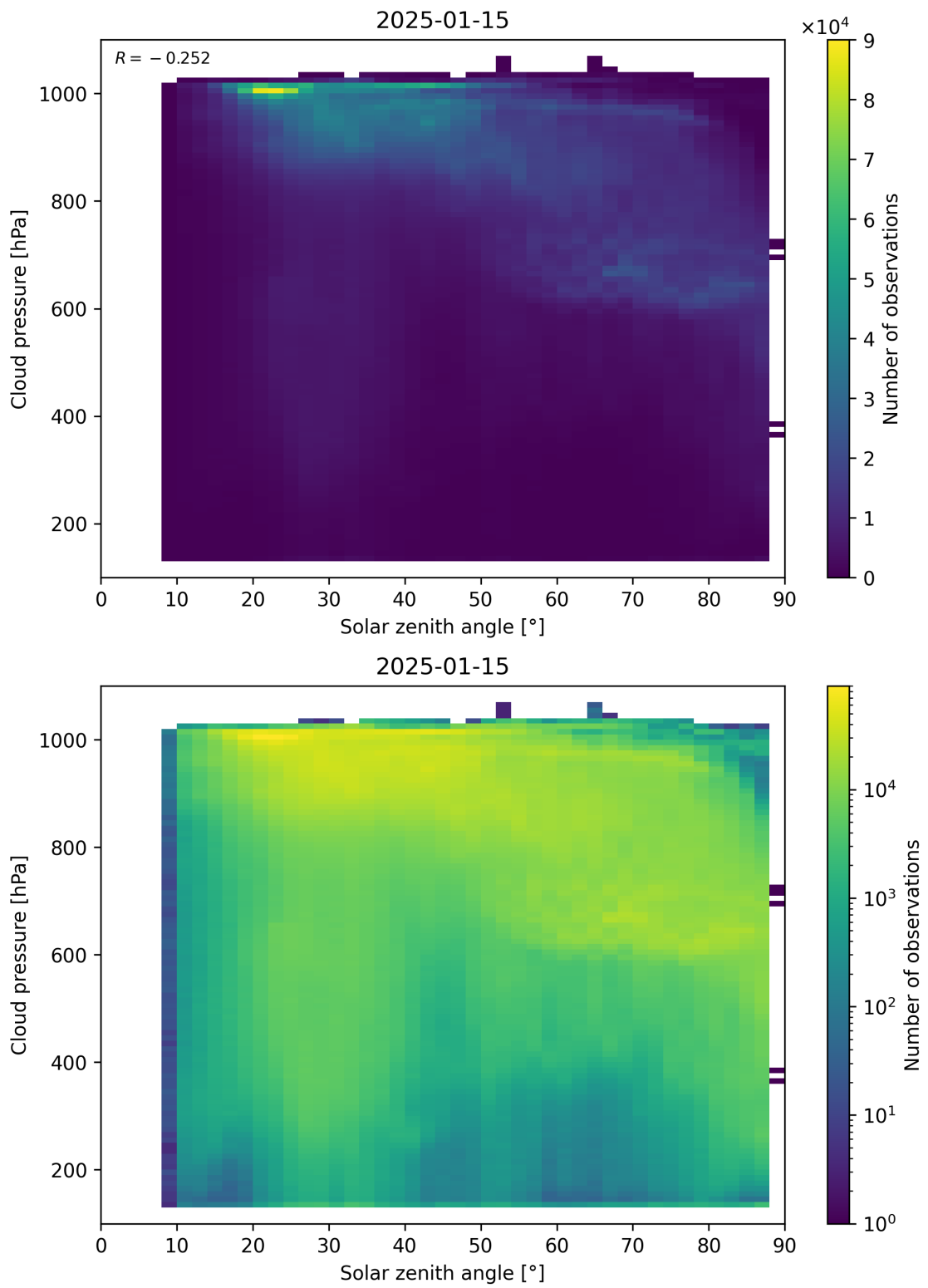


Figure 111: Scatter density plot of “Solar zenith angle” against “Cloud pressure” for 2025-01-14 to 2025-01-16.

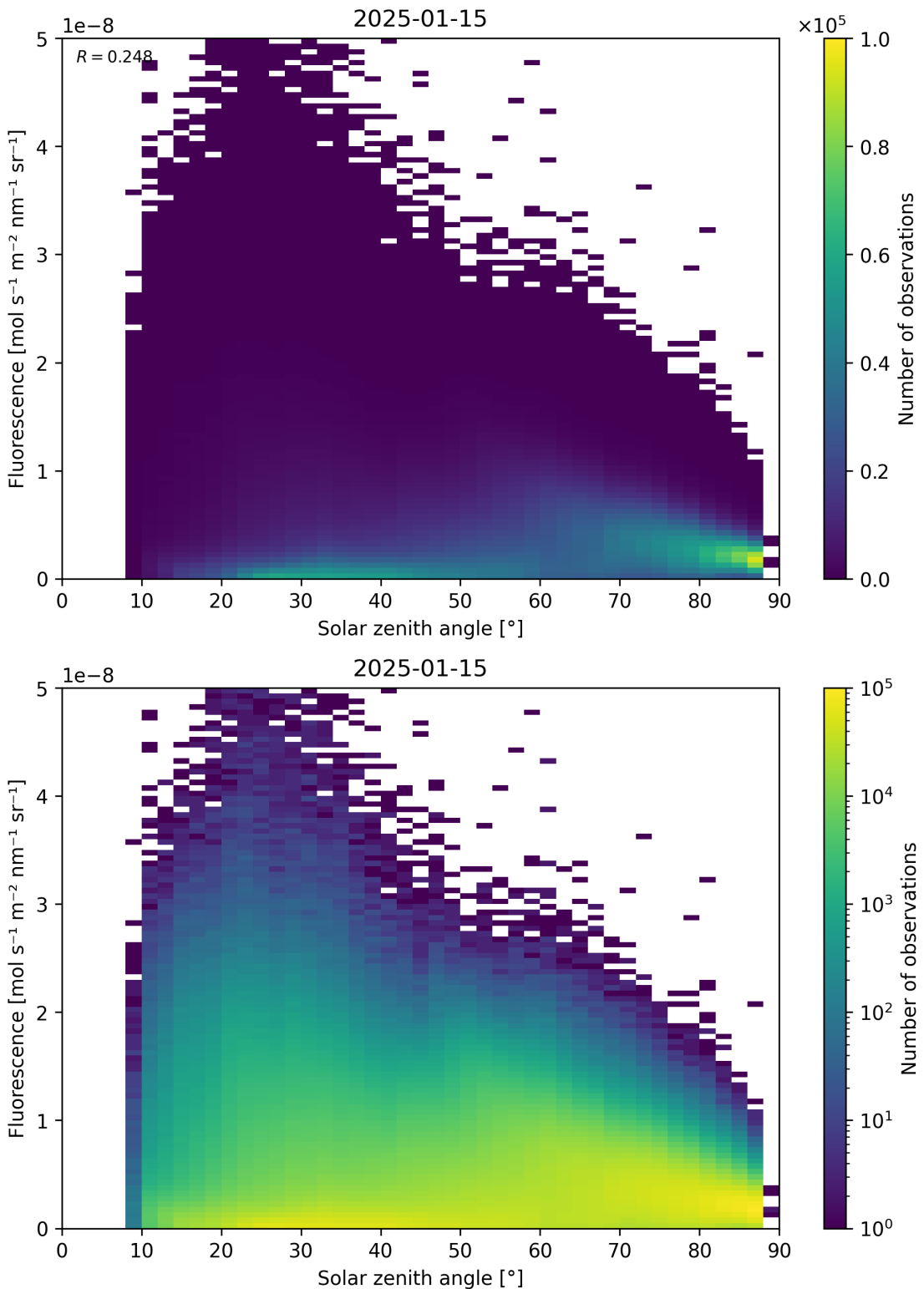


Figure 112: Scatter density plot of “Solar zenith angle” against “Fluorescence” for 2025-01-14 to 2025-01-16.

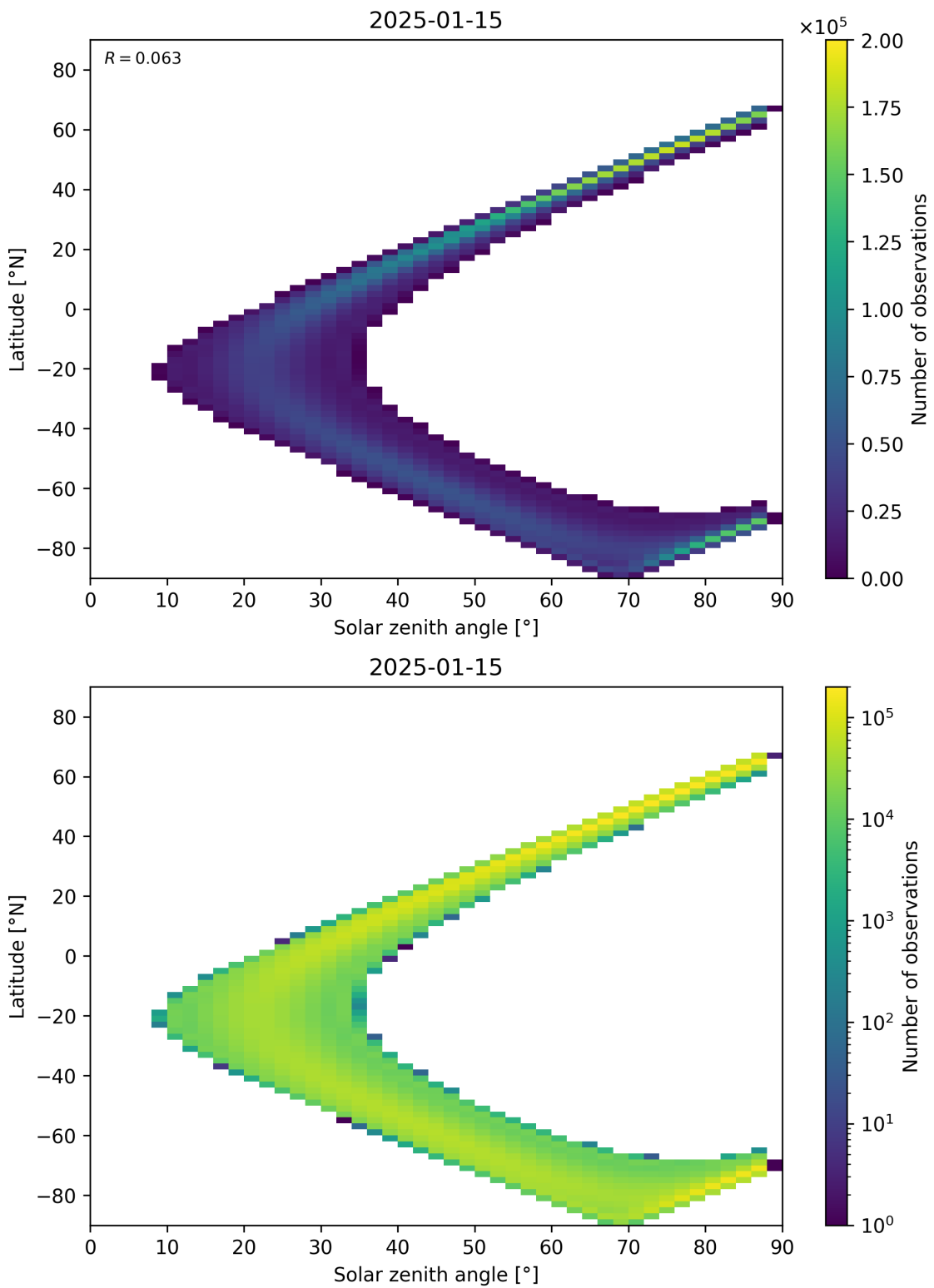


Figure 113: Scatter density plot of “Solar zenith angle” against “Latitude” for 2025-01-14 to 2025-01-16.

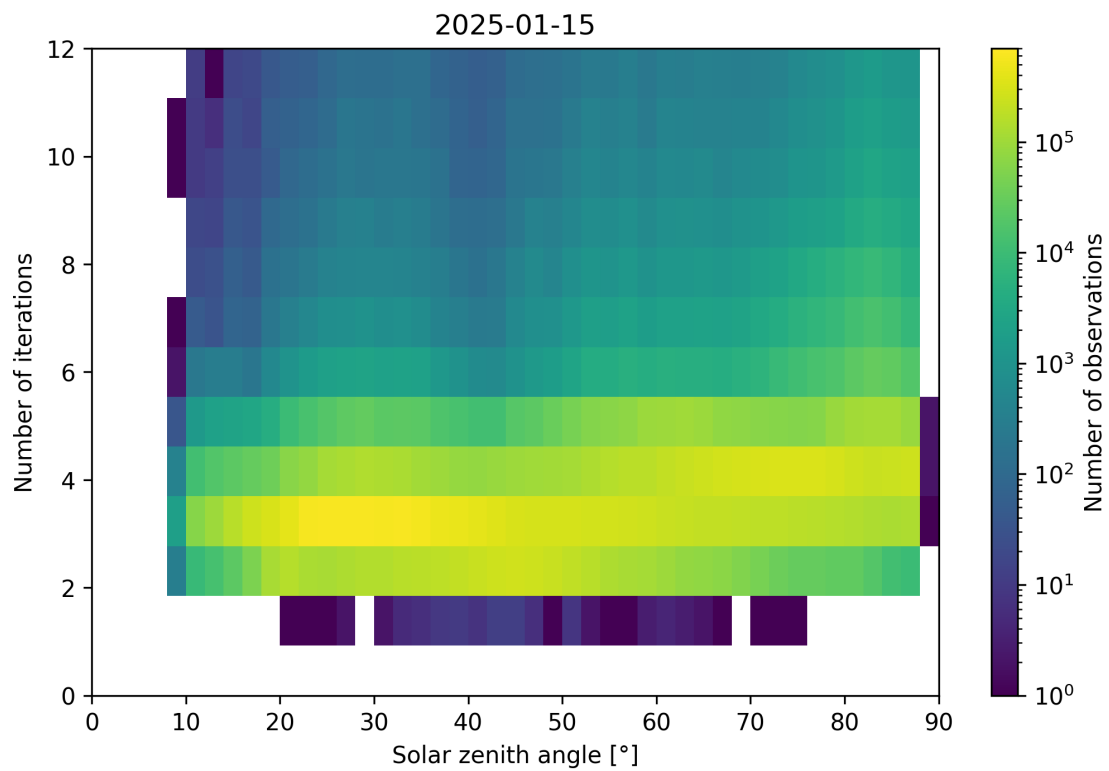
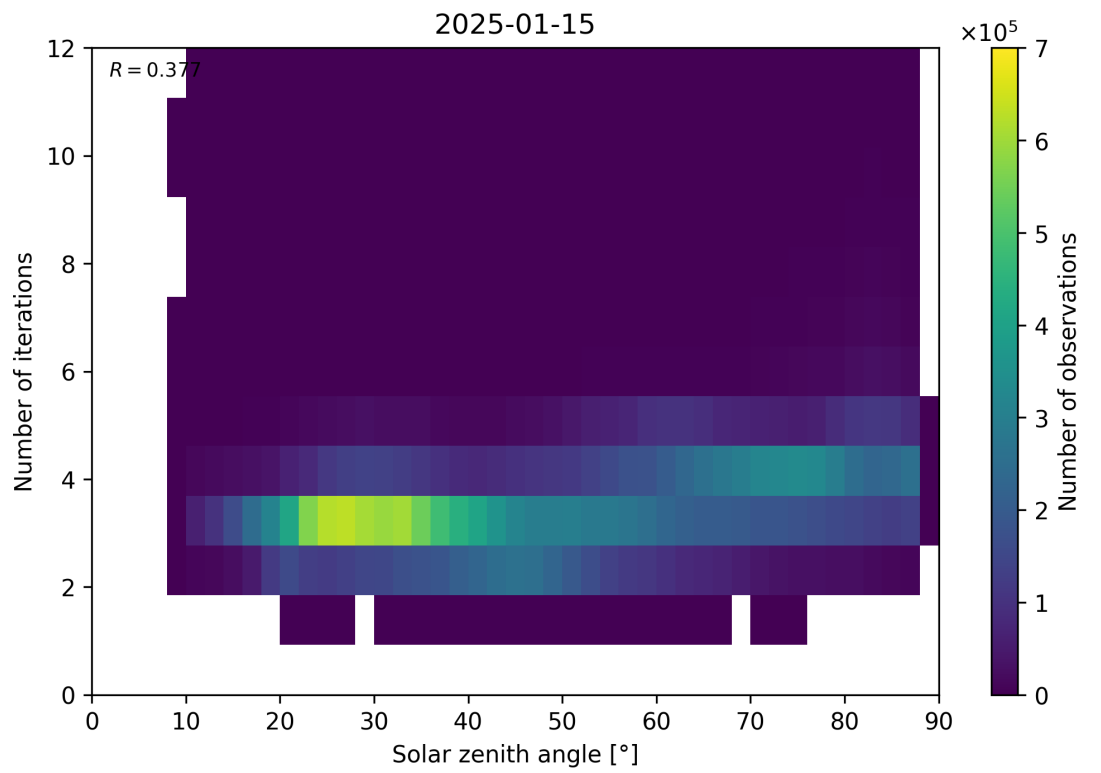


Figure 114: Scatter density plot of “Solar zenith angle” against “Number of iterations” for 2025-01-14 to 2025-01-16.

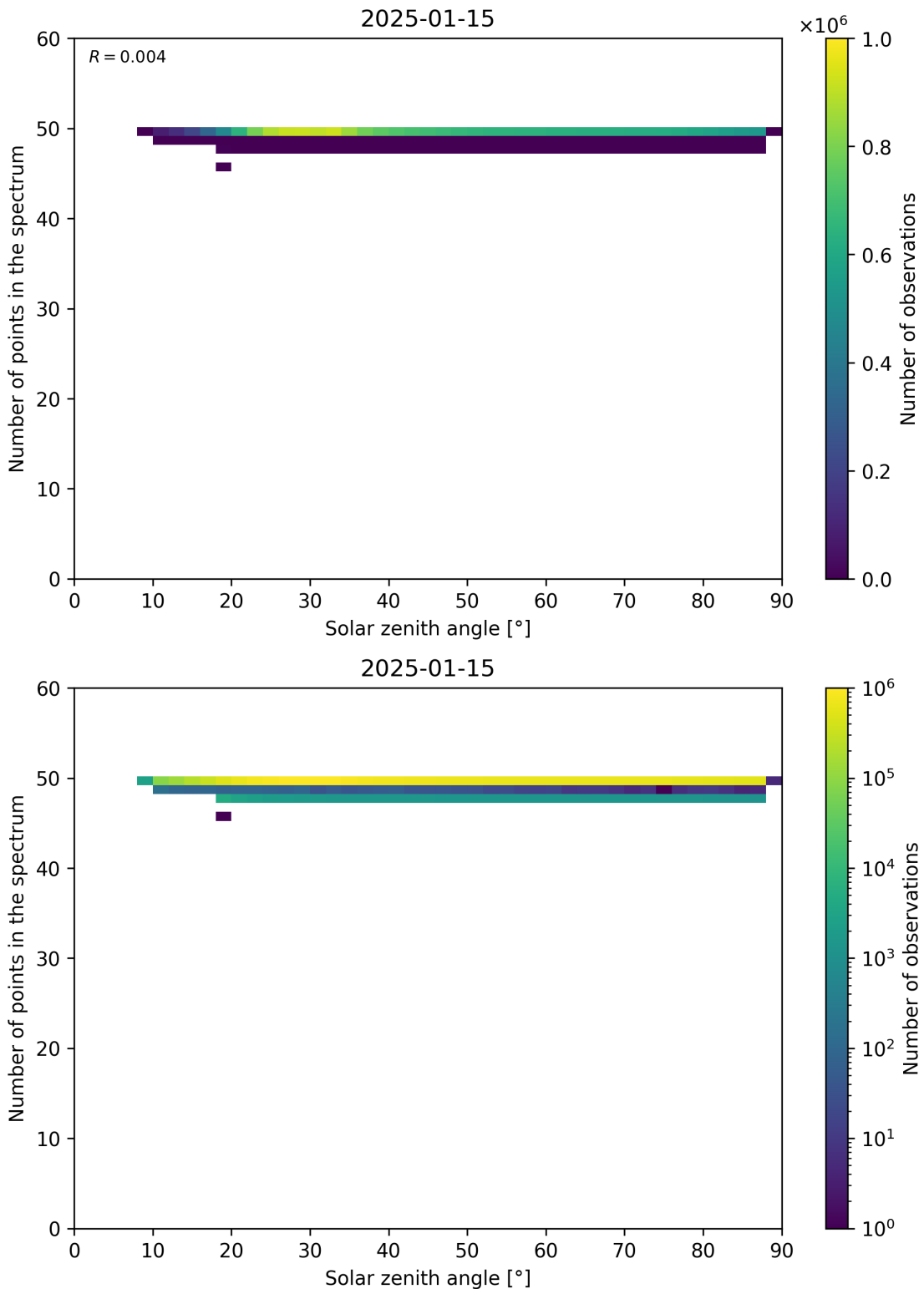


Figure 115: Scatter density plot of “Solar zenith angle” against “Number of points in the spectrum” for 2025-01-14 to 2025-01-16.

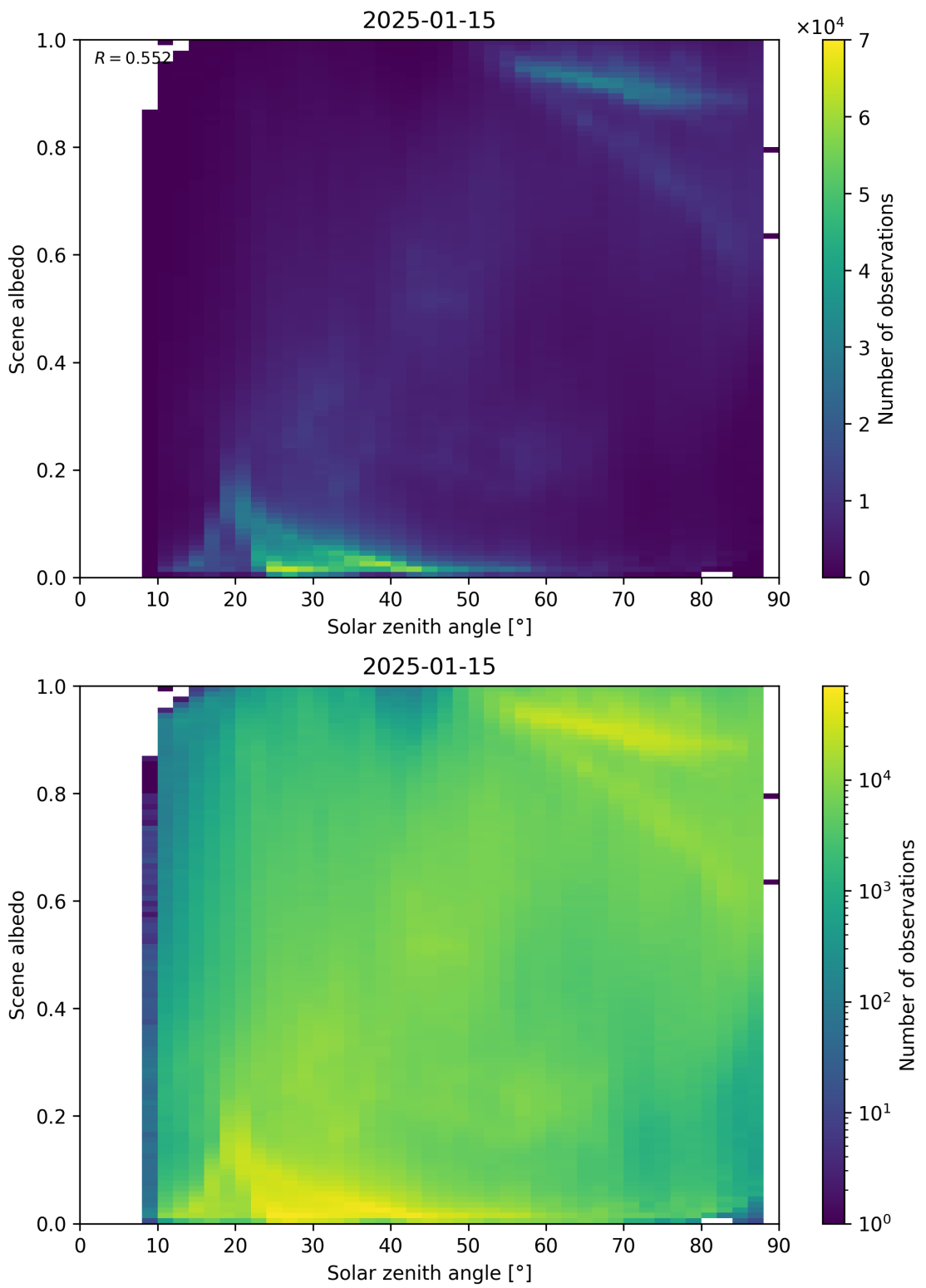


Figure 116: Scatter density plot of “Solar zenith angle” against “Scene albedo” for 2025-01-14 to 2025-01-16.

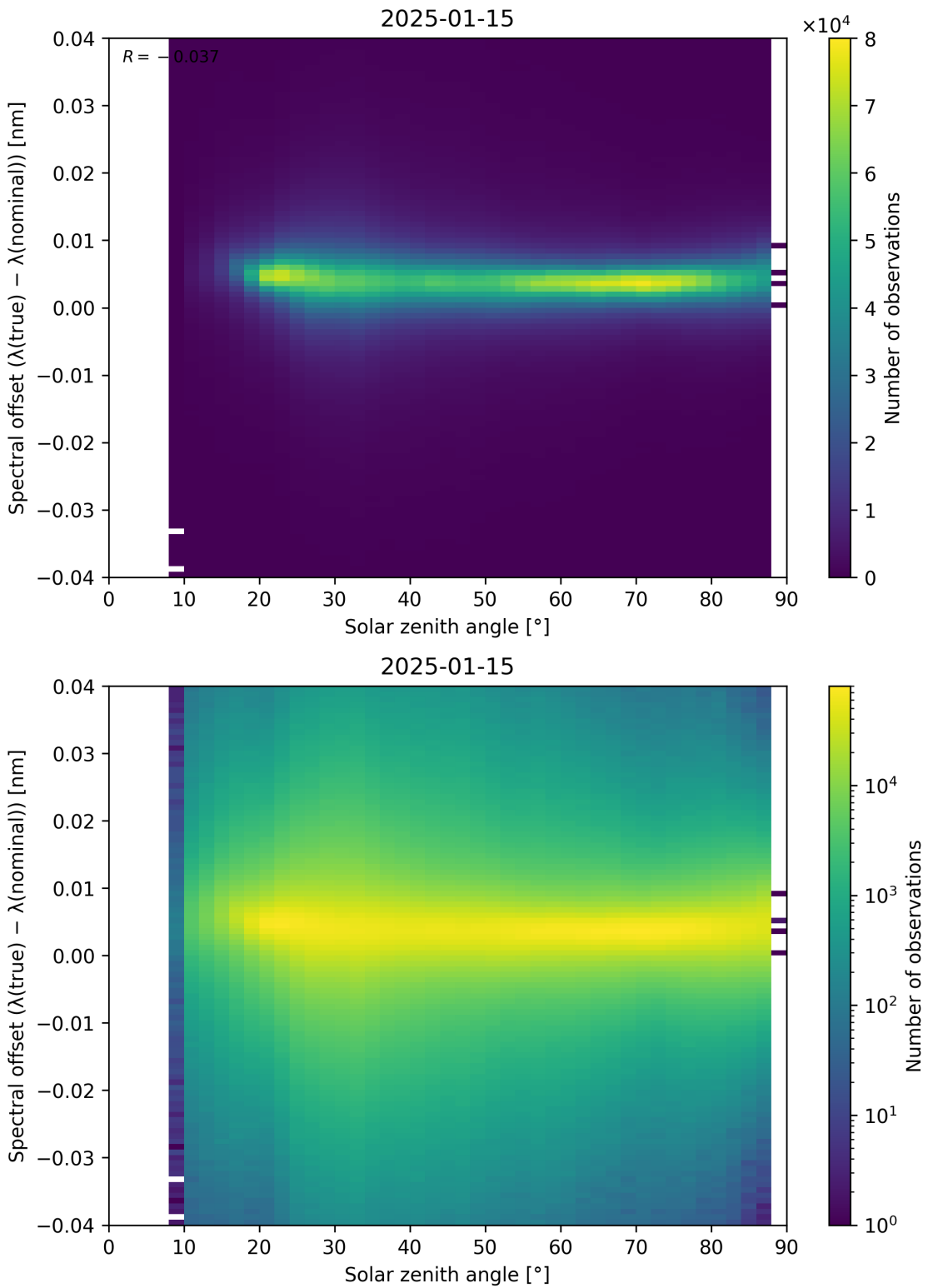


Figure 117: Scatter density plot of “Solar zenith angle” against “Spectral offset ($\lambda_{\text{true}} - \lambda_{\text{nominal}}$)” for 2025-01-14 to 2025-01-16.

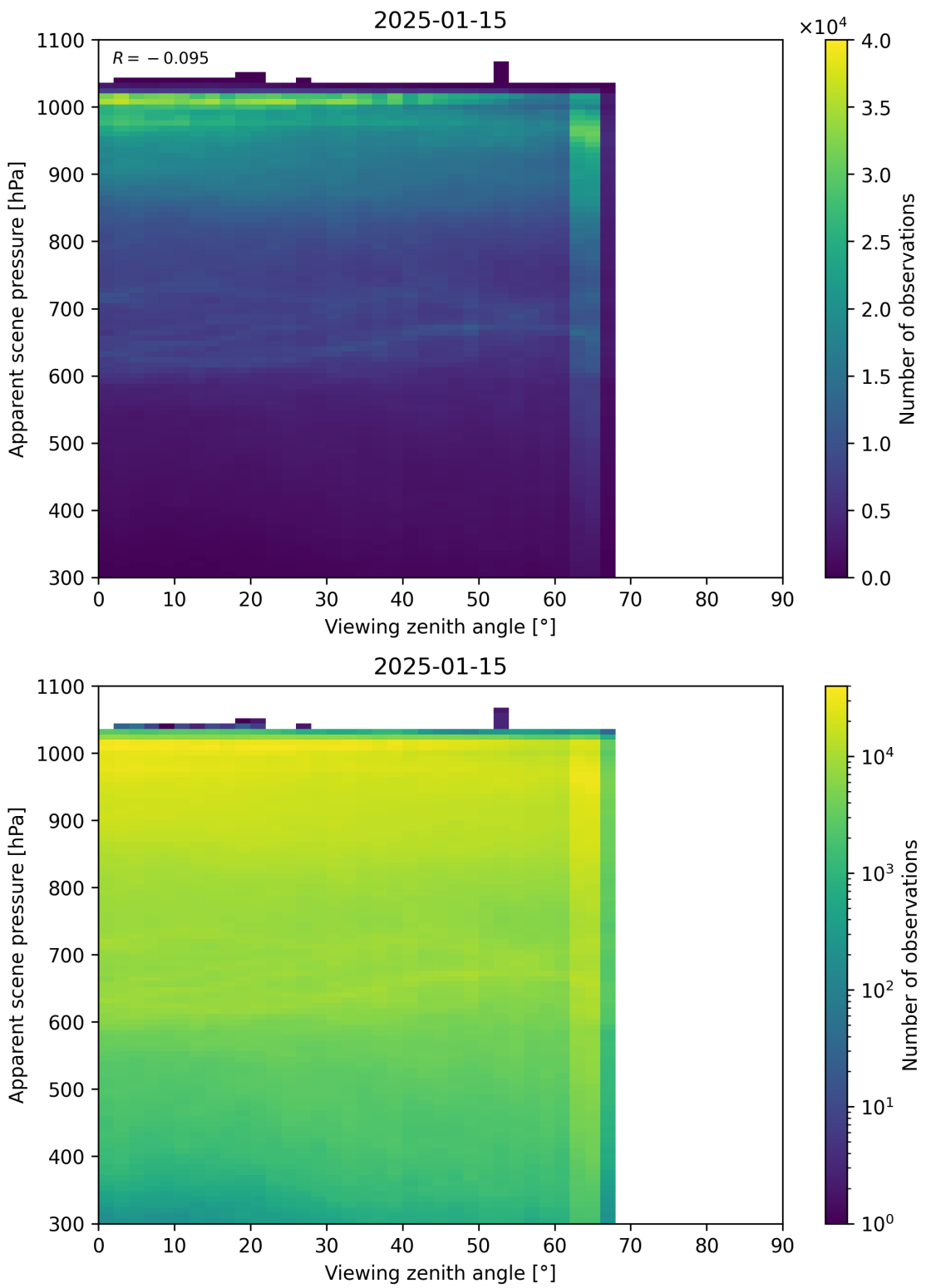


Figure 118: Scatter density plot of “Viewing zenith angle” against “Apparent scene pressure” for 2025-01-14 to 2025-01-16.

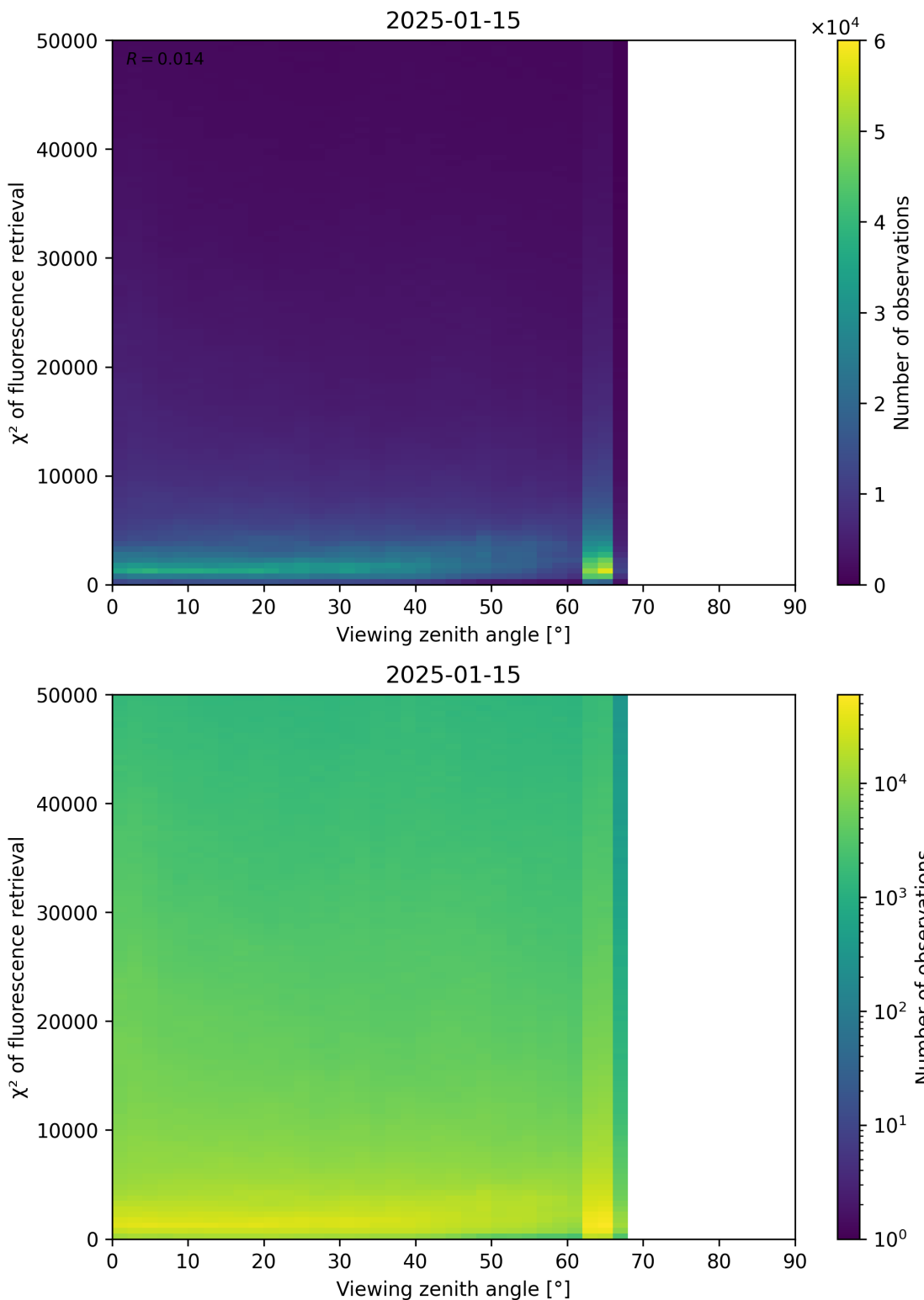


Figure 119: Scatter density plot of “Viewing zenith angle” against “ χ^2 of fluorescence retrieval” for 2025-01-14 to 2025-01-16.

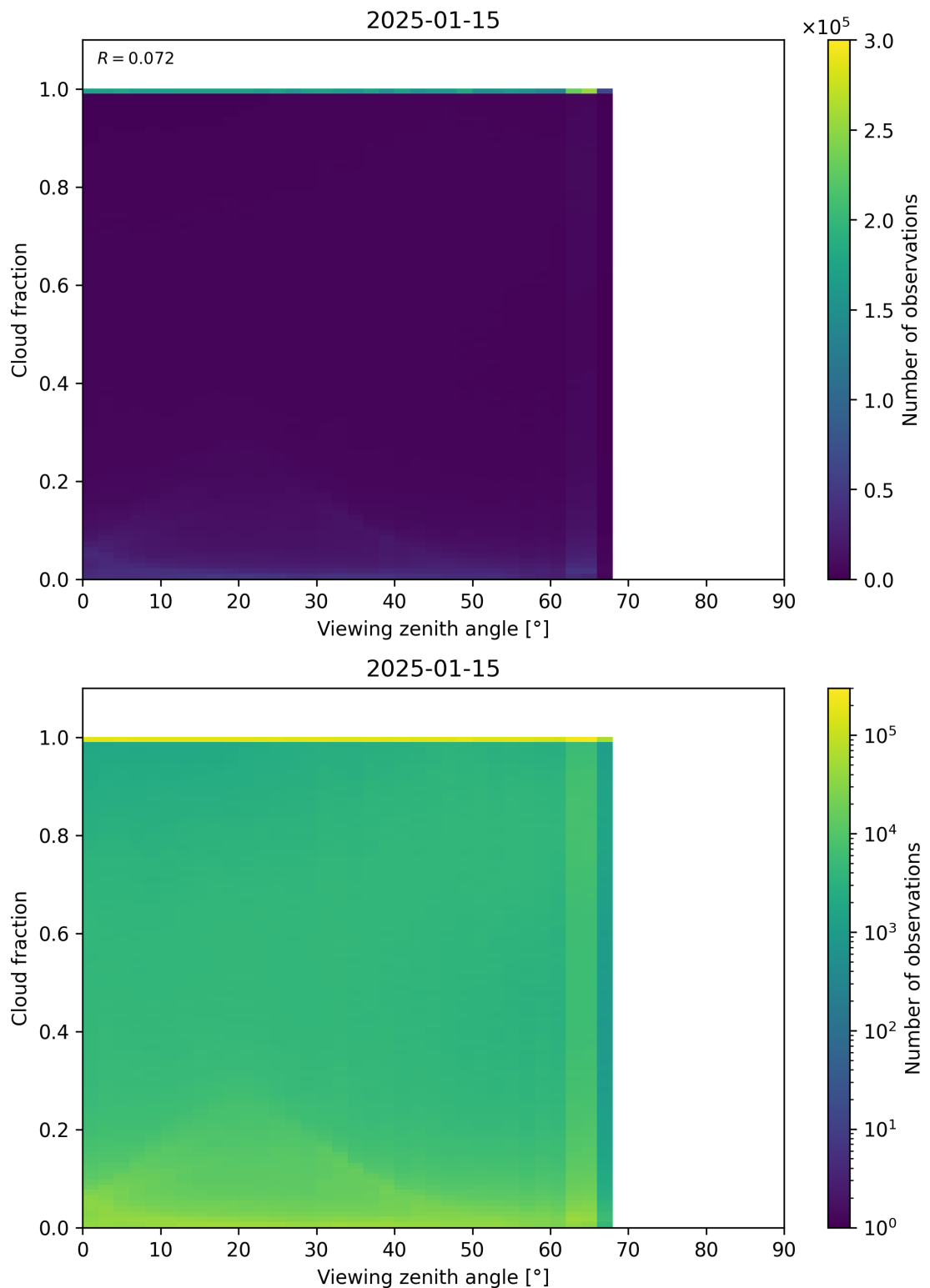


Figure 120: Scatter density plot of “Viewing zenith angle” against “Cloud fraction” for 2025-01-14 to 2025-01-16.

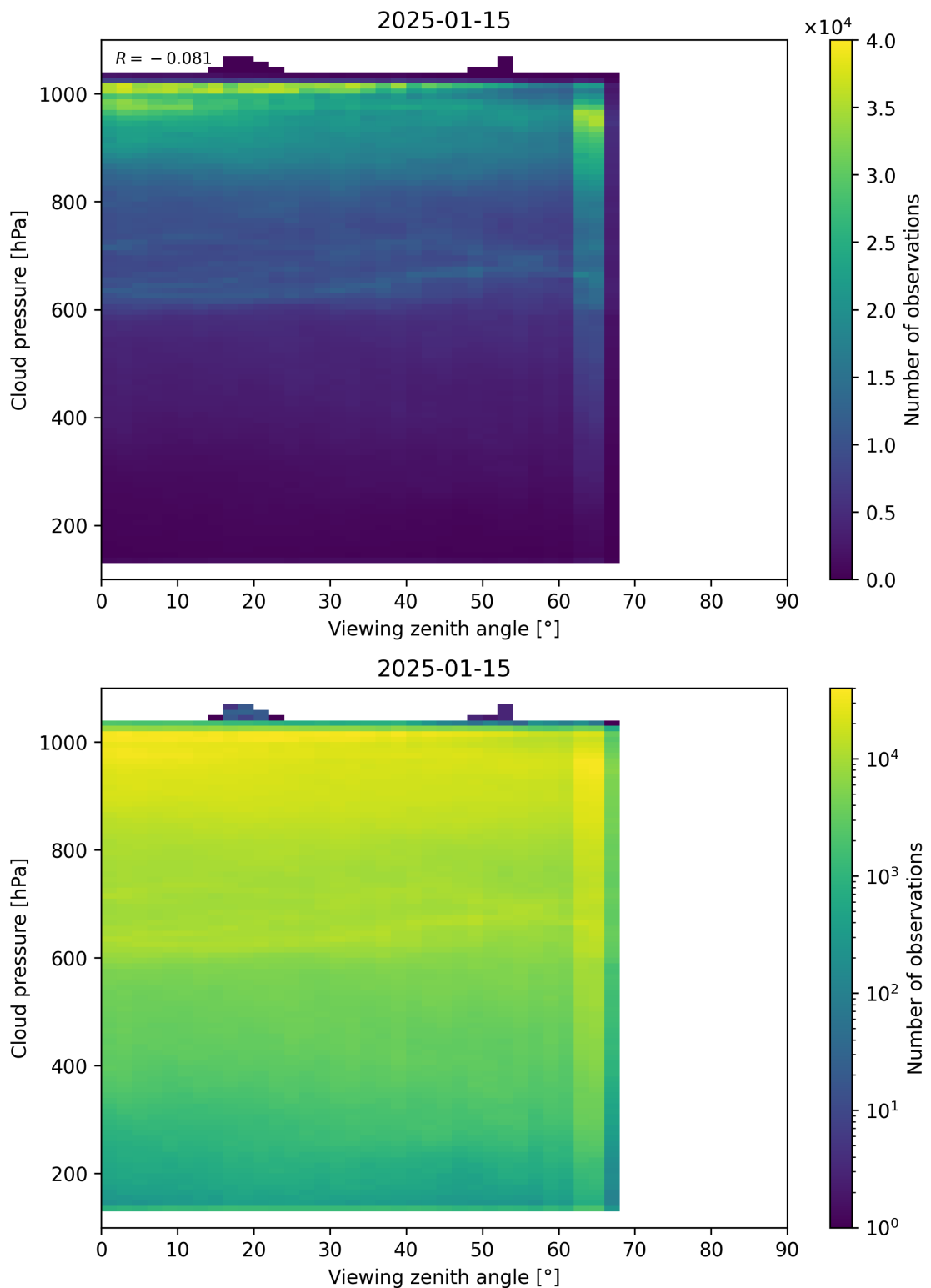


Figure 121: Scatter density plot of “Viewing zenith angle” against “Cloud pressure” for 2025-01-14 to 2025-01-16.

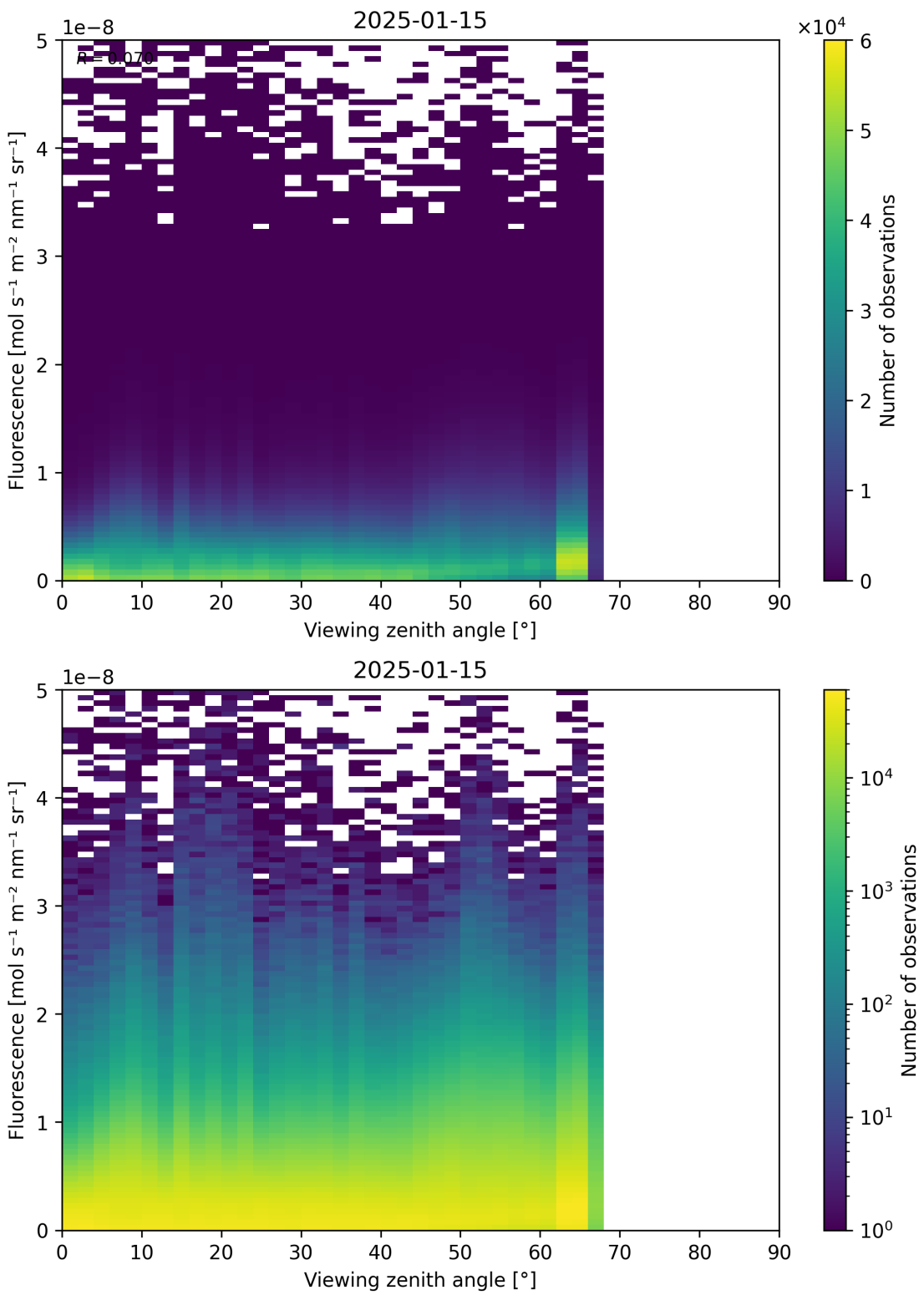


Figure 122: Scatter density plot of “Viewing zenith angle” against “Fluorescence” for 2025-01-14 to 2025-01-16.

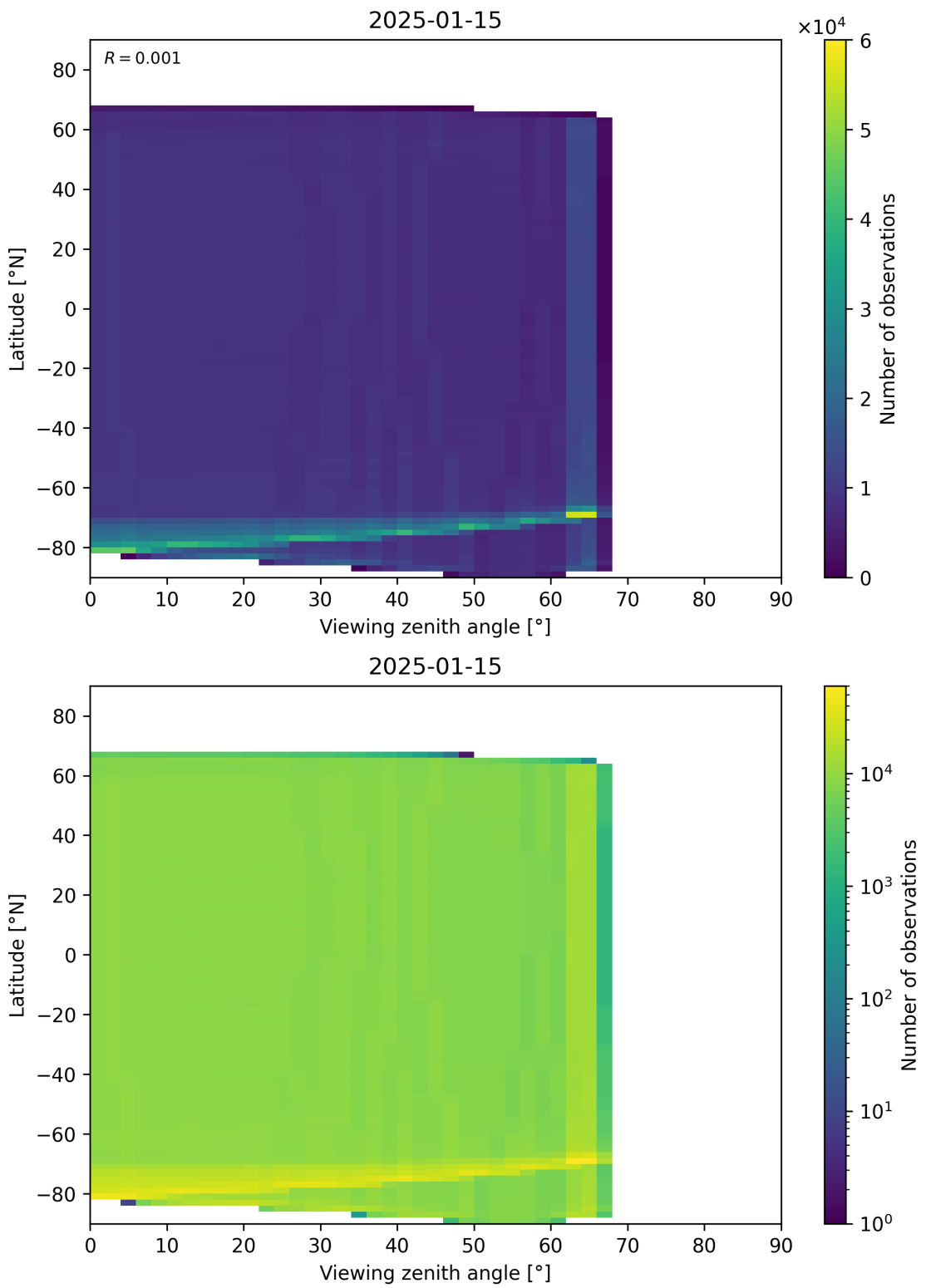


Figure 123: Scatter density plot of “Viewing zenith angle” against “Latitude” for 2025-01-14 to 2025-01-16.

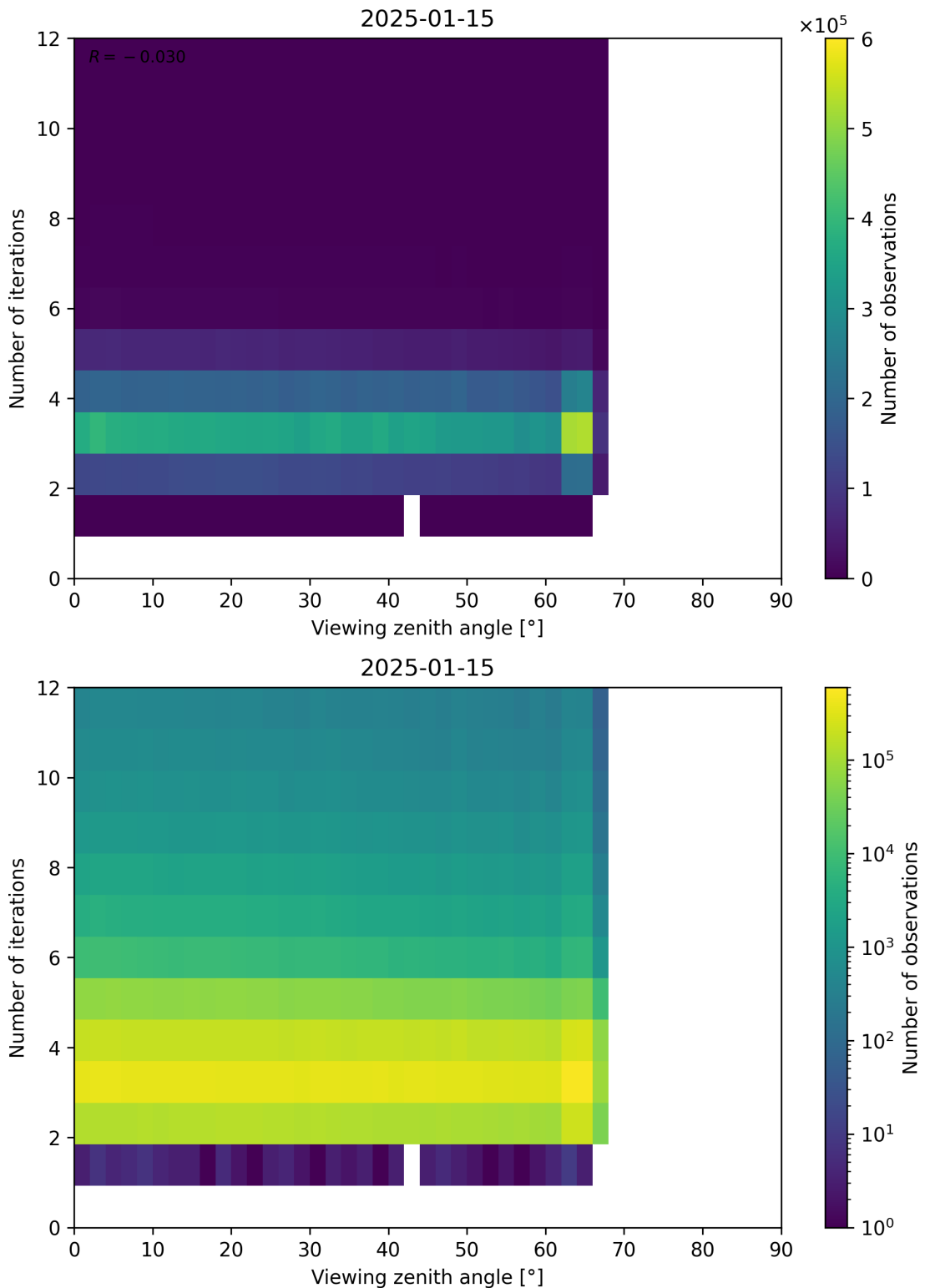


Figure 124: Scatter density plot of “Viewing zenith angle” against “Number of iterations” for 2025-01-14 to 2025-01-16.

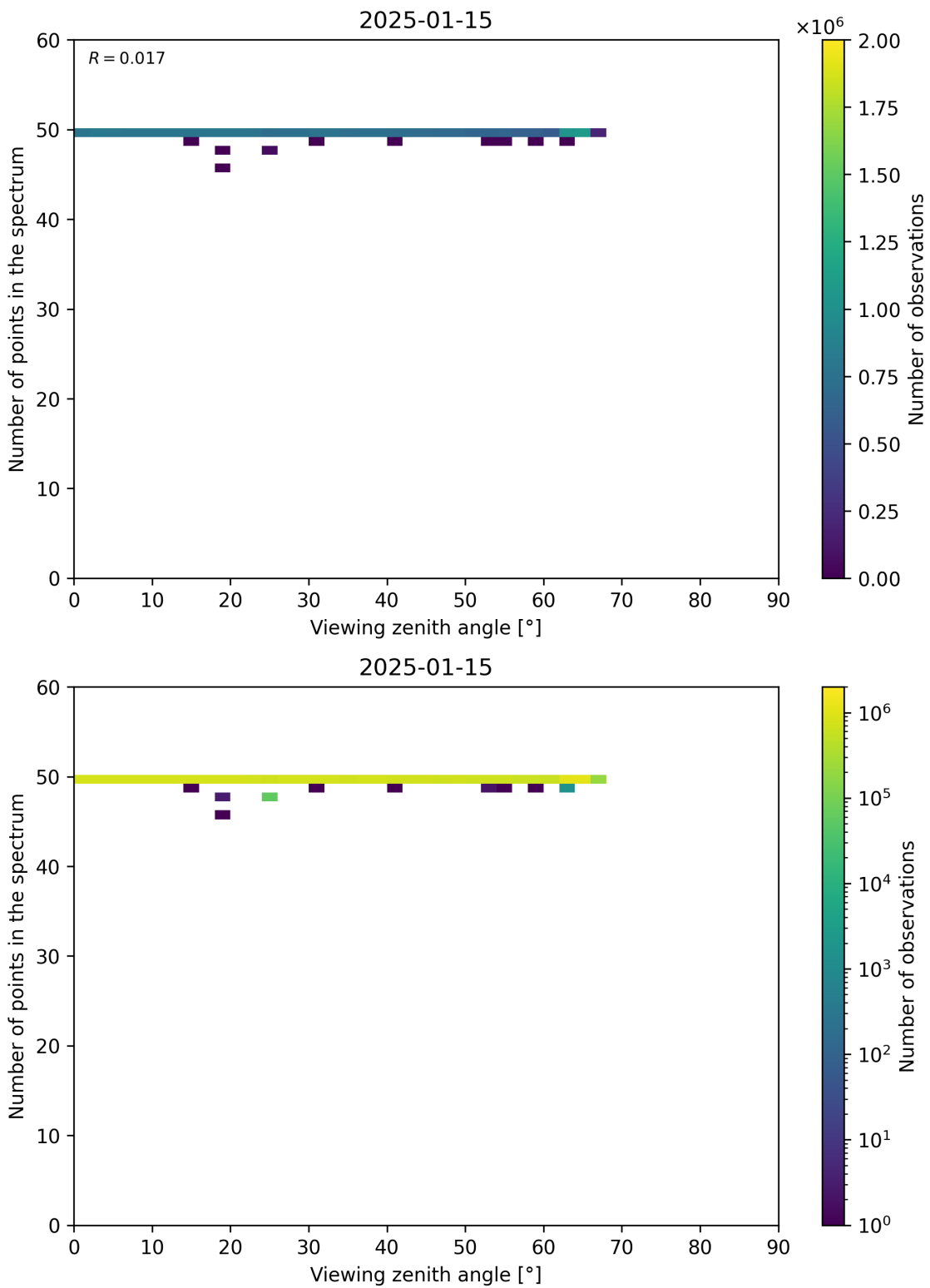


Figure 125: Scatter density plot of “Viewing zenith angle” against “Number of points in the spectrum” for 2025-01-14 to 2025-01-16.

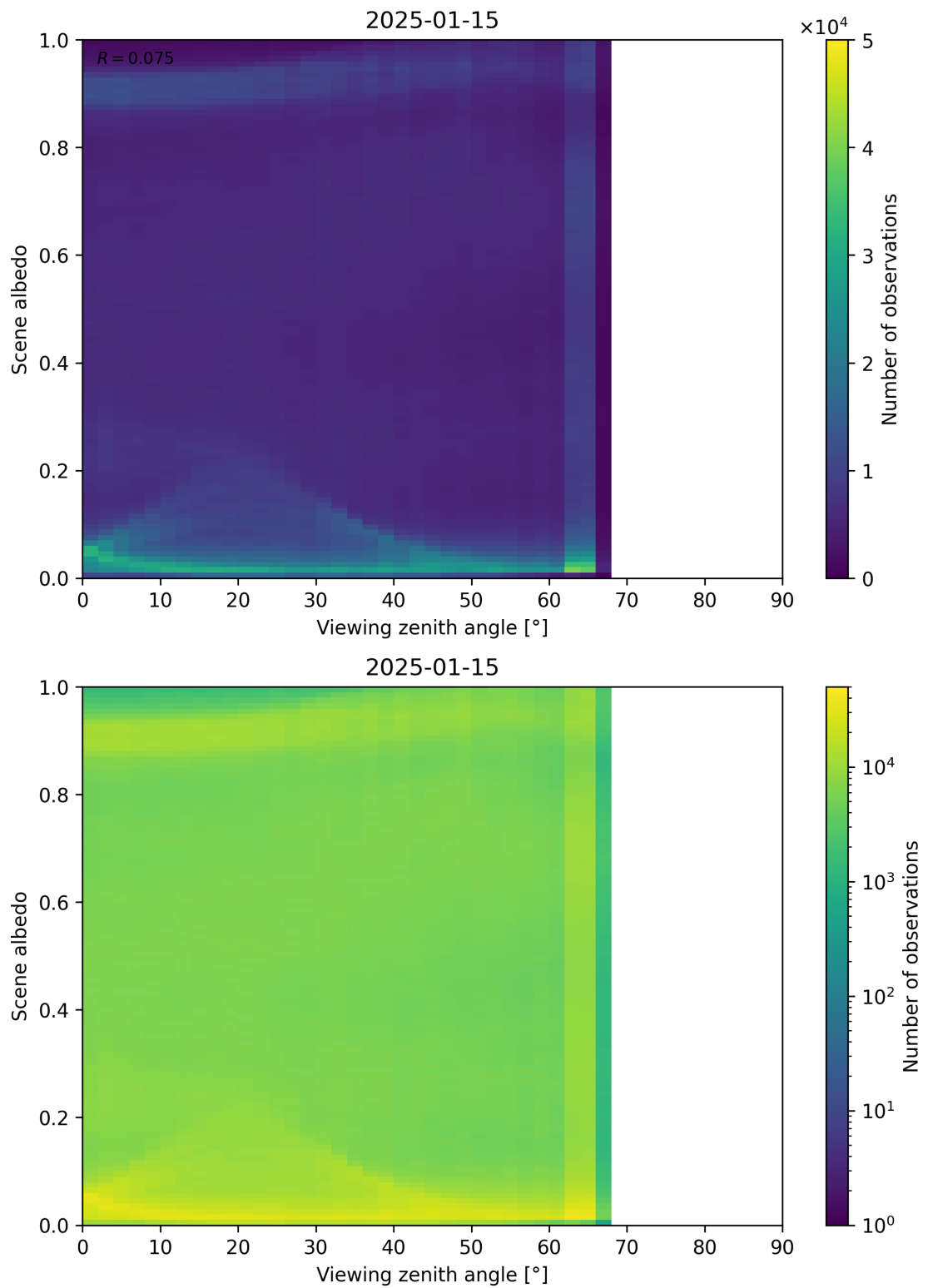


Figure 126: Scatter density plot of “Viewing zenith angle” against “Scene albedo” for 2025-01-14 to 2025-01-16.

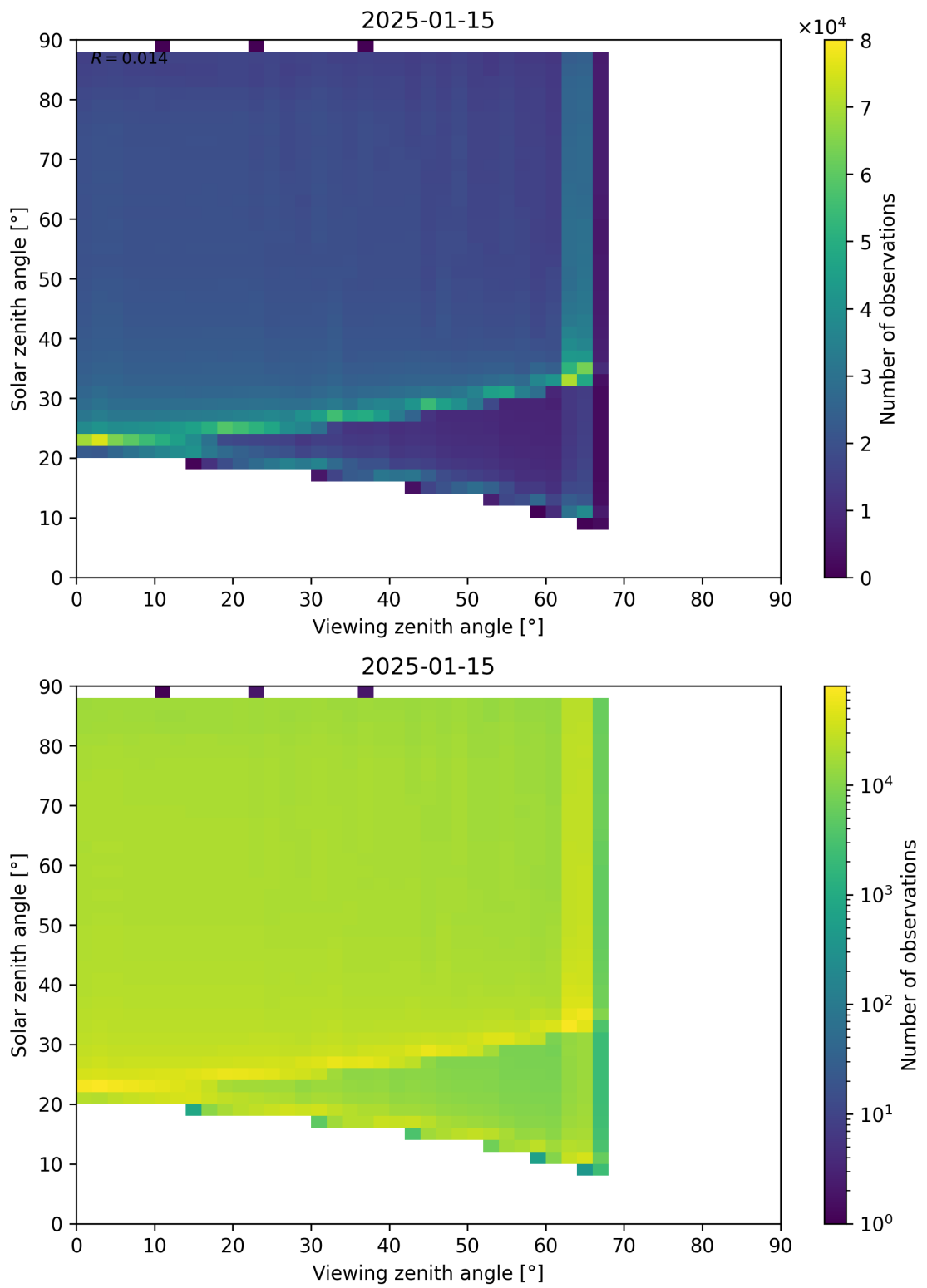


Figure 127: Scatter density plot of “Viewing zenith angle” against “Solar zenith angle” for 2025-01-14 to 2025-01-16.

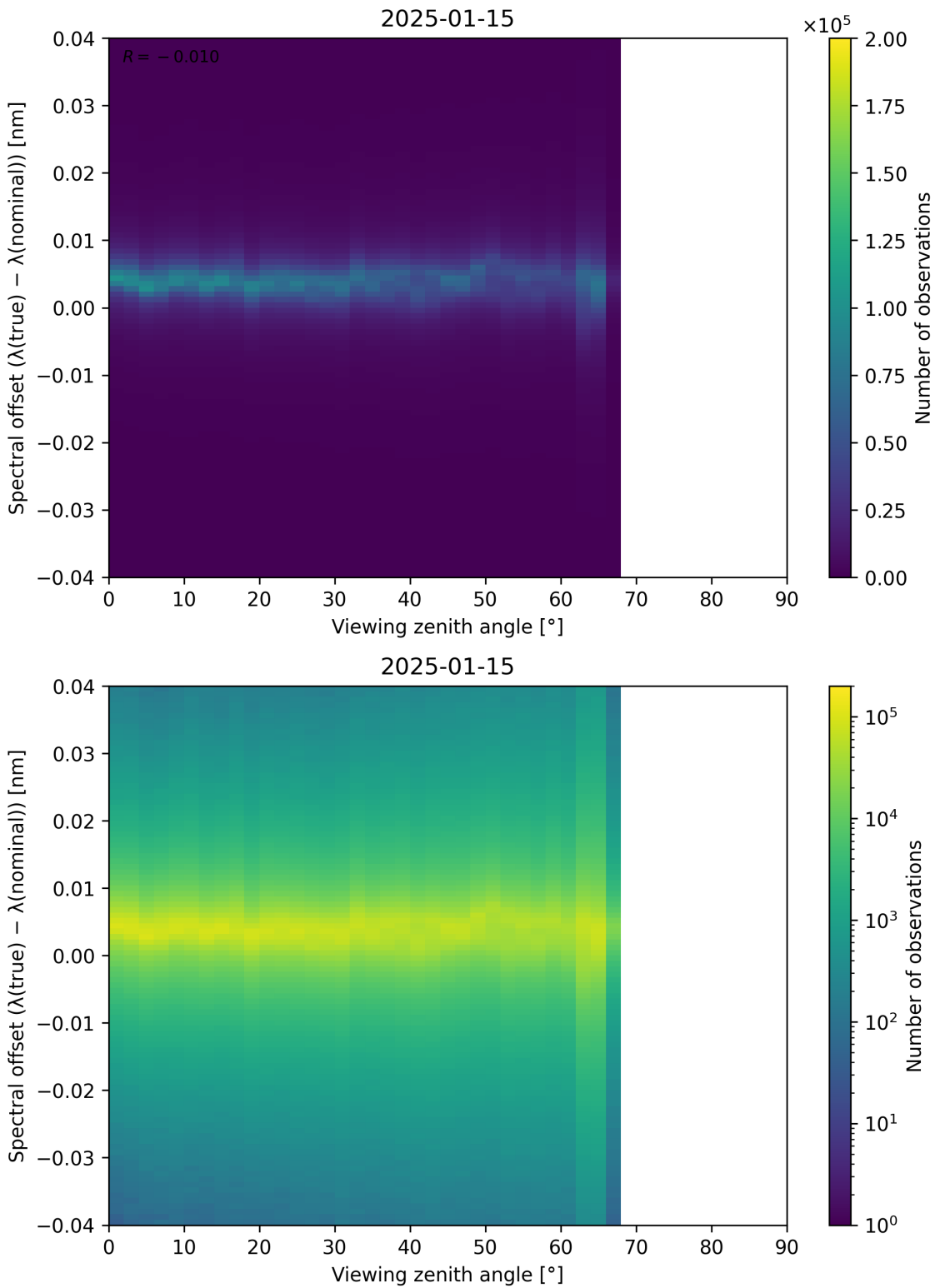


Figure 128: Scatter density plot of “Viewing zenith angle” against “Spectral offset ($\lambda_{\text{true}} - \lambda_{\text{nominal}}$)” for 2025-01-14 to 2025-01-16.

Contents

| | | |
|-----------|--|------------|
| 1 | Short Introduction | 1 |
| 1.1 | The list of parameters | 1 |
| 2 | Definitions | 1 |
| 3 | Granule outlines | 12 |
| 4 | Input data monitoring | 13 |
| 5 | Warnings and errors | 14 |
| 6 | World maps | 15 |
| 7 | Zonal average | 21 |
| 8 | Histograms | 38 |
| 9 | Along track statistics | 55 |
| 10 | Coincidence density | 72 |
| 11 | Copyright information of ‘PyCAMA’ | 138 |

List of Figures

| | | |
|----|---|----|
| 1 | Map of correlation graph for 2025-01-14 to 2025-01-16. | 10 |
| 2 | Map of correlation matrix for 2025-01-14 to 2025-01-16. | 11 |
| 3 | Outline of the granules. | 12 |
| 4 | Input data per granule | 13 |
| 5 | Fraction of pixels with specific warnings and errors during processing | 14 |
| 6 | Map of “Cloud pressure” for 2025-01-14 to 2025-01-16 | 15 |
| 7 | Map of “Cloud fraction” for 2025-01-14 to 2025-01-16 | 16 |
| 8 | Map of “Scene albedo” for 2025-01-14 to 2025-01-16 | 17 |
| 9 | Map of “Apparent scene pressure” for 2025-01-14 to 2025-01-16 | 18 |
| 10 | Map of “Fluorescence” for 2025-01-14 to 2025-01-16 | 19 |
| 11 | Map of the number of observations for 2025-01-14 to 2025-01-16 | 20 |
| 12 | Zonal average of “QA value” for 2025-01-14 to 2025-01-16. | 21 |
| 13 | Zonal average of “Cloud pressure” for 2025-01-14 to 2025-01-16. | 22 |
| 14 | Zonal average of “Cloud pressure precision” for 2025-01-14 to 2025-01-16. | 23 |
| 15 | Zonal average of “Cloud fraction” for 2025-01-14 to 2025-01-16. | 24 |
| 16 | Zonal average of “Cloud fraction precision” for 2025-01-14 to 2025-01-16. | 25 |
| 17 | Zonal average of “Scene albedo” for 2025-01-14 to 2025-01-16. | 26 |
| 18 | Zonal average of “Scene albedo precision” for 2025-01-14 to 2025-01-16. | 27 |
| 19 | Zonal average of “Apparent scene pressure” for 2025-01-14 to 2025-01-16. | 28 |
| 20 | Zonal average of “Apparent scene pressure precision” for 2025-01-14 to 2025-01-16. | 29 |
| 21 | Zonal average of “ χ^2 ” for 2025-01-14 to 2025-01-16. | 30 |
| 22 | Zonal average of “Number of iterations” for 2025-01-14 to 2025-01-16. | 31 |
| 23 | Zonal average of “Fluorescence” for 2025-01-14 to 2025-01-16. | 32 |
| 24 | Zonal average of “Fluorescence precision” for 2025-01-14 to 2025-01-16. | 33 |
| 25 | Zonal average of “ χ^2 of fluorescence retrieval” for 2025-01-14 to 2025-01-16. | 34 |
| 26 | Zonal average of “Degrees of freedom for signal of fluorescence retrieval” for 2025-01-14 to 2025-01-16. | 35 |
| 27 | Zonal average of “Number of points in the spectrum” for 2025-01-14 to 2025-01-16. | 36 |
| 28 | Zonal average of “Spectral offset ($\lambda_{\text{true}} - \lambda_{\text{nominal}}$)” for 2025-01-14 to 2025-01-16. | 37 |
| 29 | Histogram of “QA value” for 2025-01-14 to 2025-01-16 | 38 |
| 30 | Histogram of “Cloud pressure” for 2025-01-14 to 2025-01-16 | 39 |
| 31 | Histogram of “Cloud pressure precision” for 2025-01-14 to 2025-01-16 | 40 |
| 32 | Histogram of “Cloud fraction” for 2025-01-14 to 2025-01-16 | 41 |
| 33 | Histogram of “Cloud fraction precision” for 2025-01-14 to 2025-01-16 | 42 |
| 34 | Histogram of “Scene albedo” for 2025-01-14 to 2025-01-16 | 43 |
| 35 | Histogram of “Scene albedo precision” for 2025-01-14 to 2025-01-16 | 44 |
| 36 | Histogram of “Apparent scene pressure” for 2025-01-14 to 2025-01-16 | 45 |

| | | |
|----|--|----|
| 37 | Histogram of “Apparent scene pressure precision” for 2025-01-14 to 2025-01-16 | 46 |
| 38 | Histogram of “ χ^2 ” for 2025-01-14 to 2025-01-16 | 47 |
| 39 | Histogram of “Number of iterations” for 2025-01-14 to 2025-01-16 | 48 |
| 40 | Histogram of “Fluorescence” for 2025-01-14 to 2025-01-16 | 49 |
| 41 | Histogram of “Fluorescence precision” for 2025-01-14 to 2025-01-16 | 50 |
| 42 | Histogram of “ χ^2 of fluorescence retrieval” for 2025-01-14 to 2025-01-16 | 51 |
| 43 | Histogram of “Degrees of freedom for signal of fluorescence retrieval” for 2025-01-14 to 2025-01-16 | 52 |
| 44 | Histogram of “Number of points in the spectrum” for 2025-01-14 to 2025-01-16 | 53 |
| 45 | Histogram of “Spectral offset ($\lambda_{\text{true}} - \lambda_{\text{nominal}}$)” for 2025-01-14 to 2025-01-16 | 54 |
| 46 | Along track statistics of “QA value” for 2025-01-14 to 2025-01-16 | 55 |
| 47 | Along track statistics of “Cloud pressure” for 2025-01-14 to 2025-01-16 | 56 |
| 48 | Along track statistics of “Cloud pressure precision” for 2025-01-14 to 2025-01-16 | 57 |
| 49 | Along track statistics of “Cloud fraction” for 2025-01-14 to 2025-01-16 | 58 |
| 50 | Along track statistics of “Cloud fraction precision” for 2025-01-14 to 2025-01-16 | 59 |
| 51 | Along track statistics of “Scene albedo” for 2025-01-14 to 2025-01-16 | 60 |
| 52 | Along track statistics of “Scene albedo precision” for 2025-01-14 to 2025-01-16 | 61 |
| 53 | Along track statistics of “Apparent scene pressure” for 2025-01-14 to 2025-01-16 | 62 |
| 54 | Along track statistics of “Apparent scene pressure precision” for 2025-01-14 to 2025-01-16 | 63 |
| 55 | Along track statistics of “ χ^2 ” for 2025-01-14 to 2025-01-16 | 64 |
| 56 | Along track statistics of “Number of iterations” for 2025-01-14 to 2025-01-16 | 65 |
| 57 | Along track statistics of “Fluorescence” for 2025-01-14 to 2025-01-16 | 66 |
| 58 | Along track statistics of “Fluorescence precision” for 2025-01-14 to 2025-01-16 | 67 |
| 59 | Along track statistics of “ χ^2 of fluorescence retrieval” for 2025-01-14 to 2025-01-16 | 68 |
| 60 | Along track statistics of “Degrees of freedom for signal of fluorescence retrieval” for 2025-01-14 to 2025-01-16 | 69 |
| 61 | Along track statistics of “Number of points in the spectrum” for 2025-01-14 to 2025-01-16 | 70 |
| 62 | Along track statistics of “Spectral offset ($\lambda_{\text{true}} - \lambda_{\text{nominal}}$)” for 2025-01-14 to 2025-01-16 | 71 |
| 63 | Scatter density plot of “Apparent scene pressure” against “ χ^2 of fluorescence retrieval” for 2025-01-14 to 2025-01-16. | 72 |
| 64 | Scatter density plot of “Apparent scene pressure” against “Fluorescence” for 2025-01-14 to 2025-01-16. | 73 |
| 65 | Scatter density plot of “Apparent scene pressure” against “Number of iterations” for 2025-01-14 to 2025-01-16. | 74 |
| 66 | Scatter density plot of “Apparent scene pressure” against “Number of points in the spectrum” for 2025-01-14 to 2025-01-16. | 75 |
| 67 | Scatter density plot of “Apparent scene pressure” against “Spectral offset ($\lambda_{\text{true}} - \lambda_{\text{nominal}}$)” for 2025-01-14 to 2025-01-16. | 76 |
| 68 | Scatter density plot of “ χ^2 of fluorescence retrieval” against “Number of points in the spectrum” for 2025-01-14 to 2025-01-16. | 77 |
| 69 | Scatter density plot of “ χ^2 of fluorescence retrieval” against “Spectral offset ($\lambda_{\text{true}} - \lambda_{\text{nominal}}$)” for 2025-01-14 to 2025-01-16. | 78 |
| 70 | Scatter density plot of “Cloud fraction” against “Apparent scene pressure” for 2025-01-14 to 2025-01-16. | 79 |
| 71 | Scatter density plot of “Cloud fraction” against “ χ^2 of fluorescence retrieval” for 2025-01-14 to 2025-01-16. | 80 |
| 72 | Scatter density plot of “Cloud fraction” against “Fluorescence” for 2025-01-14 to 2025-01-16. | 81 |
| 73 | Scatter density plot of “Cloud fraction” against “Number of iterations” for 2025-01-14 to 2025-01-16. | 82 |
| 74 | Scatter density plot of “Cloud fraction” against “Number of points in the spectrum” for 2025-01-14 to 2025-01-16. | 83 |
| 75 | Scatter density plot of “Cloud fraction” against “Scene albedo” for 2025-01-14 to 2025-01-16. | 84 |
| 76 | Scatter density plot of “Cloud fraction” against “Spectral offset ($\lambda_{\text{true}} - \lambda_{\text{nominal}}$)” for 2025-01-14 to 2025-01-16. | 85 |
| 77 | Scatter density plot of “Cloud pressure” against “Apparent scene pressure” for 2025-01-14 to 2025-01-16. | 86 |
| 78 | Scatter density plot of “Cloud pressure” against “ χ^2 of fluorescence retrieval” for 2025-01-14 to 2025-01-16. | 87 |
| 79 | Scatter density plot of “Cloud pressure” against “Cloud fraction” for 2025-01-14 to 2025-01-16. | 88 |
| 80 | Scatter density plot of “Cloud pressure” against “Fluorescence” for 2025-01-14 to 2025-01-16. | 89 |
| 81 | Scatter density plot of “Cloud pressure” against “Number of iterations” for 2025-01-14 to 2025-01-16. | 90 |
| 82 | Scatter density plot of “Cloud pressure” against “Number of points in the spectrum” for 2025-01-14 to 2025-01-16. | 91 |
| 83 | Scatter density plot of “Cloud pressure” against “Scene albedo” for 2025-01-14 to 2025-01-16. | 92 |
| 84 | Scatter density plot of “Cloud pressure” against “Spectral offset ($\lambda_{\text{true}} - \lambda_{\text{nominal}}$)” for 2025-01-14 to 2025-01-16. | 93 |
| 85 | Scatter density plot of “Fluorescence” against “ χ^2 of fluorescence retrieval” for 2025-01-14 to 2025-01-16. | 94 |
| 86 | Scatter density plot of “Fluorescence” against “Number of points in the spectrum” for 2025-01-14 to 2025-01-16. | 95 |
| 87 | Scatter density plot of “Fluorescence” against “Spectral offset ($\lambda_{\text{true}} - \lambda_{\text{nominal}}$)” for 2025-01-14 to 2025-01-16. | 96 |
| 88 | Scatter density plot of “Latitude” against “Apparent scene pressure” for 2025-01-14 to 2025-01-16. | 97 |

| | | |
|-----|---|-----|
| 89 | Scatter density plot of “Latitude” against “ χ^2 of fluorescence retrieval” for 2025-01-14 to 2025-01-16. | 98 |
| 90 | Scatter density plot of “Latitude” against “Cloud fraction” for 2025-01-14 to 2025-01-16. | 99 |
| 91 | Scatter density plot of “Latitude” against “Cloud pressure” for 2025-01-14 to 2025-01-16. | 100 |
| 92 | Scatter density plot of “Latitude” against “Fluorescence” for 2025-01-14 to 2025-01-16. | 101 |
| 93 | Scatter density plot of “Latitude” against “Number of iterations” for 2025-01-14 to 2025-01-16. | 102 |
| 94 | Scatter density plot of “Latitude” against “Number of points in the spectrum” for 2025-01-14 to 2025-01-16. . | 103 |
| 95 | Scatter density plot of “Latitude” against “Scene albedo” for 2025-01-14 to 2025-01-16. | 104 |
| 96 | Scatter density plot of “Latitude” against “Spectral offset ($\lambda_{\text{true}} - \lambda_{\text{nominal}}$)” for 2025-01-14 to 2025-01-16. . | 105 |
| 97 | Scatter density plot of “Number of iterations” against “ χ^2 of fluorescence retrieval” for 2025-01-14 to 2025-01-16. | 106 |
| 98 | Scatter density plot of “Number of iterations” against “Fluorescence” for 2025-01-14 to 2025-01-16. | 107 |
| 99 | Scatter density plot of “Number of iterations” against “Number of points in the spectrum” for 2025-01-14 to 2025-01-16. | 108 |
| 100 | Scatter density plot of “Number of iterations” against “Spectral offset ($\lambda_{\text{true}} - \lambda_{\text{nominal}}$)” for 2025-01-14 to 2025-01-16. | 109 |
| 101 | Scatter density plot of “Number of points in the spectrum” against “Spectral offset ($\lambda_{\text{true}} - \lambda_{\text{nominal}}$)” for 2025-01-14 to 2025-01-16. | 110 |
| 102 | Scatter density plot of “Scene albedo” against “Apparent scene pressure” for 2025-01-14 to 2025-01-16. . . | 111 |
| 103 | Scatter density plot of “Scene albedo” against “ χ^2 of fluorescence retrieval” for 2025-01-14 to 2025-01-16. . | 112 |
| 104 | Scatter density plot of “Scene albedo” against “Fluorescence” for 2025-01-14 to 2025-01-16. | 113 |
| 105 | Scatter density plot of “Scene albedo” against “Number of iterations” for 2025-01-14 to 2025-01-16. | 114 |
| 106 | Scatter density plot of “Scene albedo” against “Number of points in the spectrum” for 2025-01-14 to 2025-01-16. | 115 |
| 107 | Scatter density plot of “Scene albedo” against “Spectral offset ($\lambda_{\text{true}} - \lambda_{\text{nominal}}$)” for 2025-01-14 to 2025-01-16. . | 116 |
| 108 | Scatter density plot of “Solar zenith angle” against “Apparent scene pressure” for 2025-01-14 to 2025-01-16. . | 117 |
| 109 | Scatter density plot of “Solar zenith angle” against “ χ^2 of fluorescence retrieval” for 2025-01-14 to 2025-01-16. . | 118 |
| 110 | Scatter density plot of “Solar zenith angle” against “Cloud fraction” for 2025-01-14 to 2025-01-16. | 119 |
| 111 | Scatter density plot of “Solar zenith angle” against “Cloud pressure” for 2025-01-14 to 2025-01-16. | 120 |
| 112 | Scatter density plot of “Solar zenith angle” against “Fluorescence” for 2025-01-14 to 2025-01-16. | 121 |
| 113 | Scatter density plot of “Solar zenith angle” against “Latitude” for 2025-01-14 to 2025-01-16. | 122 |
| 114 | Scatter density plot of “Solar zenith angle” against “Number of iterations” for 2025-01-14 to 2025-01-16. . | 123 |
| 115 | Scatter density plot of “Solar zenith angle” against “Number of points in the spectrum” for 2025-01-14 to 2025-01-16. | 124 |
| 116 | Scatter density plot of “Solar zenith angle” against “Scene albedo” for 2025-01-14 to 2025-01-16. | 125 |
| 117 | Scatter density plot of “Solar zenith angle” against “Spectral offset ($\lambda_{\text{true}} - \lambda_{\text{nominal}}$)” for 2025-01-14 to 2025-01-16. | 126 |
| 118 | Scatter density plot of “Viewing zenith angle” against “Apparent scene pressure” for 2025-01-14 to 2025-01-16. . | 127 |
| 119 | Scatter density plot of “Viewing zenith angle” against “ χ^2 of fluorescence retrieval” for 2025-01-14 to 2025-01-16. | 128 |
| 120 | Scatter density plot of “Viewing zenith angle” against “Cloud fraction” for 2025-01-14 to 2025-01-16. | 129 |
| 121 | Scatter density plot of “Viewing zenith angle” against “Cloud pressure” for 2025-01-14 to 2025-01-16. | 130 |
| 122 | Scatter density plot of “Viewing zenith angle” against “Fluorescence” for 2025-01-14 to 2025-01-16. | 131 |
| 123 | Scatter density plot of “Viewing zenith angle” against “Latitude” for 2025-01-14 to 2025-01-16. | 132 |
| 124 | Scatter density plot of “Viewing zenith angle” against “Number of iterations” for 2025-01-14 to 2025-01-16. . | 133 |
| 125 | Scatter density plot of “Viewing zenith angle” against “Number of points in the spectrum” for 2025-01-14 to 2025-01-16. | 134 |
| 126 | Scatter density plot of “Viewing zenith angle” against “Scene albedo” for 2025-01-14 to 2025-01-16. | 135 |
| 127 | Scatter density plot of “Viewing zenith angle” against “Solar zenith angle” for 2025-01-14 to 2025-01-16. . | 136 |
| 128 | Scatter density plot of “Viewing zenith angle” against “Spectral offset ($\lambda_{\text{true}} - \lambda_{\text{nominal}}$)” for 2025-01-14 to 2025-01-16. | 137 |

List of Tables

| | | |
|---|---|---|
| 1 | Parameterlist and basic statistics for the analysis | 2 |
| 2 | Percentile ranges | 3 |
| 3 | Parameterlist and basic statistics for the analysis for observations in the northern hemisphere | 4 |
| 4 | Parameterlist and basic statistics for the analysis for observations in the southern hemisphere | 5 |
| 5 | Parameterlist and basic statistics for the analysis for observations over water | 6 |
| 6 | Parameterlist and basic statistics for the analysis for observations over land | 7 |
| 7 | Correlation matrix | 8 |
| 8 | Covariance matrix | 9 |

11 Copyright information of ‘PyCAMA’

Copyright © 2005 – 2023, Maarten Sneep (KNMI).

All rights reserved.

Redistribution and use in source and binary forms, with or without modification, are permitted provided that the following conditions are met:

1. Redistributions of source code must retain the above copyright notice, this list of conditions and the following disclaimer.
2. Redistributions in binary form must reproduce the above copyright notice, this list of conditions and the following disclaimer in the documentation and/or other materials provided with the distribution.
3. Neither the name of the copyright holder nor the names of its contributors may be used to endorse or promote products derived from this software without specific prior written permission.

This software is provided by the copyright holders and contributors “as is” and any express or implied warranties, including, but not limited to, the implied warranties of merchantability and fitness for a particular purpose are disclaimed. In no event shall the copyright holder or contributors be liable for any direct, indirect, incidental, special, exemplary, or consequential damages (including, but not limited to, procurement of substitute goods or services; loss of use, data, or profits; or business interruption) however caused and on any theory of liability, whether in contract, strict liability, or tort (including negligence or otherwise) arising in any way out of the use of this software, even if advised of the possibility of such damage.

Maarten Sneep (maarten.sneep@knmi.nl).